

The copyright of this thesis rests with the University of Cape Town. No quotation from it or information derived from it is to be published without full acknowledgement of the source. The thesis is to be used for private study or non-commercial research purposes only.

**Development of HI-236 as an HIV NNRTI and as a component of novel
bifunctional HIV-1 RT inhibitors of the type (NRTI)-spacer-(HI-236)**

A thesis submitted to the
University of Cape Town
In fulfilment of the requirements of the
Degree of Doctor of Philosophy



By

Yassir Eltayeb Younis

Supervisor: **Professor Roger Hunter**

Department of Chemistry
University of Cape Town
Rondebosch, 7701
Cape Town

March 2009

DECLARATION

I declare that “*Development of HI-236 as an HIV NNRTI and as a component of novel bifunctional HIV-1 RT inhibitors of the type (NRTI)-spacer-(HI-236)*” is my own work and that all sources that I have used or quoted have been indicated and acknowledged by means of complete references.

Yassir Eltayeb Younis

University of Cape Town

ABSTRACT

This thesis concerns the synthesis and biological evaluation of bifunctional inhibitors of the type [NRTI]-spacer-[HI-236] as well as development of HI-236 derivatives as NNRTI's.

Following a comprehensive review on RT and HIV double drugs, in the first part of the Results and Discussion section (Chapter 2) of the thesis, a library of derivatives of the NNRTI HI-236 substituted at the C-2 oxygen of the phenyl ring is described and evaluated for their inhibitory activity against HIV (IIIB) replication in MT-2 cell culture. The compounds were synthesized in order to fine-tune the activity of HI-236 as well as to gain insight into spatial characteristics in the pocket pertaining to the positional choice of the tether in the design of [NRTI]-spacer-[HI-236] bifunctional inhibitors. Two of the thiourea derivatives bearing a butynyl (**77c**) or hydroxyethyl tether (**77m**) were endowed with improved anti-HIV activity compared to HI-236. NNRTI activity was confirmed by a cell-free RT assay on six of the derivatives in which (**77c**) returned an IC_{50} of 3.8 nM compared to 28 nM for HI-236, establishing it as an improved lead for HI-236.

The second part (Chapter 3) involves the synthesis and biological evaluation of four bifunctional inhibitors of the type [d4U]-spacer-[HI-236] varying the spacer length. This was accomplished using a divergent synthesis starting with uridine to furnish each bifunctional in between 13 and 19 steps respectively using a Sonogashira coupling as a key step in each case. Each bifunctional derivative was fully characterised using NMR, IR and MS techniques. Similarly, a phosphoramidate as a mono-phosphorylated pro-drug of the 4-PEG bifunctional was prepared, except in this case the Sonogashira coupling proceeded via coupling of an amine version of the NNRTI followed by condensation post-coupling to install the HI-236 thiourea grouping. All bifunctional compounds were tested against HIV-1 replication in MT-2 cell culture as well as in an *in vitro* RT enzyme assay. The results (EC_{50} and IC_{50}) indicated good inhibitory activity likely due to an elongated NNRTI with some binding outside the pocket. However, there was no evidence for conversion to the bifunctional triphosphate for possible full "mixed-site" inhibition.

In the final part (Chapter 4) two bifunctionals incorporating an ANP (acyclic nucleotide phosphonate) prototype instead of d4U were prepared and tested in cell-culture. The EC_{50} results indicated a similarity to those for the d4U bifunctional, hence leading support for the conclusions from Chapter 3.

Parts of this thesis have been published:

“C-2-Aryl O-Substituted HI-236 Derivatives as Non-Nucleoside HIV-1 Reverse-Transcriptase Inhibitors”. Hunter, R.; Younis, Y.; Muhanji, C-I.; Curtin, T-L.; Naidoo, K. J.; Petersen, M.; Baily, C. M.; Basavapathruni, A.; Anderson, K. S. *Bioorg. Med. Chem.* **2008**, 16, 10270-10280.

Parts of this thesis have been presented at the following conferences:

(presenting author underlined)

9th Frank Warren Conference on Organic Chemistry, 22-25 January 2006, University of Cape Town, Cape Town, South Africa.

Poster: Towards the synthesis of NRTI/NNRTI bifunctional inhibitors type [d4U]-spacer-[HI-236] as anti HIV-1.

Y. Younis and R. Hunter.

XXTH International Symposium on Medicinal Chemistry, (EFMC-ISMC 2008) organized, August 31-September 4, 2008 in Vienna, Austria.

Poster: Synthesis and evaluation of non-cleavable NRTI/NNRTI bifunctional inhibitors based on [d4U]-spacer-[HI-234].

Y. Younis and R. Hunter.

10th Frank Warren Conference on Organic Chemistry, 14-19 September 2008, Kruger National Park, South Africa.

Poster: Synthesis and evaluation of non-cleavable NRTI/NNRTI bifunctional inhibitors based on [d4U]-spacer-[HI-234].

Y. Younis and R. Hunter.

ACKNOWLEDGEMENTS

I would like to thank the following people for their contributions to this thesis:

My supervisor, Professor Roger Hunter to whom I dedicate this thesis, for his guidance, motivation, encouragement, patience and most importantly enthusiasm throughout this project and preparation of my thesis.

Professor Karen Anderson (Yale University, USA) for biological activity experiments and useful discussions.

Professor Kevin J. Naidoo (University of Cape Town) for molecular modeling experiments and helpful discussion.

Associate Professor David W. Gammon and Professor Kelly Chibale their helpful discussion.

Colleagues past and present in the Hunter/Gammon research Dr. Clare Muhanji, Dr. Sophi Rees-Jones, Dr. Seanette Wilson, Dr. Henok Kinfe, Dr Vincent Zishiri, Dr. Vincent Paul, Dr. Rajinder Singh, Dr. Philip Richards, Dr. Hayley Haupt, Dr. Melissa Petersen, Tanith-Lea Curtin, Ana Andrijevic, Rudy Cozette, Tozama Qwebani, Mythes Smith, David van der Merwe, Scebi Mkhize and my friend Ebrahim Mohammed all for their help and assistance.

A special thank you to Dr. Nashia Stellenboom for her great assistance and friendship.

Noel Hendricks, Pete Roberts, Tommie van der, Martin Brits and Dr. Marietji Stander for their analytical services.

The National Research Foundation and University of Cape Town for their financial support.

Lastly, to my family and friends for their constant support and encouragement that means so much to me.

ABBREVIATIONS

ABC	(1 <i>S</i> ,4 <i>R</i>)-4-[2-Amino-6-(cyclopropyl-amino)-9 <i>H</i> -purin-9-yl]-2-cyclopentene-1-methanol succinate
AcBr	Acetyl bromide
AcOH	Acetic acid
AIDS	Acquired Immunodeficiency Syndrome
Amino Acids	A, Alanine; C, Cysteine; D, Aspartate; E, Glutamate; F, Phenylalanine; G, Glycine; H, Histidine; I, Isoleucine; K, Lysine; L, Leucine; M, Methionine; N, Asparagine; P, Proline; Q, Glutamine; R, Arginine; S, Serine; T, Threonine; V, Valine; W, Tryptophan; Y, Tyrosine
APY	Arylpyrimidine
α -APA	α -(2,6-Dichlorophenyl)- α -(2-acetyl-5-methylanilino)acetamide
APTS	8-Aminopyrene-1,3,6-trisulfonate
aq.	Aqueous
Ar	Aromatic
AZT	3'-Azido-2',3'-dideoxythymidine
B:	Generic base
BnBr	Benzyl bromide
Boc	<i>tert</i> -Butyl carbonate
BOP	Benzotriazol-1-yloxy-tris(dimethylamino)phosphonium hexafluoro phosphate
br	Broad
brs	Broad singlet
Bu ₃ SnH	Tributyltin hydride
BuNH ₂	Butylamine
<i>t</i> -BuOK	Potassium <i>tert</i> -butoxide
BVDU	Bromovinyldeoxyuridine
CAN	Ceric ammonium nitrate
cat.	Catalytic
CD4	Cluster of differentiation 4
cDNA	Complementary deoxynucleic acid
CF ₃ COOH	Trifluoroacetic acid
CH ₂ Cl ₂	Dichloromethane / Methylene chloride
CH ₃ CN	Acetonitrile
CS ₂	Carbonylsulfide

δ	Chemical shift in ppm
d	Doublet
dd	Doublet of doublets
dt	Doublet of triplets
d ₂ U	2',3'-Dideoxyuridine
d ₄ T	2',3'-Didehydro-2',3'-dideoxythymidine
d ₄ U	2',3'-Didehydro-2',3'-dideoxyuridine
DABO	Dihydroalkoxybenzyloxypyrimidine
DAPY	Diarylpyrimidine
DATA	Diaryltriazine
DBU	1,8-Diazabicyclo[5.4.0]undec-7-ene
DCC	1,3-Dicyclohexylcarbodiimide
DCM	Dichloromethane / Methylene chloride
dCMP	deoxyribonucleoside monophosphates kinase
dCTP	Deoxycytidine triphosphate
dCyd	Deoxycytidine kinase
ddC	2',3'-Dideoxycytidine
ddl	2',3'-Dideoxyinosine
Delavirdine	1-(5-Methanesulfonamido-1 <i>H</i> -indol-2-yl-carbonyl)-4-[3-(1-methylethyl-amino)pyridinyl]piperazine monomethane sulfonate
DIA	(Diisopropylamino)phosphine
DIAD	Diisopropylazodicarboxylate
DIEA	Diisopropylethylamine
DMA	<i>N,N</i> -Dimethylacetamide
DMAP	<i>N,N</i> -Dimethylaminopyridine
DME	1,2-Dimethoxyethane
DMP	2,2-Dimethoxypropane
DMSO	Dimethylsulfoxide
DNA	Deoxyribonucleic acid
dGTP	Deoxyguanine triphosphate
dNMP	Deoxyribonucleotide monophosphate
dNTP	Deoxyribonucleotide triphosphate
dsDNA	Double-stranded deoxyribonucleic acid
dTTP	Deoxythymidine triphosphate
EDC	Ethylene dichloride
Efavirenz	(-)-6-Chloro-4-cyclopropylethynyl-4-trifluoromethyl-1,4-dihydro-2 <i>H</i> -

	3,1-benzoxazin-2-one
E1	Unimolecular elimination
E2	Bimolecular elimination
EDTA	Ethylenediaminetetraacetate monosodium
EI	Electron impact
Enfuvirtide	36-amino acid peptide
ES	Electron spray
Et ₃ N	Triethylamine
Et ₂ O	Diethyl ether
EtOAc	Ethyl acetate
EtOH	Ethanol
eq.	Equivalent
FAB	Fast atom bombardment
FDA	US Food and Drug Administration
FDU	5-Fluoro-2'-deoxyuridine
(-)-FTC	(-)-β-L-3'-thia-2',3'-dideoxy-5-fluorocytidine
(+)-FTC	(+)-β-D-3'-thia-2',3'-dideoxy-5-fluorocytidine
g	Grams
GALT	Gastrointestinal associated lymphoid tissue
gp	Glycoprotein
GR	Glutathion reductase
HAART	Highly active anti-retroviral therapy
HBY 097	(S)-4-Isopropoxycarbonyl-6-methoxy-3-(methylthiomethyl)-3,4-dihydroquinoxaline-2(1 <i>H</i>)-thione
HCl	Hydrochloric acid
HCMV	Cytomegalovirus
HEPT	1-[(2-Hydroxyethoxy)methyl]-6-(phenylthio)thymine
HI-236	<i>N</i> '-(5-bromo-2-pyridyl)- <i>N</i> -[2-(2,5-dimethoxyphenyl)ethyl]thiourea
HIV-1	Human Immunodeficiency Virus type 1
HOPT	1-Hydroxybenzotriazole
HPLC	High-pressure liquid chromatography
hr.	Hour
HRMS	High-resolution mass spectrometry
Hz	Hertz
IDU	5-Iodo-2'-deoxyuridine (Idoxuridine)
IN	Integrase

IR	Infrared spectrometry
ITU	Imidoylthiourea
<i>J</i>	Coupling constant
LAH	Lithium aluminium hydride
Lit.	Literature
LTR	Long terminal repeat
<i>m</i>	Meta
m	Multiplet
M ⁺	Molecular ion
MA	HIV-1 matrix protein
MeOH	Methanol
mg	Milligram(s)
MHz	Mega hertz
MKC-442	6-Benzyl-1-(ethoxymethyl)-5-isopropyluracil
ml	Millilitre(s)
mmol	Millimole(s)
Mp	Melting point
mRNA	Messenger ribonucleic acid
MsCl	Methanesulfonyl chloride
<i>m/z</i>	Mass to charge ratio
NBS	<i>N</i> -Bromosuccinamide
NCp	Nucleocapsid protein
NDP	Nucleoside-diphosphate kinase
NEM	Nucleotide excision mechanism
Nevirapine	11-Cyclopropyl-5,11-dihydro-4-methyl-6 <i>H</i> -dipyrido(3,2- <i>b</i> :2',3'- <i>f</i>) (1,4)diazepin-6-one
NMM	<i>N</i> -Methylmorpholine
NMR	Nuclear magnetic resonance
NNIBP	Non-nucleoside inhibitor binding pocket
NNIBS	Non-nucleoside inhibitor binding site
NNRTI	Non-nucleoside reverse transcriptase inhibitor
NNRTI-BP	Non-nucleoside reverse transcriptase inhibitor binding pocket
NRTI	Nucleoside reverse transcriptase inhibitor
<i>o</i>	Ortho
<i>p</i>	Para
PBS	Primer binding site

PG	Protecting group
P(OEt) ₃	Triethyl phosphite
Pd/C	Palladium-on-carbon
Pet ether	Petroleum ether
PETT	Phenylethylthiazolylthiourea
PFA	Phosphonoformate
Phospho	Phosphonate
PI	Protease inhibitor
PLM (II)	Plasmepsin (II)
PMBCl	<i>p</i> -Methoxybenzyl chloride
PMEA	9-(2-phosphonylmethoxyethyl)adenine
PMPA	(<i>R</i>)-9-(2-Phosphonylmethoxypropyl)adenine
PPh ₃	Triphenylphosphine
(PPh ₃) ₄ P	Tetrakis(triphenylphosphine)palladium (0)
PQ	Primaquine
PR	Protease
PT	Proton transfer
RDDP	RNA-dependent DNA polymerase
Ribavirin	1-β-D-Ribofuranosyl-1 <i>H</i> -1,2,4-triazole-3-carboxamide
RNA	Ribonucleic acid
RNase H	Ribonuclease H
RT	Reverse transcriptase
rt	Room temperature
s	Singlet
SATE	S-Acyl-2-thioethyl
S _N 1	Unimolecular nucleophilic substitution
S _N 2	Bimolecular nucleophilic substitution
ssRNA	Single-stranded ribonucleic acid
t	Triplet
TBDMSCl	<i>tert</i> -Butyldimethylsilyl chloride
TBDPS	<i>tert</i> -Butyldiphenylsilyl chloride
3TC	(-)-β-L-3'-Thia-2',3'-dideoxycytidine
td	Triplet of doublets
TFA	Trifluoroacetic acid
TFT	5-Trifluoromethyl-2'-deoxyuridine (Trifluorothymidine or Trifluridine)
THF	Tetrahydrofuran

THP	Tetrahydropyran
TIBO	(+)-(S)-4,5,6,7-Tetrahydro-8-chloro-5-methyl-6-(3-methyl-2-butenyl)imidazo[4,5,1jk][1,4]benzodiazepine-2(1H)-thione
TIPS	Triisopropylsilyl
TLC	Thin layer chromatography
TMSCI	Trimethylsilyl chloride
TSAO	2',5'-bis-O-(<i>tert</i> -Butyldimethylsilyl)-3'-spiro-5'-(4"-amino-1",2"-oxathiole-2",2"-dioxide)pyrimidine
<i>p</i> -TsOH	<i>para</i> -Toluenesulfonic acid
q	Quartet
UV	Ultra violet
w/v	Weight by volume
v/v	Volume by volume

University of Cape Town

CONTENTS

CHAPTER 1: INTRODUCTION	1
1.1 Human Immunodeficiency Virus (HIV).....	1
1.2 The Structure of the HIV-1 Virion	1
1.3 Epidemiology of HIV/AIDS.....	2
1.4 The HIV Life-Cycle.....	3
1.5 HIV Pathogenesis.....	5
1.6 The Reverse Transcriptase Enzyme (RT).....	6
1.7 Developments in Anti-HIV Chemotherapy.....	8
1.8 Nucleoside Reverse Transcriptase Inhibitors (NRTIs).....	9
1.9 The Structure of HIV-1 RT in Complex with Nucleoside Inhibitors.....	12
1.10 Nucleotide Reverse Transcriptase Inhibitors (NtRTIs).....	14
1.10.1 The Prodrug Approach (The Pronucleotide Approach).....	15
1.10.2 The Acyclic Nucleotide Phosphonates (ANPs).....	18
1.11 NRTI Resistance.....	21
1.12 Non-Nucleoside Reverse Transcriptase Inhibitors (NNRTIs).....	23
1.12.1 The NNRTI-Binding Pocket.....	26
1.12.2 The mechanism for NNRTI Inhibition of RT.....	27
1.12.3 First-and Second-Generation NNRTIs: Differences in the Mode of Binding to HIV-1 RT.....	29
1.13 Phenethylthiazolythioureas (PETT) Derivatives.....	32
1.14. NNRTI Resistance.....	35
1.15. The Double-Drugs Strategy.....	38
1.15.1 Double-Drugs in Cancer and Malaria.....	38
1.15.2 Double-Drugs in HIV.....	40
1.16 Objective of the Study.....	56

CHAPTER 2: C-2-ARYL O-SUBSTITUTED HI-236 DERIVATIVES AS NON-NUCLEOSIDE HIV-1 RT INHIBITORS	59
2.1 Modeling of HI-236.....	60
2.2 Overview on Synthesis of the PETT Derivatives.....	62
2.3 Retrosynthetic Analysis of HI-236 Derivatives 77	64
2.4 Biological Results, Modeling and Discussion.....	81
CHAPTER 3: SYNTHESIS OF [d4U]-SPACER-[HI-236] DOUBLE-DRUGS	89
3.1 Introduction.....	89
3.2 Overview on the Synthesis of d4T.....	90
3.2.1 Synthesis of d4T from 5-Methyluridine.....	91
3.3 Strategies for the Synthesis of [d4U]-spacer-[HI-236].....	93
3.4 Overview on Sonogashira Coupling.....	95
3.5 Route (A): Synthesis of Target Compounds 51 , 78 and 79	99
3.5.1 Synthesis of [d4U]-butyne-[HI-236] 51	99
3.5.1.1 Synthesis of 5'-O-Benzoyl iodo-d4U.....	99
3.5.1.2 Sonogashira Coupling, Deprotection and Condensation.....	101
3.5.1.3 The End-Game.....	103
3.5.2 Synthesis of [d4U]-monpPEG-propyne-[HI-236] 78	103
3.5.3 Synthesis of [d4U]-diPEG-propyne-[HI-236] 79	106
3.6 Route (B): Synthesis of Target Compounds 80 and 81	110
3.6.1 Synthesis of [d4U]-tetraPEG-propyne-[HI-236] 80	110
3.6.2 Synthesis of [d4U]-phosphoramidate]-teraPEG-propyne-[HI-236] 81	113
3.6.2.1 Synthesis of Iodo-d4U-Phosphoramidate.....	113
3.7 Biological Results and Rationale.....	119
CHAPTER 4: SYNTHESIS OF [ANP]-SPACER-[HI-236]	123
4.1 Synthesis of [ANP]- <i>n</i> -PEG-propyne-[HI-236]: (<i>n</i> = 4 and 6).....	124

4.1.1 Retrosynthetic analysis of [ANP]- <i>n</i> -PEG-propyne-[HI-236].....	125
4.1.2 Synthesis of the ANP moiety.....	126
4.1.3 Synthesis of [ANP]- <i>tetra</i> PEG-propyne-[HI-236] 134	131
4.1.4 Synthesis of [ANP]- <i>hexa</i> PEG-propyne-[HI-236] 135	132
4.2 Biological results and rationale.....	134
CHAPTER 5: EXPERIMENTAL SECTION	137
REFFERANCES	199

University of Cape Town

CHAPTER 1: INTRODUCTION

1.1 HUMAN IMMUNODEFICIENCY VIRUS (HIV)

The Human Immunodeficiency Virus (HIV) is an intracellular parasite, belonging to a class of viruses called retroviruses (viral family *Retroviridae*), and is the causative agent of Acquired Immunodeficiency Syndrome (AIDS). Retroviruses are ribonucleic acid (RNA) viruses, and in order to replicate they must make a deoxyribonucleic acid (DNA) copy of their RNA. It is DNA genes that allow the virus to replicate. HIV exists as two distinct viruses: type-1 (HIV-1) and type-2 (HIV-2), which both have a similar molecular structure in that they contain a single-stranded RNA genome but which differ in origin and gene sequence. The difference between them is that HIV-1 carries a *vpu* gene whereas HIV-2 carries the *vpx* gene, and HIV-2 is more geographically restricted to West Africa compared to HIV-1. HIV-2 also tends to have slower rates of disease progression to AIDS than HIV-1, although when this occurs the symptoms are almost indistinguishable between the two types.^{1,2}

1.2 THE STRUCTURE OF THE HIV-1 VIRION

The HIV-1 structure involves outer and inner cores. The outer core consists of a lipid bilayer acquired from the host cell, while the inner core contains two proteins, p24 and p17, as matrix proteins surrounding the nucleocapsid containing the genetic material. A single virion has an icosahedral shape with a knobby-looking envelope. The knobs are comprised of the envelope glycoproteins gp-120 and gp-41.^{3,4} Beneath the envelope are the viral matrix proteins p17 and p24, which, aside from structural maintenance, houses the nucleocapsid containing the viral genome for transmission to the host nucleus. The HIV genome transcribes nine genes: *gag*, *pol*, *env*, *tat*, *rev*, *nef*, *vif*, *vpu* and *vpr*, which carry all the information needed to make new viruses (Fig. 1.1).^{5a} Copies of reverse transcriptase (RT), integrase (IN) and protease (PR) necessary for replication purposes are also housed together with the HIV viral RNA.

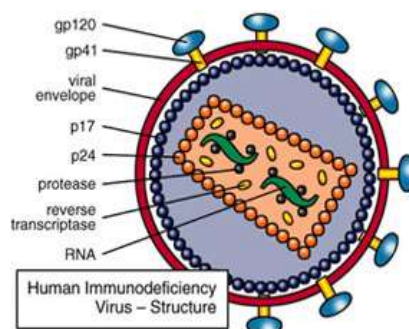


Figure 1.1 Structure of an HIV-1 virion.^{5b}

1.3 EPIDEMIOLOGY OF HIV/AIDS

According to statistics released by UNAIDS and WHO for July 2008, everyday, over 6800 people become infected with HIV and over 5700 people die from AIDS. The estimated number of people having died from HIV/AIDS-related illnesses is around 2.1 million per annum for 2007. The annual number of new HIV infections (for 2008) stands at around 2.5 million, while the total number of people estimated to be living with HIV/AIDS is approximately 33.2 million [30.6-36.1 million]. Sub-Saharan Africa presents itself as the region most heavily affected by HIV with 22.0 million people living with HIV (Fig. 1.2), accounting for 67% of all people living with HIV and 75% of global AIDS deaths. Of these an estimated 5.7 million of these people live in South Africa.⁶

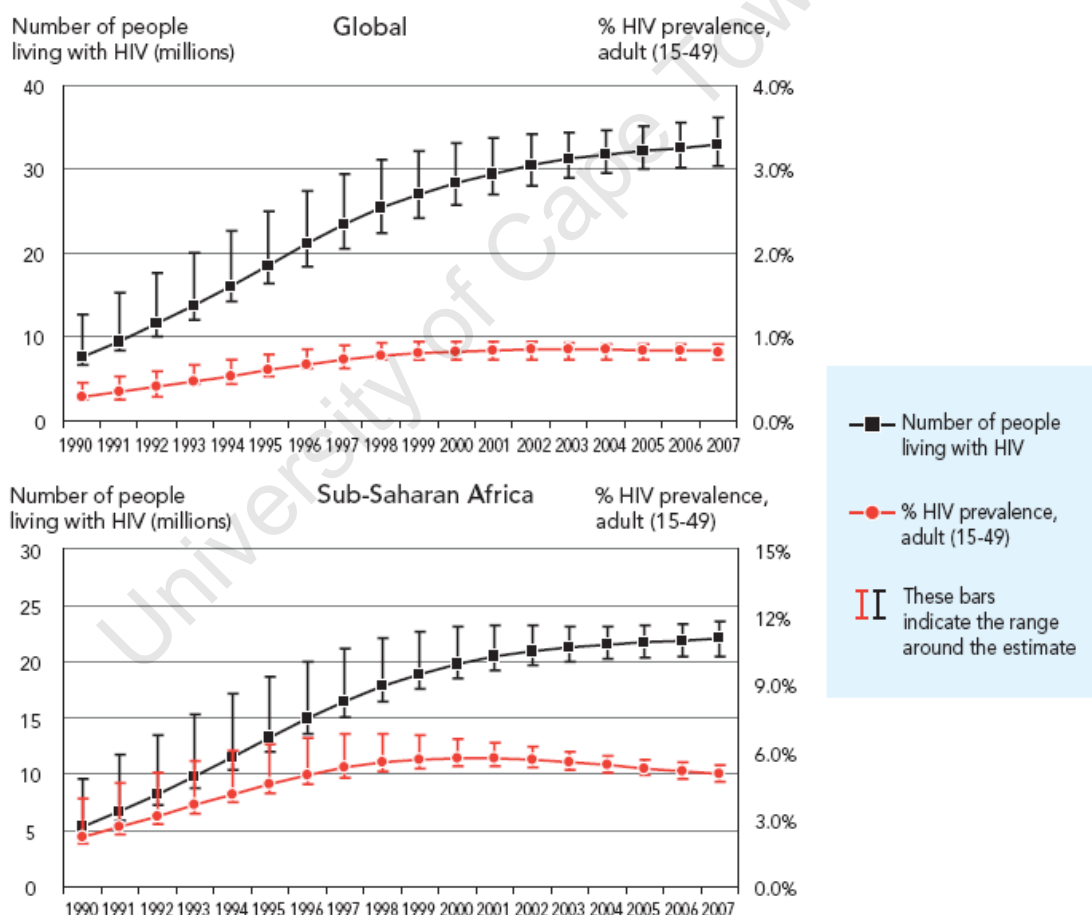


Figure 1.2 Estimated number of people living with HIV and adult HIV prevalence. Global HIV epidemic, 1990-2007, and HIV epidemic in Sub-Saharan Africa, 1990-2007 (2008 report on the global AIDS Epidemic).⁶

1.4 THE HIV LIFE-CYCLE

Like all viruses, HIV-1 needs a host-cell to proliferate itself, which it uses for replication, Figure 1.3.

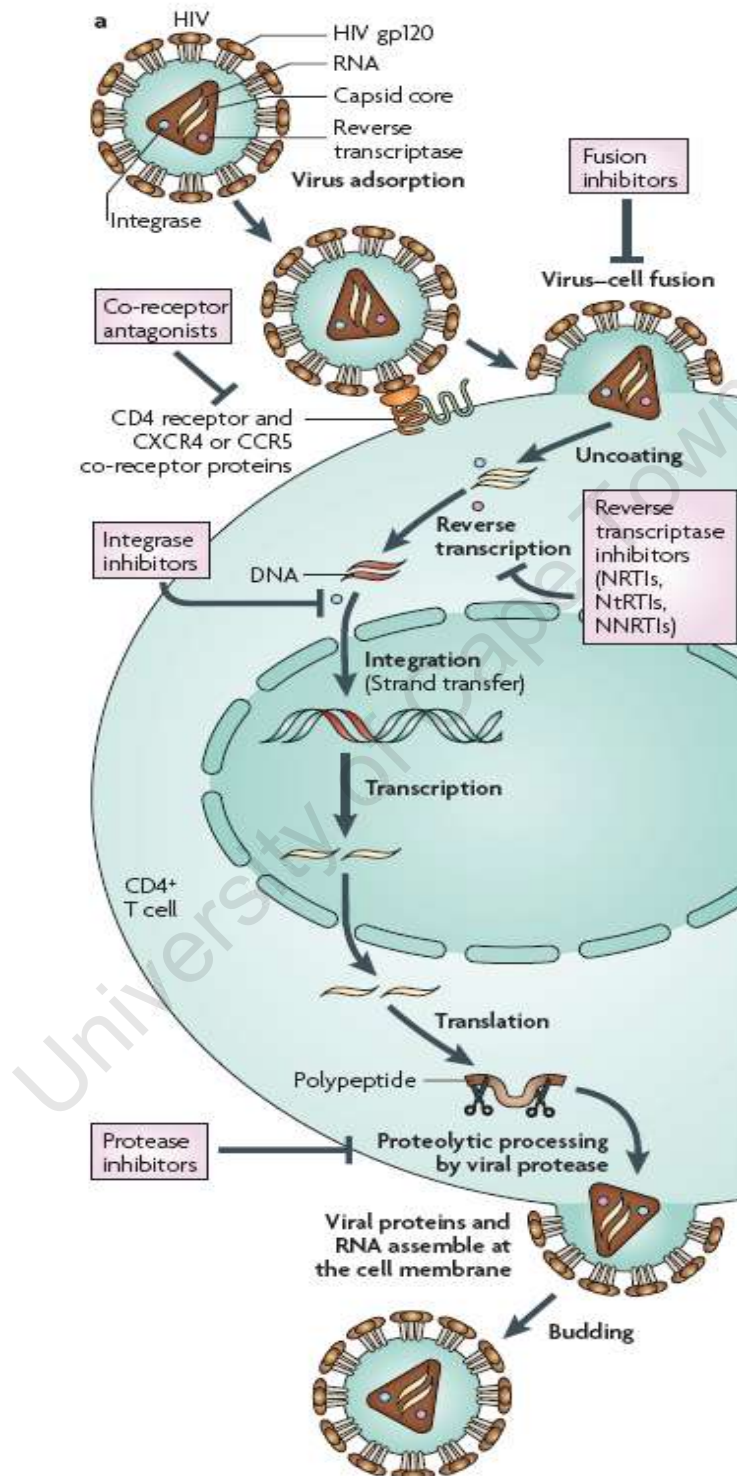


Figure 1.3 The Life-cycle of the HIV-1 virus.⁷

However, what differentiates HIV from other viruses and what makes it so lethal, is that HIV mostly infects cells of the immune system. HIV-1 will only infect a human cell that bears a

CD4 surface marker.⁸ Such cells include macrophages, some dendritic cells, and most importantly, CD4+ T-lymphocytes, also referred to as “T-helper cells”, which play an important role in the body’s immune-defence when foreign entities invade the body. HIV-1 entry into CD4+ cells involves several sequential steps (Fig. 1.4) that involve firstly the interaction of gp-120 with the host CD4 receptor. This gp-120/CD4 complex leads to a loss of entropy (i.e. ordering) in the HIV receptor gp-120, which counteracted by a large enthalpy of formation ($\Delta H < 0$). This interaction leads to conformational changes in gp-120, and to extent CD4, that enable the interaction of gp-120 with the CCR5 or CXCR4 co-receptor. The subsequently formation of a CD4-gp-120-CCR5/CXCR4 complex triggers conformational changes in the gp-41 that eventually allows fusion between the cellular and viral membranes leading the viral core into the cytoplasm.^{9,10,11,12}

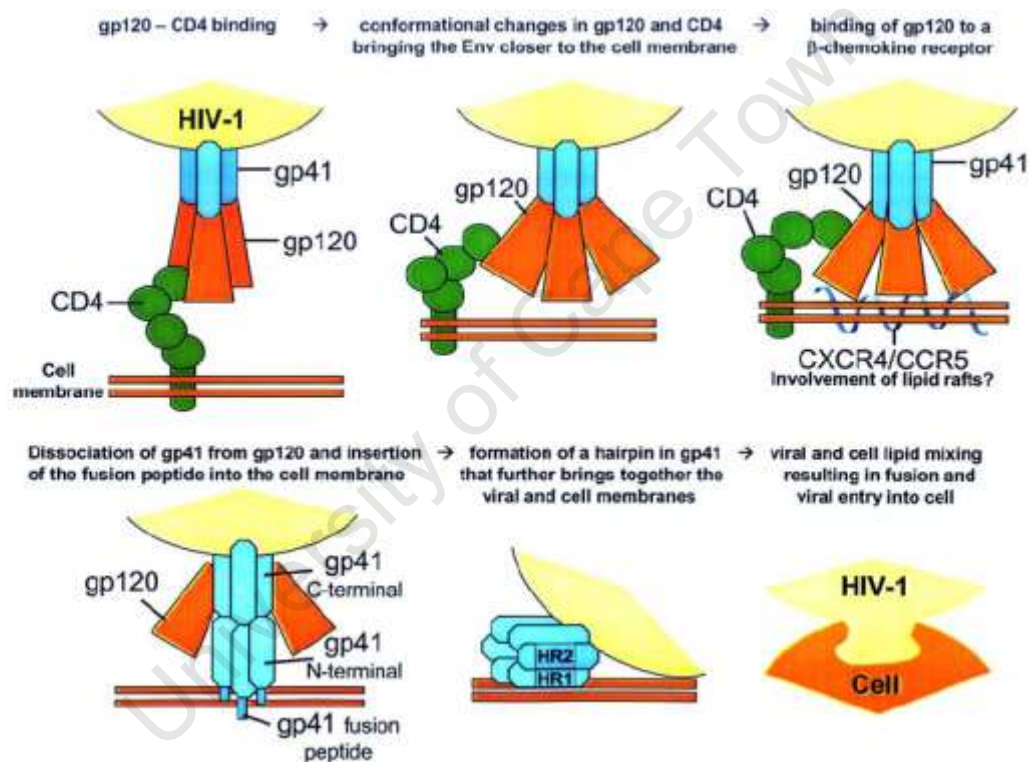


Figure 1.4 HIV-1 attachment and fusion to CD4+ cell.¹²

Viral entry thus involves the following three distinct steps: CD4 binding, chemokine receptor engagement and the structural changes in the viral envelope required for fusion between viral and cellular membranes. HIV-1 entry inhibitors thus encompass three mechanistically distinct classes of agents known as attachment inhibitors (PRO-452, PRO-2000), co-receptor inhibitors such as MaravirocTM (Met-RANTES, T-22, T-134), and the fusion inhibitor FuzeonTM (Enfuvirtide, T-20).¹³ Once the HIV nucleocapsid enters the cell (Fig. 1.3), partial uncoating of the viral core occurs to release the genetic material of the virus into the host cell cytoplasm, where the viral enzyme reverse transcriptase (RT) transforms the ssRNA genome

to a dsDNA form.¹⁴ RT promotes (catalyst) three types of reactions: RNA-directed DNA synthesis, DNA-directed DNA synthesis both of which carried out by the polymerase moiety of RT, and RNA hydrolysis directed by ribonuclease (RNase H). The dsDNA is subsequently transported into the cell nucleus, where another virion-associated enzyme, HIV integrase, catalyses the integration of the viral DNA into the host-cell genome. Importantly though, the viral DNA lies dormant until called upon to transcribe, when transcription of the integrated viral DNA leads to the production of genomic messenger RNA (mRNA) molecules that are transported back to the cell cytoplasm, where translation takes place leading to the production of Gag and Gag-Pol proteins. Immature Gag and fused Gag-Pol precursor are transported to the cell membrane, where viral progeny begin assembling and “budding” from the infected cells. Viral particles released following budding, however, do not contain the characteristic HIV condensed core and are not infectious. Virus infectivity is acquired after particle maturation, which is mediated by the virion-associated HIV aspartyl protease. This enzyme cleaves the immature Gag and Gag-Pol precursors into functional polypeptides.¹⁵

1.5 HIV PATHOGENESIS

AIDS results from selective depletion of CD4+ helper T-lymphocytes.^{16a,b} Progressive CD4 cell depletion has been identified as the fundamental basis of AIDS, but the specific mechanism by which this cell death occurs is still not well understood. It is well accepted that in chronic disease less than 15% of all CD4 cells are infected. The proportional loss of CD4 cells in AIDS far exceeds this prevalence of cell infection, implying that a direct cytopathic effect of the virus cannot be the sole explanation of CD4 cell depletion. In recent years, it has been shown that during acute infection there is massive depletion of CD4 cells in the gastrointestinal associated lymphoid tissue (GALT) and other mucosal tissues. Importantly, CD4 cell depletion in these tissues appears to be significantly greater than that observed in peripheral blood.^{16b}

The function of CD4 cells is to help CD8+ cytotoxic T-lymphocytes to destroy other cells that express foreign antigens and also to enhance antibody production by B-lymphocytes. Thus, CD4 cells represent a key component of the immune system. In a healthy individual, about 1200 CD4 cells circulate per μL blood; when CD4 counts drop below 400 μL , opportunistic infections start to occur.² HIV eventually kills the helper T-cell that are vital for the immune system, and the decline in CD4+ T-cells eventually has a great effect on humoral response functions, specifically the functioning of the B-cells. Helper T-cell depletion inhibits the B-cells from differentiating into plasma cells and memory cells, thus impairing the immune system's ability to fight against foreign antigens that have entered the body.¹⁷ A person with a CD4 level below 200/ μL defines a state of AIDS.

1.6 THE REVERSE TRANSCRIPTASE ENZYME (RT)

HIV reverse transcriptase (RT) is a multifunctional enzyme (Fig. 1.5) responsible for catalytic transformation of single-stranded viral RNA into double-stranded DNA (dsDNA) that in turn gets integrated into host cell chromosomes by integrase.¹⁸ In summary again, HIV-1 RT carries out reverse transcription by the following catalytic activities:

- (i) RNA-dependent DNA polymerization to form an RNA-DNA hybrid.
- (ii) RNase H degradation of the RNA strand from RNA-DNA hybrid.
- (iii) DNA-dependent DNA polymerization to form a dsDNA.

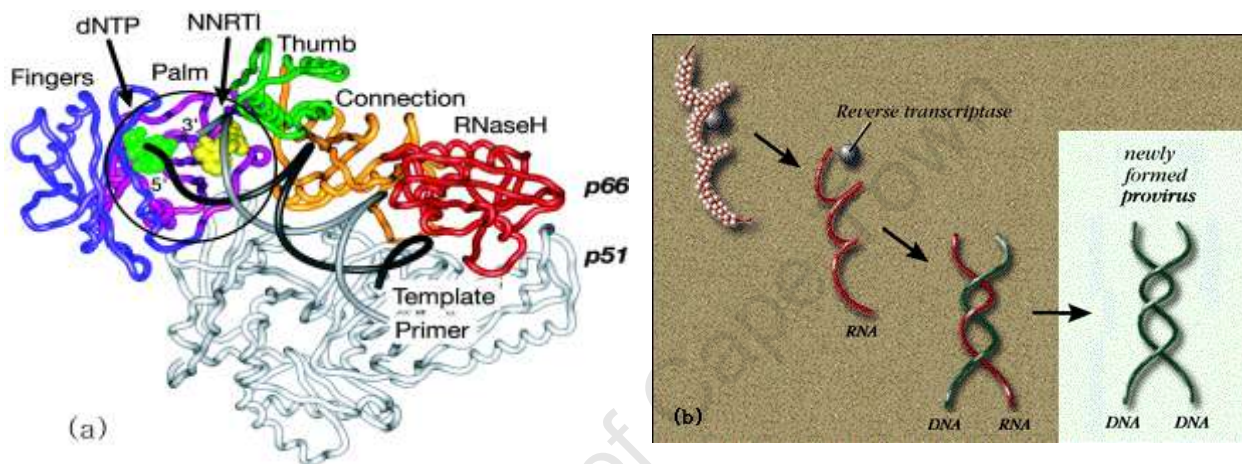


Figure 1.5 (a) Structure of the HIV-1 reverse transcriptase enzyme adapted from Pata *et al.*¹⁹ (b) RNA-directed followed by DNA-directed synthesis.

From a structural point of view, HIV-1 RT is a heterodimer consisting of two subunits: a 66 kDa one and a 51 kDa one (p66 and p51). The p66 subunit contains an N-terminal polymerase domain and a C-terminal RNase H domain. The p51 subunit is derived either from p66 or from a large gag-pol precursor by proteolytic cleavage with HIV-1 protease, and has the same amino acid sequence as the polymerase domain of p66. Crystal structures of RT have revealed the part of the p66 subunit responsible for transcription to resemble a right hand with fingers, palm, thumb, and connection subdomains. The p66 palm contains the polymerase active site that is defined by Asp110, Asp185, and Asp186 residues located in the $\beta 9$ - $\beta 10$ sheet. These amino acids bind the divalent magnesium cations required for catalysis (more details later).^{20,21,22}

The primary function of reverse transcriptase is to build a DNA strand from an RNA template, which is performed at the polymerase active site of the p66 subunit. This process is complex and requires the concerted function of two enzyme active sites in RT (Fig.1.6).

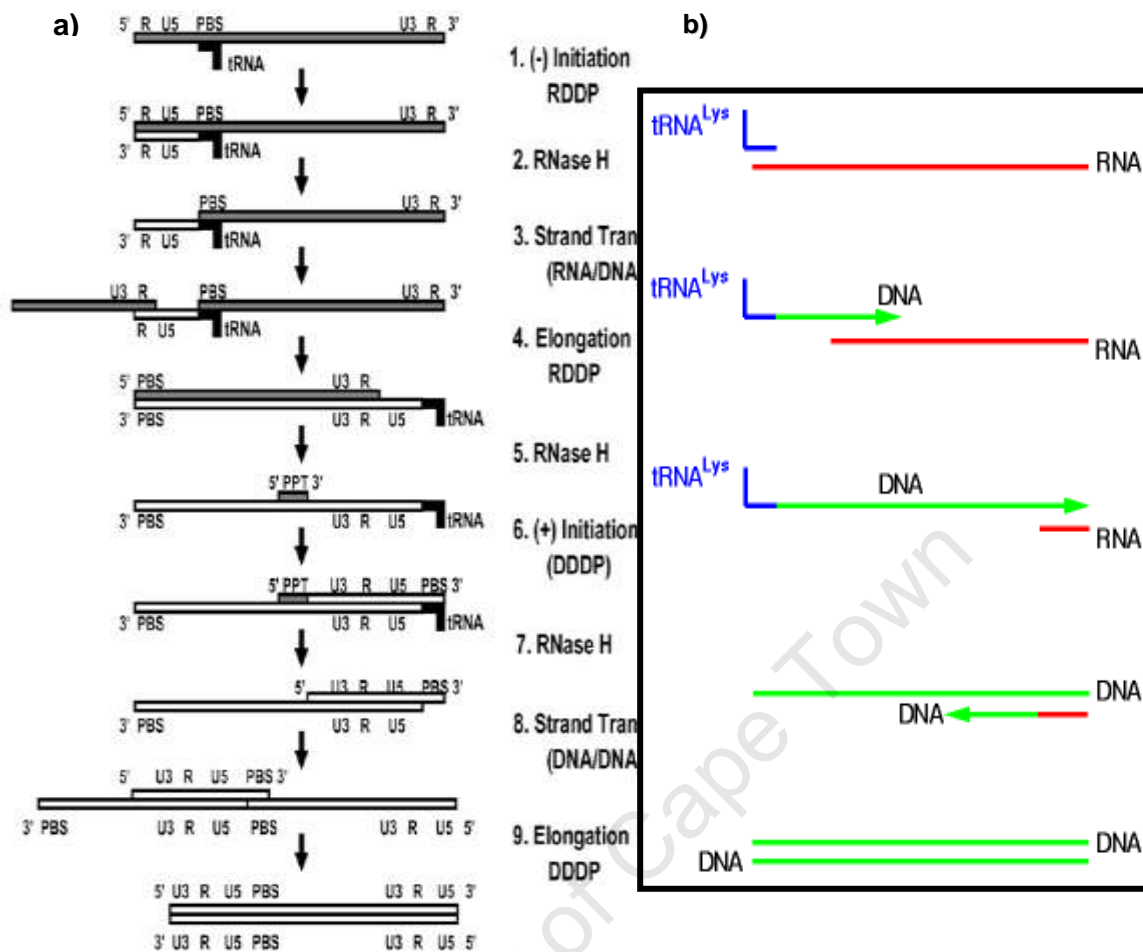


Figure 1.6 a) HIV reverse transcription mediated by the DNA polymerase, RNase H and the transfer activities of the viral RT.²² b) simplification of the transcription process.

Reverse transcription is initiated at the 3'-end of a cellular lysyl-tRNA^{Lys,3}, hybridized to the primer binding site (PBS) of the HIV RNA genome, by the RNA-primed RNA-dependent DNA polymerase activity (RDDP) of the RT. This elongates to produce viral DNA until the 5'-end of the HIV-1 RNA is reached (Fig. 1.6, Step 1). The product formed from this reaction is termed the minus-strand strong-stop DNA. RT ribonuclease H (RNase H) activity then hydrolyzes the HIV genomic RNA (Fig. 1.6, Step 2) to allow the nascent DNA to hybridize with the repeat sequence (R) at the 3'-end of the HIV genomic RNA (Fig. 1.6, Step 3). After this strand transfer, the nascent DNA strand is further elongated by RT DNA-primed RDDP activity (Fig. 1.6, Step 4). RNase H activity is again required to hydrolyze the rest of genome RNA except for the a purine rich sequence, termed the polypurine tract (PPT), which serves as a primer for the initiation of second strand DNA synthesis (Fig. 1.6, Step 5). RNA-primed DNA-dependent DNA polymerase activity (DDDP) then elongates the PPT primer (Fig. 1.6, Step 6). Removal of the PPT and tRNA primers by RT RNase H activity (Fig. 1.6, Step 7) then allows second strand transfer to take place by interaction of the complementary PBS

sequences (Fig. 1.6, Step 8). HIV-1 RT DNA-primed DDDP activity including strand-displacement activity completes the synthesis of the double-strand proviral DNA precursor. The final product of the complete reaction carries U3-R-U5 long terminal repeats (LTR) at both ends (Fig 1.6, Step 9).²²

As a result, the reverse transcriptase enzyme has played a key role in the HIV-1 life-cycle, making it a primary target for development of new anti-HIV drugs used in the treatment of HIV/AIDS.^{14,23}

1.7 DEVELOPMENTS IN ANTI-HIV CHEMOTHERAPY

With the onslaught of drug-resistant mutations, combination therapy comprising of at least three anti-HIV drugs, has become the standard treatment of HIV-infected patients.²³ Drugs used in Highly Active Anti-retroviral Therapy (HAART) fall into one of three categories: (i) nucleoside/nucleotide RT inhibitors (NRTIs) that following two phosphorylation steps (for nucleotides) or three phosphorylation (for the nucleosides) steps act as chain terminators at the substrate binding site (Fig. 1.7) of RT; (ii) non-nucleoside RT inhibitors (NNRTIs) that are able to interact with reverse transcriptase at an allosteric, non-substrate binding site; and (iii) protease inhibitors (PIs) that inhibit the virus-associated protease.²³ Generally, drug combinations involve two NRTI's plus one NNRTI, or two NRTI's plus one PI. Entry inhibitors, Integrase inhibitors and Protease inhibitors will not be dealt with in any further detail.

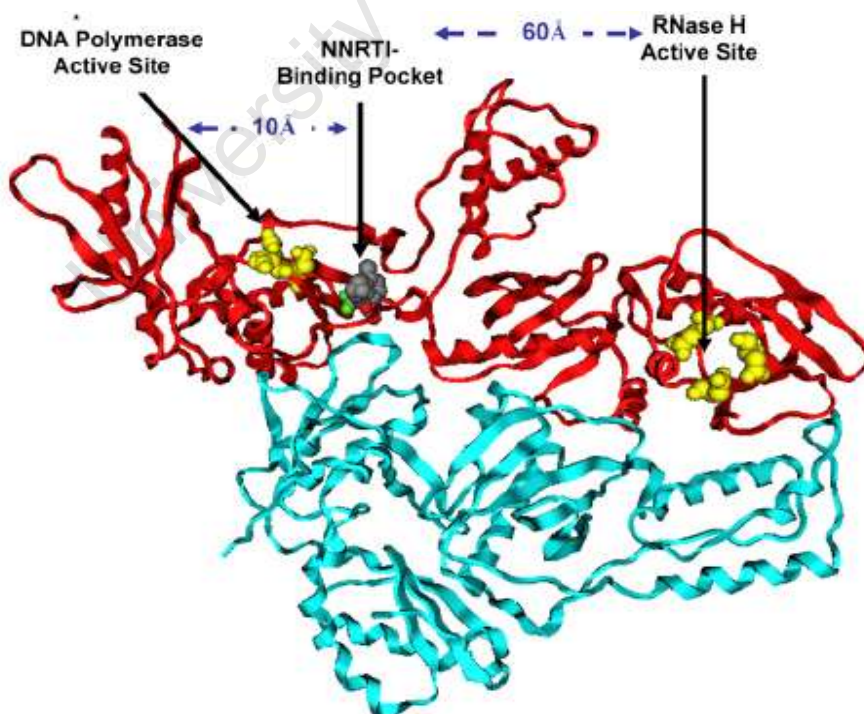


Figure 1.7 Ribbon representation of HIV-1 RT in complex with efavirenz. The p66 and p51 domains of RT is highlighted in red in blue respectively. The DNA active site and the RNase H active site is highlighted with yellow spheres.²²

Recent studies have shown that the combination therapy of NRTIs, NNRTIs and PIs are able to significantly reduce the viral load, increase CD4 count, decrease mortality and delay disease progression.²³ This type of therapy has been shown to work particularly well in AIDS patients with advanced immune suppression.²⁴ In addition, there has been found to be a significant benefit in early aggressive anti-HIV chemotherapy, especially in patients showing no symptoms of the disease (asymptomatic stage).²⁵ HAART is able to partially restore the immune system in patients with advanced HIV infection, but also exacerbates cryptococcal meningitis.²⁶ Thus, HAART has profound repercussions on various AIDS-associated diseases.

Therefore, almost all current HIV-drug candidates, either in preclinical or advanced clinical development, target well-defined steps in the HIV replicative life cycle. These drugs fall into categories associated with the life cycle such as (i) viral adsorption (gp-120) inhibitors; (ii) viral co-receptor antagonists; (iii) viral fusion (gp-41) inhibitors; (iv) nucleocapsid protein (NCp7) Zn finger-targeted agents; (v) HIV integrase inhibitors; (vi) transcription (transactivation) inhibitors and (vii) HIV protease inhibitors.²³

The inhibitors that lie at the core of this project are the *reverse transcriptase inhibitors*.

1.8 NUCLEOSIDE REVERSE TRANSCRIPTASE INHIBITORS (NRTIs)

The substrate (dNTP) binding site of HIV-1 reverse transcriptase is the obvious target for a large variety of NRTI analogues,²³ and the HIV-1 binding site has been targeted for many years now as an efficient way of combatting HIV. In 1987, zidovudine (AZT), a nucleoside RT inhibitor (NRTI), was approved in USA as the first chemotherapeutic agent against HIV/AIDS. However, resistance to anti-HIV compounds develops rapidly, sometimes within a few days of initiating treatment. Errors made by the viral enzyme RT and cellular RNA polymerase II result in about one mutation per viral replication cycle (1 base change in 10 000 RNA nucleotides), which together with the rapid replication of the virus, is responsible for rapid emergence of drug-resistant mutants. This problem led many in pursuit of developing other NRTIs, and over 21 years of research has culminated in seven US Food and Drug Administration (FDA) approved NRTIs. Examples of such NRTIs are zidovudine²⁷ (AZT, 1987), didanosine²⁸ (ddI, 1991), zalcitabine²⁹ (ddC, 1992), stavudine³⁰ (d4T, 1994), lamivudine³¹ (3TC, 1995), abacavir³² (ABC, 1998) and emtricitabine³³ (racemic FTC, 2000) all of which are FDA-clinically approved drugs (Fig. 1.8).

These NRTIs are pro-drugs and need to firstly be phosphorylated by cell-derived kinases to their 5'-triphosphate forms, before they can halt the chain propagation step at the reverse transcriptase level as illustrated in Figure 1.9. The active metabolites then act as competitive

inhibitors (alternative substrates) with respect to the normal substrates (dATP, dGTP, dCTP or dTTP), and lead to the termination of chain elongation.²³

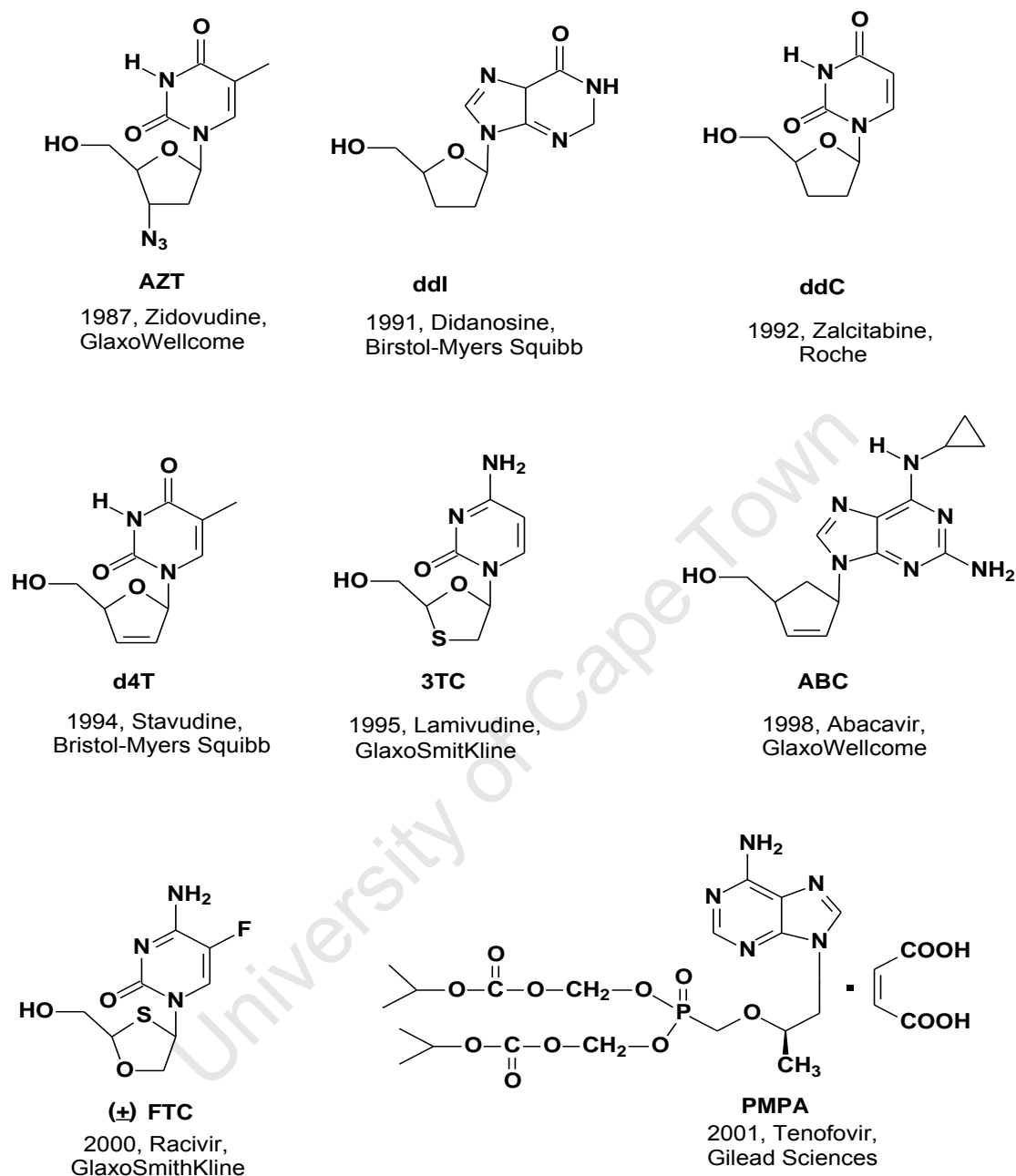


Figure 1.8 Nucleoside reverse transcriptase inhibitors and Tenofovir (PMPA).

D4T shows selective anti-HIV activity comparable to that of AZT *in vitro*. However, d4T is more toxic than AZT,^{34a} and is thought to be the worst culprit for lipodistrophy and other body composition changes associated with antiretroviral therapy. However, there is some evidence that reducing or stopping the drug can slow or halt the changes in body

composition and metabolism. Lowering the dose of d4T has also been shown to help to alleviate peripheral neuropathy, another side effect of the drug. The World Health Organization recommended in 2007 that d4T dosing should be reduced to 30mg twice a day in order to counter toxicity.^{34b}

It has also been shown, though, that under physiological conditions, RT can remove these chain-terminators, thus unblocking the primer terminus with great efficiency and thus restoring DNA synthesis.³⁵

In contrast to the nucleoside analogues, the nucleotide analogues (NtRTIs), e.g. PMPA are mono-phosphorylated pro-drugs in the form of phosphonates, and thus only require a further two phosphorylation steps by cellular kinases in order to be transformed into the active metabolite. NtRTIs can therefore by-pass the nucleoside-kinase reaction, the later well documented to be the rate-determining step en route to the active triphosphate, and which can limit the activity of the dideoxynucleoside analogues.⁷ An included bonus is that the phosphonate, unlike the phosphate, cannot be cleaved by esterases that would normally convert nucleoside monophosphates back to their parent nucleoside.

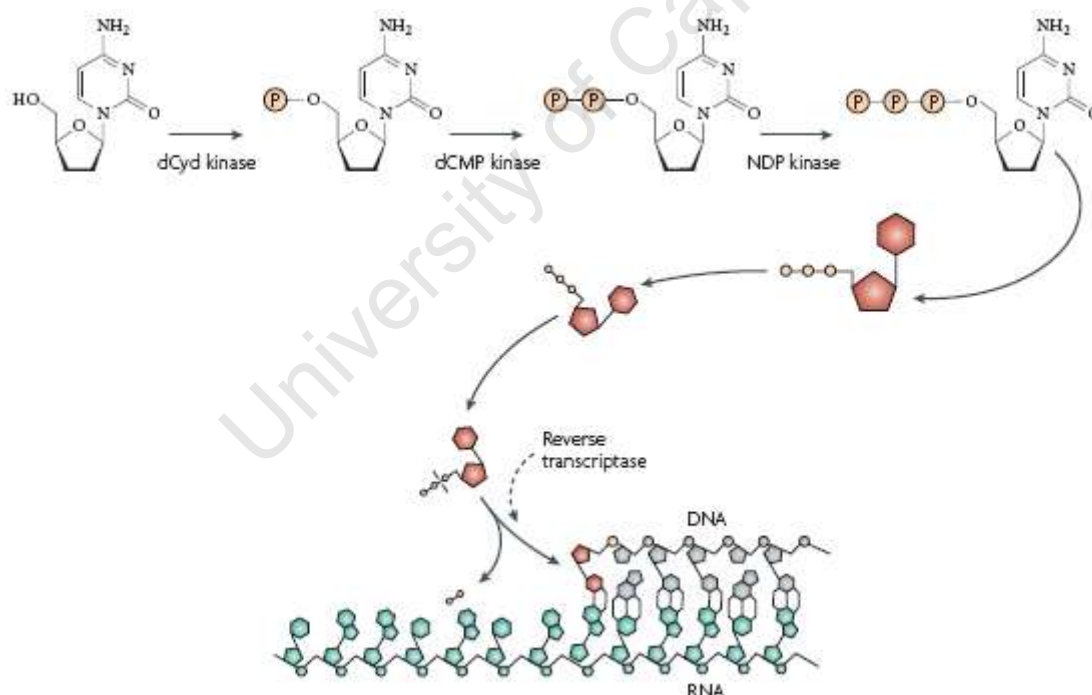


Figure 1.9 Mechanism of anti-HIV action of 2', 3'-dideoxynucleoside analogues- shown for 2,3'-dideoxycytidine.⁷

Tenofovir³⁶, which is FDA clinically approved, has proven to be antivirally active and has showed favourable activity/resistance profiles. It is currently the only approved NtRTI for

treatment in HIV chemotherapy. It is scarcely affected by HIV-1 RT mutations while at the same time retains its full potency as an antiretroviral.

At present, the existing drugs still find it remarkably difficult to comply with the ever-increasing demands of higher activity (potency), lower toxicity (side-effects) and favorable resistance profiles required for anti-HIV drugs. As a result, several new NRTIs are in clinical development.³⁷ Zalcitabine, also known as (±) FTC, is one such inhibitor. Its mechanism of action is precisely the same as that of zidovudine³⁸, in that after successful phosphorylation to the active metabolite, the ddNTP competes with the normal substrates. Upon expulsion of the β , γ -diphosphate, following nucleophilic substitution by the HIV DNA 3'-hydroxyl with an incoming ddNTP, ddNMP is incorporated in the 3'-end of the DNA chain, leading to chain termination since the decoy inhibitor does not possess the necessary 3'-hydroxyl functionality for further elongation (Fig. 1.9). Zalcitabine comprises of a 50:50 racemic mixture of the two enantiomers^{39a} and is thus considered a form of combination therapy. (-) FTC is moderately more potent than (+) FTC. Pharmacokinetic studies carried out by Anderson and co-workers revealed that compared to the (+)-isomer, (-)-FTC is more efficiently taken up into the cell and phosphorylated to its active triphosphate form. Also, by serving as a much poorer substrate of cytidine deaminase than the (+)-isomer, (-)-FTC is not degraded back to its parent nucleoside. FTC has also shown diminished resistance profiles.^{39b} Further successes have come in the form of NtRTI prodrugs.^{40,41,42} Attempts have been made to synthesize 2', 3'-dideoxynucleotide (ddNMP) prodrugs, as well as other forms of prodrugs that are taken up into the cell immediately in the nucleotide form. Successes have been achieved using this approach for a number of NRTIs such as d4T (more later).

1.9 THE STRUCTURE OF HIV-1 RT IN COMPLEX WITH NUCLEOSIDE INHIBITORS

Nucleotide analogues bind at the dNTP-binding site (Fig. 1.10), adjacent to the 3' terminus of the primer strand that is located in the palm subdomain of the p66 subunit.⁴³ The catalytic triad of aspartic acids, (Asp110, Asp185 and Asp186), which are conserved in most polymerases are also located at this site. The nucleotide analogue binding site is composed of both protein and nucleic acid. The nucleic acid part of the binding site is made up of the 3'-primer terminus, which possesses the 3'-OH group that is the site for the covalent attachment of the incoming substrate. The base of the 3'-primer terminal nucleotide also helps to bind incoming substrate *via* base-stacking interactions. The first base in the template overhang contributes base-specific H-bond donor and acceptor groups that guide dNTP selection based on Watson-Crick base pairing rules. Based on modelling experiments, residues

Asp185 and Asp186 of the conserved Tyr-Met-Asp-Asp motif and Asp110 are believed to bind the triphosphate moiety of the incoming dNTP *via* two chelated Mg^{2+} ions (Fig. 1.11).⁴³ Once again, substitution with expulsion of the diphosphate (as described before) leads to incorporation of the resulting dNMP at the 3'-end of DNA chain.

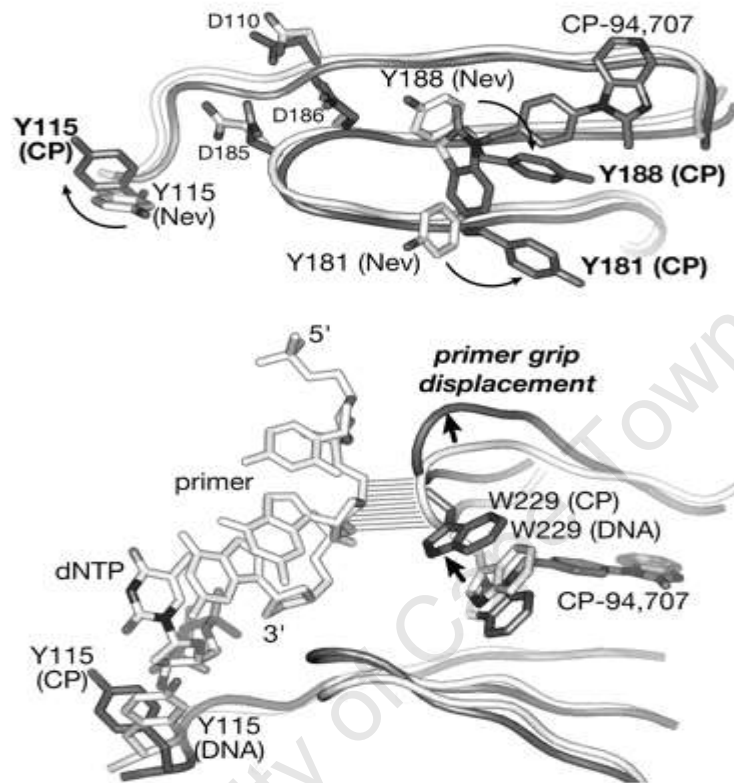


Figure 1.10 Superposition of HIV-1 RT in complex with an inhibitor and in ternary complex with primer template DNA and incoming dNTP. Displacement of TRP-229 and concomitant displacement of the primer grip are indicated with arrows. Nonspecific contacts between the primer grip and the primer strand DNA are indicated with parallel lines.¹⁹

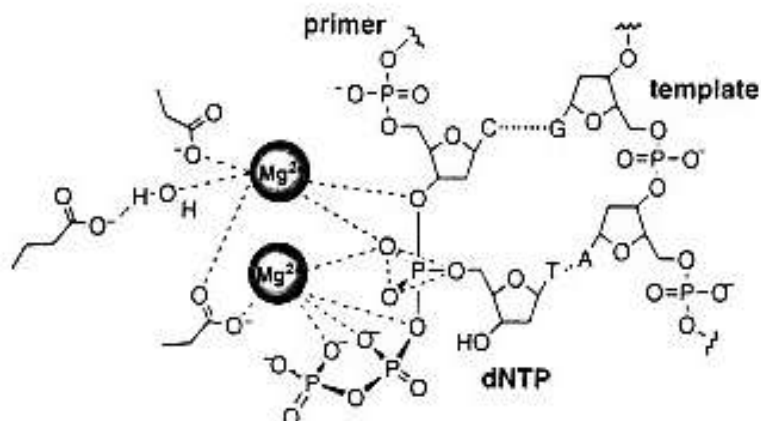


Figure 1.11 Proposed transition state of DNA polymerase-catalyzed nucleotide insertion.⁴⁴

1.10 NUCLEOTIDE REVERSE TRANSCRIPTASE INHIBITORS (NtRTIs)

The ultimate bottleneck in the metabolic pathway leading from 2',3'-dideoxynucleoside (ddN) analogues to their active 5'-triphosphate form is the first phosphorylation step.²³ Unlike adefovir dipivoxil [9-(2-phosphonylmethoxyethyl)adenine (PMEA)] and tenofovir disoproxil [(*R*)-9-(2-phosphonylmethoxypropyl)adenine (PMPA)] (Fig. 1.12) which are already equipped with a phosphonate group and therefore only require two more phosphorylations to be converted to their active metabolites (PMEApp and PMPApp, respectively), nucleoside analogues lack this advantage. (Fig.1.12) depicts various known versions of mono-phosphorylated nucleotide pro-drugs, which will be discussed.

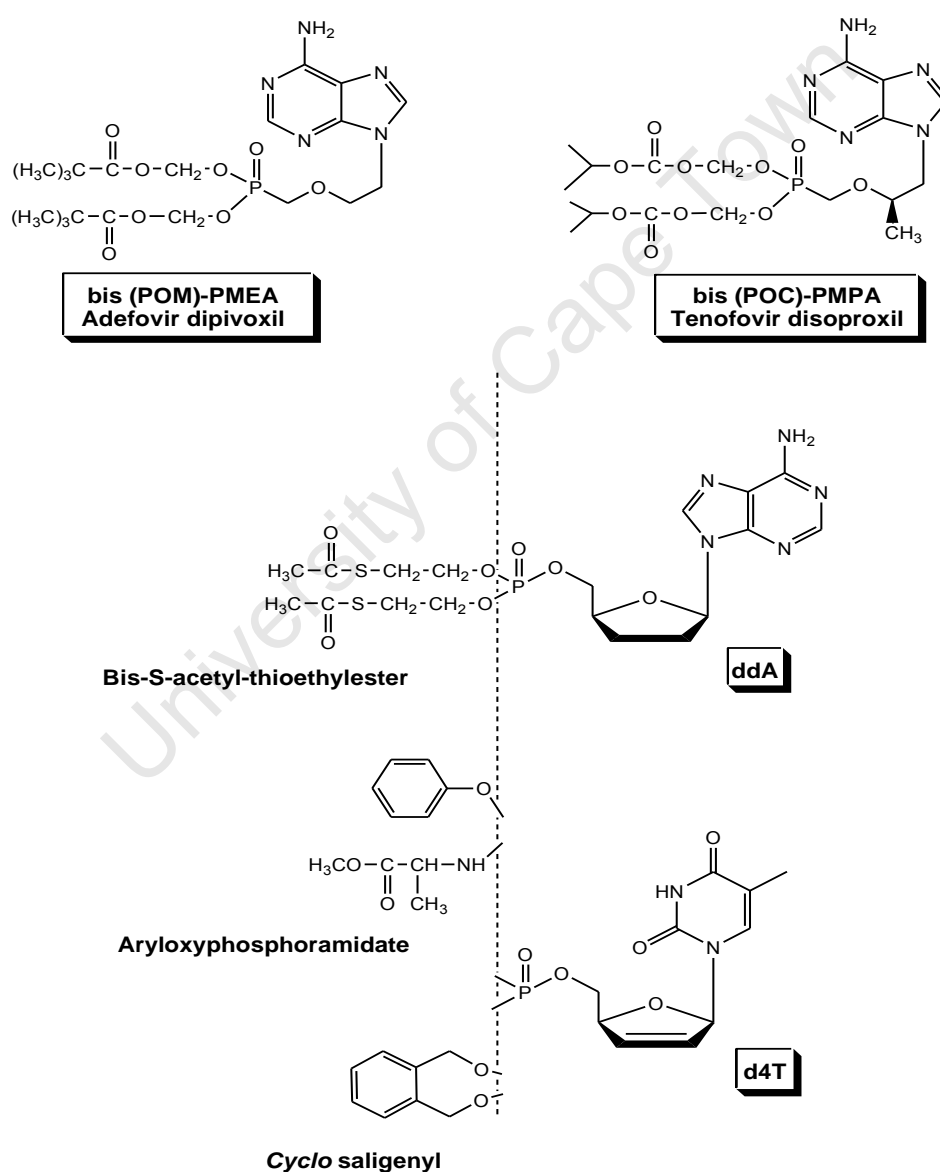


Figure 1.12 Acyclic nucleotides phosphonates: PMEAs and PMPAs in their prodrug forms. Prodrugs of ddNMPs.²³

Many research groups have focused their attention on constructing 2',3'-dideoxynucleotide (ddNMP) prodrugs as esters or amides that once taken up by the cells, deliver the nucleotide (ddNMP) form. This so-called pronucleotide or prodrug approach (discussed in detail later) has proven successful for a number of NRTIs such as 2',3'-dideoxyadenosine (ddA) and d4T (Fig. 1.12). The bis(S-acetyl-2-thioethyl)phosphotriester of ddA [bis(SATE)ddAMP] was synthesized by Imbach and co-workers⁴⁵ and found to be 1000-fold more potent than the parent nucleoside. This increase in potency can be attributed to direct delivery of bis(SATE)ddAMP into the cells, which circumvents adenosine deaminase enzymes rapidly degrading ddA to ddl.⁴⁵

Similarly, McGuigan and co-workers^{46,47,48} have over a number of years synthesized and evaluated the highly potent arylphosphoramidate derivatives of d4T, AZT and ddU as prodrugs (Fig. 1.12). This prodrug comprises a phosphate derivative bearing aryloxy and alaninyl (methyl ester) O- and N-based groups respectively as a phosphoramidate derivatives. Direct intake of aryloxyphosphoramidate derivatives of d4T, d4A and ddA intracellularly (via the alaninyl nucleoside-MP intermediate⁴⁹) have provided anti-HIV activities that are 25- to 625-fold greater than the parent nucleosides.⁵⁰

Similarly, Meier and co-workers^{51,52} having introduced the cyclic saligenyl group (Fig. 1.12), which by-passes the rate-determining, thymidine kinase (in the case of d4T) and adenosine deaminase (in the case of ddA) enzymatic step. *CycloSaligenyl* pronucleotides deliver the monophosphate nucleotides of d4T and ddA exclusively under intracellular conditions of pH.^{53,54} To fully understand how this works, the 'the Prodrug Approach' will now be discussed in detail.

1.10.1 THE PRODRUG APPROACH (The Pronucleotide Approach)

The first introduction of prodrugs to the field of medicinal chemistry is kindly attributed to Albert⁵⁵ in 1951 who wrote: "A prodrug is a molecule which does not have any intrinsic biological activity but which is capable during the different phases of its metabolism to generate a biologically active drug". Furthermore, a potent suitable prodrug should overcome the crucial paradox: to be lipophilic enough to by-pass a membrane or metabolic barrier and to be hydrophilic enough to fulfill solubility, bioavailability or transport criteria.⁵⁶ The systematic enzymatic cleavage of the chemical bond allowing efficient prodrug-to-drug conversion is of particular interest since it depends on the type of cleavable linkage: -carbonate, -ester, -amide, carbamate, -phosphate, -phosphonate, -phosphoramidate, or -amidine.⁵⁶ The enzymatic stability of the resulting prodrug is characterized by its half-life, which can vary from a few minutes to several weeks.

All of the above is schematically depicted in Figure 1.13 for d4T.

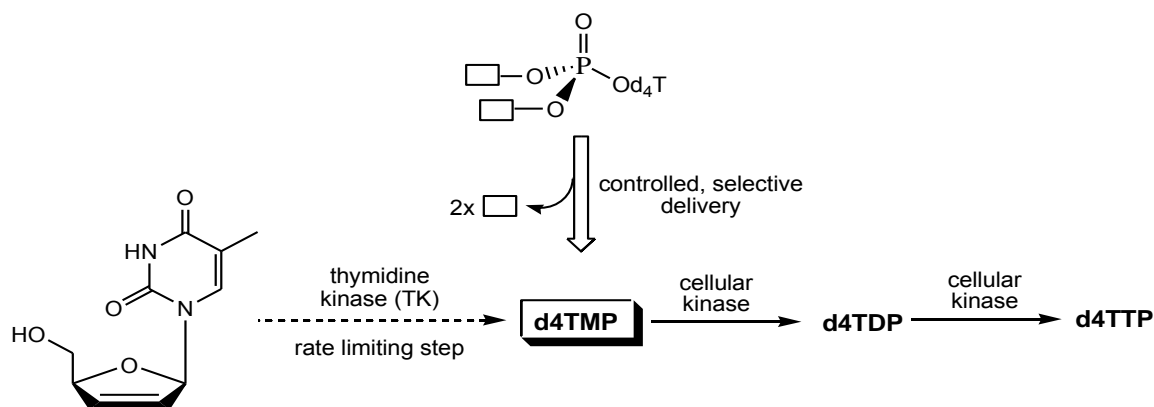


Figure 1.13 Metabolic transformation of d4T into active ddNTPP, after controlled selective delivery, i.e. the prodrug approach.⁵⁷

In contrast to d4T, the fate of the majority of nucleoside analogues has not yet been studied in detail. After being tested, many parent nucleosides are discarded after not displaying any biological activity. Thus, it is likely that such a lack of understanding of the metabolic blockade has prevented the successful development of certain nucleosides into active nucleotide prodrugs.⁵⁷

Nucleotides are very polar molecules that do not easily pass through cellular membranes and are dephosphorylated in the serum by non-specific phosphorylases.⁵⁷ However, this problem can be overcome by masking the phosphate or phosphonate moiety of the nucleotide with degradable lipophilic carrier groups as illustrated in Figure 1.13. This leads to neutral, membrane-permeable nucleotide delivery systems, which is known as the pronucleotide approach. Under physiological conditions nucleotides are charged species (phosphate monoester pK_a values are about 1.6 and *ca.* 6.6). Therefore, as reported by Meier, one requires two masking groups to obtain a neutral lipophilic phosphate triester.⁵⁷ Several methods with corresponding mechanisms for achieving this have been employed. Strategies involving pure chemical hydrolysis of dialkyl, dibenzyl and diphenyl phosphate triesters have proven to be successful in *in vitro* and *in vivo* studies.⁵⁸ However, recent pronucleotide approaches are based on enzymatic or chemical activation of the masking groups. These approaches use carboxyesterase activity and specific pH conditions.^{58,59}

An example of this is the neutral lipophilic phosphotriesters using pivaloyloxymethyl (POM) phosphate-masking groups (Fig. 1.14), which can penetrate into cells *via* passive diffusion.⁶⁰ Cleavage of one of the POM groups by non-specific cellular carboxylate esterases yields the hydroxymethyl analogue which is inherently chemically labile and spontaneously dissociates with elimination of formaldehyde to give the phosphodiester.⁶⁰

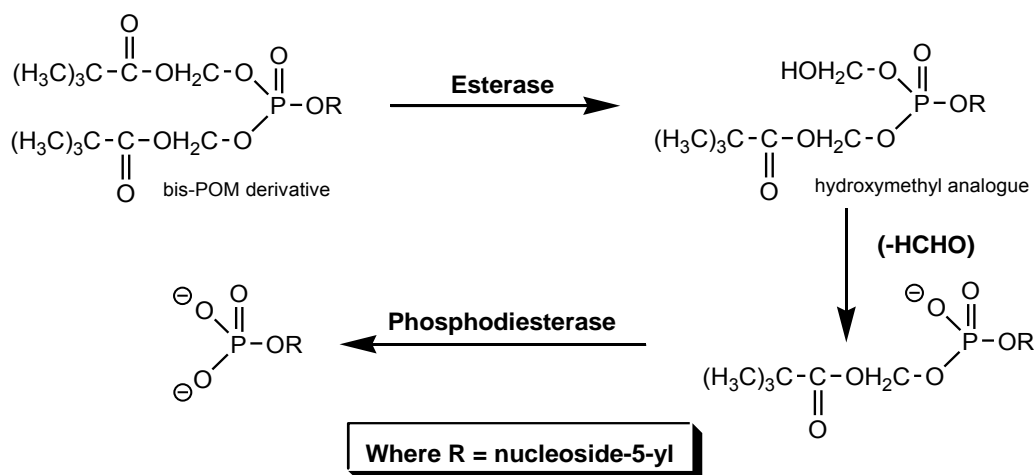


Figure 1.14 Metabolic transformation of d4T into active ddNTPP, after controlled selective delivery, i.e. the prodrug approach.⁶⁰

Cleavage of the second POM group by cellular phosphodiesterases regenerates the desired parent nucleoside 5'-monophosphate. These enzyme-triggered approaches on POC and POM phosphate-masking groups have proven very successful in *in vitro* intracellular delivery systems.⁶⁰

However, thus far, the only successful intracellular pH-driven nucleotide delivery strategy is the *cycloSal* approach.^{61,62} This designed chemically induced coupling, follows a cascade mechanism^{61,62}, and gives as follows (Fig. 1.15): following nucleophilic attack of hydroxide at the phosphorus atom of *cycloSal* triester **1**, the phenolate is displaced preferentially in an $\text{S}_{\text{N}}\text{P}$ reaction, since it is the best leaving group of the three OR groups. This leads to 2-hydroxybenzylphosphate diester **2** via proton transfer. The resulting *ortho* substituent of the benzyl ether is changed from a very weak electron-donating group (phosphate) to a strong electron-donating group (hydroxy). This electronic change activates the remaining masking group and induces a spontaneous rupture of diester **2** to yield the nucleotide and salicyl alcohol **8** (cascade reaction; steps b_1 and b_2). The bond cleavage proceeds after intramolecular proton transfer (intermediate **4**) via zwitterion **5** or 2-quinone methide **6**.⁵⁷

The disfavoured pathway involves cleavage of the benzyl ester bond (step c), in which cation **3** is rapidly trapped by water to yield phenyl phosphate diester **7**. However, no further chemical hydrolysis of the phosphate diester takes place at physiological pH and **7** comes to a dead end. Thus, the pathway via step c does not occur.⁵⁷

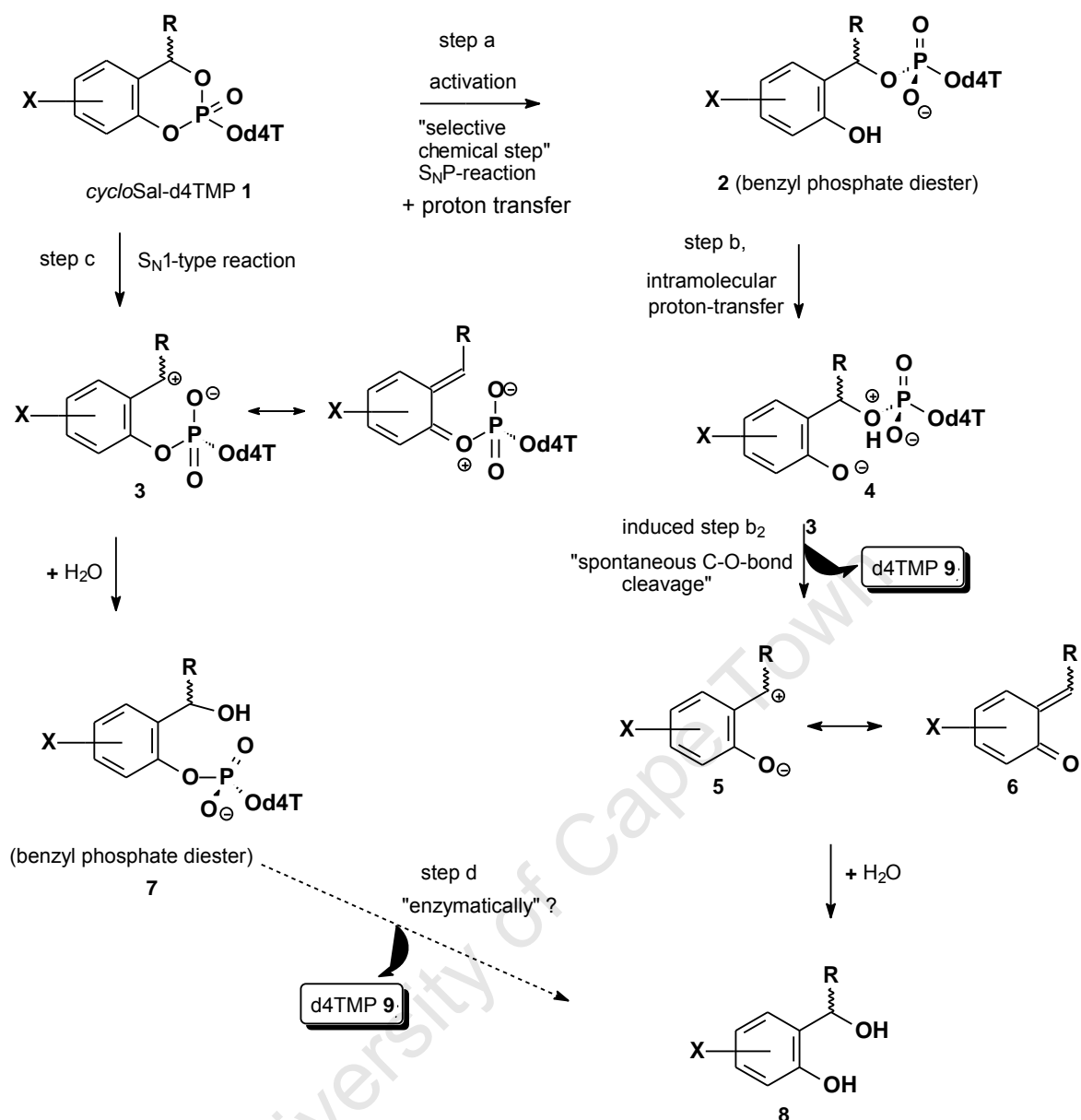


Figure 1.15 Two possible mechanisms for the hydrolysis of *cycloSal*-d4TMP triester 1.^{57a,b}

In summary, the *cycloSal* strategy requires one bifunctional masking group per equivalent nucleotide and is chemically triggered intracellularly at physiological pH to render the desired parent nucleotide-MP.

1.10.2 THE ACYCLIC NUCLEOTIDE PHOSPHONATES (ANPs)

The acyclic nucleotide phosphonates (ANPs) represent a new dimension for the treatment of DNA virus and retrovirus infections.⁶³ These ANPs encompass three compounds that have been formally licensed for the treatment of (i) HCMV (human cytomegalovirus) infections (i.e. HCMV retinitis) in AIDS patients (cidofovir, Vistide®) (Fig. 1.16), (ii) chronic HBV (hepatitis B

virus) infections (adefovir dipivoxil, Hepsera ®), and (iii) HIV (human immunodeficiency virus) infections (AIDS) [tenofovir disoproxil fumarate (TDF), Viread ®].⁴⁰

ANPs have therefore proved to be the cornerstone of anti-viral therapy. The question would therefore be: What is the significance of an acyclic nucleoside 'phosphonate'? In regular nucleotides (or nucleoside phosphates), the phosphate group is attached, to the 5'-oxygen as an ester sugar.

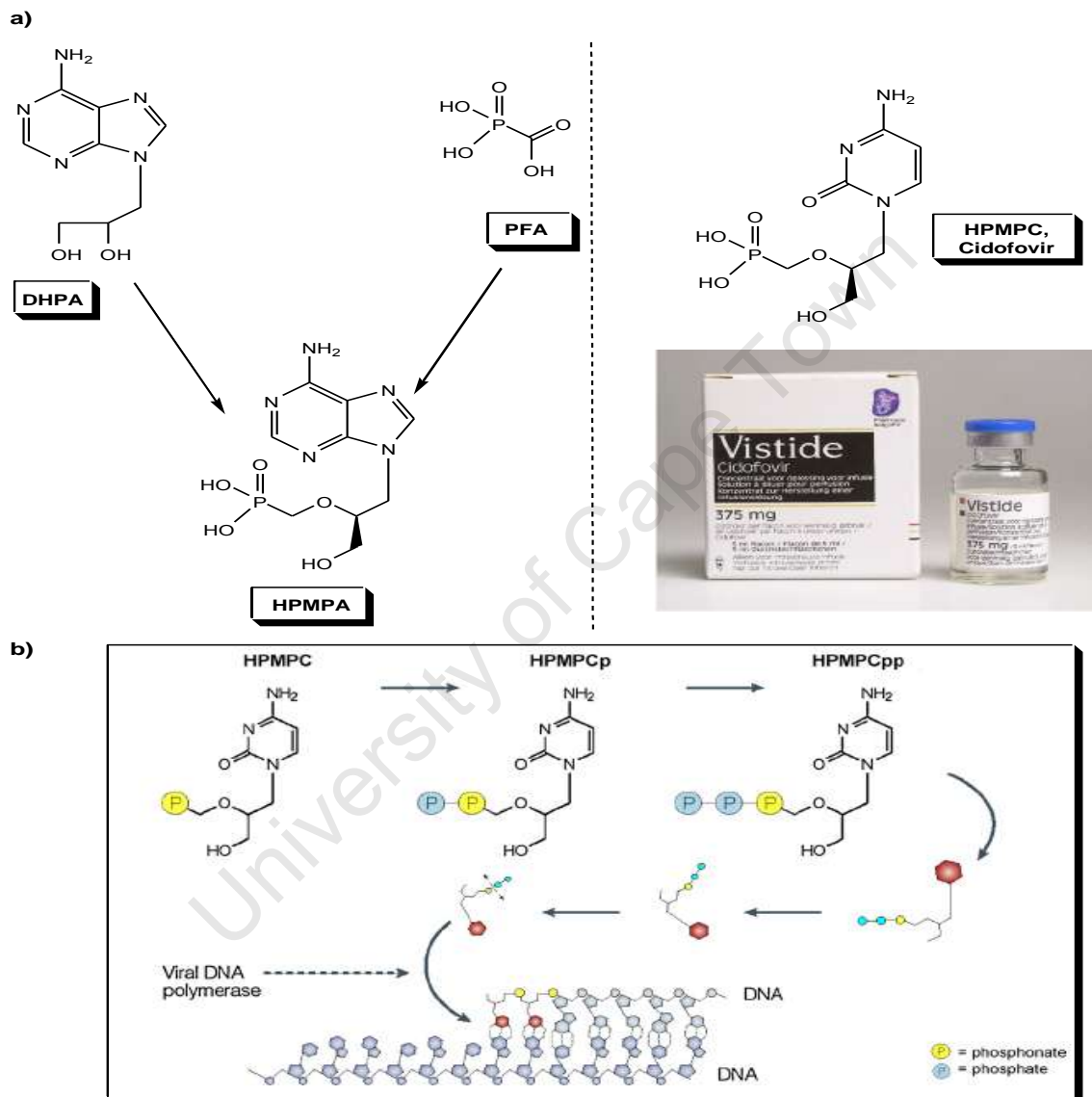


Figure 1.16 a) Broad spectrum of acyclic nucleotide phosphonates (ANPs); b) Mechanism of action of cidofovir.⁴⁰

bound to the nucleoside.⁴⁰ In the ANPs, the phosphate group, is attached to the nucleoside via of a phosphonmethyl ether phosphonate grouping, which, unlike the phosphate ester linkage, should resist any attack from esterases, or any catabolic enzymes at large, by virtue of it having a more P-C bond over a P-O bond.

The concept of ANPs was born in 1986 with the discovery of the ANP prototype, (S)-9-(3-hydroxyl-2-phosphonylmethoxypropyl)adenine (HPMPA) (Fig. 1.16), as a broad spectrum anti-DNA virus agent.⁶⁴ HPMPA itself could be envisaged as a kind of construct resulting from the replacement of the carboxylate group of phosphonoacetic acid [PAA, the predecessor of the antiviral agent phosphonoformic acid (foscarnet, Foscavir ®) by the acyclic nucleoside analogue DHPA [(S)-9-(2,3-dihydroxypropyl)adenine], which was described in 1978 as an acyclic nucleoside analogue with broad spectrum antiviral activity.⁶⁵ Cidofovir, adefovir, tenofovir and several others show high potential as therapeutic agents. According to their activity spectrum, the ANPs can be classified into two categories: (i) the 'HPMP' derivatives, represented by HPMPA (cidofovir), which are active against a broad variety of DNA viruses (polyoma-, papilloma-, adeno-, herpes- and poxvirus, and (ii) the 'PME' and 'PMP' derivatives, represented by PME (adefovir) and PMP (tenofovir) (Fig. 1.12, pg. 14), which are primarily active against hepadna- and retroviruses. Their clinical usages, approved and potential are represented in Table 1.1.

Table 1.1 Clinical applications of acyclic nucleotide phosphonates.⁴⁰

Compound <i>Commercially available</i>	Dosage and route of administration	Approved clinical use	Off-label (potential) clinical use
Cidofovir (Vistide®)	Intravenous (5 mg/kg weekly or two-weekly) Topical (gel/cream) 1%	CMV retinitis in AIDS patients	- Severe polyoma-, papilloma-, adeno-, herpes- and pox-virus infectious - HPV-, HSV-1-, HSV-2-, MCV-, and poxvirus
Adefovir dipivoxil (Hepsera®)	Oral (10 mg daily)	Chronic hepatitis B (HBV infection)	
Tenofovir disoproxil fumarate (TDF) (Viread®)	Oral (300 mg daily)	AIDS (HIV infection)	Chronic hepatitis B (HBV infection)
TDF in fix-dose combinations with emtricitabine (Truvada®)	Oral (300 mg TDF daily) (200 mg emtricitabine daily)	AIDS (HIV infection)	Chronic hepatitis B (HBV infection)
TDF in fix-dose combinations with emtricitabine and efavirenz (Atripla®)	Oral (300 mg TDF daily) (200 mg emtricitabine daily) (600 mg efavirenz daily)	AIDS (HIV infection)	

1.11 NRTI RESISTANCE

HIV-1 RT is very tolerant to non-standard base pairs and modified sugars which has advantages for chemotherapy. However, one drawback are the resultant mutations (no proof-reader), due to misincorporation ranging from 1/1700 to 1/4000 nucleotides. One estimate suggests about 10 base changes in the HIV genome per replication cycle, and the resultant mutant strains can exhibit NRTI resistance. There are two currently known biochemical mechanisms of NRTI drug resistance. The first is mediated mutations in the RT enzyme that allow it to discriminate against NRTIs during DNA synthesis, thereby preventing their addition to the growing DNA chain. The second mechanism “nucleotide excision mechanism” “NEM” involves an increase in nucleotide excision rate in the mutant strain, resulting in continued DNA synthesis.^{66,67} In the second mechanism, the oxygen anion of a nucleoside diphosphate or triphosphate is used as a pyrophosphate nucleophile to attack and cleave the 3'/5'-phosphate bond of the primer, producing an unblocked primer and a dinucleoside tri- or tetraphosphate containing the dideoxynucleoside monophosphate from the primer terminus linked through its phosphate group to the distal phosphate of the free nucleoside di- or triphosphate (Fig. 1.17).⁶⁷

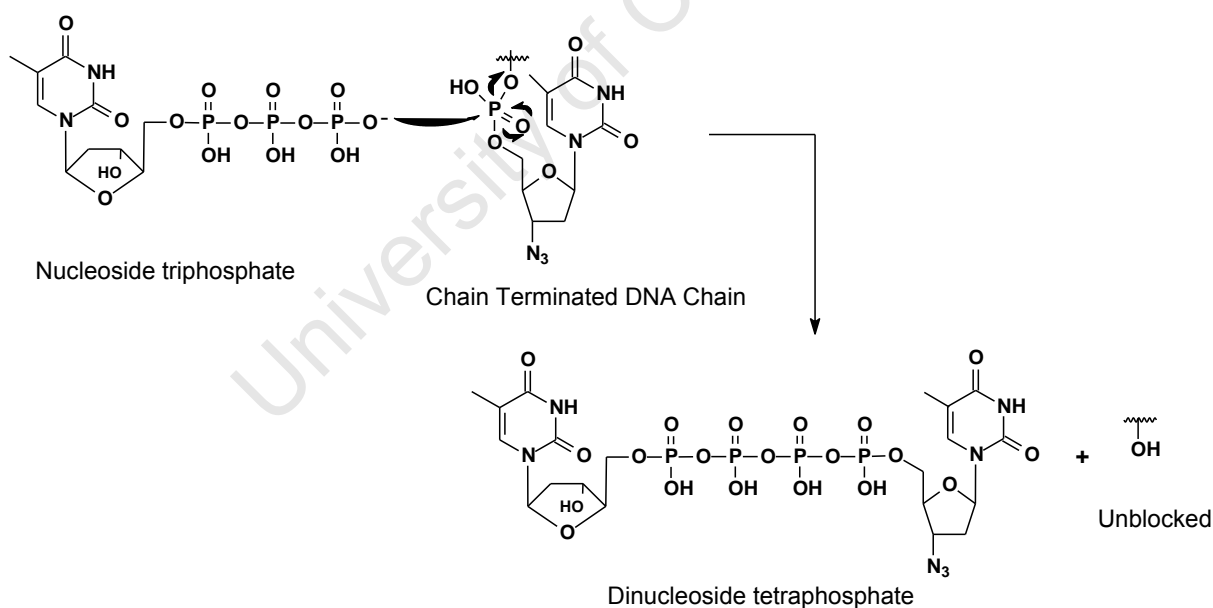


Figure 1.17 Removal of NRTI from the primer terminus through dinucleoside polyphosphate synthesis

Biochemical and modelling studies suggest that incorporation of AZT results in steric strain between the azido group and Asp185 of the mutant, resulting in an enhanced excision rate (Fig. 1.18). This explains why NEMs cause the highest levels of phenotypic resistance to AZT.

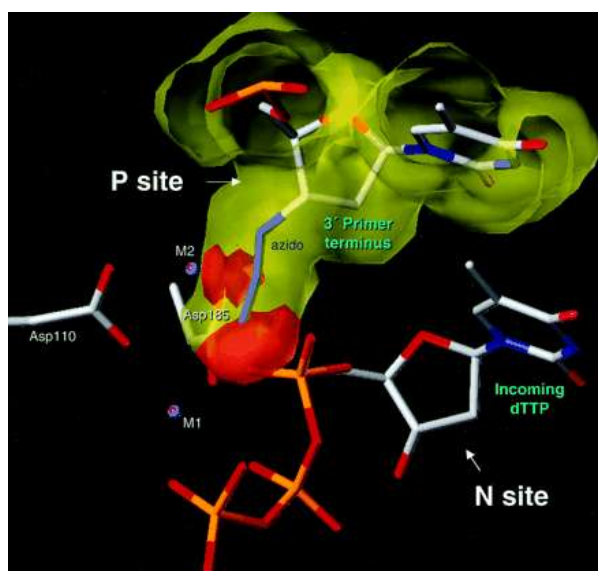


Figure 1.18 Steric hindrance when an AZT-terminated primer is bound to RT at the P site. The figure, based on the structure of the ternary RT-DNA-dNTP complex, shows that the distance between the azido of AZT and D185 (mutant) would cause steric conflict; the distance between D185 and the first and second azido nitrogens is less than the sum of the van der Waals radii.

The M184V mutation causes the high-level of lamivudine resistance observed and emerges rapidly in patients receiving lamivudine monotherapy. This mutation (M184V) and other NRTI resistance mutations interfere with the effects of the NEMs. The mutational antagonism between the NEMs and several of the mutations that act by allowing RT to discriminate against NRTIs explains the clinical synergism observed with dual NRTI combinations such as Zidovudine/Lamivudine, Stavudine/Lamivudine, Zidovudine/didanosine and Stavudine/didanosine.⁶⁶

1.12 NON-NUCLEOSIDE REVERSE TRANSCRIPTASE INHIBITORS (NNRTIs)

More than 30 structurally different classes of NNRTIs (Fig. 1.19) have been synthesized,^{68,69a-c} since the well known TIBO derivatives⁷⁰ were first discovered by the Janssen group in 1987. More than 29 NNRTIs have been approved by the FDA, with the most recent one being Etravirine.^{69b} NNRTIs are a chemically diverse set of compounds, largely specific for HIV-1 RT, although some examples of NNRTI inhibition of HIV-2 RT have reported, including certain members of the PETT series.^{14a,b} And unlike the NRTIs, they do not require intracellular metabolism for activity.

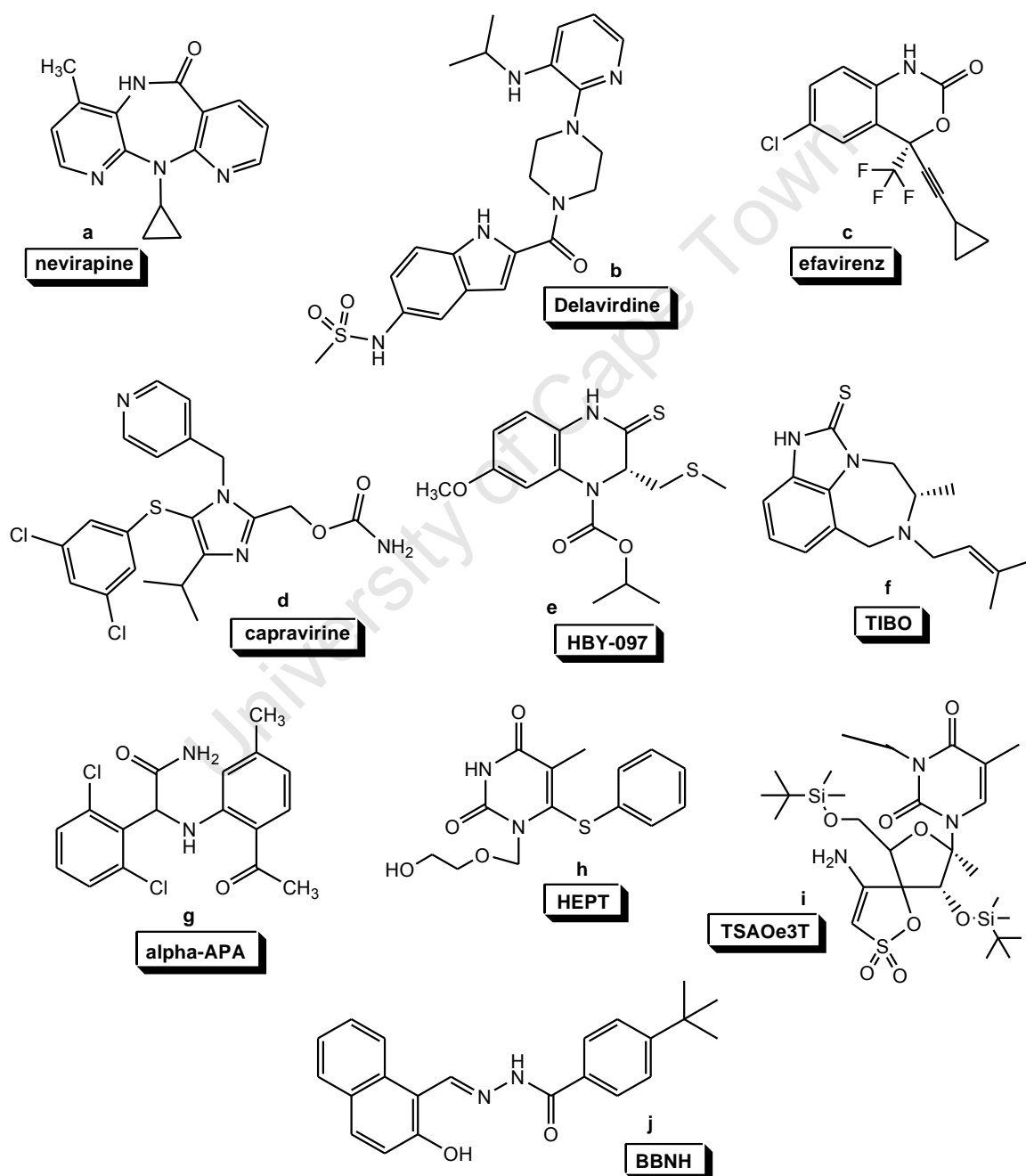


Figure 1.19 Non-nucleoside reverse transcriptase inhibitors.⁶⁹

In general, NNRTIs are a group of small (< 600 Da) hydrophobic compounds with diverse structures, as can be seen in Figure 1.19. They specifically inhibit HIV-1, but not HIV-2 RT, which is unable to form the required pocket for binding.

By far and the chief pioneer for nearly 17 years in NNRTI development is the late Dr. Paul Janssen. Beginning in 1987, Janssen and his co-collaborators (Das, Clark, Arnold, De Corte, De Clercq, Pauwels, Lewi, Kukla and others) engineered the field of non-nucleoside reverse transcriptase inhibition of HIV-1 RT. Figure 1.20 provides crucial insight in the form of a historical synopsis of the developments that ultimately led to the discovery of TMC278.⁷⁰

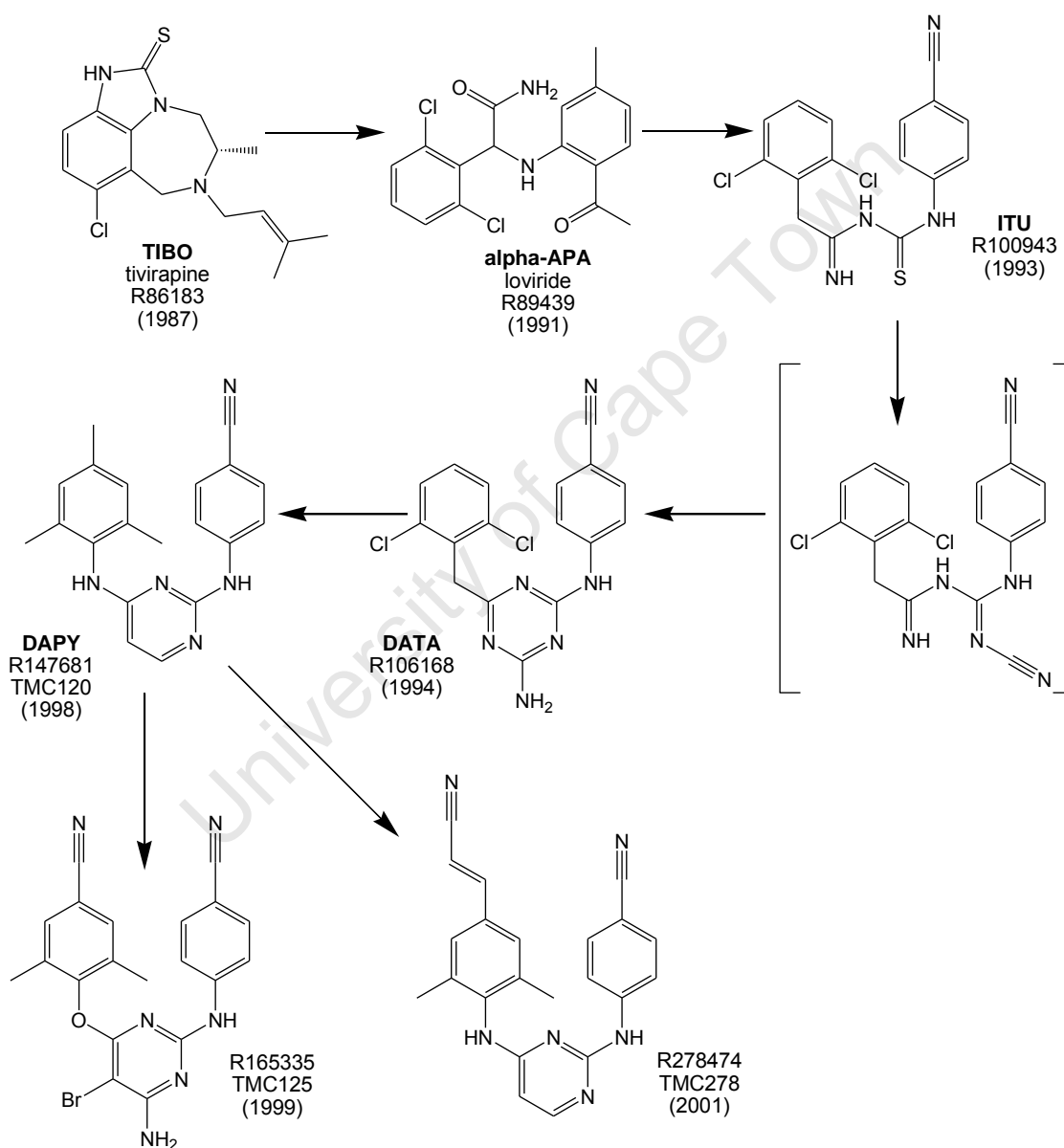


Figure 1.20 Chemical evolution from TIBO to TMC278, starting in 1987.⁷¹

TIBO (*t*etrahydro*i*madazo*b*enzodiazepin*o*ne) analogues were discovered by screening a subset of a Janssen compound library in a cell-based anti-HIV test at the Rega Institute.⁷⁰

Subsequent screening of the Janssen compounds led to the discovery (2nd lead series) of the α -APA (α -*anilinophenylacetamide*) class of NNRTIs.⁷² Further chemical modification led to the class of potent ITU (*iminothiourea*) NNRTIs.⁷³ In an attempt to synthesize the corresponding imino-*N*-cyanoguanidine derivatives of ITU, an unexpected ring closure occurred, producing the first compound of the DATA (*diaryltriazine*) class of NNRTIs.⁷⁴

Molecular modeling studies suggested in 1996 that replacing the central aminotriazine ring of DATA with a pyrimidine ring would lead to greater activity. This was the birth of the DAPY (*diarylpyrimidine*) NNRTIs, of which TMC120 (R147681) is the prototype. TMC120 and TMC125 have subsequently proved to be highly active in reducing viral loads.⁷⁵

Further collaborative work among medicinal chemists, crystallographers, and molecular modelers led in 2001 to the discovery of the cyanovinyl DAPY compounds, of which the *E*-isomer TMC278 (R278474) is the prototype. The potency of TMC278 against wild-type and mutant HIV-1 RTs are compared in Table 1.2 below with those of two other DAPY compounds (TMC120 and TMC125) as well as with three approved NNRTI drugs.⁷⁶

Table 1.2 Potency studies of DAPY compounds and the three approved NNRTIs.⁷⁶

Compound	EC ₅₀ (μ M) {fold resistance} ^{**}					
	Wild-type	K103N	Y181C	K103N/Y181C	L100I	L100I/K103N
TMC278	0.0004	0.0003	0.0001	0.0008	0.0005	0.008
TMC125	0.002	0.001	0.006	0.005	0.003	0.01
TMC120	0.001	0.004	0.008	0.044	0.016	>10
Efavirenz	0.001	0.039	0.002	0.04	0.038	>10
Delavirdine	0.016	>1	>1	>10	>1	N/A
Nevirapine	0.085	>1	>1	>100	0.6	N/A

^{**} EC₅₀ is defined as the concentration of compound required to inhibit syncytia formation in HIV-1 infected cells. The fold resistance is the ratio of mutant/wild type EC₅₀s for each compound. Table 1 is adapted from reference 2.

Table 1.2 reveals how first-generation NNRTIs (Nevirapine and Delavirdine) are effective in inhibiting wild-type HIV-1 RT, but are poor at overcoming single and double point mutations because of their rigidity. Efavirenz, often referred to as a second-generation NNRTI is very good (1 nM range) at inhibiting HIV-1 RT, as well as being capable of inhibiting single point mutations. The flexible third-generation DAPY compounds, especially TMC125 and TMC278, display an outstanding anti-HIV profile for inhibition against all single point mutations as well

as a remarkable 8 nM activity for TMC278 against the double point mutation of L100/K103N. The mechanism by which this works will be discussed later.

1.12.1 THE NNRTI-BINDING POCKET

All NNRTIs bind to a single site on the p66 subunit of the HIV-1 RT p66/p51 heterodimer termed the NNRTI binding pocket (NNRTI-BP) (see Fig. 1.7 again), despite being a heterogeneous class of inhibitors with diverse chemical structures. The NNRTI-BP is situated between the β 6- β 10- β 9 and β 12- β 13- β 14 sheets in the palm subdomain of the p66 subunit. This is also approximately 10Å away from the RT DNA polymerase aspartic acid catalytic triad.²⁰ The NNRTI-BP is predominantly hydrophobic in nature with substantial aromatic character (Y181, Y188, F227, W229 and Y232), but also contains hydrophilic residues (K101, K103, S105, D192, and E224 of the p66 subunit and E138 of the β 7- β 8 loop of the p51 subunit). A likely entrance to the NNRTI-BP is located at the p66/p51 interface, ringed by residues L100, K101, K103, V179, and Y181 (p66 subunit) and E138 (p51 subunit).⁷⁷ In the absence of ligand, the side chains of Y181 and Y188 of p66 point into the hydrophobic core, and thus, the NNRTI-BP does not exist in the free 'apo'-enzyme (Fig. 1.21).^{77,78} NNRTI-binding to HIV-1 RT causes the Y181 and Y188 to rotate away from their positions in the hydrophobic core thereby creating space for ligand accommodation.⁷⁷ Effectively, this equates to an approx. 30° twisting of the β 12- β 13- β 14 sheet, which leads to an expansion of the NNRTI-BP.⁶⁹



Figure 1.21 Close-up of the future binding pocket area in unliganded RT. Amino acid residue 100 (shown in blue) makes contact with residues Y181 and Y188 (shown in red) which undergo major structural rearrangement prior to non-nucleoside inhibitor binding. L100 also makes contact with K101 and K103 (purple) in the uncomplexed state.⁷⁹

In NNRTI-bound RT, the p66 fingers and RNase H domain fluctuate in opposite directions (anti-correlated motions), giving rise to open and close conformations (Fig. 1.22).⁶⁹ The p66 palm and connection serve as a rigid support for the flexible regions. The p66 thumb, on the

other hand, is subject to orthogonal, but cooperative motions, with respect to the p66 fingers and RNase H. Thus, the net effect of NNRTI-binding to RT is to change the direction of domain movements.⁸⁰ To understand this, the mechanism of NNRTI-RT inhibition will be discussed in details.

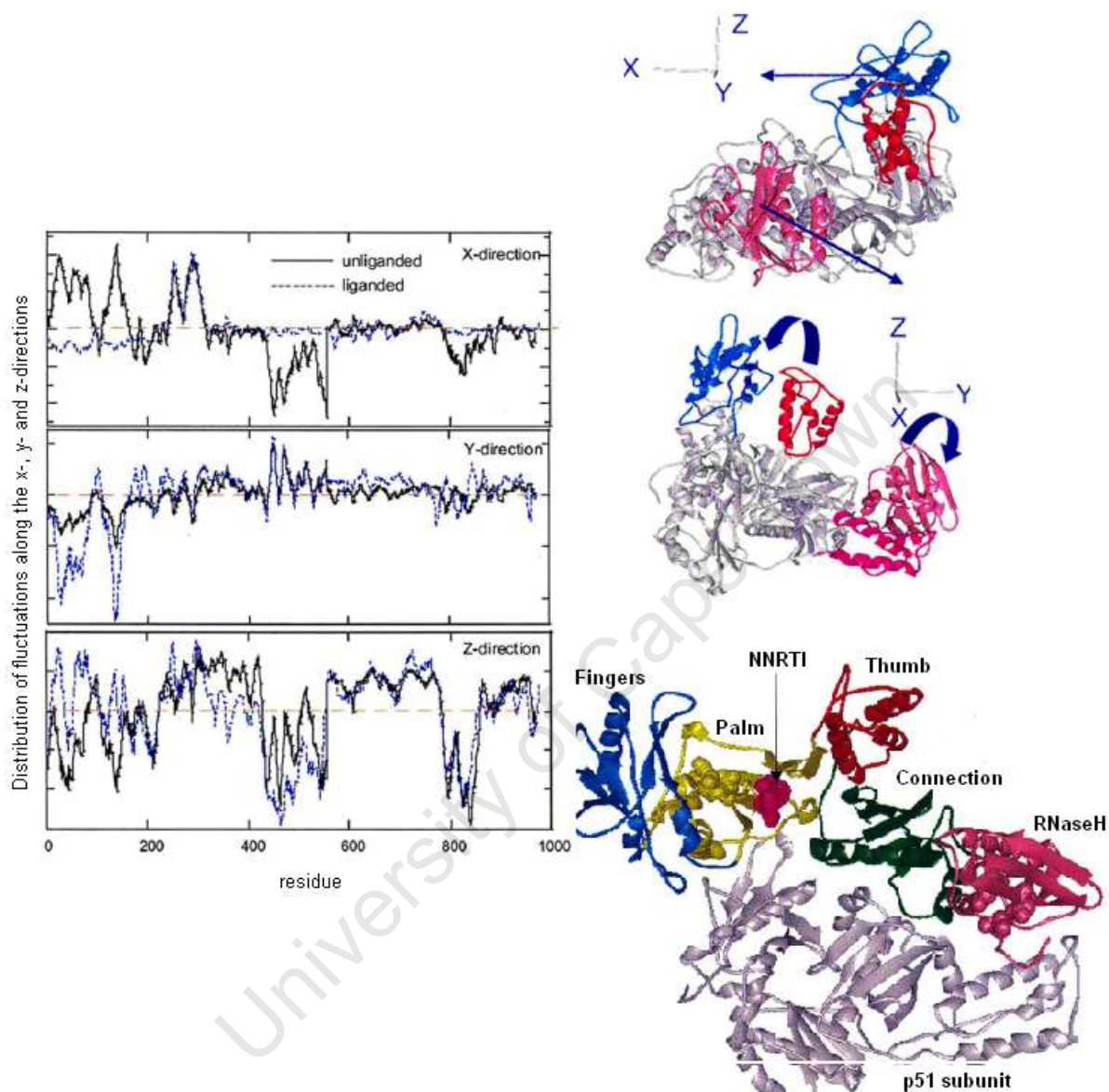


Figure 1.22 Residue fluctuations along the x-, y- and z-directions for unliganded (black line) and nevirapine-bound (blue line) RT. The X axis coincides with the out-of-plane direction; the Y and Z axis lie along the in-plane directions. The ribbon diagrams on the right represent the p66 fingers, thumb, RNase H, and the p51 thumb are coloured blue, red, pink and magenta, respectively.⁶⁹

1.12.2 THE MECHANISM FOR NNRTI INHIBITION OF RT

A number of different mechanisms for NNRTI inhibition of RT have been proposed. 1992, Kohlstaedt and co-workers²⁰ suggested that binding of nevirapine induces so-called 'molecular arthritis' whereby relative domain movements, similar to Figure 1.22 above, though to be necessary for the catalytic cycle of the enzyme, are inhibited.²⁰ Crystal

structures of RT with bound NNRTIs generally have the p66 thumb subdomain in an extended position. For unliganded RT, the thumb subdomain can either be folded down into the DNA-RNA binding cleft⁸¹ or can adopt a more extended position.⁸² Examination of various crystal forms of RT with different NNRTIs bound showed significant variations in relative domain positioning.⁸³ Thus, there is no clear evidence that NNRTI binding induces a single positioning of the p66 thumb subdomain. Comparing the NNRTI bound and free forms of RT indicated a significant and consistent movement of the strands β 2- β 3 containing the critical Asp110, Asp185 and Asp186 active site triad,⁸¹ which ultimately explains the inhibition of RT by the NNRTIs (Fig. 1.23).

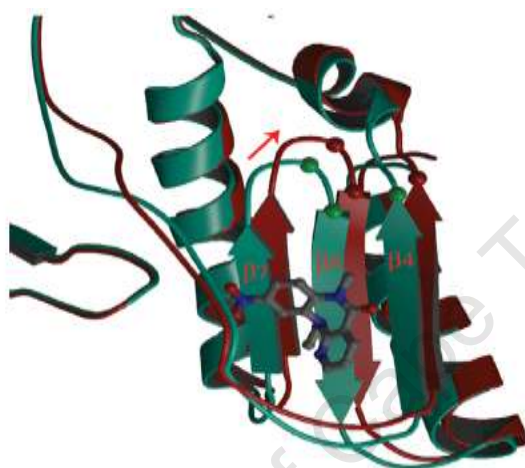


Figure 1.23 Diagram comparing the NNRTI site and polymerase active site in RT for the apo enzyme (in green) and for the inhibitor-bound form (I051U91, shown in grey as ball and stick representation) in brown. The three key aspartic acid residues in the polymerase active site (110, 85 and 186) are shown as small spheres which mark their $C\alpha$ atoms. The three-stranded β -sheet (strands β 4, β 7 and β 8) moves as a rigid body on binding an NNRTI, thereby causing inhibition of the enzyme. The direction of movement is indicated by the arrow; the $C\alpha$ atom of Asp186 is displaced by 1.9 Å.^{82,84}

Parallel rapid reaction kinetic experiments showed that the rate limiting step inhibiting was the chemical bond formation, in line with the proposed structural mechanism.⁸⁵ An alternative to the active site displacement mechanism was proposed by Das and co-worker in 2007, in which the NNRTI distorts the catalytic triad position into a conformation incompatible with the binding of divalent cations Mn^{2+}/Mg^{2+} .⁸⁶ This idea was built on the back of an RT crystal structure determined in the absence of NNRTI and with ATP bound but in a mode significantly different to dNTP binding in the complex.⁸⁸ The loss of the Mn^{2+} or Mg^{2+} counter ion would be expected to significantly weaken the binding of dNTPs, since charge repulsion between the nucleotide phosphate groups and the catalytic aspartates would result. In fact, the opposite is the case as kinetic data shows that the presence of an NNRTI in fact significantly strengthens the binding of the deoxynucleoside triphosphate in the initial collision

complex for the quaternary complex.^{85,88} Additionally, there is a metal-ion dependency of dTTP binding in the complexes with nevirapine/delavirdine or efavirenz present, giving further evidence that the cations remain in place after an NNRTI is bound.⁸⁸ These data hence argue against the proposal of the NNRTI-shifted aspartates being unable to bind divalent cations.

An alternative mechanism of NNRTI inhibition has been described which relates to movement of residues in the region of the primer grip.⁸⁹ This region, containing residue Pro236, is however extremely flexible taking up very variable conformations which are unrelated to NNRTI potency.⁹⁰ Interference of the catalytic step of the polymerase would thus be via an indirect route involving perturbation of the primer position. The effects of NNRTIs on the stability of RT heterodimer formation do not appear to significantly contribute to the mechanism of inhibition of the enzyme.²² The status quo in 2009, on the NNRTI mechanism of RT inhibition is that any of the above mechanisms are acceptable and that the precise mechanism is still not known.

1.12.3 FIRST-AND SECOND-GENERATION NNRTIs: DIFFERENCES IN THE MODE OF BINDING TO HIV-1 RT

NNRTIs can be broadly categorized into first- and third-generation compounds. Efavirenz appears to be the odd one out as a bridging second-generation type. First generation NNRTIs such as nevirapine, delavirdine, TIBO and loviride were mainly discovered by random screening but are associated with rapid development of mutations due to their inherent rigidity. By comparison, third-generation NNRTIs, such as DAPY compounds in view of flexibility and hydrogen bonding ability to K101 were developed with 'rational drug-design' strategies in mind. These strategies include molecular modeling, rational-based drug synthesis and biological and pharmacokinetic evaluations. In general, third-generation NNRTIs tend to be more potent than first generation counterparts and are more active against a broader spectrum of drug-resistant strain of HIV-1.⁹¹

The common pharmacophores^{92,93} that are crucial for tight and specific binding to the RT NNRTI-BP include an aromatic ring capable of π -stacking interactions at the back of the pocket, NH-C=O or NH-C=S groups able to participate in hydrogen-bonding, and a few more hydrocarbon-rich regions for hydrophobic contacts.⁶⁹ The X-ray crystal structure analysis of HIV-1 RT has demonstrated similarities in the geometry of the binding modes both generation types.⁹⁴ Generally, the binding of first-generation NNRTIs in the pocket resembles a 'butterfly' (Fig. 1.24) resting on the β 6- β 10- β 9 sheet.

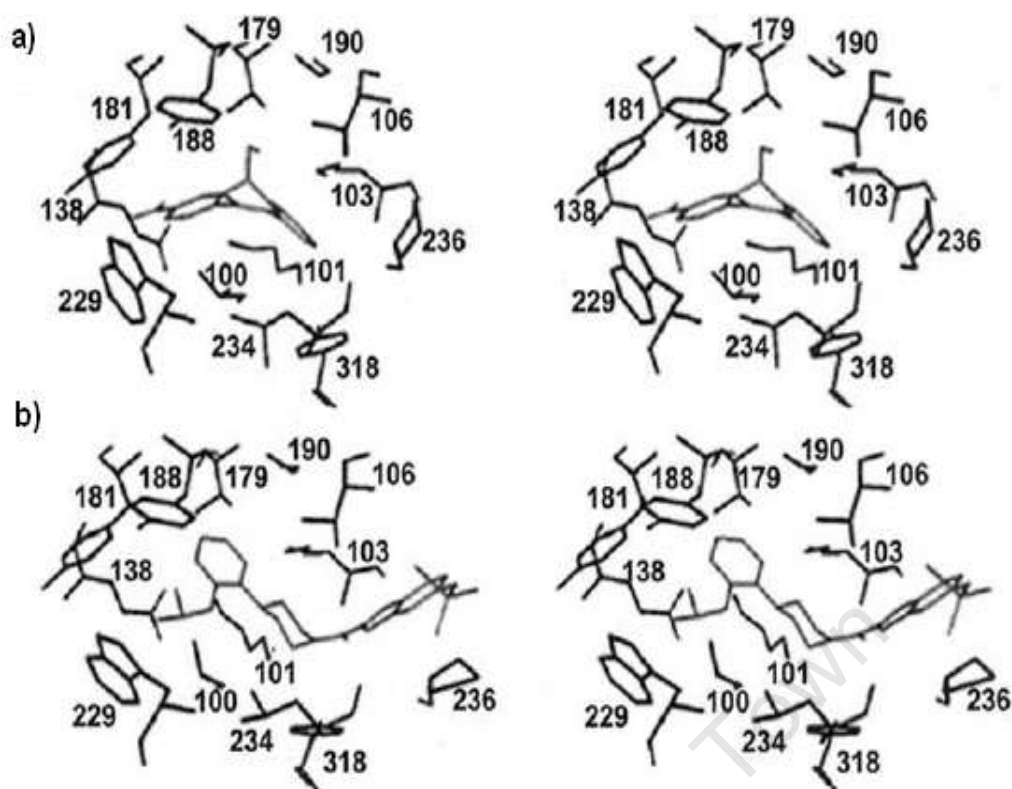


Figure 1.24 Stereoview of a) nevirapine and b) delavirdine in a clear butterfly binding mode in the NNRTI-BP.⁶⁹

This butterfly-like mode is defined by Wing I, Wing II and the body/linker modular segments to which specific pharmacophores bind. The Wing II region is lined with aromatic amino acid residues Y181, Y188 and W229 at the back of the pocket that have favorable π - π interactions. Wing I has fewer hydrophobic interactions compared to Wing II and involves the side chains of K101, K103, V106, V179 and Y318. The body of the 'butterfly' has interactions with the main chain atoms of Y188, Y189 and G190, and with the side chains of V106 and V179. The back of the 'butterfly' is flanked with residues L100 and L234, which interact with both wings.⁶⁹

The crystal structures of second-generation NNRTIs (ITU, DATA and DAPY compounds) bound to HIV-1 RT show a different, unique 'horseshoe' or 'U' mode⁹⁵ compared to the butterfly-like nevirapine above. The torsional flexibility of the DAPY structure permits access to numerous conformational variants, and their compact structure permits repositioning and reorientation (Fig. 1.25) when mutations are present in the NNRTI-BP.^{96,97} The ability of etravirine (TMC125) to bind the RT enzyme in more than one conformationally distinct mode explains the exceptional spectrum of activity observed for this compound (Table 1.2 above).⁹⁶

Depicted in Figure 1.26, the proposed docking of TMC125 and X-ray structure of TMC120, sees the pyrimidine-unit firmly embedded into the Wing I compartment of RT, together with

the less-substituted phenyl ring (attached to C-2 of the pyrimidine) into the hydrophobic Wing II (interacting with Lys101, Tyr188 and Tyr181). However, the more substituted phenyl ring (attached to C-4 of the pyrimidine) clearly exits the hydrophobic pocket and leads off towards Glu188 and the p66 subunit of RT.

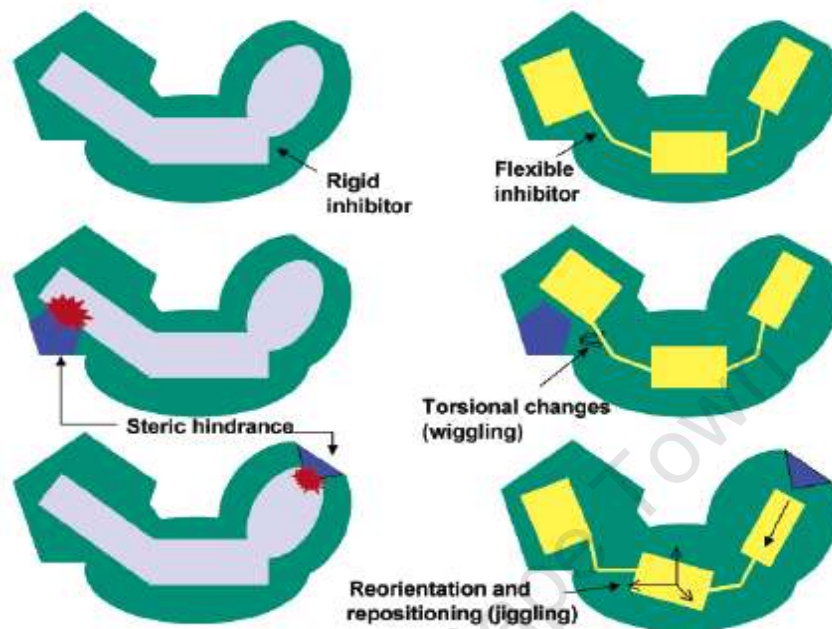


Figure 1.25 Schematic representation depicting how flexibility of an inhibitor can assist in overcoming resistant mutations.⁹⁷

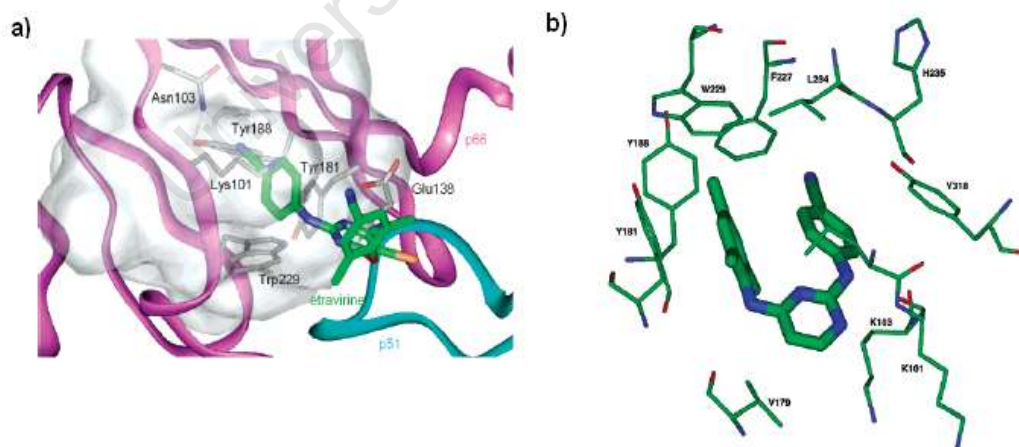


Figure 1.26 a) Proposed docking site for TMC125 at the entrance of NNRTI binding pocket of HIV-1 RT,⁹⁸ b) X-ray crystallographic structure of TMC120 in the NNRTI-BP.⁷²

1.13 PHENETHYLTHIAZOLYTHIOUREAS (PETT) DERIVATIVES

Recent studies including crystallographic analysis and computational modeling have made it possible to develop drugs based on a deeper understanding of the structural features required for anti-HIV activity as well as conformational changes that may help in minimizing the drug resistance. Trogirdine (LY 300046.HCl) represents a second-generation NNRTI developed by Eli Lilly and Medivir in 1995.^{99,100,101} This NNRTI was generated through a multidisciplinary approach involving synthesis, molecular modelling and biological assaying starting from LY 73497, a lead compound prototypic of the PETT series of antiviral agents (Fig. 1.27).⁷²

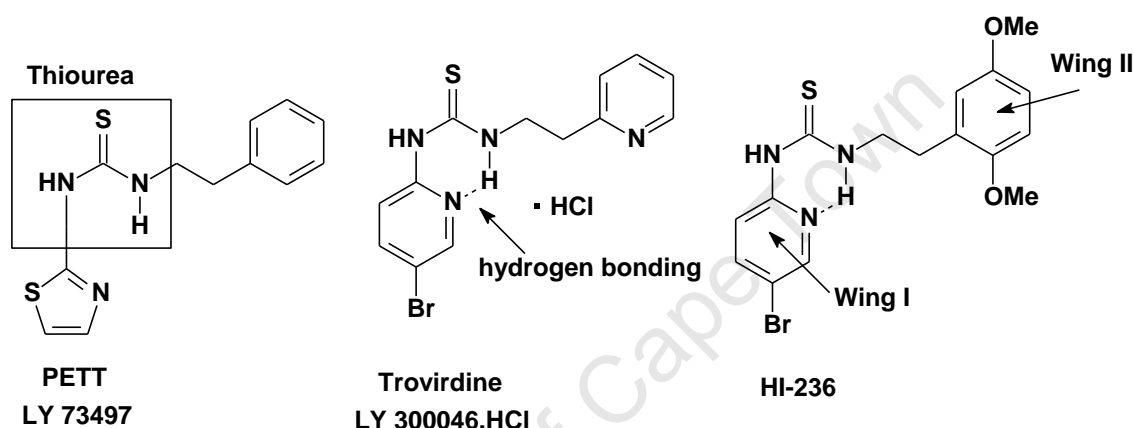


Figure 1.27 Structures of LY 73497 (PETT), Trogirdine and HI-236.

From the structural point of view, PETT NNRTIs have two chemical moieties joined together by a thiourea group. The one end of the compound is either a thiazole ring (PETT) or a 5-bromopyridine ring (Trogirdine) in which the rings are capable of forming an intramolecular hydrogen-bond between the thiourea and the heterocyclic ring.^{102,103,104} The other end of the molecule is a pyridine or phenyl ring separated from the thiocarbonyl group by an ethyl linker (Fig. 1.27).

A comparison of PETT inhibitors, revealed that PETT-1 (Fig. 1.28) inhibits HIV-1 RT with an IC_{50} of 6 nM but showed only weak inhibition of HIV-2, whereas PETT-2 retains similar potency against HIV-1 RT (IC_{50} of 5 nM) and also inhibits HIV-2 RT (IC_{50} of 2.2 μ M). These inhibitors adopt conformations that occupy similar volumes of the space within the drug pocket despite their diverse structures.¹⁰⁵

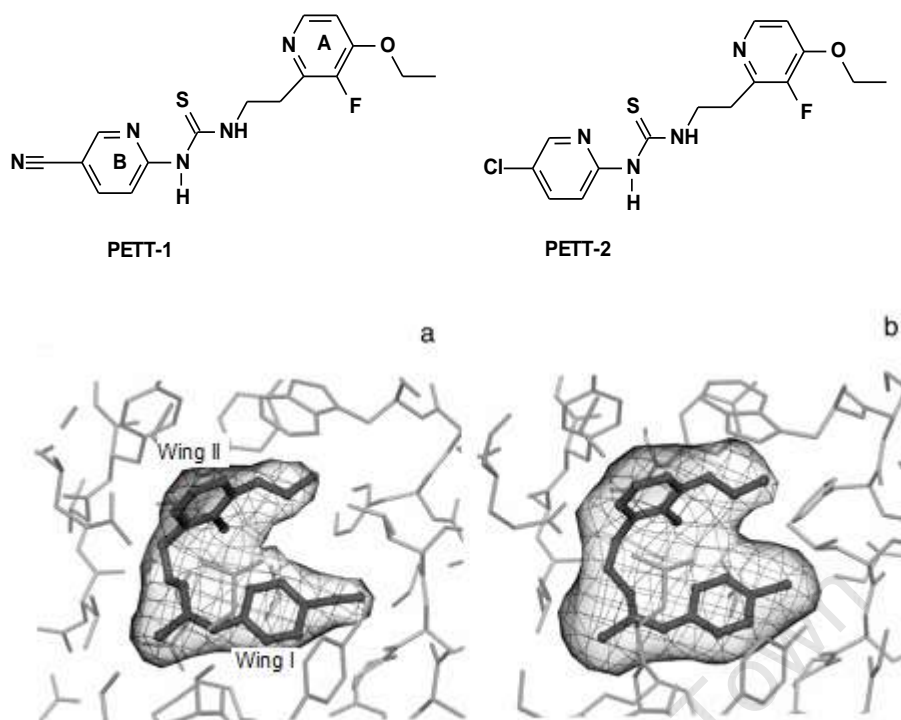


Figure 1.28 Simulated annealing omit electron density maps showing the bound inhibitors at the NNRTI pocket of HIV-1 RT. *a*, PETT-1; *b*, PETT-2.¹⁰⁵

Uckun and co-workers in their modelling studies reported that trovirdine and other PETT molecules docked into the composite binding site, had a greater binding score than the parent compound (PETT) based on a “butterfly”-shaped binding with one residue in Wing I and the other in Wing II. The composite binding pocket showed space around the pyridine ring in the Wing II (ring B) region of the binding site. The 5-bromopyridyl group binds tightly in Wing I,¹⁰⁵ with an intramolecular hydrogen bond between the ring B pyridyl nitrogen atoms and one of the nitrogen atoms of the thiourea group (Fig. 1.29 and Fig. 1.30). Ring A is positioned at the back of the NNRTI pocket in Wing II, and thus forms ring stacking interactions with the side chains of both Tyr188 and Tyr 181. The sulphur atom makes a number of van der Waals contacts with the backbone of Lys101, while there is a single hydrogen bond to the main chain from one of the thiourea nitrogens to the carbonyl of Lys101 (Fig. 1. 29).¹⁰¹

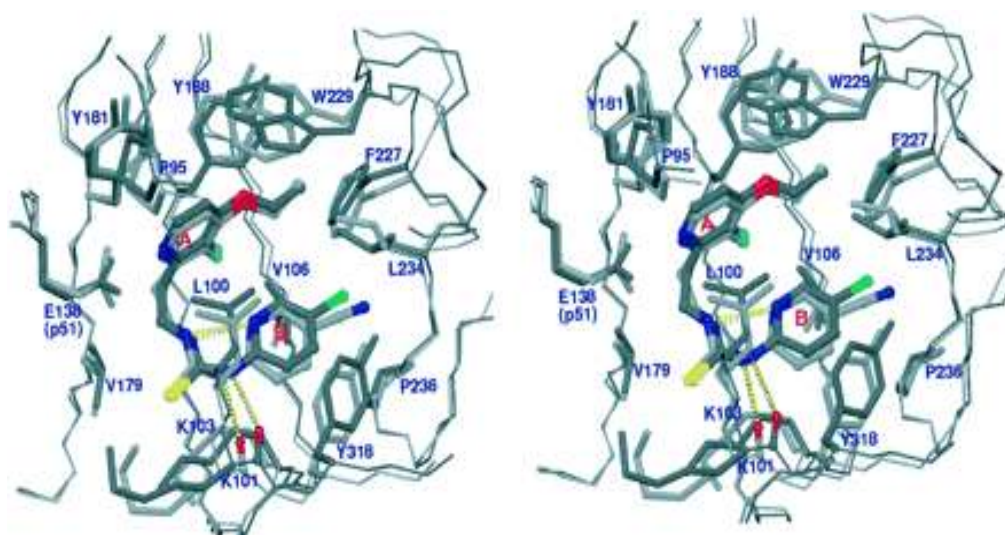


Figure 1.29 Stereo view showing PETT-1 and PETT-2 positioned in the NNRTI binding pocket of HIV-1 RT. RT side chains that form the NNRTI binding site are marked. The inhibitors are in atom colours with PETT-2 shown in a darker hue. The protein for the PETT-1 complex is shown in *light gray*, whereas that for the PETT-2 complex is shown in *dark gray*. The positions of hydrogen bonds are marked in *broken yellow lines*.¹⁰⁵

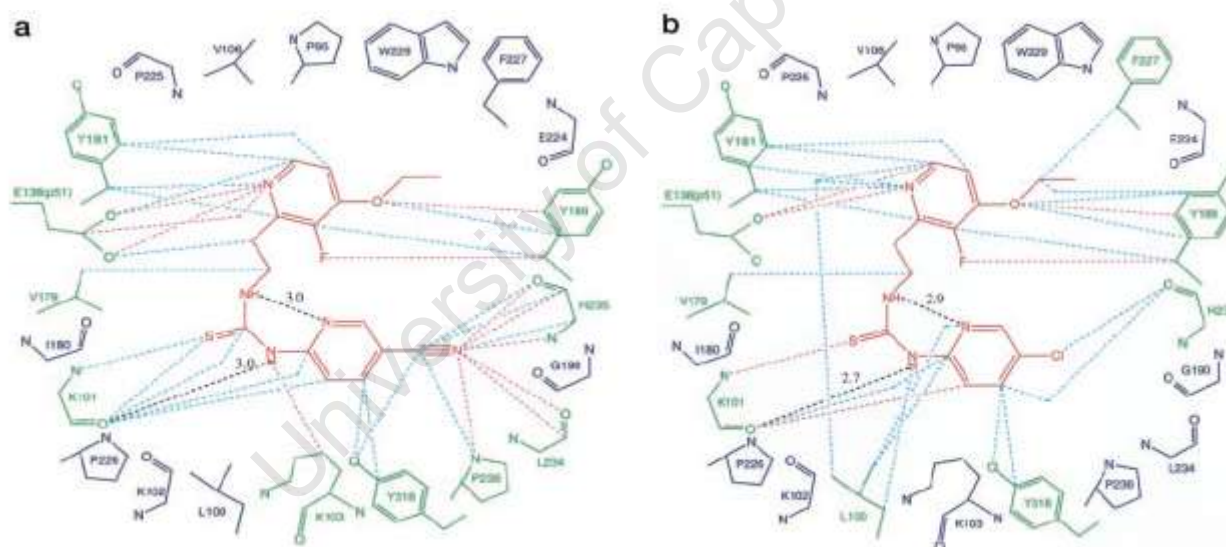


Figure 1.30 Schematic diagrams showing the intermolecular interactions between PETT inhibitors (in *red*) and the surrounding residues of HIV-1 RT for (a) PETT-1 and (b) PETT-2. Residues that contact the NNRTI with a minimum inter-atomic distance of 3.6 Å are shown in *green*, whereas other residues lining the binding pocket are shown in *blue*. The individual distances between the NNRTI and the protein atoms are shown as *dashed lines* (distances 3.3 Å in *pink* and 3.6 Å in *light blue*). Hydrogen bonds together with their distances are shown in *black*.¹⁰⁵

Once again, docking studies with PETT and trovirdine revealed that the Wing II space of both had a substantial molecular volume (~160 Å³) surrounding the pyridine or phenyl ring that could be more efficiently occupied by a larger functional group to achieve a high binding affinity even against the problematic Y181C and Y188C RT mutants. When Y181 and Y188

are mutated to a cysteine residue, the volume change for NNRTI binding is larger and the ability of the NNRTI to inhibit the RT mutant would be attenuated. Uckun and co-workers concluded that a larger NNRTI would perform better against mutants such as the Y181C and Y188C mutants. In accordance this composite binding pocket, a series of thiourea NNRTIs or (PETT) derivatives were synthesized to generate more potent thiourea compounds, by substituting the phenyl ring with various functional groups. Replacement of the pyridylethyl ring of trovirdine with a 2,5-dimethoxy-substituted phenyl ring led to the discovery of *N*-[2-(2,5-dimethoxyphenylethyl)]-*N'*-[2(5-bromopyridyl)]-thiourea as HI-236 (Fig. 1.26), which was designed to optimize occupancy at the Wing II of the binding pocket in order to have an advantage against Wing II mutants such as the Y181C and Y188C mutants Table 1.3.^{106,107}

Table 1.3 Resistance of the Y181C and the Y181C + K103N strains HIV RT inhibition by NNI, relative to wild-type (WT) RT¹⁰⁷

RT inhibitors	rRT*	WT/RT	Y181C mutant (A17)		Y181C +K103N mutant (A17 variant)	
	IC ₅₀ (μM)	IC ₅₀ (μM)	IC ₅₀ p24(μM)	Resistance relative to WT RT (fold)	IC ₅₀ p24 (μM)	Resistance relative to WT RT (fold)
HI- 236	0.1	< 0.001	0.1	> 100	11	11,000
HI-240	0.1	< 0.001	0.2	> 200	41	41,000
HI-241	0.7	< 0.001	ND [†]	ND	ND	ND
HI-253	0.7	< 0.001	ND	ND	ND	ND
HI-280	5.6	< 0.001	> 100	> 100,000	> 100	> 100,000
HI-281	7.0	0.02	38	1,850	55	2,750
HI-443	0.8	0.030	0.048	1.5	3.3	110
Delavirdine	2.3	0.009	50	5,556	38	4,222
Nevirapine	19.8	0.034	> 100	> 2,941	> 100	> 2,941
AZT	ND	0.004	0.006 [‡]	1.5	0.005 [‡]	1.2

* rRT, recombinant RT assay

[†] ND, not determined

[‡]AZT binds to a different site on RT than NNI; therefore it would be as affected by NNI binding site mutations.

1.14 NNRTI RESISTANCE

Resistance mutations associated with NNRTI treatment failure occur primarily in and around the NNRTI-BP. The most common NNRTI-resistance mutations (Fig. 1.31) include Leu100Ile, Lys103Asn, Tyr181Cys, Tyr 188Leu, and Gly190Ala.^{108,109} Structural and molecular modeling studies of drug-resistant HIV-1 mutants¹¹⁰, both in the presence and in the absence of bound NNRTIs, have suggested possible mechanisms by which key mutations confer resistance to NNRTIs.

The Gly190Ala mutation, which causes high-level resistance to loviride and HBY-097, has no significant effect on the ITU, DATA, and the DAPY inhibitors. The resistance was proposed to be caused by filling the area of the binding pocket that would otherwise be occupied by the linker/body portion of the butterfly-shaped NNRTIs like loviride or by the quinoxaline ring of HBY-097.¹¹¹ The ITU, DATA, and DAPY inhibitors are not affected by the mutation. Since a C β atom introduced by the Gly190Ala mutation would point toward the central part of the inhibitors (a thiourea, triazine or pyrimidine group). A minimum distance of 6.0 Å between the C α atom of Gly190 and the central part of these inhibitors suggests that there would be no serious steric conflict between the alanine at position 190 and the bound NNRTI.⁹⁷

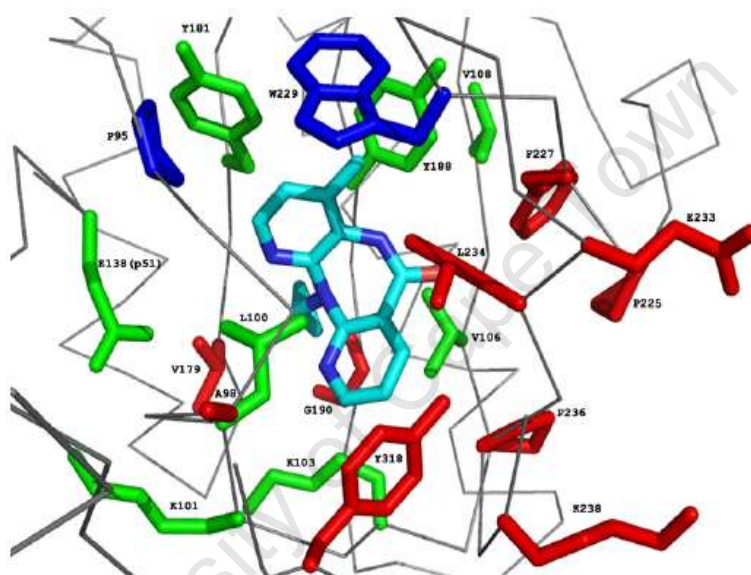


Figure 1.31 Diagram showing the NNRTI site with the principle drug-resistance mutation sites coloured either in green (crystal structures known) or red (structures not reported as yet). Residues where no mutations have been reported are coloured in blue. The NNRTI shown is nevirapine.¹¹²

Leu100,¹¹³ Tyr181,¹¹⁴ and Tyr188¹¹⁵ amino acid residues form a portion of the hydrophobic core of the binding pocket that interacts with Wing I of the ITU, DATA, and DAPY NNRTIs. Mutations of one or more of these amino acids can affect inhibitor-protein interactions and the size, shape, and chemical environment of the binding pocket.¹⁰⁷ Previous studies have shown that the Tyr181Cys¹¹⁵ and Tyr188Leu¹¹¹ mutation affect the binding of an NNRTI by loss of favorable aromatic ring interactions. The Lys103Asn mutation possibly affects the kinetics of inhibitor-binding by stabilizing the unbound state of RT *via* the generation of an additional hydrogen bond between the Tyr188 phenoxy group and the Asn103 side chain.¹¹¹

A connection of the NNRTI binding pocket and the NRTI substrate site through the use of a double-drug was previously suggested by both Arnold *et al.*¹¹⁶ and Anderson *et al.*⁸⁵ The first suggestion came from Arnold *et al.*¹¹⁶ in 1993 who wrote: "An interesting approach that would take optimal advantage of the currently available structural information would be to *design and synthesize inhibitors that would incorporate structural features from both nucleoside analog and non-nucleoside inhibitors.....*Synthesis of these agents could be challenging but there are a number of substituent positions that could be used for the linkage. Site of attachment for the linkers to nucleoside analogs include sugar ring positions (e.g. 2', 3' and 5' substitutions), extensions of mono-, di- and tri-phosphate esters, and positions on the nucleoside base (e.g., the 5-position of a pyrimidine ring). Selection of sites of attachment on the non-nucleoside moieties would vary according to the inhibitor type."

This was followed by a Science article in 1995 in which Anderson⁸⁶ wrote: "We have established the mechanism of inhibition of RT by the three (clinically approved) NNRTIs. Although the long-term inhibition of RT is limited by the high frequency of mutations of the enzyme, this detailed understanding of the action taken by RT when presented with these inhibitors (i.e that binding of a NNRTI does not stop the binding process of a NRTI) should assist in the search for effective drugs to attenuate the AIDS virus. In particular, the interaction between the nucleotide binding site may provide a means to increase the effectiveness of drugs used in combination therapy. *A single drug combining the functionalities of nucleotide analog and a non-nucleoside inhibitor would bind much more tightly because of the cooperative interaction between the sites.*" These two research contributions gave birth to the field of HIV bifunctional double-drugs.

1.15 THE DOUBLE-DRUG STRATEGY

The double-drug strategy involves a chemotherapeutic approach combining two different inhibitors into a single chemical entity via a linker, with the aim of improving the physicochemical characteristics of the individual compounds.

1.15.1 DOUBLE-DRUGS IN CANCER AND MALARIA

5-Fluoro-2'-deoxyuridine (FDU) either as its 5'-O-butanoate or its 5'-O-butanoate-3'-O-retinoate (from retinoic acid) diester (FDU) (Fig. 1.32) have been synthesized to act as anticancer double prodrugs that would serve as a mean of releasing at least two active drugs that act through different mechanisms. The FDU once released could act as a competitive inhibitor for thymidylate synthase whereas retinoic acid and butyric acid once released were expected to induce cell differentiation. The ester derivatives exhibited comparable activity to FDU.¹¹⁷

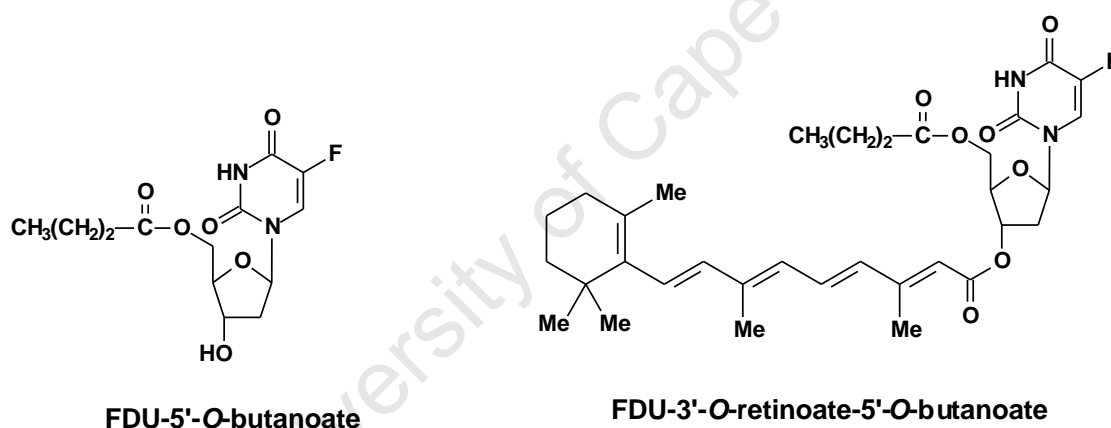


Figure 1.32 Example of 5-fluoro-2'-deoxyuridine (FDU) either as its 5'-O-butanoate or its 5'-O-butanoate-3'-O-retinoate.

Retinoids have been reported to induce differentiation and arrest proliferation in a wide spectrum of cancer cells and are currently used for treatment of promyelocytic leukaemia. Butyric acid is an effective inhibitor of cell proliferation and inducer of cytodifferentiation. In the case of 5'-O-Butanoate-3'-O-retinoate, a mutual prodrug combining butyric acid and *all-trans*-retinoic acid into FDU, it was evaluated for anticancer activity and was found to be more potent than the parent drugs.¹¹⁸ Furthermore, the differentiation activity elicited by the double-drug was greater than that of the combined parent acids. The large increase in activity was attributed to two factors:

- (i) The *all-trans*-retinoic acid fragment imparted lipophilicity and facilitated the penetration of butyric acid to the cellular target site.
- (ii) The intracellularly released *all-trans*-retinoic acid and butyric acid affected the cells synergistically.

Similarly, the statine-based inhibitor of Plasmeprin (II) (PLM II) was linked to the antimalarial drug Primaquine (PQ) using a dicarboxylic acid linker (Fig. 1.33). PLM II is one of the aspartic proteases involved in the degradation of haemoglobin during the intraerythrocytic cycle of *Plasmodium falciparum*. Primaquine is highly active against all malaria species infecting humans. Its toxicity levels can be minimised and its activity increased by converting it into a peptide prodrug. The PQ-Statine double-drugs showed remarkable improvement in the inhibition of both PLM II and *P. falciparum* growth in vitro. The double drugs kill the parasites mainly by inhibiting PLM II together with digestion of haemoglobin that is essential for the survival of the parasite.¹¹⁹

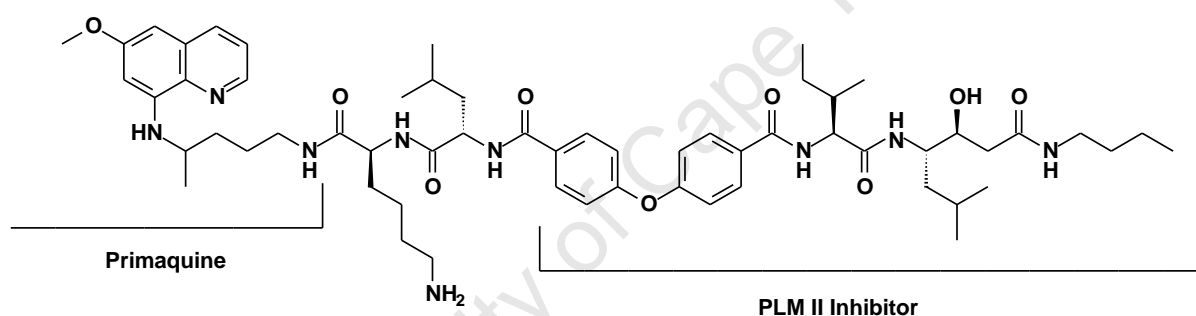


Figure 1.33 Structure of [Primaquine]-4,4'-oxy-bis(benzoic acid)-[PLM II].

Biot *et al.*^{120,121} synthesized double-headed antimalarial prodrugs that target two essential functions of the malarial parasite, namely glutathione regeneration and heme detoxification, with the aim of exploring their synergistic or additive effects. The double drugs combined a glutathione reductase (GR) inhibitor to a 4-aminoquinoline moiety with a bioreversible linker. However, these double-drugs exhibited poor inhibition activity (Fig. 1.34).

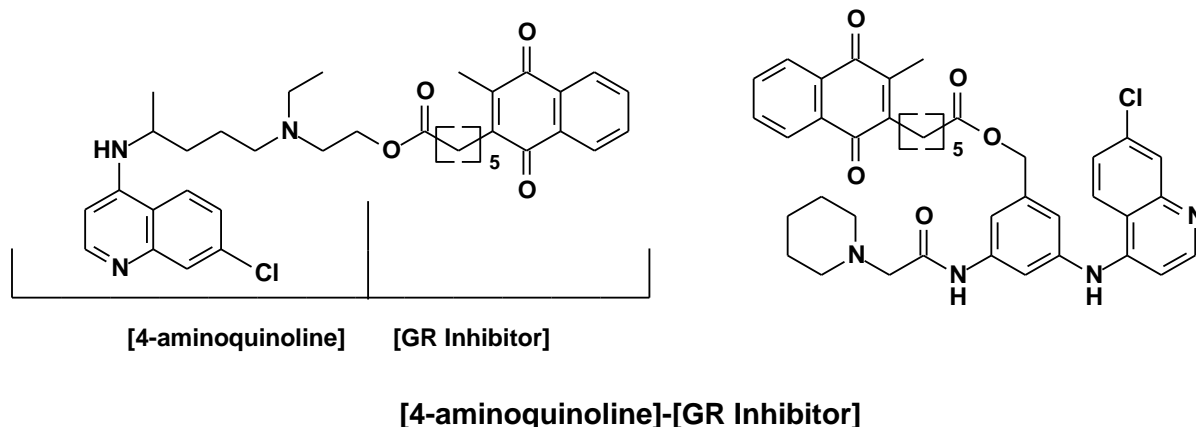


Figure 1.34 Structure of [4-aminoquinoline]-[GR Inhibitor].

1.15.2 DOUBLE-DRUGS IN HIV

Several strategies have been employed in the chemotherapy and chemoprophylaxis of HIV infections. The most effective current strategies involve the following targets: (i) CD4 as primary cell receptor for viral entry into the cell; (ii) gp120 as the viral glycoprotein involved in virus adsorption to the cells; (iii) CXCR4 and CCR5 as co-receptors for viral entry; (iv) gp41 as viral glycoprotein required for virus-cell fusion; (v) NRTI binding site of the HIV reverse transcriptase (RT) enzyme; (vi) NNRT binding site of RT; (vii) integration of the proviral DNA into the host genome by the HIV integrase; (viii) proviral DNA expression (ix) HIV protease. As mentioned in Section 1.7. Based on a combination of inhibition for these targets, the double-drug inhibitors of HIV can be divided into the following classes:

(A) Fused: Two drugs fused together, to create a single entity that is active on two different drug-targets corresponding to the individual drugs.

(B) Cleavable: Two drugs joined by a cleavable (via hydrolysis) linker (spacer) that can target either the same or different drug-target. The cleavable linkers are stable outside the target cell, but are cleaved to individual drugs once in the cell cytoplasm.

(C) Non-cleavable: Stable (to hydrolytic cleavage) bifunctional entity (“mixed-site inhibitors”) whose rationale is to interact the drug entities simultaneously at distinct sites that are in close proximity on the same drug target.¹²²

(A) Fused double-drug inhibitor for RT and IN

Vince and co-workers¹²³ synthesized fused double-drug inhibitors, also referred to as “*portemanteau inhibitors*” based on the fusion of a non-nucleoside reverse transcriptase (RT) inhibitor (NNRTIs) with a diketoacid (DKA) integrase (IN) inhibitor pharmacophore (Fig. 1.35). (IN) is the third virally encoded enzyme that lacks a mammalian counterpart and represents a

validated target for anti-HIV chemotherapeutic. Intriguingly, active sites for RT and IN require one or two Mg^{+2} ions. Further more, catalytic cooperation and even physical interaction between RT and IN, certain peptide fragments from RT inhibit IN activity *in vitro*. The double-drug had a low cytotoxicity (EC_{50} : 24 nM against RT; 4.4 μM against IN; 10 nM against HIV-1 in a cell-based assay; $CC_{50} > 10 \mu M$ $SI \Rightarrow 1000$).

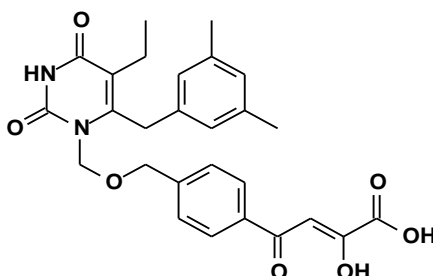


Figure 1.35 Structure of a portemanteau inhibitor combining an RT inhibitor with an IN inhibitor.

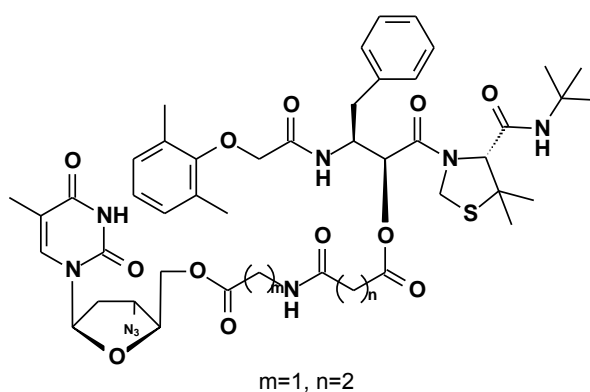
(B) CLEAVABLE DOUBLE-DRUG INHIBITORS

These have been by far the most common type studied with the emphasis on the synergistic effects of the two drugs released in combination.

The cleavable double-drug inhibitors can be divided into two categories:

(1) Cleavable double-drugs on different targets:

A combination of an HIV protease inhibitor and AZT into a single molecule has also been successfully used to improve poor membrane permeation. The protease inhibitor KNI-727, unable to penetrate the cell membrane was linked to AZT by a cleavable linker (Fig. 1.36) resulting in a considerable boost in potency according to a MTT-cell assay by virtue of the parent components being released intracellularly ($EC_{50} = 5.3$ nM for the double drug, compared to 92.0 nM for KNI-727 and 6.2 nM for AZT).¹²⁴



[AZT]-succinic-[KNI-727] conjugate

Figure 1.36 Structure of [AZT]-succinic-[KNI-727] conjugate

Similarly, Tamamura *et al.*¹²⁵ employed the double-drug strategy to synthesize a bifunctional drug that incorporated a CXCR4 inhibitor (T140) as a co-receptor antagonist with an NRTI (AZT) linked by succinate (Fig. 1.37). T140 is a 14-amino acid peptide which inhibits infection of target cells by T cell-line-tropic strains of HIV through specific binding to its chemokine receptor, CXCR4. An equimolar mixture of AZT and T140 caused a remarkable increase in anti-HIV activity compared to the single compounds. This result led to the synthesis of conjugated compounds which combined each entity into a single molecule. The conjugated drug exhibited a synergistic effect for anti-HIV in vitro ($EC_{50} = 4.6$ nM in MT-4 cells with HIV-1, $SI = > 4300$; AZT = 20 nM; T140-succinic acid = 310 nM). The mechanism of action is based on the hydrolysis of the enzymatically labile ester 5'-O-bond between the NRTI and the spacer.

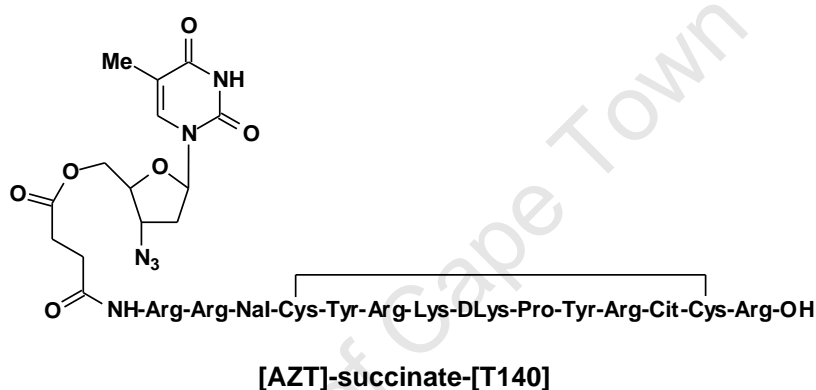
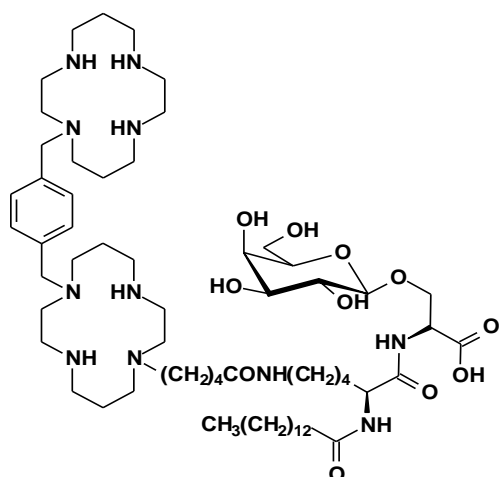


Figure 1.37 Structure of [AZT]-succinate-[T140]

Daoudi *et al.*¹²⁶ synthesized bifunctional compounds combining bicyclam AMD3100 and a galactosylceramide (GalCer) analogue into a single molecule with the aim of inhibiting several steps of the complex virus/cell cascade interactions (virus-cell adsorption/fusion processes). The double-drug [Gal]-[AMD3100] conjugate (Fig. 1.38) exhibited superior potency to that of AMD3100 ($EC_{50} = 65$ nM in MT-4 cells with HIV-1; AMD = 2.9 μ M; GalCer >100 μ M). AMD3100 is a CXCR4 antagonist and interferes with viral binding to the cellular co-receptors, whereas GalCer provides an attachment platform (alternative receptor in CD4⁺ cells) for the virus (through its gp120 and/or gp41) onto the cell. When compared to the activity of GalSer, the bipharmacophore conjugate moderately increased its anti-HIV activity.



Gal-AMD3100 Conjugates

Figure 1.38 Structures of Gal-AMD3100 Conjugates.

Similarly, AZT coupled onto κ -carrageenan using a succinate diester spacer was synthesized with the aim of enhancing AZT intracellular uptake as well as to test the synergism of the prodrug.¹²⁷ Carrageenans are naturally occurring sulphated polysaccharides extracted from different species of red seaweed that have a common structural backbone of D-galactose residues. The κ -form is characterised by a repeating unit of 4-sulfate- β -D-galactopyranose linked 1 \rightarrow 3 and 3,6-anhydro- α -D-galactopyranose linked 1 \rightarrow 4. The κ -carrageenan was expected to act not only as a drug-delivery carrier for AZT, but also as an anti-HIV agent which would act synergistically with AZT. Carrageenans possess anti-HIV activity and inhibit the binding of the virions to the cell as gp-120 adsorption inhibitors, as well as cell-to-cell fusion inhibition. The [κ -carrageenan]-succinate diester-[AZT] (Fig.1.39) conjugate inhibited the binding of the virions to the MT-4 cells and concomitantly delivered AZT to these cells to further inhibit the RT ($EC_{50} = 6.8$ nM, SI = 3000; AZT = 25 nM).

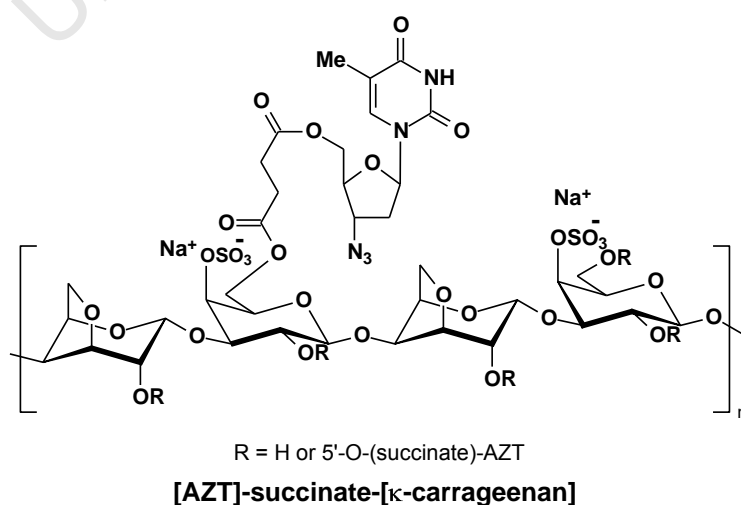
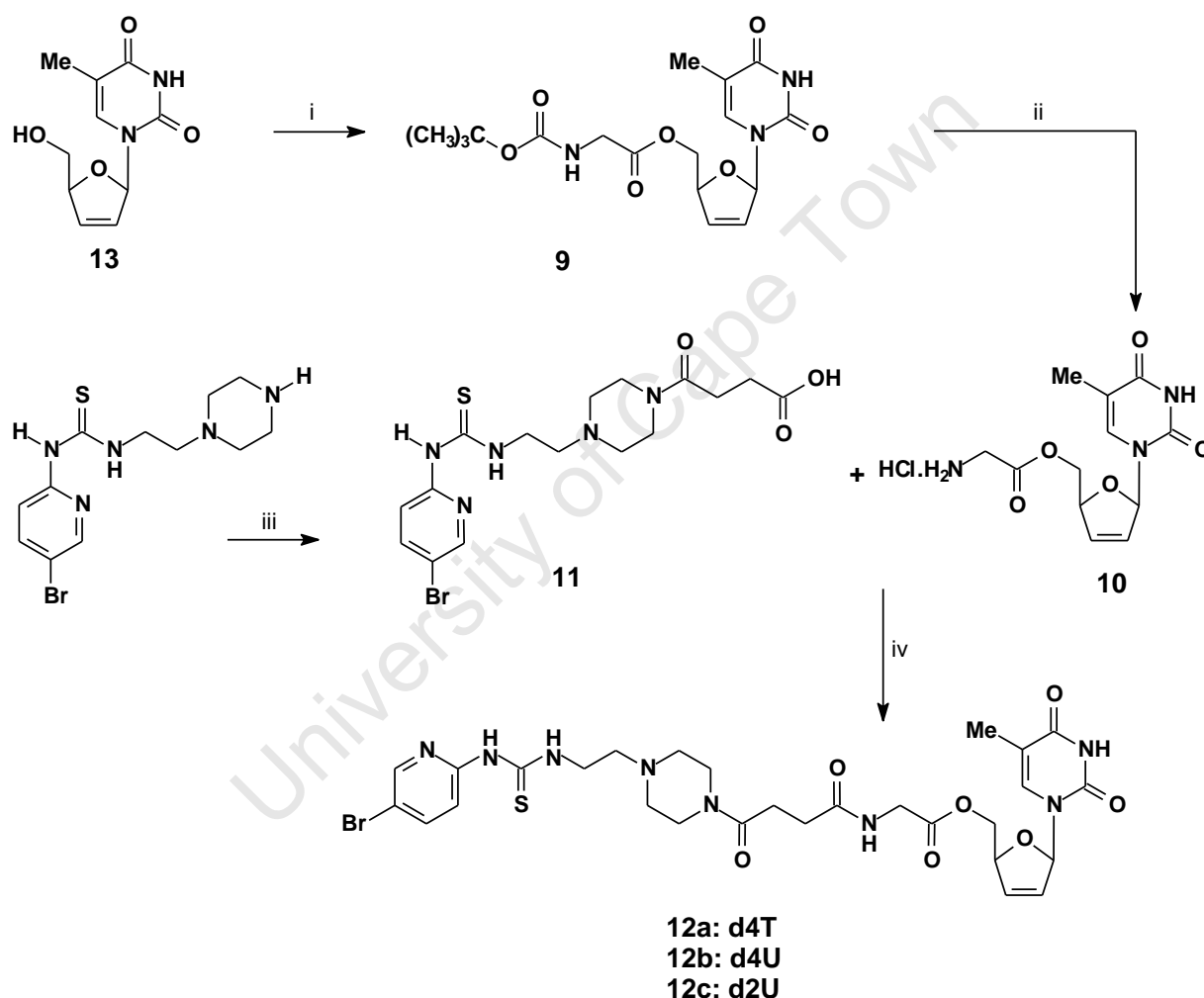


Figure 1.39 Structure of [AZT] -succinate diester-[κ -carrageenan].

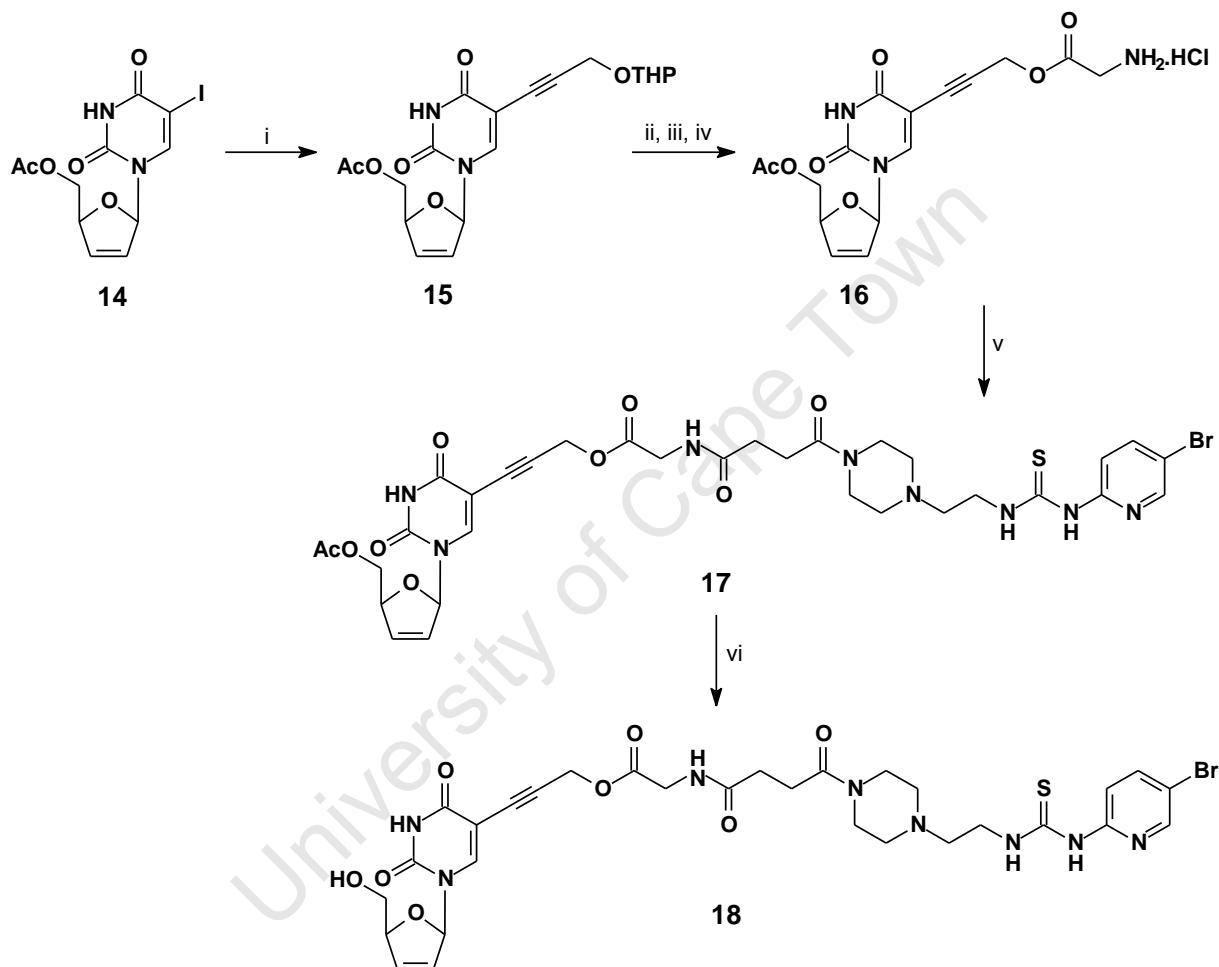
The Ladurée group has reported the synthesis of a NRTI/NNRTI heterodimer of the formula [NRTI]-Glycyl-Succinyl-[Trovirdine].¹²⁸ Nucleosides d4U, d2U and d4T were varied as the NRTI and spacer linking was achieved via the C-5' hydroxyl group of the NRTI with the *N*-piperazine of a modified trovirdine. A succinyl-glycine moiety was chosen as a spontaneously cleavable linker, and introduced via coupling of the NRTIs with Boc-gly-OH using DCC in the presence of DMAP in DMF to give the 5'-esters **9**. Deprotection of Boc using 4M HCl/dioxane afforded the amine hydrochlorides **10** which were condensed with modified trovirdine analogue **11** using BOP/HOBt in the presence of triethylamine in DMF to afford the heterodimers **12 a-c** in 35-45% yield. The heterodimers were unfortunately devoid of antiviral activity at non-toxic concentrations (Scheme 1.1).



Scheme 1.1 Reagents and Conditions: (i) HOOC-CH₂-NHBoc, DCC, DMAP, DMF; 78%. (ii) 4M HCl/Dioxane; 87%. (iii) succinic anhydride, CH₂Cl₂; 64%. (iv) Et₃N, HOBt, BOP, DMF; 35-45%.

The synthesis of an analogous system using C-5/NRTI as the attachment point^{129,130} (Scheme 1.2) was accomplished employing a Sonogashira reaction. Pd(0)-mediated Sonogashira coupling at C-5 of **14** with a C-3 propynyloxy spacer protected as its THP ether produced **15**. Deprotection of THP using CF₃COOH in CH₂Cl₂ followed by condensation of

the resultant alcohol with Boc-Gly-OH using DCC in the presence of DMAP and subsequent deprotection of the Boc group using 4M HCl in dioxane afforded the amine hydrochloride **16**. Condensation of amine **16** with modified trovirdine derivative **11** followed by deprotection of the acetate group with cyanide ion gave the heterodimer **18** in 35-45% yield for the last step. The heterodimers displayed inferior anti-HIV activity (compound **18** displayed an $IC_{50} > 20 \mu\text{M}$) compared to the parent compounds. The lack of activity was attributed to the wrong positioning of the linker to either NRTI or NNRTI with respect to their active sites in the enzyme.

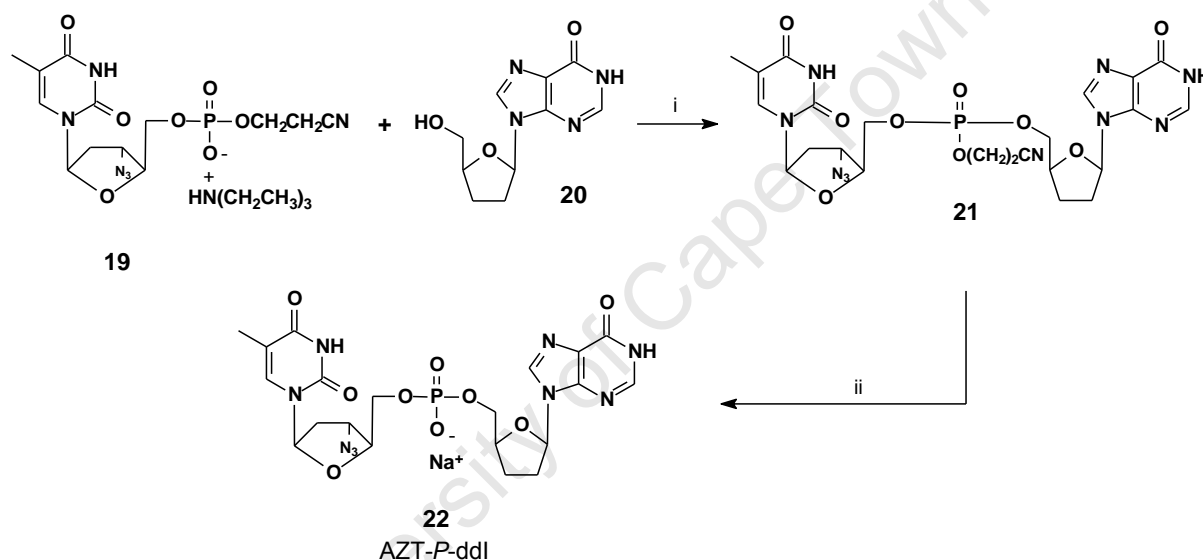


Scheme 1.2 Reagents and Conditions: (i) alkyne, $(\text{PPh}_3)_4\text{Pd}$, CuI, Et_3N , DMF; 67%. (ii) CF_3COOH , CH_2Cl_2 , CH_3OH (iii) $\text{HOOC-CH}_2\text{-NHBoc}$, DCC, DMAP, DMF (iv) 4M HCl/Dioxane (v) **11**, Et_3N , HOBT, BOP, DMF; 48%. (vi) NaCN, MeOH; 38%.

(2) Cleavable double-drugs on the same target site

Several NRTI homo- and heterodimers targeting the HIV reverse transcriptase enzyme have been synthesized by attaching the linker at the 5', 5' or N-3 positions of the nucleosides. Ijichi *et al.*¹³¹ have reported the synthesis of nucleotide heterodimers of AZT, ddI and Ribavirin.

The dimers were formulated as a mixed phosphate diester via the 5'-hydroxyl groups of the nucleoside, with the aim of releasing two nucleosides at the active site. Thus, 5'-O-phosphorylation of AZT gave AZT cyanoethyl phosphate **19**, which condensed with ddl **20** in the presence of *p*-toluenesulfonyl chloride to afford heterodimer [AZT]-cyanoethylphosphate-[ddl] **21**. Deprotection of the cyanoethyl group with 1N NaOH led to the heterodimer **22** (Scheme 1.3). Similarly, [ddl-phospho-Ribavirin] **23** ($EC_{50} > 17.5 \mu\text{M}$) and [AZT-phospho-Ribavirin] **24** ($EC_{50} = 0.004 \mu\text{M}$) heterodimers (Fig. 1.40) were synthesized using the same procedure. The heterodimers **22** and **24** showed enhanced anti-HIV activity relative to their monomers. Furthermore, AZT-P-ddl **22** ($EC_{50} = 0.002 \mu\text{M}$, $CC_{50} = 18.2 \mu\text{M}$) was ~2-fold times less toxic than AZT to human granulocytes macrophage progenitor cells ($EC_{50} = 0.002 \mu\text{M}$, $CC_{50} = 10.7 \mu\text{M}$ for AZT; $EC_{50} = 13.3 \mu\text{M}$, $CC_{50} = 226 \mu\text{M}$ for ddl).



Scheme 1.3 Reagents and Conditions: (i) *p*-TsCl, CH_2Cl_2 (ii) NaOH.

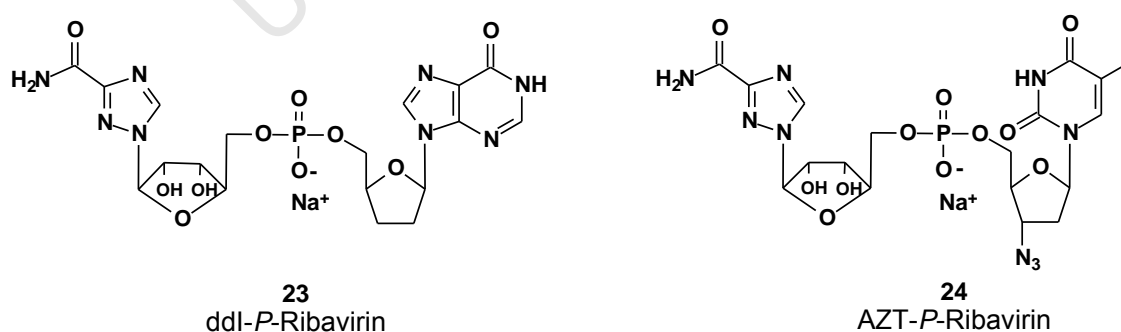
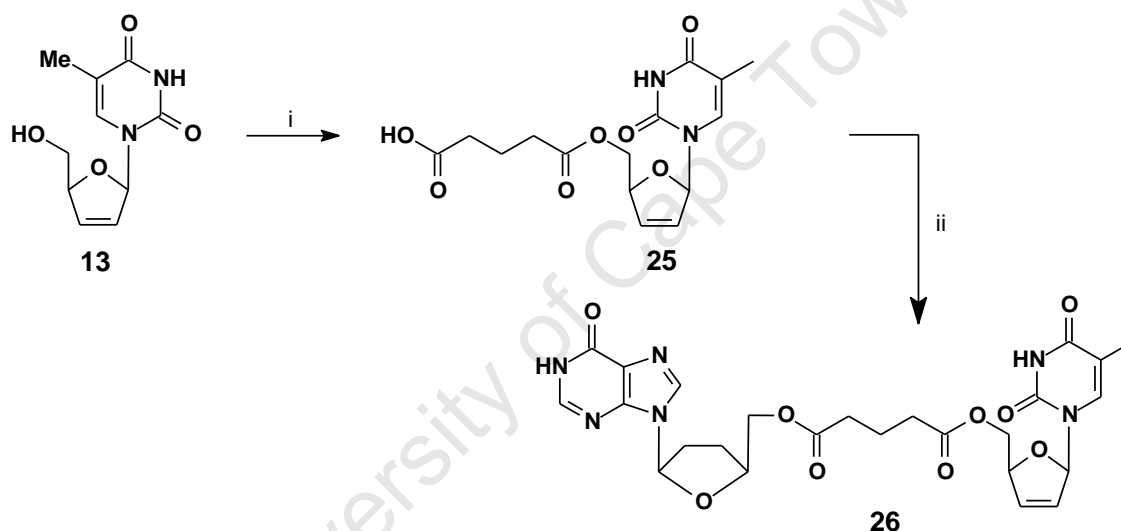


Figure 1.40 Structures of AZT, ddl, Ribavirin and HEPU heterodimers

In a similar fashion, homo- and heterodimers of ddl, AZT and d4T have been synthesized by Mohamed *et al.*¹³² with the aim of enhancing the antiviral activity of their components

(Scheme 1.4). An ester linkage was used to link to a glutaric acid spacer. The synthetic strategy involved converting d4T **13** into half ester **25** by treatment with glutaric anhydride in methylene chloride, followed by an EDC-promoted esterification of the glutarate with ddl to form the heterodimer **26** in good yield (Scheme 1.4). AZT-ddI and ddl-ddI heterodimers bearing an ester linkage were also synthesized using this methodology. Other spacers used in this class of compounds were carbonate and carbamate based to form AZT and d4T homo- and heterodimer carbonates **27** and carbamates **28**, respectively (Fig. 1.41). Following intracellular hydrolysis of the carbonate or carbamate, the two nucleosides would be regenerated in the cytoplasm. The carbonates displayed anti-HIV activity comparable to AZT, while the carbamates displayed low anti-HIV activities. No synergistic effects on the inhibition of HIV replication was detected for either the carbonates **27 a-c** and carbamates **28a-c**.



Scheme 1.4 Reagents and Conditions: (i) Glutaric anhydride, Et₃N, CH₂Cl₂; 85%. (ii) ddl/DMAP/EDC, HCl, CH₂Cl₂/DMF; 80%.

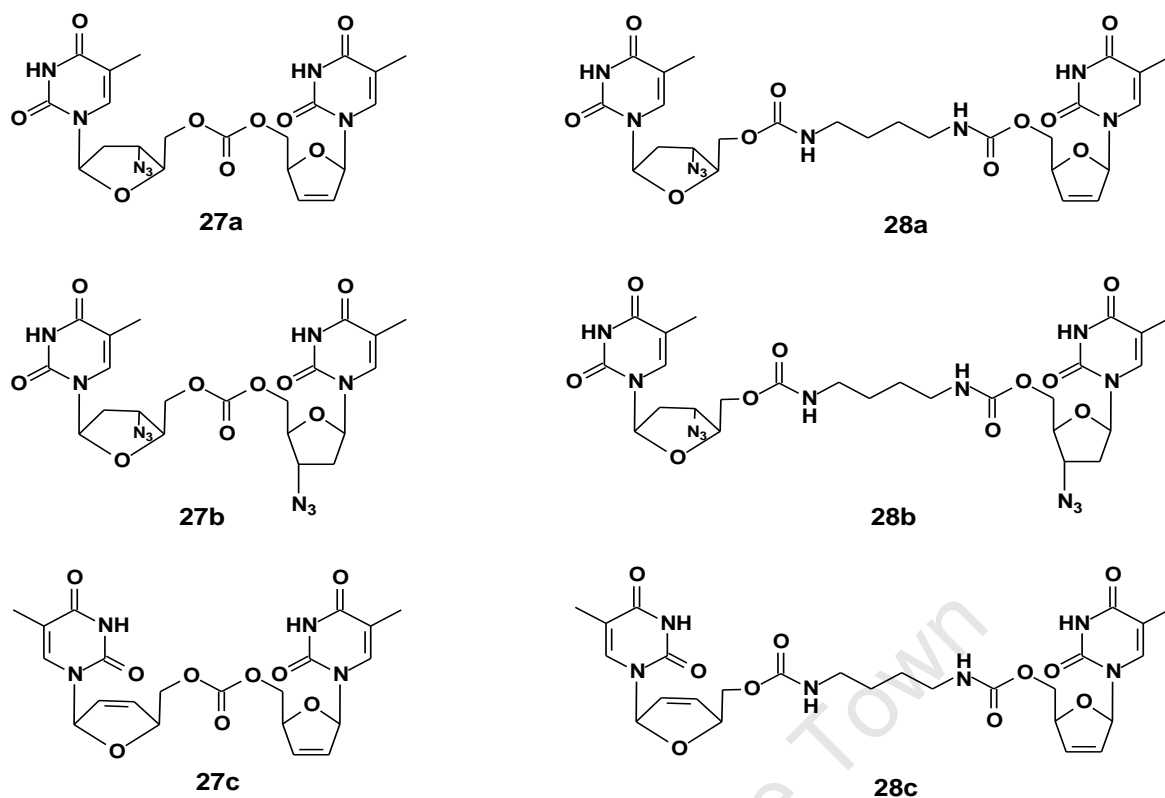


Figure 1.41 Structure of AZT/d4T homo- and heterodimer linked by a carbonate or carbamate spacer.

Pederson *et al.*¹³³ has been recently reported the synthesis and antiviral activities of cleavable [NRTI/ NNRTI] double-prodrugs against HIV based on the mixed S-acyl-2-thioethyl (SATE) prodrug approach. The SATE prodrugs were first introduced in 1993 by Imbach. *et al.*^{117a,b} as a carboxyesterase-labile protecting group for the ddU nucleotide. The double prodrug in question incorporated d4T as a 5'-phosphate and as a SATE ester linking through the phosphate to N-3 of MKC-442 (a HEPT derivatives) via a cleavable *p*-hydroxybenzoyl linker. The double-prodrug (Fig. 1.42) had good activities against HIV-1 ($EC_{50} = 0.03 \mu\text{M}$) and the Y181C mutant strain ($EC_{50} = 2.7 \mu\text{M}$). Most probably, the activity of the SATE prodrug given in Figure 1.42 is due to the activity of the separate compounds, in which MKC442 strongly loses activity against the Y181C mutant. The activity was thus mainly attributed to the NNRTI (MKC-442) part of the molecule (Fig. 1.42).

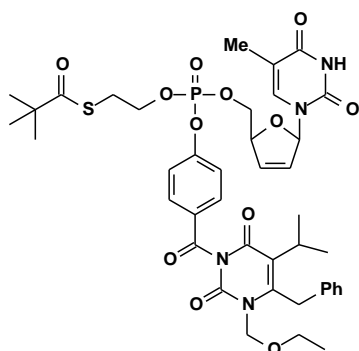
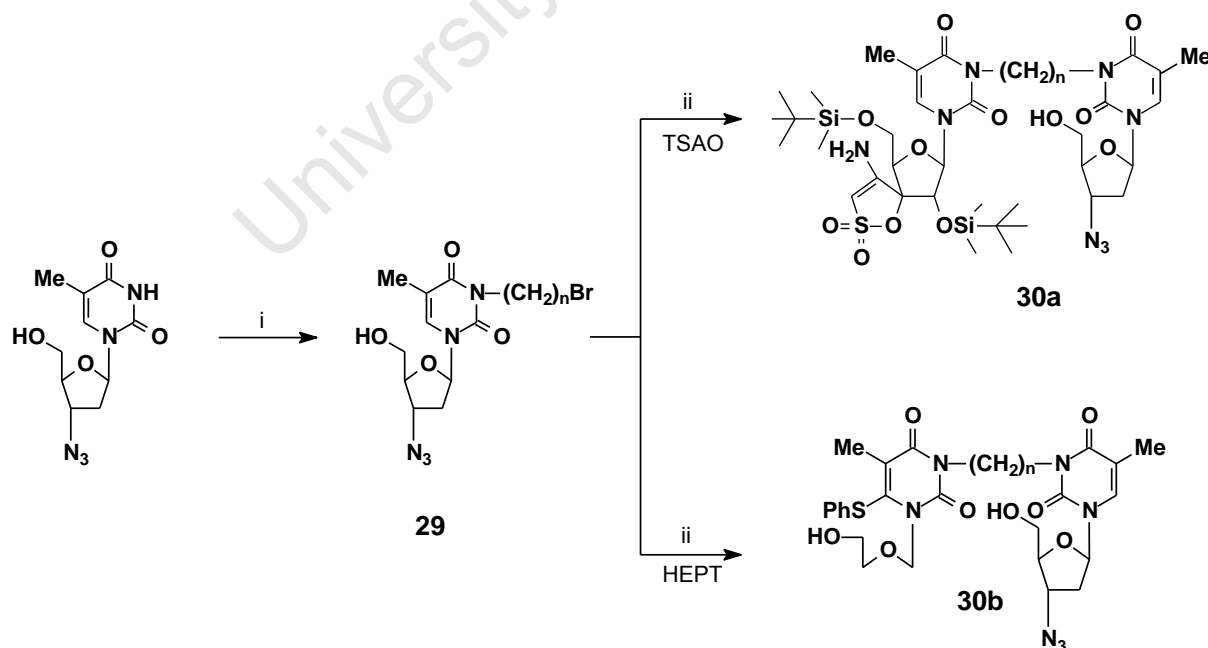


Figure 1.42 SATE pro-drug

(C) NON-CLEAVABLE DOUBLE-DRUG (“MIXED-SITE INHIBITORS”)

The combination of a nucleoside and a non-nucleoside RTI into a single molecular entity was advocated by Arnold *et al* in 1993.¹¹⁶ This was supported by structural^{18,116} and biochemical^{185,134} studies which indicated that linking the compounds with an appropriate spacer might result in an improved inhibitory capacity. The first heterodimers incorporating an NRTI with an NNRTI were synthesized by the Camarasa group in 1995.¹³⁵ They reported the synthesis of a family of anti-HIV heterodimers based on combining AZT with either TSAO-T or HEPT via a polymethylene spacer between the N-3 of the thymine base of both compounds (Scheme 1.5). TSAO derivatives were first synthesized in 1992 and represent a unique structural class of NNRTI as they specifically interact at the interface between the p51 and p66 subunits of HIV-1 RT. The prototype compound of this family is the thymine derivative designated TSAO-T and the most active compound is its 3-*N*-methyl substituted derivative TSAO-m³T. The synthetic strategy for formation of **30a** and **30b** involved selective N-3 alkylation of AZT with a dibromoalkyl reagent followed by N-alkylation of the N-3-bromoalkyl AZT intermediate with TSAO-T or HEPT. The polymethylene spacer was varied in length from $n = 4 \rightarrow 7$. Thus, treatment of AZT with 2 equiv of 1,3-dibromopropane in dry acetone: DMF (1:1) in the presence of K_2CO_3 gave the N-3 substituted derivative **29**. Subsequent reaction of **29** with TSAO-T or HEPT under basic conditions gave heterodimers **30a** and **30b** in 50-60% yield.



Scheme 1.5 Reagents and Conditions: (i) $(CH_2)_nBr_2$ ($n = 3-9$), K_2CO_3 , acetone, DMF (1:1); (ii) K_2CO_3 , acetone, DMF (1:1).

The most active compound in the series was [TSAO-T]-(CH₂)₃-[AZT] **30a** (EC₅₀ = 0.10 μM; TSAO-T = 0.06 μM) incorporating a short spacer. Heterodimers bearing polymethylene linkers [-(CH₂)_n-] with n = 4-6 showed good antiviral activity, while longer spacers with n > 7 showed diminished activity. The precursors to the dimers were also tested. Specifically, AZT derivatives such as **29** proved inactive irrespective of the chain length of the methylene spacer. The activity of the TSAO-T-spacer derivatives **31c** decreased with increasing length of the spacer. Replacement of AZT with d4T resulted in improved anti-HIV activity. No marked differences in activity were observed when the spacer consisted of 1-butynyl, 1-butenyl or ethoxyethyl moieties. Similarly, heterodimers **31a,c** were synthesized using the C-5 of the NRTI for attachment, and these showed comparable activities to that of **30a**, whereas the corresponding d4T analogue of **31b** led to a 5-fold decrease in anti-HIV potency.

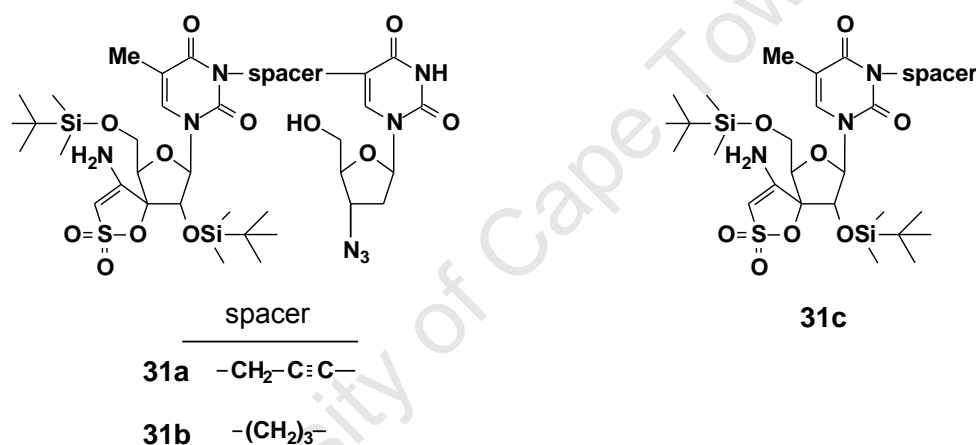


Figure 1.43 [TSAO-T]-spacer-[AZT]

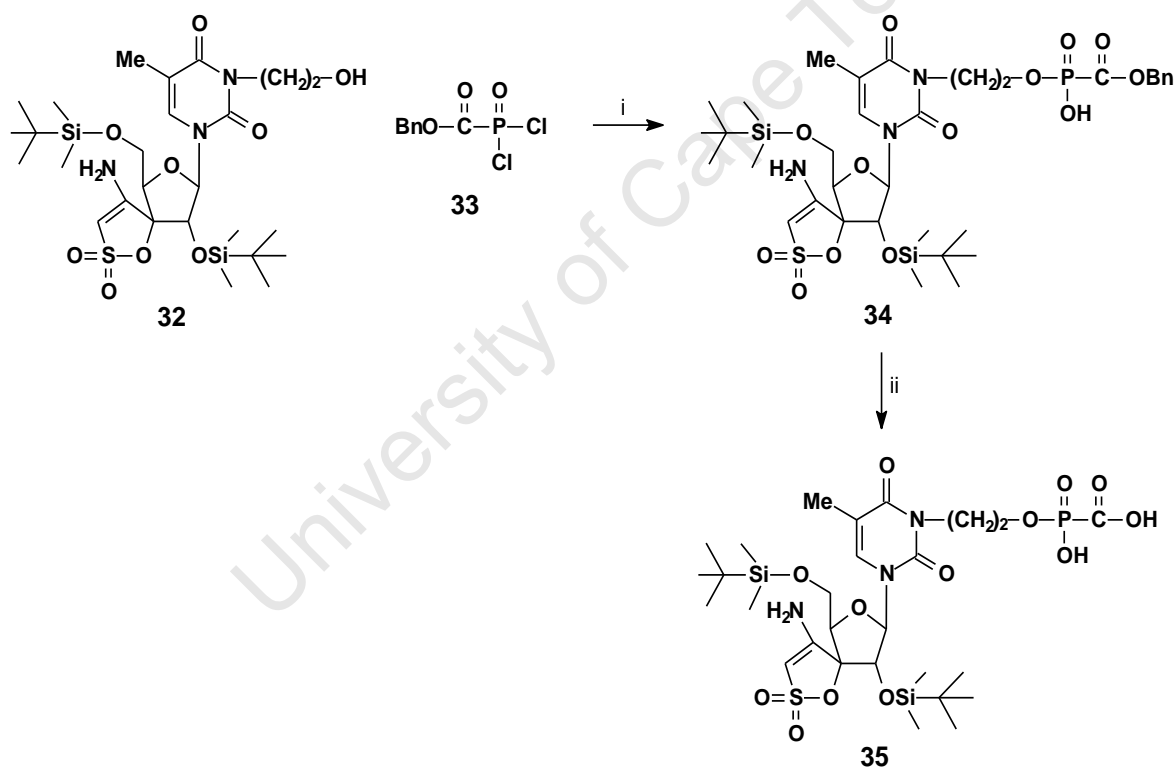
Spacer rigidity in the C-5 series did not markedly influence the antiviral potency since the heterodimer **31b** bearing a flexible propyl group as spacer was endowed with anti-HIV-1 activity comparable to that of the corresponding propynyl analogue **31a** (Fig. 1.43). Converting AZT, d4T and thymidine heterodimers to phenoxyphosphoramidate¹³⁶ heterodimers had no improved activity over the corresponding non-phosphorylated analogues. Overall, the d4T heterodimers had better inhibitory efficacy than the AZT ones.

By comparison, combinations of TSAO-m³T and foscarnet (PFA) (Fig. 1.44), also synthesized by the Camarasa group as individual entities, at a variety of concentrations revealed that these compounds displayed additive antiviral activity.¹³⁷ These results inspired the synthesis of a single molecule combining a TSAO derivative with foscarnet through a

labile phosphate ester bond, hence making it a cleavable double-drug. PFA is an effective antiviral agent approved for intravenous treatment of Human Cytomegalovirus (HCMV) Retinitis in patients with AIDS.¹³⁸ It is also effective against HIV replication and inhibits HIV-1 RT by blocking the pyrophosphate binding site.¹³⁹



Figure 1.44 Structure of TSAO-m³T and Foscarnet

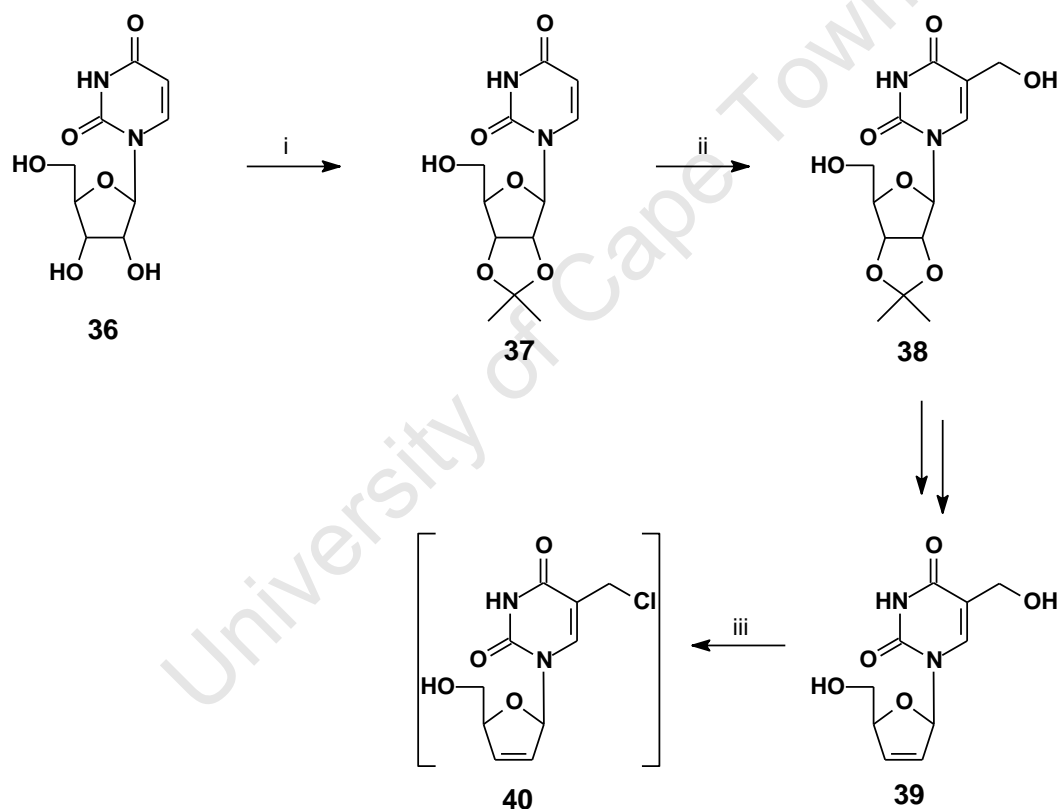


Scheme 1.6 Reagents and Conditions: (i) (a) **33**, Et₃N, CH₂Cl₂, -20 °C (b) H₂O; 54%. (ii) H₂, Pd/C, MeOH; 60%.

Thus, treatment of TSAO derivative **32** with the foscarnet-based phosphorylating reagent **33** in the presence of triethylamine led to the formation of the PFA diester **34** in moderate yield. Catalytic hydrogenolysis of **34** yielded the [TSAO-T]-[PFA] conjugate **35** in 60% yield (Scheme 1.6). Unfortunately, conjugate **35** was less active than the parent compound **32**,

displaying no additive or synergistic anti-HIV activity and thus indicating the activity to be due to the TSAO part of the molecule and not the PFA part.

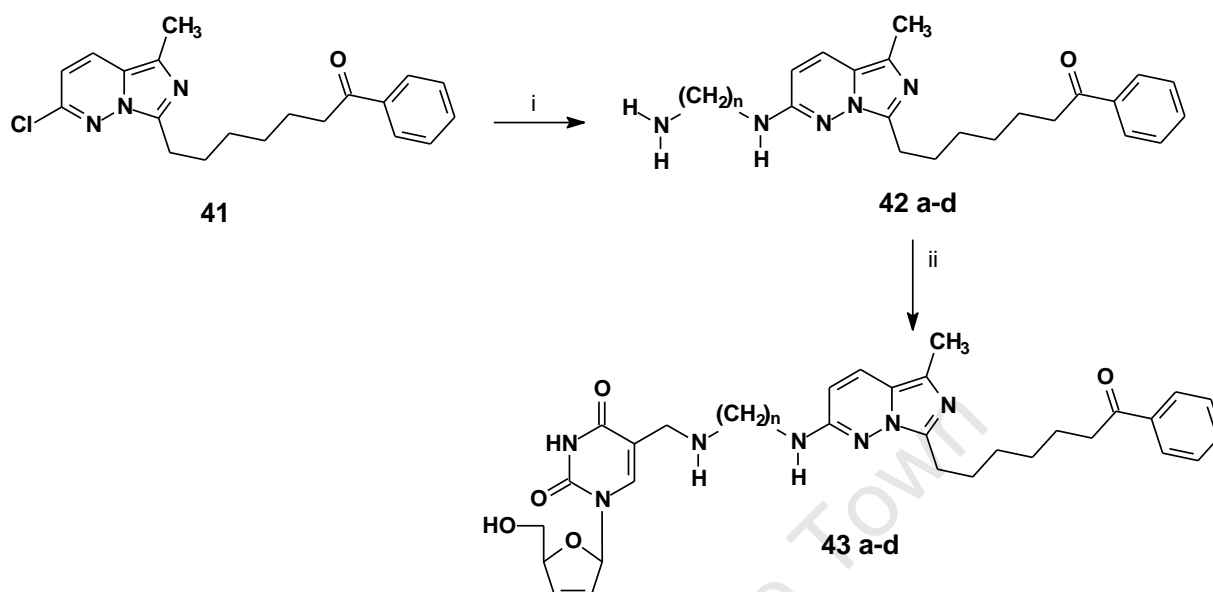
The design, synthesis and anti-HIV-1 evaluation of several non-cleavable heterodimers of the general formula [d4T]-NH(CH₂)_n-NH-[imidazo[1,5-*b*]pyridazine] (*n* = 6-12) involving a C-5 linkage to d4T was reported by Ladurée *et al.*¹⁴⁰ in 1998. Imidazo[1,5-*b*]pyridazine was chosen as the NNRTI due to its exceptional potency. The synthetic strategy involved synthesis of the NNRTI linked to a 1,*n*-diaminoalkyl spacer followed by substitution onto d4T via a C-5 chloromethyl group. The synthesis of the d4T coupling derivative (Scheme 1.7) involved C-5 hydroxymethylation of protected uridine **37** to give **38** in good yield followed by C-2'/3' double-bond introduction to afford **39** and selective chlorination of the hydroxymethyl group in the presence of the C-5' hydroxyl group of **39** to give **40**.



Scheme 1.7 Reagents and Conditions: (i) 2,2-DMP, APTS, MeCOMe. (ii) CH₂O, Et₃N, 60 °C; 93%. (iii) TMSCl, 1,4-dioxane, 60 °C.

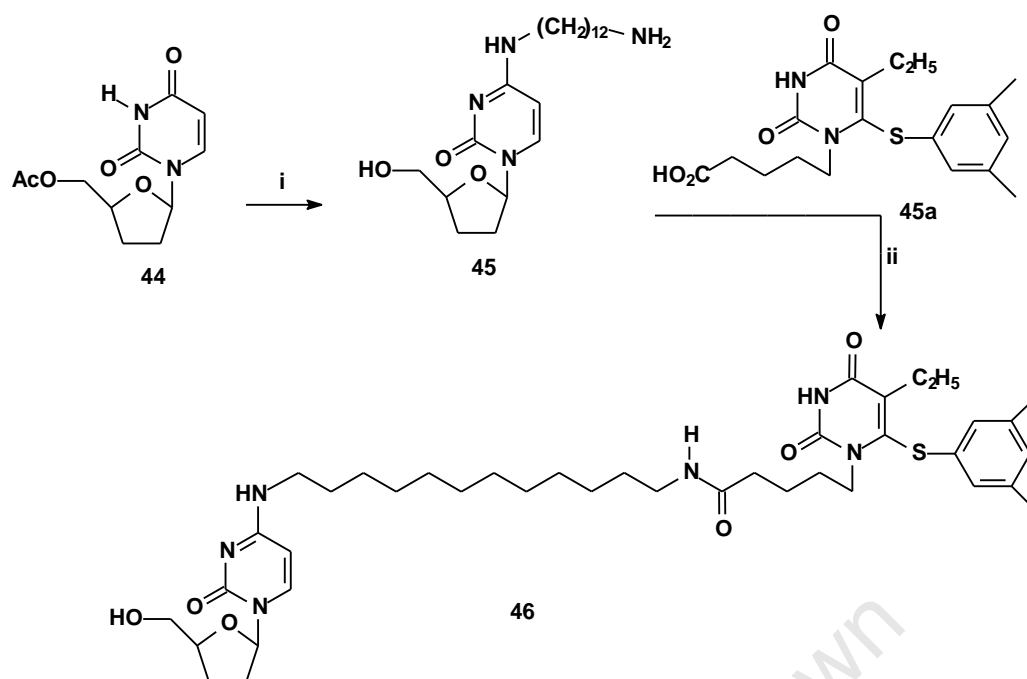
Imidazo[1,5-*b*]pyridazine **41** was synthesized in seven steps from alanine, and was heated with a 1,*n*-diaminoalkane at 120 °C to give monomers **42 a-d** via aromatic nucleophilic substitution. Condensation of **42 a-d** with **40** in DMF gave heterodimers **43 a-d** in 72-85% yield (Scheme 1.8). The anti-HIV activity of the NNRTI linked to its spacer **43 a-d** was

evaluated independently and the results revealed a decrease in activity compared to the unsubstituted NNRTI. The activity of the heterodimers **43 a-d** was comparable to that of d4T and thus mainly due to the nucleoside part of the molecule.



Scheme 1.8 Reagents and Conditions: (i) $\text{H}_2\text{N}-(\text{CH}_2)_n-\text{NH}_2$; a: $n=6$, b: $n=8$, c: $n=10$, d: $n=12$. (ii) $d_4\text{CIMUrd}$ **40**, DIEA, DMF.

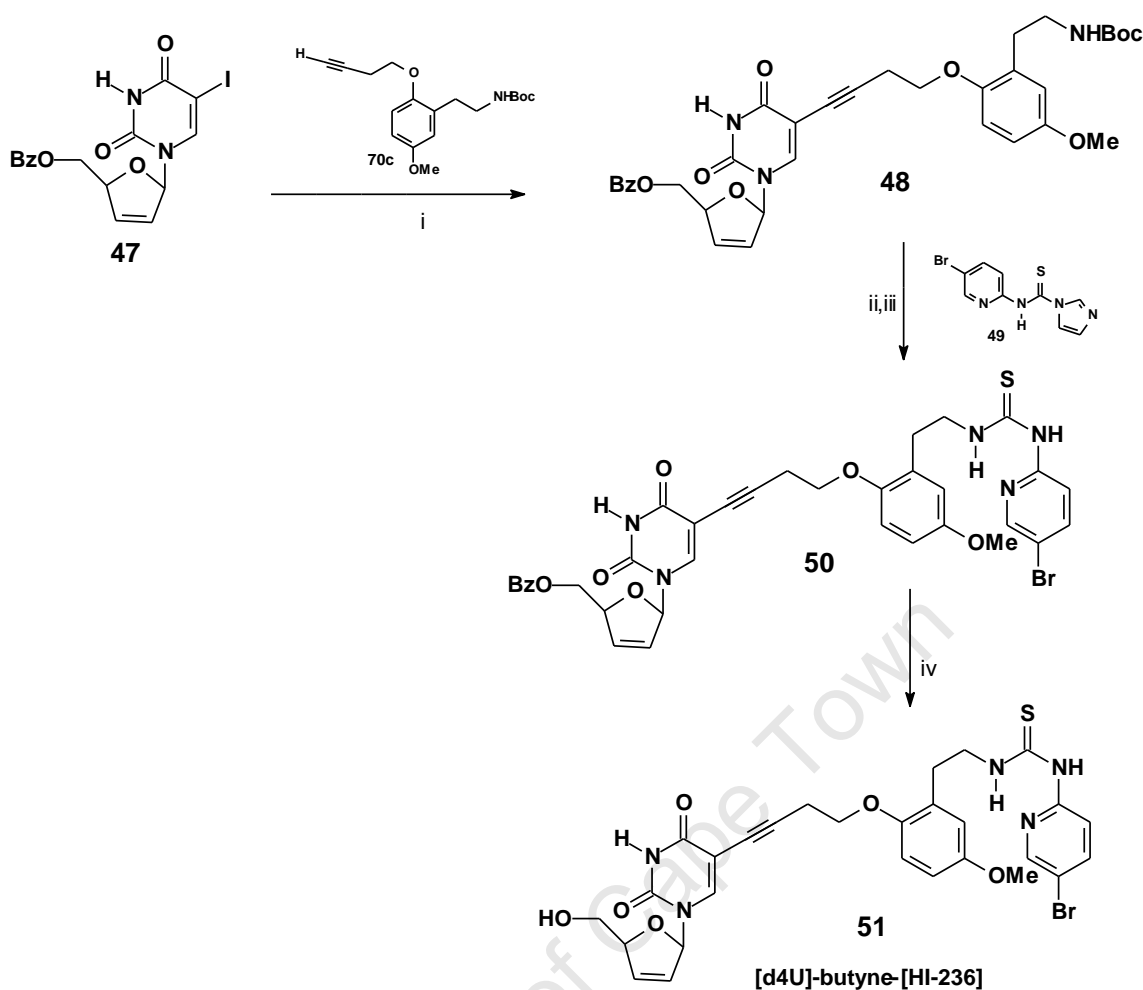
Similarly in 2000, Monneret¹⁴¹ and co-workers synthesized a variety of (N-3 and C-5)AZT - HEPT bifunctional conjugates displaying anti-HIV activity ranging between 2-5 μM . In the same report, a non-cleavable ddC-HEPT conjugate was found to exhibit an anti-HIV potency of 0.45 μM against HIV-1 (wild-type and the Y181C nevirapine-resistant strain) and HIV-2 in cell culture. The ddC component in the mixed inhibitor **46** (Scheme 1.9) was prepared in a one-pot procedure (33% yield), involving reaction of 5'-O-acetyl-2',3'-dideoxyuridine **46** with triisopropylbenzenesulfonyl (TPS) chloride, followed by treatment with 1,12-diaminododecane. Coupling of amino derivative **45** with **45a** using N-methylmorpholine (NMM) and 2-chloro-4,6-dimethoxy-1,3,5-triazine (CMDT) provided **46** in good yield.



Scheme 1.9 Reagents and Conditions: (i) TPSCI, Et_3N , DMAP, DCM, then $\text{NH}_2(\text{CH}_2)_{12}\text{NH}_2$ (33%); (ii) CDMT, NMM, DMF, then **45a** (69%).

No synergistic effects were observed, and **38** appeared to inhibit RT through interaction of only one component (NNRTI) in its bis-substrate structure. A plausible reason offered by the authors is that the tethering arm is poorly adapted to permit the nucleoside and the NNRTI motifs to communicate simultaneously with their respective sites.

Recently ongoing research at University of Cape Town by Hunter *et al.*¹⁴² has reported the synthesis of a non-cleavable [d4U]-butyne-[HI-236] bifunctional using a Sonogashira strategy similar to that used by Ladurée (Scheme 1.10). These compounds are the subject of this thesis. Thus, coupling of 5'-benzoyl-5-iodo-d4U **47** with an *N*-Boc-protected alkyne that was prepared in a number of steps from 2-hydroxy-5-methoxybenzaldehyde furnished nucleoside **48**. The latter underwent Boc-deprotection with trifluoroacetic acid followed by condensation with thiourea **49** to furnish benzoylated bifunctional **50**. Methoxide deprotection of **50** gave the target bifunctional [d4U]-butyne-[HI-236] **51**, which showed an impressive inhibitory activity ($\text{EC}_{50} = 0.25 \mu\text{M}$; HI-26 = $0.048 \mu\text{M}$; d4T = $1 \mu\text{M}$) against HIV-1 (IIIB) replication in MT-2 cell cultures using an MTT assay. The biological results suggest that the prototype compound behaves as an extended NNRTI.



Scheme 1.10 *Reagents and Conditions:* (i) alkyne **70c**, $(\text{PPh}_3)_4\text{Pd}$ (10%), CuI (50%) Et_3N (2 eq), DMF: THF (1: 2), rt, 4h, 69%; (ii) CF_3COOH , CH_2Cl_2 , 0°C ; (iii) $\text{EtN}(\text{i-Pr})_2$ followed by **49**, THF, rt/ over night, 60% for 2 steps; (iv) NaOMe (cat), MeOH , 0°C , 20 min, 51%.

In conclusion, most approaches have pursued the easier synthetic option of connecting the tether via the C-5' OH or N-3 of the nucleoside base. For the C-5 heterodimers, linker attachment has been achieved via a Pd(0) Sonogashira coupling (compounds **18** and **51**) or hydroxymethylation of uridine (compound **43a-d**). Most of the heterodimers have been designed as prodrugs linked with a cleavable tether, with the aim of regenerating the parent drugs once in the cell cytoplasm. Non-cleavable systems have as yet not suggested connection between the two sites to fulfil the conceptual objective of “mixed-site” inhibition, probably mainly as a result of poor choice of the spacer attachment.

1.16 OBJECTIVE OF THE STUDY

The use of combinations of different drugs as in HAART is designed to prevent resistant HIV strains by effectively suppressing viral replication, thus denying HIV the opportunity to produce new mutations. This principle holds provided that there is minimised cross-resistance between the drugs. NNRTIs act by slowing down the chemical step catalyzed by RT, and this retardation allows the two-step binding of NRTI to come to equilibrium leading to tighter binding of the nucleotide. The objective of this study was thus to join these concepts by synthesizing and evaluating HIV bifunctional non-cleavable double-drugs of the type NRTI-spacer-HI-236 in order to probe the possibility of “mixed-site” inhibition.

HI-236 was selected owing to its potency against wild-type and NNRTI resistant HIV-1 strains (carrying the NNRTI resistant mutations K103N, V106A and Y181C). Furthermore, the relative simplicity of its structure, ease of its synthesis and options for spacer attachment also made HI-236 an attractive NNRTI choice. The NRTI's chosen were d4T, which is currently used to treat HIV, as well as an acyclic nucleotide phosphonate based on the Tenofovir concept.

The site of attachment of the linker on the d4U (NRTI) was chosen as an alkynyl linker at the C-5 position on the pyrimidine ring of the base, since this was considered to exit the substrate binding site with anticipated low interference with base-pairing in DNA in accordance with the study by Ruth and Chen.¹⁴³ Also, linking at the C-5 position with a flexible linking chain of about 10Å has been reported by Arnold¹¹⁶ to permit the triphosphate to be generated and be incorporated into the nucleic acid.

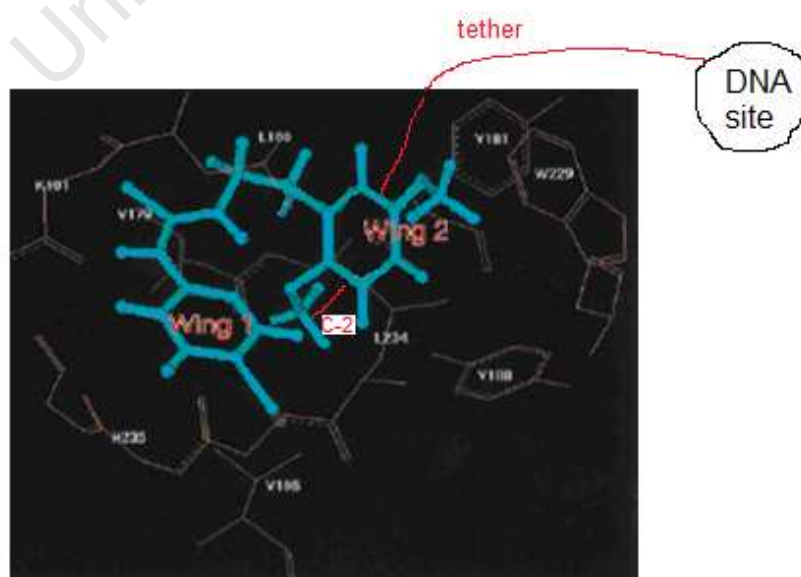


Figure 1.45 HI-236 docked into the HIV pocket.¹⁰⁷

On the HI-236 side, it was decided to extend at the C-2 phenolic oxygen for synthetic reasons as well as because of studies conducted by Uckun and co-workers^{107,144} regarding the binding mode of HI-236 in the RT pocket, which showed that the C-5-methoxy group forges cooperative C-H π interactions with the highly conserved W229, while the phenyl ring interacts with Y188. The C-2 methoxy group (labelled in Fig. 1.45) is positioned underneath the phenyl ring, pointing into available space near Y188 in Wing 2. Thus a tether connected to the C-2 methoxy position might plausibly point downwards and exit the front of the pocket making its way towards the substrate binding site as shown in Fig. 1.45. Note that the view in Fig. 1.45 is from the “back” of the pocket. A tether exiting the “front” would have to find its way to the substrate binding site shown in Fig. 1.45 to the “right” as one looks at the Figure. In reality, the DNA site is “behind” W229 shown at the “back” of the NNRTI pocket in Fig. 1.45. Varying the spacer lengths would be needed to probe the length needed to join the two sites.

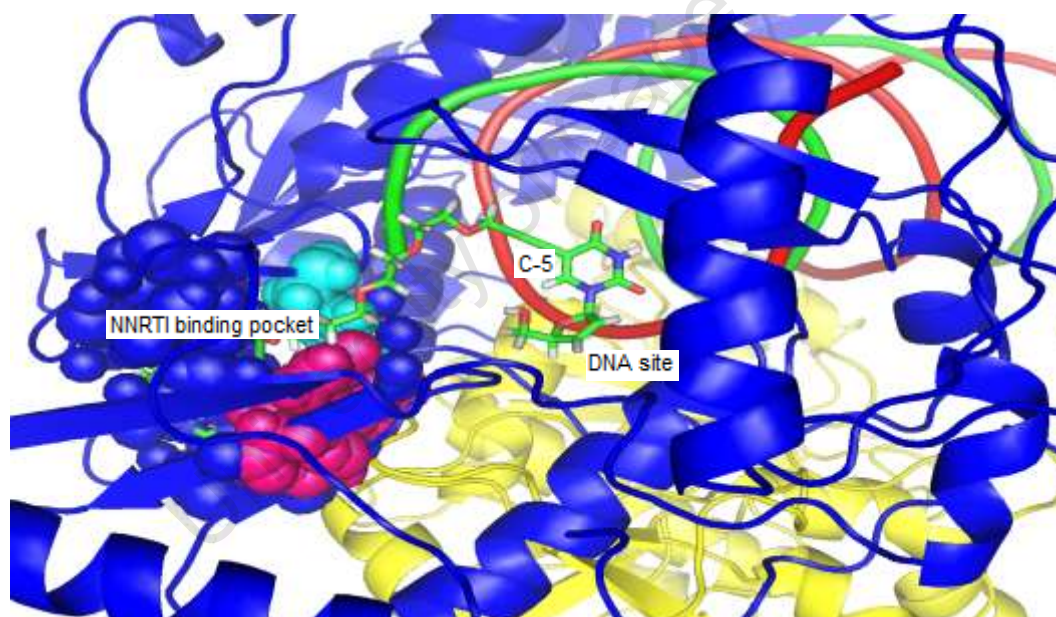


Figure 1.46 Shows a d4U-spacer-TMC-120 bifunctional exiting from the “back” of the NNRTI pocket.

Figure 1.46 also assists this visualisation and was generated in conjunction with a different system based on TMC-120 as the NNRTI from a sister project at University of Cape Town. It shows the tether exiting from the “back” of the pocket. In the HI-236 case, such an exit was not possible because of the way the tether was attached to HI-236. Thus the hope was that the tether might exit out of the “front” and make its way to the “right” towards the DNA site for NRTI.

Thus, the overall objectives of the project were the following:

- (i) Synthesize HI-236 derivatives substituted at the C-2 oxygen of the phenyl ring and evaluate them for their inhibitory activity against HIV-1 (IIIB) replication in MT-2 cell culture in order to fine-tune the activity of HI-236 as well as to establish a structure-relationship (SAR) between the spacer and activity.
- (ii) Synthesize and test a library of bifunctional [d4U]-spacer-[HI-236] derivatives varying the spacer length in order to establish a structure-activity relationship in the search for evidence of synergism between the two drugs and hence sites.
- (iii) Synthesize a phosphoramidate pro-drug of one of the bifunctionals in order to apply a pronucleotide strategy to this class of compound.
- (iv) To synthesize and study the influence of changing d4U as the NRTI component of the double-drug to an acyclic phosphonate modeled on the Tenofovir concept.

CHAPTER 2: C-2-ARYL O-SUBSTITUTED HI-236 DERIVATIVES AS NON-NUCLEOSIDE HIV-1 RT INHIBITORS

This thesis concerns the synthesis and biological evaluation of bifunctional inhibitors of the type [d4U]-spacer-[HI-236] shown in Figure 2.1.

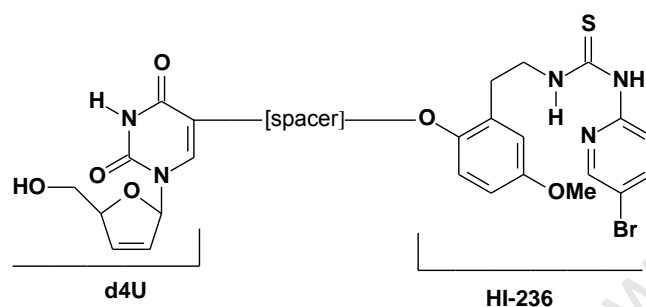


Figure 2.1 General formula [d4U]-spacer-[HI-236]

The main difference between this target and the others previously studied by other workers in the field was the choice of NNRTI as HI-236. This was made on the basis that HI-236 had emerged in the late 1990's as a potent inhibitor with a solid profile against resistant strains. Furthermore, HI-236 offered relatively attractive synthetic connection points, and the modeling data of it in the NNRTI pocket had been reported by Uckun¹⁴⁴ giving crucial insight into the all important question of where to attach the tether on the NNRTI so as to lead out of the pocket to the NRTI substrate binding site. The story of HI-236, though, is predated by that of the Phenethylthiazolylthiourea (PETT) derivatives, which were first synthesized by Bell and co-workers at the Eli Lilly Company and reported in 1995.¹⁰¹ Changing the thiazole ring to pyridine ring as *N*-(5-bromo-2-pyridinyl)-*N'*-(2-pyridylethyl)-thiourea (Trovirdine) resulted in enhanced activity and a detailed structural analysis of it carried out by the Uckun group in 1999 revealed abundant sterically usable space surrounding the pyridyl group as well as the ethyl linker.^{102,107} They postulated that an efficient use of this space would lead to more potent anti-HIV agents with higher affinity for the NNRTI binding pocket, and this resulted in several more potent derivatives including the highly potent HI-236,^{107,144} with a much superior inhibition profile in which the pyridyl ring of Trovirdine was replaced by a 2,5-dimethoxyphenyl group (Fig. 2.2a and Fig. 2.2b).

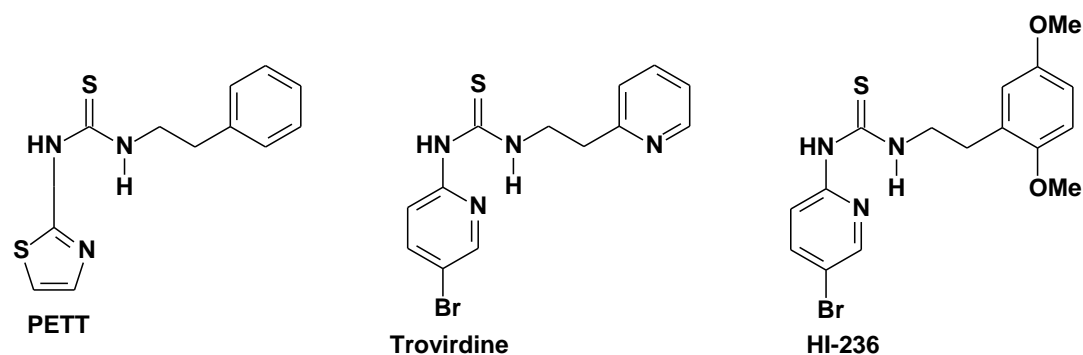


Figure 2.2a Structures of PETT, Troviridine and HI-236.

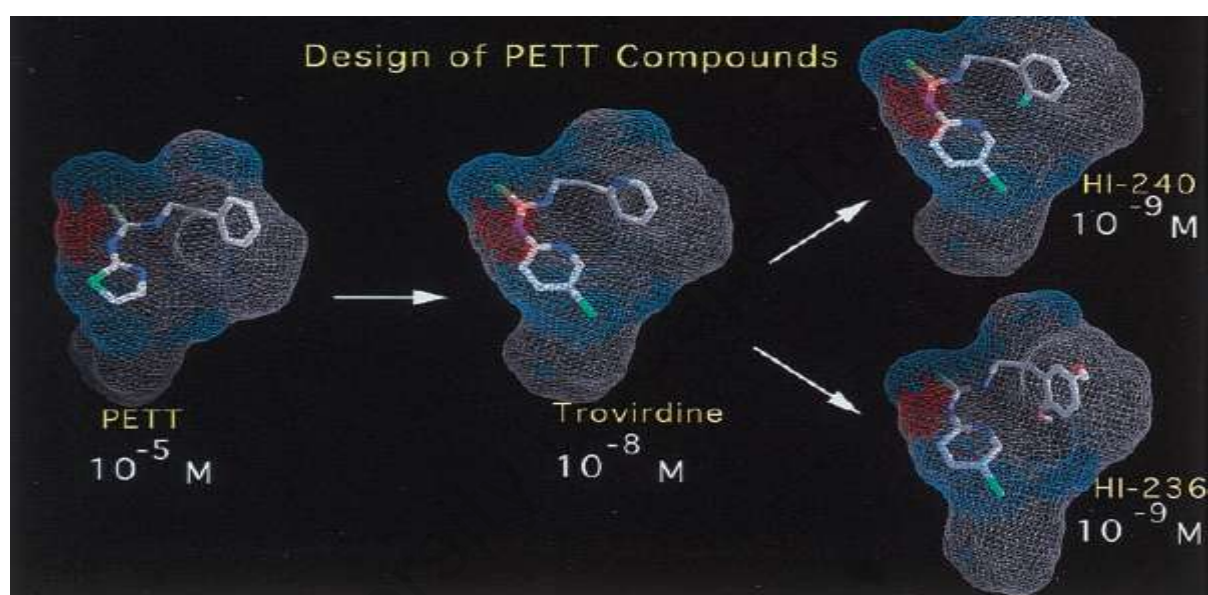


Figure 2.2b Design of PETT compounds from PETT to Troviridine as lead to HI-236. The IC_{50} values against HIV-1 replication of these compounds are shown below each compound. The surface of the composite binding pocket is color-coded for chemical preference: gray for hydrophobic regions, blue for polar regions, and red for hydrogen bonding regions.¹⁰⁷

2.1 Modeling of HI-236

Structural studies around HI-236 revealed, as with other PETT derivatives, that the thiourea portion interacts in Wing 1 toward the front of the pocket via H-bonding with K101.^{144,107} Conversely, the C-5-methoxy group forges cooperative C-H π interactions with the highly conserved W229, while the phenyl ring interacts with Y188. The methoxy group at C-2 was found to lie underneath the ethyl linker and was considered to occupy some of the vacant

spacer near Y188 in wing 2, an issue which assumes a greater weight of importance for the drug-resistant strains where there is an increase in the pocket size due to mutated residues of smaller size such as Y181C and Y188L. Figure 2.3 depicts HI-236 docked into the NNRTI pocket with the C-2 methoxy group positioned underneath the ring and pointing into available space.

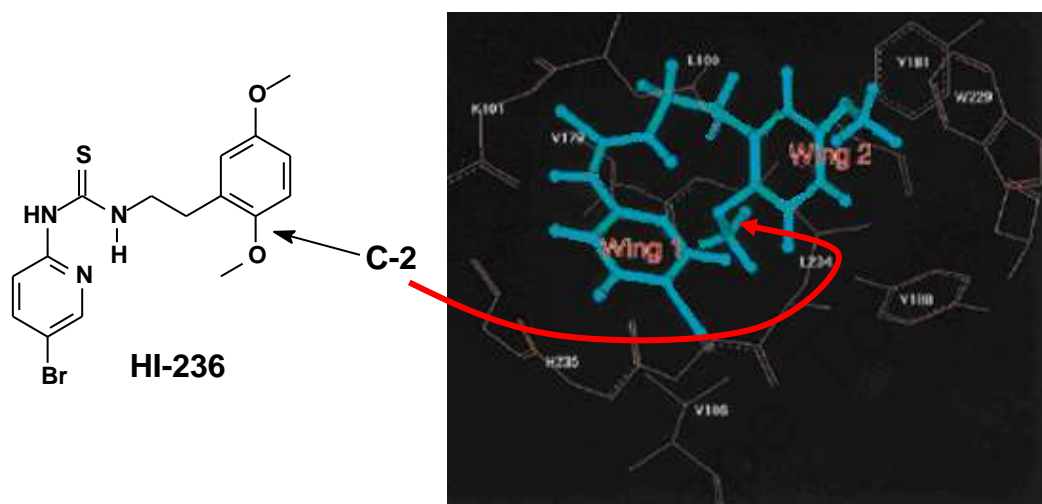
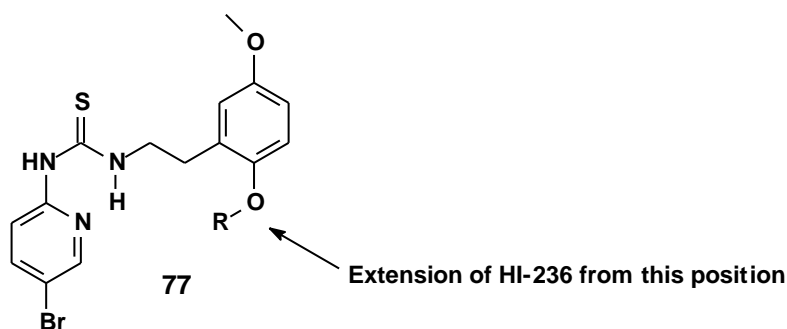


Figure 2.3 HI-236 docked into the HIV pocket.¹⁰⁷

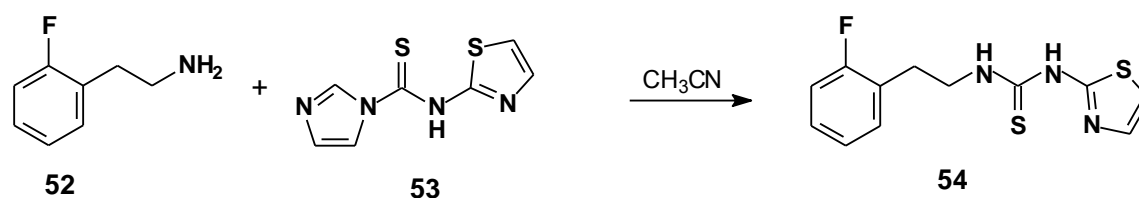
It was thus conjectured whether extending from this position might allow a tether to exit the pocket as already discussed in the objective. Thus, the first part of the study, it was decided to synthesize and evaluate the biological activity of a small library of C-2 tethered HI-236 derivatives, the objective being not only to shed light on NNRTI attachment at the C-2 oxygen for the bifunctional design, but also to probe the possibility of further binding in the region of the pocket just mentioned in an attempt to improve the activity of HI-236 even further. Tethers (R) attached to the C-2 phenolic oxygen were chosen to probe length, functionality and polarity (Table 2.1).

Table 2.1 HI-236 derivatives synthesized with different tethers (R).⁵

R	R	R
Me (HI-236)	CH ₂ 77a	CH ₂ 77b
CH ₂ CH ₂ 77c	CH ₂ CH ₂ CH ₂ 77d	CH ₂ 77e
CH ₂ 77f	MeO-C(=O)-CH ₂ 77g	N≡CH ₂ 77h
N≡CH ₂ CH ₂ CH ₂ 77i	BnO-CH ₂ 77j	CH ₂ O-CH ₂ 77k
CH ₂ O-CH ₂ -O-CH ₂ 77l	HO-CH ₂ 77m	HO-CH ₂ 77n
HO-CH ₂ -O-CH ₂ -CH ₂ 77o	HO-CH ₂ -O-CH ₂ -O-CH ₂ -O-CH ₂ -O-CH ₂ 77p	HO-CH ₂ -O-CH ₂ -[O-CH ₂ -O] ₃ -CH ₂ 77q

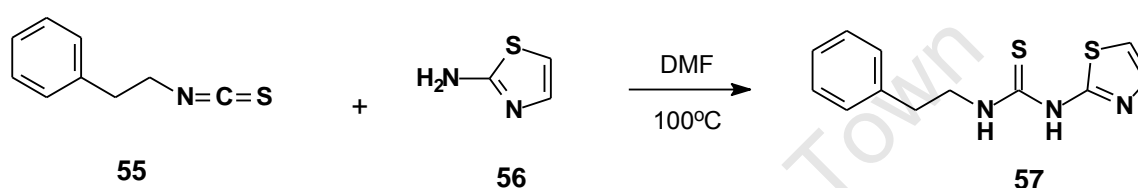
2.2 Overview on synthesis of the PETT derivatives

Phenethylthiazolylthiourea (PETT) compounds were first synthesized in 1995 by Bell *et al.*¹⁰¹ as lead inhibitors of HIV-1 RT, resulting in a structure-activity relationship profile involving various substituents in their structure. The PETT derivatives were synthesized according to two general methods. In the first route, thiourea analogue **54** (as a representative example) was prepared by condensation of the amine **52** with the thiocarbonyl reagent **53** derived from 2-aminothiazole and thiocarbonyldiimidazole (Scheme 2.1).



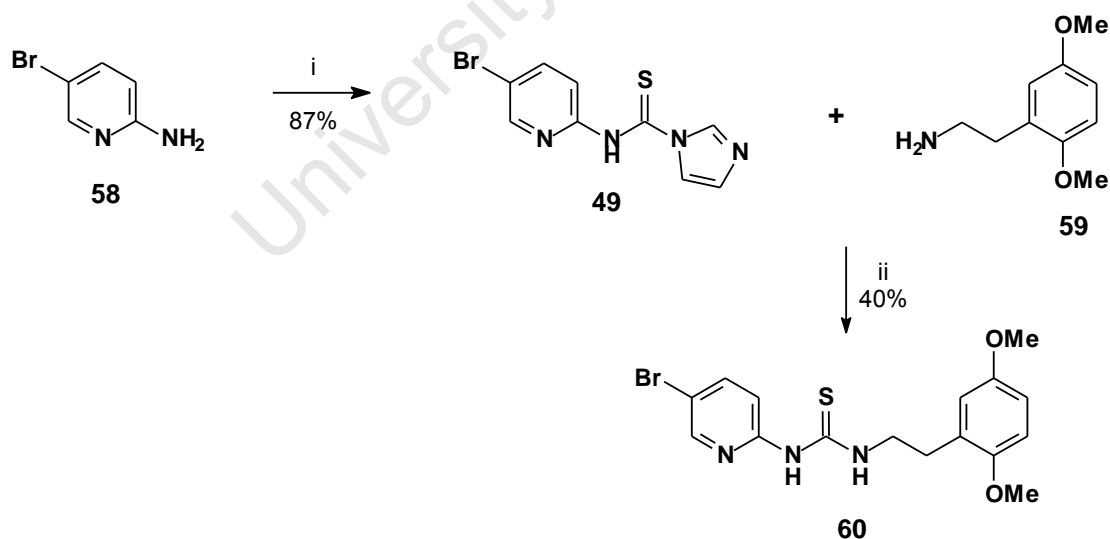
Scheme 2.1 Synthesis of PETT compounds from thiourea **53**.

The second method, exemplified by synthesis of thiourea analogue **57**, involved reacting an isothiocyanate such as phenethyl isothiocyanate **55** with a heterocyclic amine (2-aminothiazole) **56** (Scheme 2.2).



Scheme 2.2 Synthesis of PETT compounds from phenethyl isothiocyanate.

In Uckun's study,¹⁰² HI-236 **60** was synthesized according to the first method by high-temperature condensation of amine **59** with thiocarbonyl reagent **49** derived from 1,1'-thiocarbonyldiimidazole and 2-amino-5-bromopyridine **58** (Scheme 2.3).¹⁴⁵



Scheme 2.3 Reagents and Conditions: (i) 1,1'-thiocarbonyldiimidazole, acetonitrile, rt, 12-15h. (ii) DMF, 100°C , 16h.

2.3 Retrosynthetic analysis of HI-236 derivatives 77

The retrosynthetic analysis of the generic structure **77** (Fig. 2.4) in this project involved a similar set of disconnections to those for Uckun's HI-236 synthesis, and identified phenolic amine **66** as a key intermediate, which was readily available in multigram quantities using chemistry reported by Glennon^{146a} via a three-step sequence from commercially available 2-hydroxy-5-methoxybenzaldehyde **61**. In this project, amine **66** was isolated as its *N*-Boc carbamate **68**. Catalytic hydrogenolysis of **68** would furnish **69**, which was considered to be a key intermediate in the synthesis of the target molecules (**77a-q**) via alkylation.

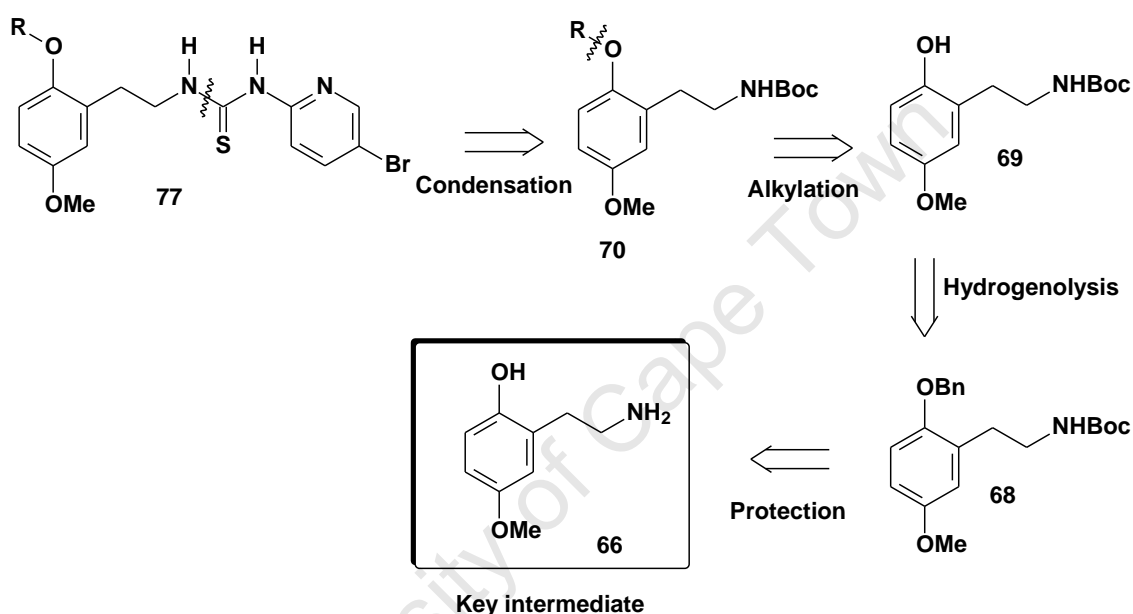
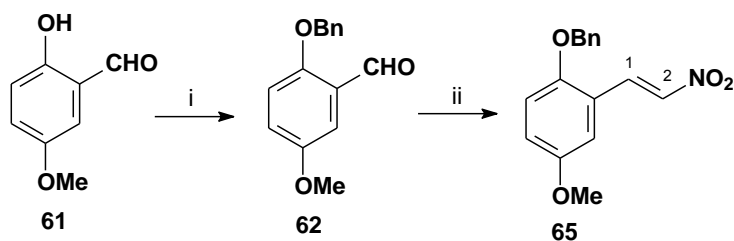


Figure 2.4 Retrosynthetic analysis of HI-236 derivatives.

Thus, for the actual synthesis, the phenolic hydroxyl group of aldehyde **61** was first protected so as to avoid complications with the phenolic hydroxyl group later in the synthesis. A benzyl ether protecting group was chosen in view of facile chemoselective removal, and conversion of **61** under standard phenolic benzylation conditions furnished **62** in excellent yield (Scheme 2.4). Its ¹H NMR spectrum displayed diagnostic peaks at δ_{H} 7.43 (5H, m) for the aromatic protons and a methylene singlet at δ_{H} 5.16 for the benzyl group, while its ¹³C NMR spectrum displayed corresponding signals at δ_{C} 136.3, δ_{C} 128.7, δ_{C} 128.3 and δ_{C} 127.4 for the aromatic carbons and δ_{C} 71.4 for the benzylic carbon. The melting point (44-46 °C) of the recrystallised sample was in agreement with the literature value of (47-48 °C),^{146b} and the sample returned an acceptable combustion microanalysis.



Scheme 2.4 Reagents and conditions: (i) BnBr, K₂CO₃, EtOH, reflux, 16 h; 94%; (ii) CH₃NO₂, NH₄OAc, 70 °C, 14 h; 80%.

In the next step, the benzylated aldehyde **62** was condensed with nitromethane as both solvent and reagent in a Henry reaction¹⁴⁷ at 70 °C using ammonium acetate as promoter to give nitrostyrene derivative **65** in 80 % yield as a bright-yellow solid after recrystallization from EtOH. The temperature of the reaction was carefully monitored to minimize by-product **67** formation as a result of subsequent Michael addition onto **65**.

Mechanistically, the ammonium acetate provides both a proton source to activate the carbonyl oxygen as well as a base to abstract the acidic proton on the nitromethane. The nitromethane anion formed then attacks the electrophilic carbonyl carbon generating intermediate **63**. Following proton transfer, an E1_{CB} elimination of water, which proceeds via a conformation in which NO₂ and the aromatic ring are anti-periplanar subsequently results in the formation of β-nitrostyrene **65** (Fig. 2.5) exclusively as an *E*-isomer. At higher temperatures, the nitrostyrene **65** acts as a Michael acceptor and undergoes a conjugate addition with a second nitromethane anion to form by-product **67**, which was not observed due to controlling the reaction temperature at 70 °C.

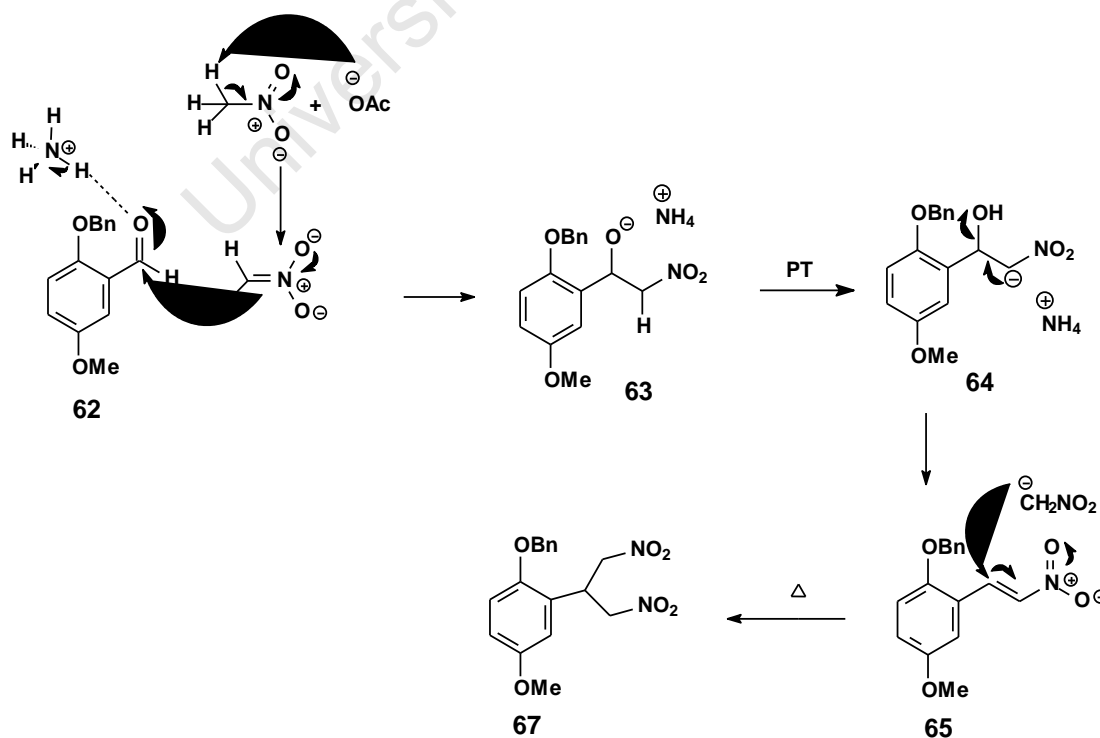
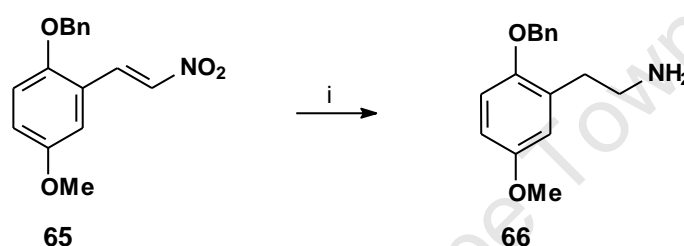


Figure 2.5 Mechanism of formation of nitrostyrene **65**.

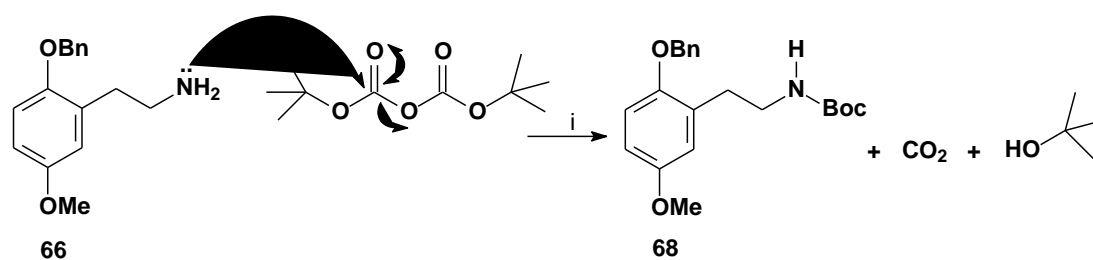
The spectroscopic and analytical data for **65** was in agreement with the assigned structure. Its ^1H NMR spectrum displayed two doublets at δ_{H} 8.17 and δ_{H} 7.83 for the nitroethenyl group with a large coupling constant $J_{1,2}$ of 13.6 Hz for an *E*-configuration, while its ^{13}C NMR spectrum displayed diagnostic signals at δ_{C} 136.1 for C-1 and δ_{C} 135.1 for C-2. The melting point of this compound was in agreement with the literature value.¹⁴⁷ The absence of formyl signals for both the ^1H (at δ_{H} 10.53) and ^{13}C (at δ_{C} 189.5) in the NMR spectra of **65** confirmed the assigned structure. The large coupling constant between H-1 and H-2 indicated a *trans*-configuration. If the protons had been *cis*, the coupling constant J_{cis} would have been around 10 Hz. Reduction of nitrostyrene **65** by lithium aluminum hydride (LAH) in refluxing THF yielded the amine **66** in good yield (Scheme 2.5).



Scheme 2.5 Reagents and conditions: (i) LiAlH_4 , THF, reflux, 4 h; 91%

The reaction could be followed by tlc towards the formation of a polar spot assigned as the amine. Conventional extractive work-up could not be pursued in view of the amine's water solubility. Thus, the work-up involved adding a saturated aq. Na_2CO_3 solution dropwise at 0°C . The precipitate formed was filtered and the filter-cake washed with large volumes of methanol, followed by complete evaporation of all solvent. As expected, the amine was very polar towards tlc, running with an $R_f = 0.3$ in an EtOAc/ MeOH (9:1) system. Thus it was not purified but used directly in the next step.

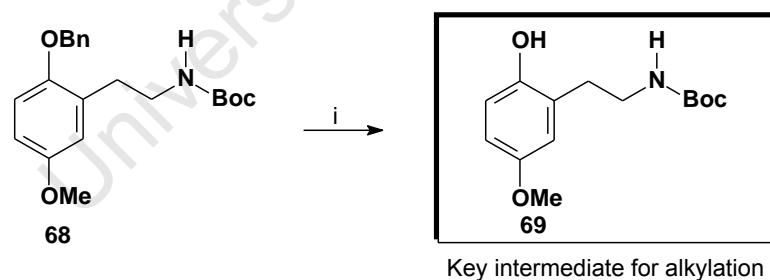
Protection of the amine **66** as a *N*-Boc carbamate **68** was considered to provide a more workable route to the desired thioureas in terms of the polarity of **68**. Also the protecting group would serve appropriately in subsequent steps including the Sonogashira coupling reaction. The Boc group is relatively stable under basic conditions since the carbonyl group is relatively hindered and its electrophilicity diminished due to mesomeric stabilization by oxygen and nitrogen. To this end, amine **66** was protected as its Boc-carbamate by reaction with *di-tert*-butyldicarbonate (1.2 equiv.) in acetonitrile at room temperature to give **68** in an overall 88% yield after purification by column chromatography (Scheme 2.6).



Scheme 2.6 Reaction condition and mechanism of formation of *N*-Boc carbamate **68**. (i) $(\text{Boc})_2\text{O}$, CH_3CN , rt, 20 h, 88%.

The ^1H NMR spectrum of **68** revealed the presence of a methyl singlet at δ_{H} 1.44 for 9H, and a downfield shift in the methylene protons adjacent to nitrogen at δ_{H} 3.40. The ^{13}C NMR spectrum of **68** revealed the presence of a carbamate carbonyl carbon at δ_{C} 155.9 and a methyl carbon (*t*-butyl) at δ_{C} 28.4. The presence of a carbonyl group was also confirmed by a stretch at 1703 cm^{-1} in the IR spectrum.

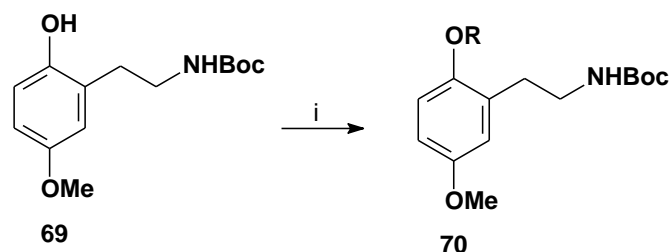
Hydrogenolytic debenylation of **68** in the presence of palladium-on-carbon in ethanol at room temperature led to phenol **69** in good yield (Scheme 2.7). The ^1H NMR spectrum of **69** revealed the absence of a benzylic methylene singlet at δ_{H} 5.04. The debenylation was also confirmed by its ^{13}C NMR spectrum, which showed only six aromatic carbons and no benzylic methylene carbons at δ_{C} 70.8. The IR spectrum of **69** displayed a diagnostic broad peak between $3457\text{--}3326\text{ cm}^{-1}$ for the hydroxyl stretch.



Scheme 2.7 Reagents and conditions: (i) H_2 , Pd/C, EtOH, rt, 5 h; 74%.

Initially, a range of short chains as tethers were selected to probe steric and electronic effects in the hydrophobic NNRTI pocket and the various groups are shown in Table 2.1 (**77a-i**) and Fig. 2.6 for the *N*-Boc derivatives (**70a-i**). Of particular interest was the incorporation of a triple bond in the chain not only to address the Sonogashira chemistry but also to probe the possibility of π - π stacking with aromatic residues in the pocket. Other functionalities included cyano and ester as groups as well as hydroxyl for probing hydrogen bonding interactions (**77g-n**).

For **70a-i**, the derivatives could be synthesized under standard alkylation conditions (Scheme 2.8) using a simple electrophile, which was readily available either commercially or via a one-step derivatisation (Fig. 2.6).



Scheme 2.8 Reagents and Conditions: (i) K_2CO_3 , CH_3CN , reflux, 20 h, with ROTs or RBr.

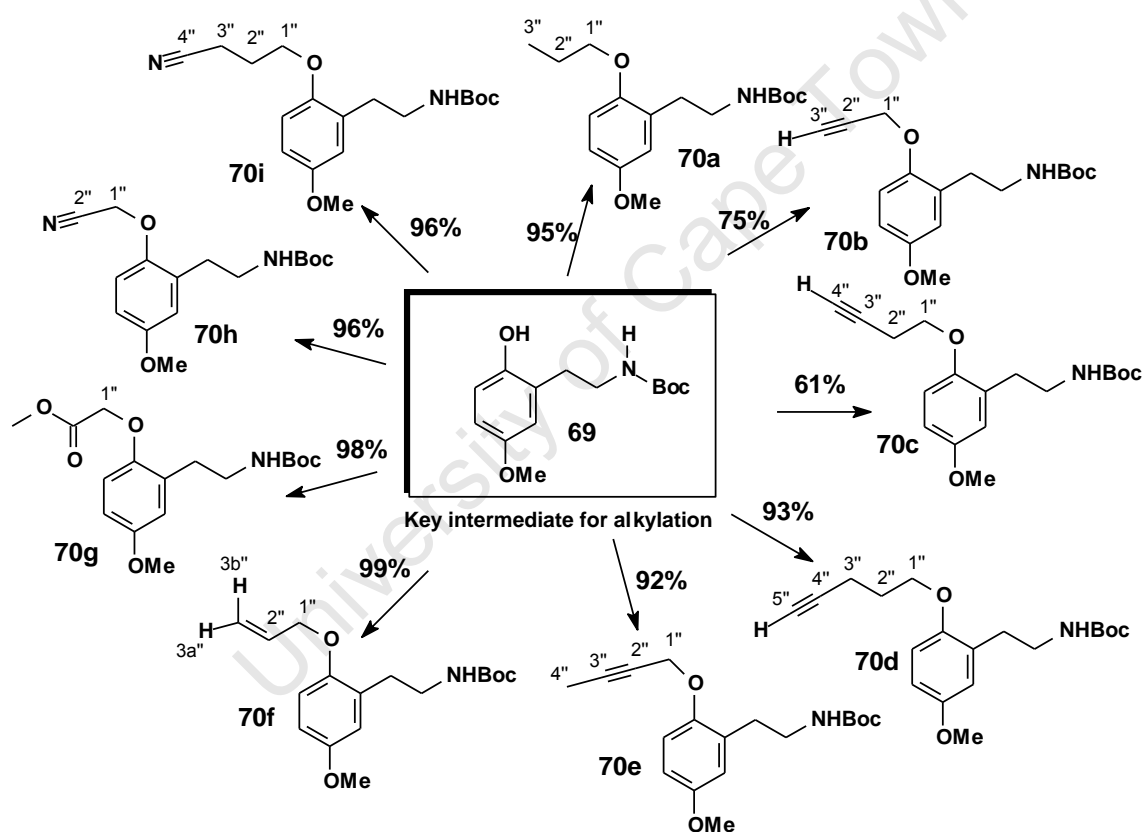


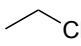
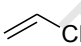
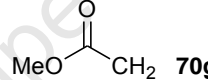
Figure 2.6 A library of oxy-alkylated *N*-Boc derivatives **70** (simple chain).¹⁴⁸

Thus, **69** was reacted with the appropriate tosylate or bromide (2.0 equiv.) electrophile using K_2CO_3 (4.0 equiv.) in acetonitrile at reflux for around 20 h. The reaction was monitored by tlc, and was easily chromatographed to give the desired product in excellent yield (Fig. 2.6).

A full spectroscopic analysis using 1H and ^{13}C NMR spectroscopy was carried out on each compound (**70a-i**) to return acceptable data as well as microanalytical and IR data. The 1H NMR spectra for compounds **70b-d** displayed a signal for the alkyne proton at around δ_H 2.03

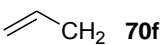
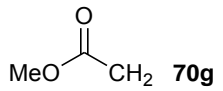
which appeared as a triplet with a small coupling constant of $J = 2.7$ Hz, due to allylic coupling with the propargylic methylene protons. The ^{13}C NMR spectra of **70b-d** as well as their IR spectra similarly gave diagnostic signals for the triple bond around 80 and 70 ppm and 3300 ($\equiv\text{CH}$) and 2120 ($\text{C}\equiv\text{C}$) respectively. Similarly, the other side chains could be easily identified in their ^1H and ^{13}C NMR spectra in terms of normal resonances for the allyl group and the methyl ester. The nitriles **70h** and **70i** could be identified from their IR $\text{C}\equiv\text{N}$ stretching frequencies at 2240 cm^{-1} as well as relaxed ^{13}C NMR resonances for the cyano carbon at around 110 ppm. Table 2.2 summarizes NMR data for H-1" and C-1" as the first carbon of the alkylated chain of the various derivatives.

Table 2.2 ^1H and ^{13}C NMR chemical shifts for H-1" and C-1" for compounds **70a-i**

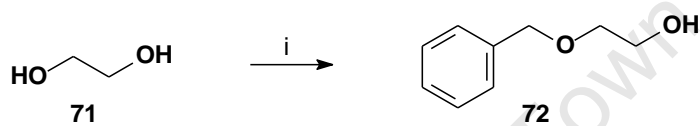
R	δ_{H} H-1"	δ_{C} C-1"	R	δ_{H} H-1"	δ_{C} C-1"
 70a	3.88	70.2	 70f	4.50	69.5
$\equiv\text{—CH}_2$ 70b	4.65	56.7	 70g	3.40	66.0
$\equiv\text{—CH}_2\text{CH}_2$ 70c	4.05	66.8	$\text{N}\equiv\text{—CH}_2$ 70h	4.73	54.9
$\equiv\text{—CH}_2\text{CH}_2\text{CH}_2$ 70d	4.02	66.9	$\text{N}\equiv\text{—CH}_2\text{CH}_2\text{CH}_2$ 70i	4.03	66.3
$\text{—}\equiv\text{—CH}_2$ 70e	4.60	57.3			

Finally, microanalytical data for the compounds that were isolated as solids, confirmed a correct molecular formula, Table 2.3.

Table 2.3 Elemental analysis results for compounds **70f**, **70g** and **70i**.

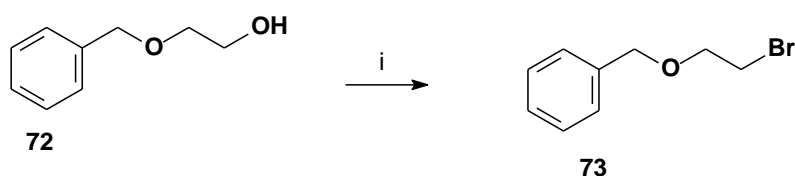
Atom	 70f		 70g		$\text{N}\equiv\text{—CH}_2\text{CH}_2\text{CH}_2$ 70i	
	Calculated	Experimental	Calculated	Experimental	Calculated	Experimental
C	66.43%	66.41%	60.16%	60.37%	64.65%	63.62%
H	8.20%	8.21%	7.16%	7.36%	7.84%	7.82%
N	4.56%	4.40%	4.13%	3.91%	8.38%	8.06%

In the second set of derivatives, the electrophile needed to be prepared (**77j-q**) from the commercially available diol. For **70j**, which could be used to prepare **70k** and **70m**, the synthesis began with mono-protection of ethylene glycol **71** *via* alkylation with benzyl bromide in tetrahydrofuran using NaH as base at room temperature, following the method described by Marshall *et. al.*¹⁴⁹ to afford **72** in 49% yield (Scheme 2.9). The product was easily isolated by distillation (bp: 98-103 °C/0.7 mm Hg), and although obtained in only a moderate yield, the mono-benylation could be carried out on a large scale. The presence of a benzyl group in the product was confirmed by the ¹H NMR spectrum, which revealed aromatic protons integrating for 5 protons resonating at δ_{H} 7.36 as well as methylene protons resonating at δ_{H} 4.56. The ¹³C NMR spectrum displayed a methylene carbon at δ_{C} 73.3 as well as the appearance of four aromatic singlets.



Scheme 2.9 Reagents and Conditions: (i) BnBr, NaH, THF, reflux, 20 h; 49%

Treatment of alcohol **72** with carbon tetrabromide and triphenylphosphine in methylene chloride smoothly yielded the bromide **73** in 92% yield (Scheme 2.10). Isolation involved evaporating the solvent and purifying the crude product directly by column chromatography. Mechanistically, the reaction of triphenylphosphine with carbon tetrabromide generates a bromophosphonium ion *in situ* which then reacts with the alcohol to give an alkoxyphosphonium ion (Fig. 2.7). The phosphonium ion intermediate then undergoes nucleophilic attack by the bromide ion, displacing triphenylphosphine oxide. The driving force for the cleavage of the C-O bond is the formation of the strong phosphine oxide bond (P=O). The ¹H NMR spectrum of compound **73** revealed the disappearance of the hydroxyl proton at δ_{H} 2.58 in **72**, while its ¹³C NMR spectrum revealed an upfield shift of the carbon at C-1 from 61.8 for **72** to δ_{C} 30.4 in **73**, thus confirming that substitution by bromine had taken place.



Scheme 2.10 Reagents and Conditions: (i) PPh₃, CBr₄, CH₂Cl₂, 0 °C, 30 min; 92%.

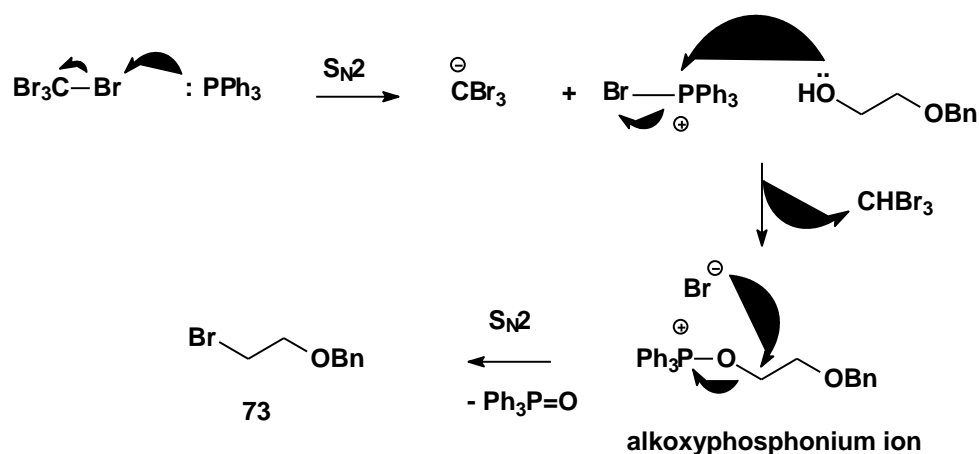
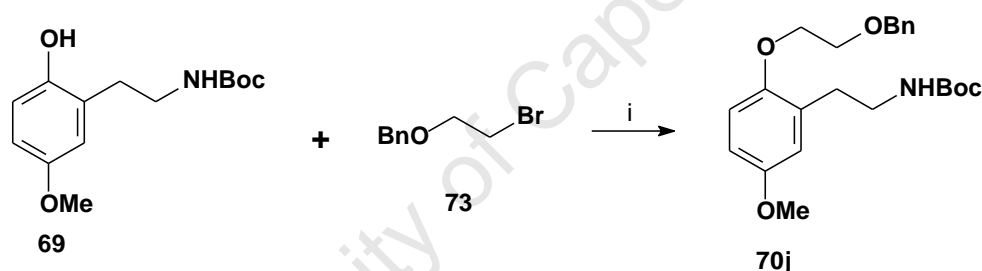


Figure 2.7 Mechanism for formation of bromide **73**.

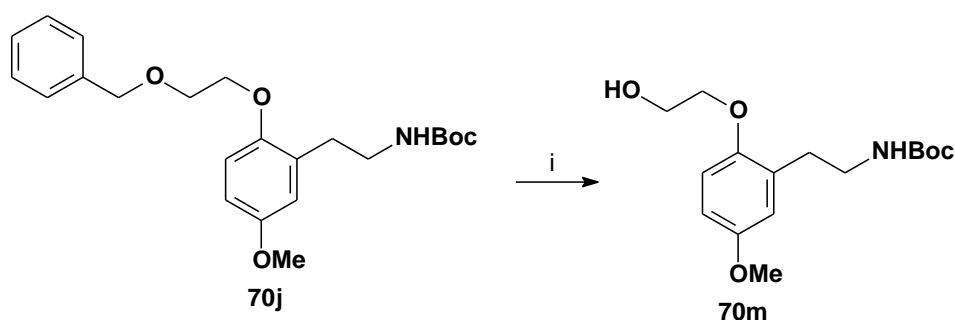
With electrophile **73**¹⁸⁰ in hand, nucleophilic substitution of it by phenol **69** in the presence of K_2CO_3 as a base in acetonitrile was carried out to afford the desired compound **70j** smoothly in a good isolated yield (85%) (Scheme 2.11).



Scheme 2.11 Reagents and Conditions: (i) K_2CO_3 , CH_3CN , reflux, 20 h; 85%.

The ^1H NMR spectrum of alkylated carbamate **70j** revealed a downfield shift of the proton α to bromine at δ_{H} 3.51 for the bromide **73** to δ_{H} 4.01 as well as the presence of signals for the phenolic moiety. The ^{13}C NMR for **70j** displayed a downfield shift of the carbon α to bromine at δ_{C} 30.4 for the bromide **73** to δ_{C} 68.7, thus confirming that the alkylation had taken place.

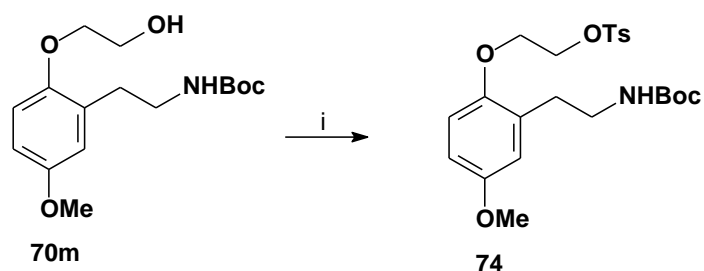
After the C-2 phenolic alkylation reaction, compound **70j** was submitted to hydrogenolytic debenzylation using 10% palladium-on-carbon catalyst in ethanol under hydrogen gas at rt for 18 h. Column chromatography gave the desired alcohol **70m** in an excellent yield (93%) (Scheme 2.12).



Scheme 2.12 Reagents and Conditions: (i) H₂, Pd/C, EtOH, rt, 18 h; 93%

The ¹H NMR spectrum of **70m** revealed the disappearance of five aromatic protons and the singlet benzylic methylene peak. In addition, there was the appearance of a hydroxyl proton as a broad singlet resonating at δ_{H} 1.25, while the ¹³C NMR spectrum of **70m** revealed the disappearance of four aromatic singlets and the methylene singlets at δ_{C} 73.2. The presence of the hydroxyl group of **70m** was also confirmed by the IR spectrum, which revealed a stretch around 3681-3449 cm⁻¹.

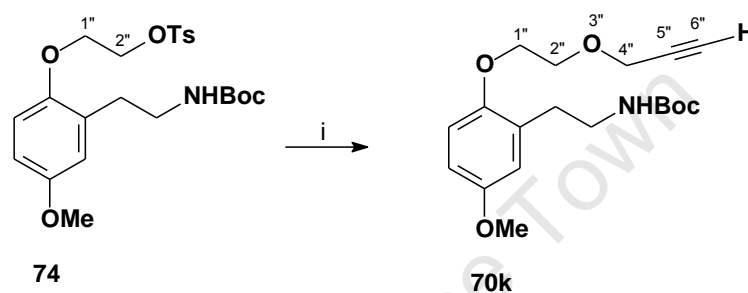
With alcohol **70m** in hand, three possible reactions were considered for the conversion of alcohol **70m** to alkyne **70k**. The first involved direct alkylation with propargyl bromide to furnish alkyne **70k** in a single step. The second strategy relied on Mitsunobu coupling of propargyl alcohol with **70m**. The last strategy was conversion of the hydroxyl group to a good leaving group, in this case a tosylate, followed by substitution with propargyloxide anion. The second method was attempted first and resulted in the desired target in low yield. Of the other two methods, it turned out to be more efficient to substitute with propargyloxy anion, rather than alkylate with propargyl bromide, probably due to the softness of propargyloxy anion. Thus, the hydroxyl group on **70m** was converted to its tosylate **74** in a good yield (77%) by reacting it with *p*-toluenesulfonyl chloride in the presence of triethylamine and a catalytic amount of DMAP in methylene chloride for 16 h at room temperature (Scheme 2.13).



Scheme 2.13 Reagents and Conditions: TsCl, Et₃N, DMAP, CH₂Cl₂, 0 °C-rt, 16 h; 77%.

Evidence for the formation of the tosylate **74** was obtained from the ^1H and ^{13}C NMR spectra which confirmed the appearance of four aromatic protons as an AB doublet pair (J_{AB} 8.2 Hz) resonating at δ_{H} 7.80 and δ_{H} 7.34 as well as a methyl singlet at δ_{H} 2.43. The presence of additional aromatic signals in the ^{13}C NMR spectrum further confirmed the presence of a tosylate group. The appearance of a sulfonate (O-SO_2^-) group was also confirmed by a stretch in the IR spectrum at 1176 cm^{-1} .

Alkylation of tosylate **74** then processed successfully in the presence of NaH and a large excess of propargyl alcohol in THF at reflux. An aqueous work-up followed by column chromatography furnished the alkyne **70k** in a good yield (77%) (Scheme 2.14).



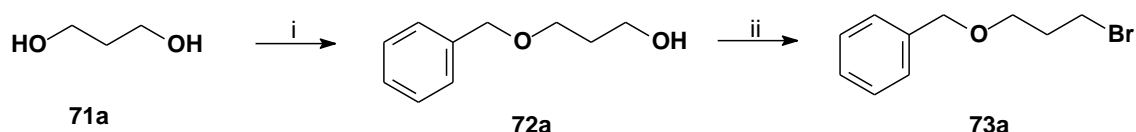
Scheme 2.14 Reagents and Conditions: (i) Propargyl bromide, NaH, reflux, 20 h; 77%.

The ^1H NMR spectrum of compound **70k** revealed an upfield shift for the H-2'' protons in tosylate **74** at δ_{H} 4.35 to δ_{H} 3.88 in the alkyne **70k** as well as the disappearance of aromatic peaks for the tosylate and the methyl singlet. The ^{13}C NMR of **70k** displayed diagnostic signals around δ_{C} 79.5 and δ_{C} 74.7 for the alkyne carbons, thus confirming that alkylation had taken place. The presence of an alkyne was further confirmed by the IR spectrum, which displayed a weak signal around 3304 cm^{-1} for the $\equiv\text{CH}$ stretch as well as a weak signal around 2123 cm^{-1} for the alkyne $\text{C}\equiv\text{C}$ stretch.

Similarly, for **70n**, the same methodology was used to elongate the chain by one more carbon in order to investigate the H-bonding effect. Thus mono-benylation of propane-1,3-diol **71a** using the standard procedure above gave the desired product **72a** in 37% after column chromatography (Scheme 2.15). The product structure was confirmed using ^1H and ^{13}C NMR spectroscopy, which revealed a new benzyl group.

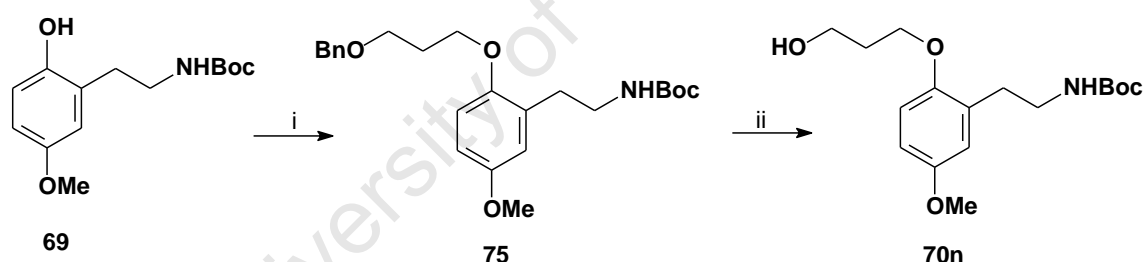
The mono-benzylated glycol **72a** was then converted to its bromide **73a** using carbon tetrabromide in methylene chloride as before to give the desired product in 91% yield (Scheme 2.15). Once again, the ^1H NMR spectrum of compound **73a** revealed the disappearance of the hydroxyl proton at δ_{H} 2.56, while its ^{13}C NMR spectrum revealed an

upfield shift of the carbon at C-1 from δ_{C} 61.4 to **72a** to δ_{C} 33.0 in **73a**, supporting the structure **73a**.



Scheme 2.15 Reagents and Conditions: (i) BnBr, NaH, THF, reflux, 20 h; 37% (ii) PPh₃, CBr₄, CH₂Cl₂, 0 °C, 30 min; 91%.

Using the standard alkylation conditions (K₂CO₃ as a base in acetonitrile at reflux) for nucleophilic substitution of **73a** by phenol **69** afforded the desired product **75** in an excellent yield (100%) after column chromatography (Scheme 2.16). All the expected resonances were observed in much the same positions as for compound **70j** (Scheme 2.11). Its ¹H NMR spectrum revealed a downfield shift of the protons α to bromine at δ_{H} 3.55 for the bromide **73a** to δ_{H} 4.04 as well as the presence of signals for the phenolic moiety. The ¹³C NMR spectrum of **75** displayed a downfield shift of the carbon α to bromine at δ_{C} 33.0 for the bromide **73a** to δ_{C} 66.9, thus confirming that alkylation to **75** had taken place.

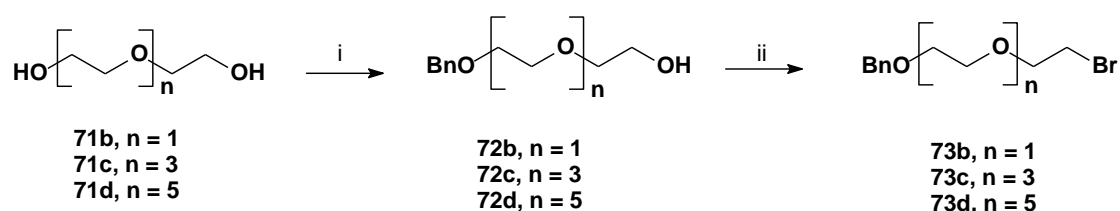


Scheme 2.16 Reagents and Conditions: (i) **73a**, K₂CO₃, CH₃CN, reflux, 20 h; 100%. (ii) H₂, Pd/C, EtOH, rt, 18 h; 93%.

75 was subjected to hydrogenolytic debenzoylation using 10% palladium-on-carbon catalyst in ethanol under hydrogen gas to give the alcohol **70n** as the desired product in 93% (Scheme 2.16). Similar trends in the ¹H and ¹³C NMR spectra of **70n** were noted as **70m** containing the shorter tether.

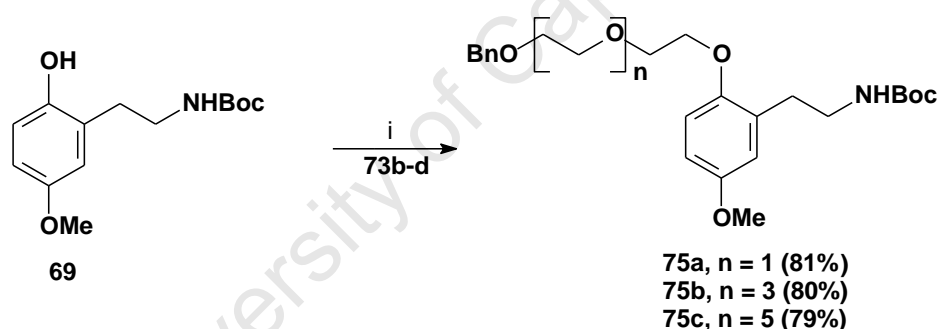
The methodological procedures just described were used to prepare the remaining elongated derivatives **77l**, **77o**, **77p** and **77q**. Once again, the mono-protection of diols **71b-d**, were carried out using the benzylation to give the desired products **72b-d** (Scheme 2.17). ¹H and ¹³C NMR spectroscopy data for each compound **72b-d** confirmed benzylation had occurred.

Subsequently, alcohols **71b-d** were converted into their bromides using carbon tetrabromide and triphenylphosphine as described before to give the desired products **73b-d**, whose spectroscopic data were consistent with previous trends.



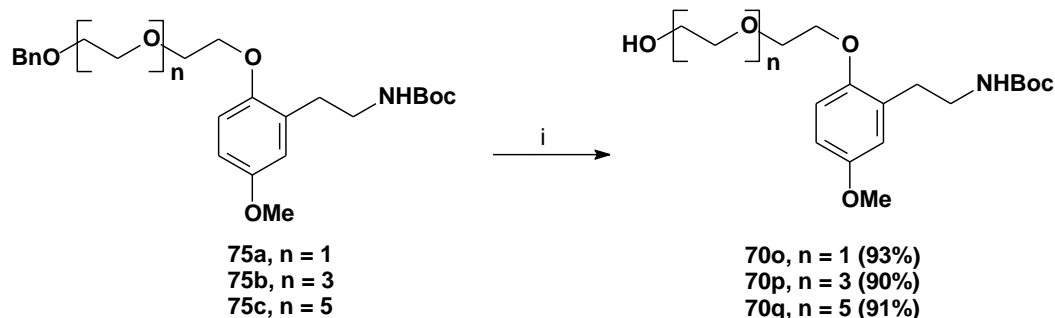
Scheme 2.17 Reagents and Conditions: (i) BnBr, NaH, THF, reflux, 20 h; (n = 0, 44%), (n = 3, 39%), (n = 5, 38%); (ii) PPh₃, CBr₄, CH₂Cl₂, 0 °C, 30 min; (n = 0, 91%), (n = 3, 88%), (n = 5, 77%).

Once again, C-2 O-alkylation of **69** with bromides **73b-d** employing K₂CO₃ in refluxing CH₃CN as described before afforded the alkylation products **75a-c** in a good yield as shown in Scheme 2.18. A full spectroscopic analysis using ¹H and ¹³C NMR spectroscopy was carried out on each compound to return acceptable data. Mass spectrometry and IR were also used.



Scheme 2.18 Reagents and Conditions: (i) **73b-d**, K₂CO₃, CH₃CN, reflux, 20 h.

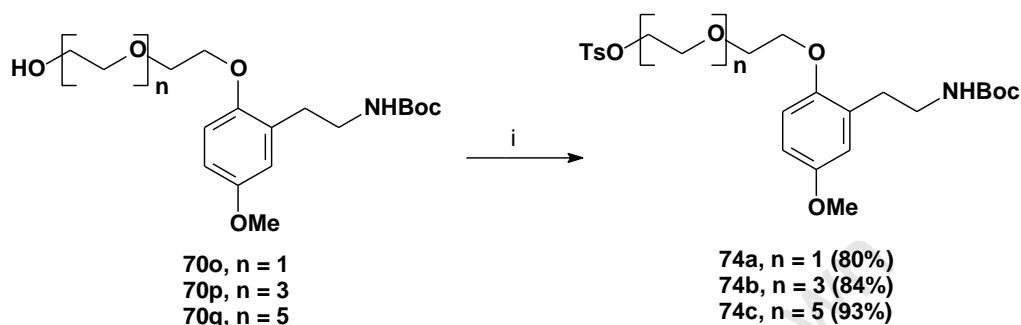
Carbamates **75a-c** were then debenzylated using 10% palladium-on-carbon catalyst in ethanol under hydrogen gas as before to afford desired alcohols **70o-q** as shown in Scheme 2.19 in an overall yield of about 90%.



Scheme 2.19 Reagents and Conditions: (i) H₂, Pd/C, EtOH, rt, 18 h.

Similar trends for **70o-q** as for **70m,n** in the ^1H and ^{13}C NMR spectra were noted which, provided sufficient evidence that debenzoylation had taken place.

For the Sonogashira coupling reaction which will be discussed later, alcohols **70o-q** were tosylated and then converted to the desired alkynes **70i, r, s** (Scheme 2.20 and Scheme 2.21) as described before in Scheme 2.13 and Scheme 2.14.

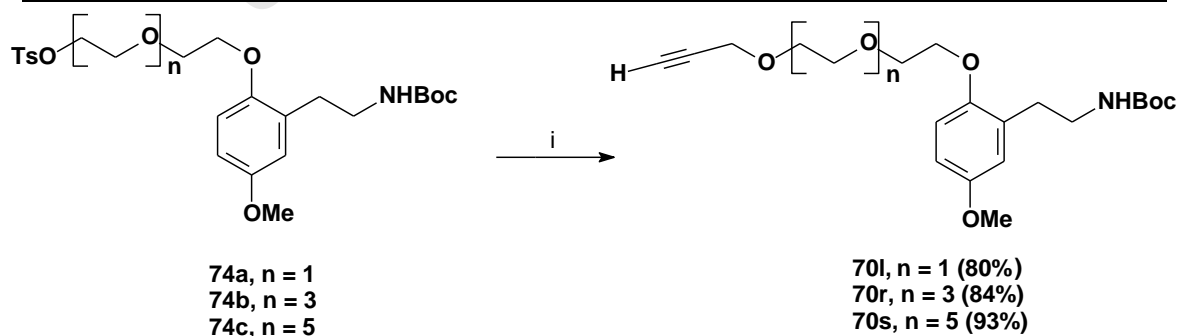


Scheme 2.20 Reagents and Conditions: TsCl, Et₃N, DMAP, CH₂Cl₂, 0 °C-rt, 16 h.

The ^1H and ^{13}C NMR for **74a-c** returned the correct number of the resonances in each case, while HRMS (ES/I) as shown in Table 2.4 for **74a-c** was used to confirm correct molecular formula to four decimal places.

Table 2.4 High resolution mass spectrum HRMS(ES/I) observed for **74a-c**.

Compound	Mass (experimental)	Mass (calculated)
74a ($n = 1$)	509.2067 (M^+)	509.2083 (M^+)
74b ($n = 3$)	598.2673 ($M^+ + H$)	598.2686 ($M^+ + H$)
74c ($n = 5$)	686.3192 ($M^+ + H$)	686.3210 ($M^+ + H$)



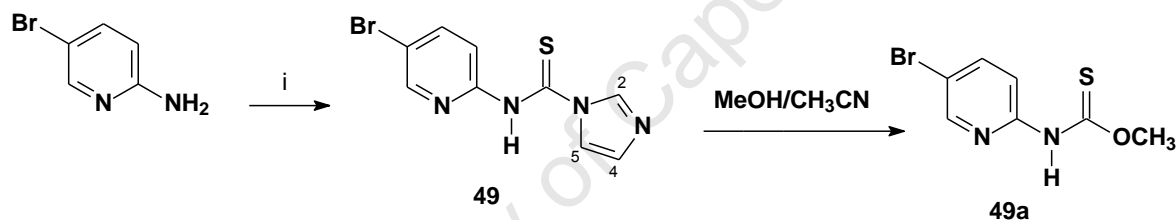
Scheme 2.21 Reagents and Conditions: (i) Propargyl alcohol, NaH, THF, reflux, 20 h.

These compounds **70i**, **70r** and **70s** were fully characterised by NMR, IR and high resolution mass spectrometry. The IR spectra of these compounds indicated characterization peak for

(C≡C) around V_{\max} 3309-3304 cm^{-1} and for $\equiv\text{CH}$ around V_{\max} 2123-2116 cm^{-1} . The ^1H and ^{13}C NMR spectra data for **70l**, **70r** and **70s** revealed the disappearance of the aromatic peaks as well as the appearance of the alkyne signals, thus, confirming that alkylation had taken place.

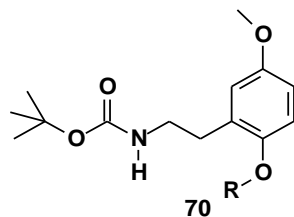
The end-game of HI-236 derivatives **77**

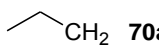
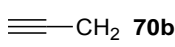
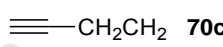
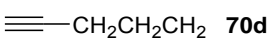
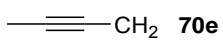
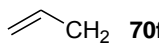
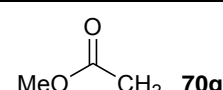
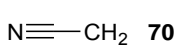
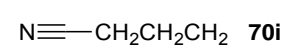
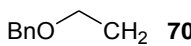
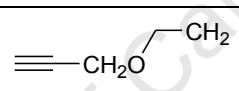
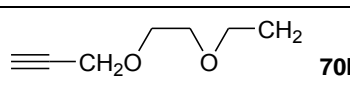
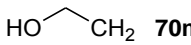
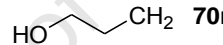
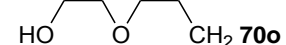
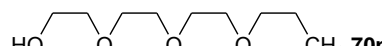
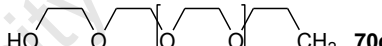
To complete the synthesis of the targets **77** required Boc deprotection to the amine and condensation with thiourea reagent **49**. As described by the Eli Lilly group,¹⁰¹ **49** was synthesized by condensation of 2-amino-5-bromopyridine with 1,1'-thiocarbonyl diimidazole in CH_3CN at room temperature for 20 h (Scheme 2.22). The precipitate formed was filtered to give **49** in good yield, which was recrystallized from methanol/ CH_3CN . This treatment resulted in substitution of the imidazole group by methoxy to form **49a** as evidenced by ^1H NMR. Therefore, the material was used directly without further purification.



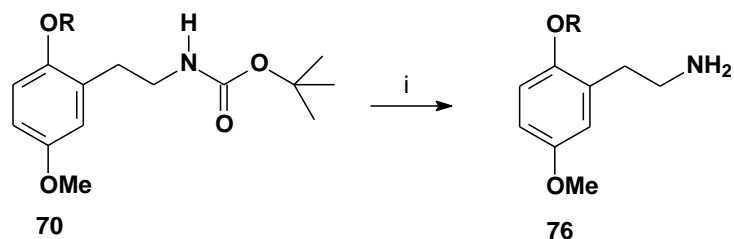
Scheme 2.22 Reagents and Conditions: (i) 1,1'-Thiocarbonyldiimidazole, CH_3CN , rt, 20 h; 92%.

The ^1H NMR spectrum of compound **49** displayed the following diagnostic peaks: a singlet at δ_{H} 7.79 for H-2 of the imidazole ring and a broad singlet at δ_{H} 10.19 for the NH proton. The presence of a carbamate carbonyl was indicated by the ^{13}C NMR spectrum, which revealed a downfield peak at δ_{C} 176.8 (C=S).

Strategy for deprotection and condensation of *N*-Boc derivatives **70**Table 2.5 *N*-Boc derivatives synthesized with different tethers (R).⁵

R	R	R
 70a	 70b	 70c
 70d	 70e	 70f
 70g	 70h	 70i
 70j	 70k	 70l
 70m	 70n	 70o
 70p	 70q	

Deprotection of *N*-Boc derivatives **70** show in Table 2.5 were accomplished with trifluoroacetic acid in methylene chloride at 0 °C for 1-3 h to provide the desired amines **76** (scheme 2.23).

Scheme 2.23 Reagents and Conditions: (i) CF₃COOH, DCM, 0 °C, 1-3 h.

The tlc revealed complete deprotection to a polar amine spot, and in view of the amine's anticipated water solubility, the final step was conducted without using an aqueous work-up.

Thus, following complete removal of all volatiles including any excess trifluoroacetic acid, Hünig's base ($\text{EtN}(\text{i-Pr})_2$) was added to liberate the free amine.

The mechanism for deprotection of the Boc group involves protonation of the carbonyl oxygen to form intermediate **I** (Fig. 2.8), which fragments with elimination of a stable *tert*-butyl carbocation **III** via an E1 mechanism to give carbamic acid **II**, which undergoes decarboxylation to give the desired amine. The reaction is driven by the relative stability of the *tert*-butyl cation **III**.

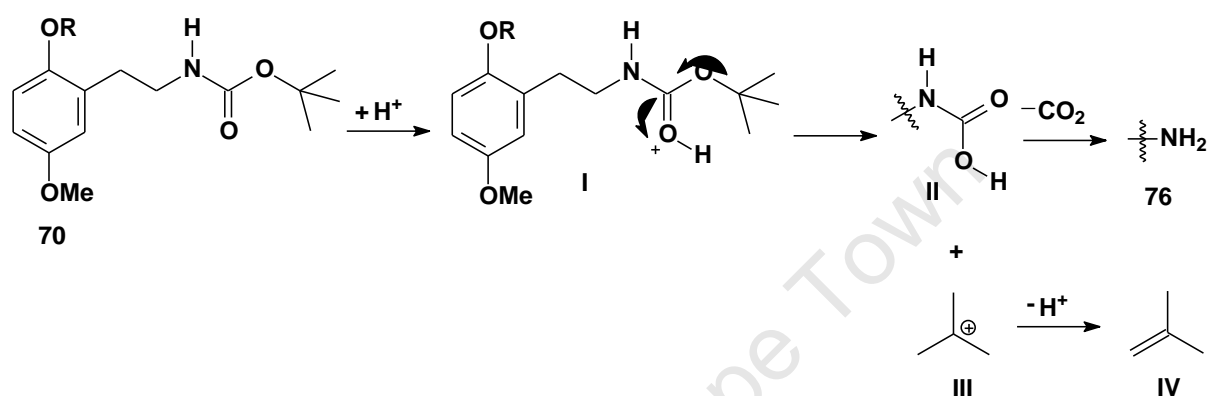
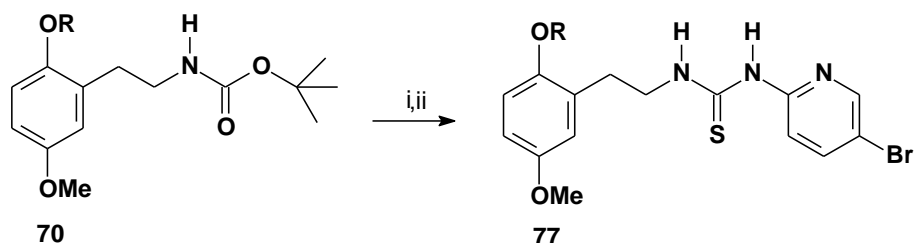


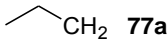
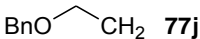
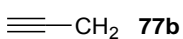
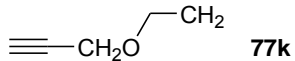
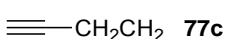
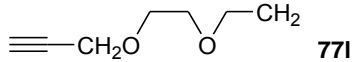
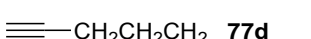
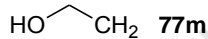
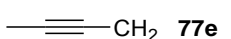
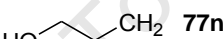

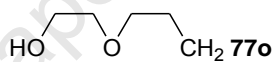
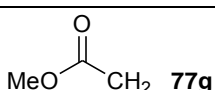
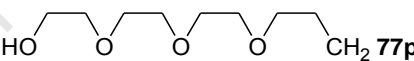
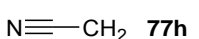
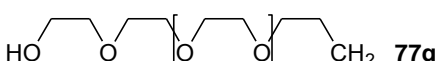

Figure 2.8 Mechanism for the deprotection of the Boc protecting group.

Subsequently, condensation between the amine and thiourea reagent **49** could be realized in DMF at 100 °C as described by Bell and co-workers¹⁰¹ to afford the targets **77** in an overall yield of around 30% for the two steps (Scheme 2.24). However, later on, it was discovered that condensation could be carried out under much milder conditions in THF or DMF at room temperature to increase the two-step yield to around 60% as shown in Table 2.6. Some of the targets were isolated by silica-gel column chromatography as crystalline solids that were crystallized to a constant, sharp melting point to return acceptable combustion analysis data.



Scheme 2.24 Reagents and Conditions: (i) CF_3COOH , DCM, 0 °C, 1-3 h; (ii) $\text{EtN}(\text{i-Pr})_2$, 0 °C, 10 min, followed by thiourea **49**, DMF at 100 °C (**77b**, **77c**) and THF at rt, 20 h.

Table 2.6 Two-step yield for Compound **77** from **70**.¹⁴⁸

R	Yield%	R	Yield%
 77a	65	 77j	58
 77b	17 ^a	 77k	62
 77c	25 ^a	 77l	60
 77d	69	 77m	65
 77e	60	 77n	51
 77f	67	 77o	62
 77g	50	 77p	63
 77h	68	 77q	52
 77i	53		

^a DMF at 100 °C; others involved THF at rt.

A full spectroscopic analysis using ¹H and ¹³C NMR spectroscopy was carried out on each derivative to return acceptable data. Notably, the aromatic region in the ¹H NMR spectra provided convenient markers for the aromatic and heteroaromatic rings to demonstrate that condensation had taken place. The thiourea N-H's could be discerned downfield as two separate resonances. The C=S carbon resonated at around 179 ppm in the ¹³C NMR. The retention of bromine in the pyridine ring was confirmed by ¹³C NMR ($\delta_{C-Br} \sim 112.6$ ppm), and microanalytical data confirmed the correct molecular formulae, Table 2.7. Finally, IR data confirmed the disappearance of the carbonyl group of the Boc and the appearance of a thiocarbonyl group (C=S) at around 1475-1464 cm⁻¹.

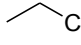
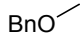
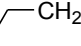
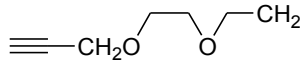
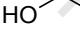
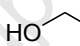
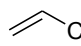
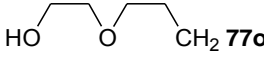
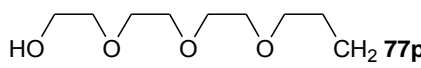
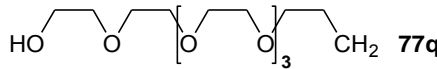
Table 2.7 Elemental analysis results for solids **77m**, **77g**, **77d**, **77l**, **77k**, and **77h**.¹⁴⁸

Atom	HO-CH ₂ 77m		BnO-CH ₂ 77j		≡-CH ₂ CH ₂ CH ₂ 77d	
	Calculated	Experimental	Calculated	Experimental	Calculated	Experimental
C	47.89%	47.96%	55.82%	56.07%	53.58%	53.54%
H	4.86%	4.61%	5.07%	4.86%	4.95%	4.78%
N	9.86%	9.77%	8.14%	7.37%	9.37%	7.81%
S	7.52%	7.01%	6.21%	5.80%	7.15%	5.62%
Atom	N≡-CH ₂ CH ₂ CH ₂ 77i		N≡-CH ₂ 77h		≡-CH ₂ O-CH ₂ 77k	
	Calculated	Experimental	Calculated	Experimental	Calculated	Experimental
C	50.78%	50.61%	48.38%	48.38%	51.73%	51.76%
H	4.71%	4.78%	4.07%	4.04%	4.78%	4.72%
N	12.47%	12.37%	13.30%	12.38%	9.05%	8.66%
S	7.135	6.92%	7.61%	6.76%	6.91%	6.86%

2.4 Biological results, modeling and discussion

The biological activities of the compounds synthesized in this part of the project were determined by project collaborators at the Division of Pharmacology, Yale University, USA, in the laboratories of Professor Karen Anderson. The inhibitory activities of compounds **77** were measured against HIV-1 (IIIB) replication in MT-2 cell culture using an MTT assay¹⁵⁰ (see Appendix). HI-236 was included as a reference compound. The results are shown in Table 2.8.

Table 2.8 Inhibition and cytotoxicity assay^a results for **77a** –**77q** against HIV -1 (IIB) in MT-2 cell culture.¹⁴⁸

R	EC ₅₀ ^b (μM)	CC ₅₀ ^c (μM)	T.I. ^d	R	EC ₅₀ ^b (μM)	CC ₅₀ ^c (μM)	T.I. ^d
CH ₃ HI-236	0.048	1.0	21	N≡—CH ₂ CH ₂ CH ₂ 77i	0.050	3.8	76
 CH ₂ 77a	0.095	0.1	1	BnO  CH ₂ 77j	2.0	5.8	3
≡—CH ₂ 77b	0.052	0.1	2	≡—CH ₂ O  CH ₂ 77k	0.095	9.5	100
≡—CH ₂ CH ₂ 77c	0.026	1	38	≡—CH ₂ O  CH ₂ 77l	0.39	6.8	17
≡—CH ₂ CH ₂ CH ₂ 77d	0.25	10.0	40	HO  CH ₂ 77m	0.012	1.0	83
—≡—CH ₂ 77e	0.27	20.0	74	HO  CH ₂ 77n	0.098	8.5	94
 CH ₂ 77f	0.20	11.0	55	HO  CH ₂ 77o	0.80	9.5	12
MeO—C(=O)—CH ₂ 77g	12	48	4	HO  CH ₂ 77p	0.32	8.5	27
N≡—CH ₂ 77h	0.12	5.5	46	HO  CH ₂ 77q	1.20	53	44

^a Reference 16; MOI was 0.1^b Effective concentration that inhibits viral-mediated T-cell death by 50% and as an average of three measurements.^c Concentration that kills 50% of the T-cells and as an average of three results.^d In vitro therapeutic index (IC₅₀ /EC₅₀).

Regarding a general comparison of all derivatives, the results from the cell culture shown in Table 2.8 were taken to reveal important trends within classes of different tether (polar vs lipophilic). Four of the compounds returned activities equal to HI-236 (**77b** and **77i**) or greater (**77c**, twofold increase; **77m**, fourfold increase). In order to assist with interpretation of the results, docking studies were carried out in the laboratories of Professor Kevin J. Naidoo (University of Cape Town) using Auto-Dock 3.05¹⁵¹ based on the recently published HIV-1 RT protein crystal structure of *N*-(5-chloro-2-pyridinyl)-*N*-[2-(4-ethoxy-3-fluoro-2-

pyridinyl)ethyl]-thiourea as template.¹⁰⁵ The conformation of the PETT derivatives studied was set to accommodate the well-documented^{102,105,152} intramolecular hydrogen bond between the hydrogen of the thiourea nitrogen attached to the alkyl side and the nitrogen of the pyridinyl ring to form a flat six-membered pseudo-ring (Fig. 2.9).

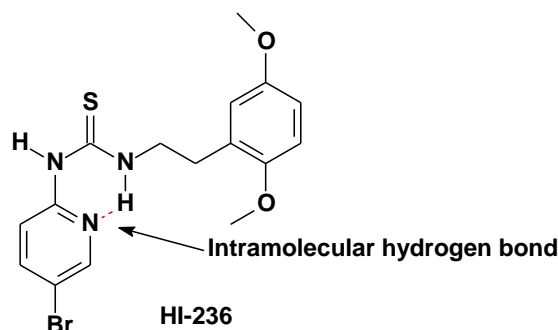
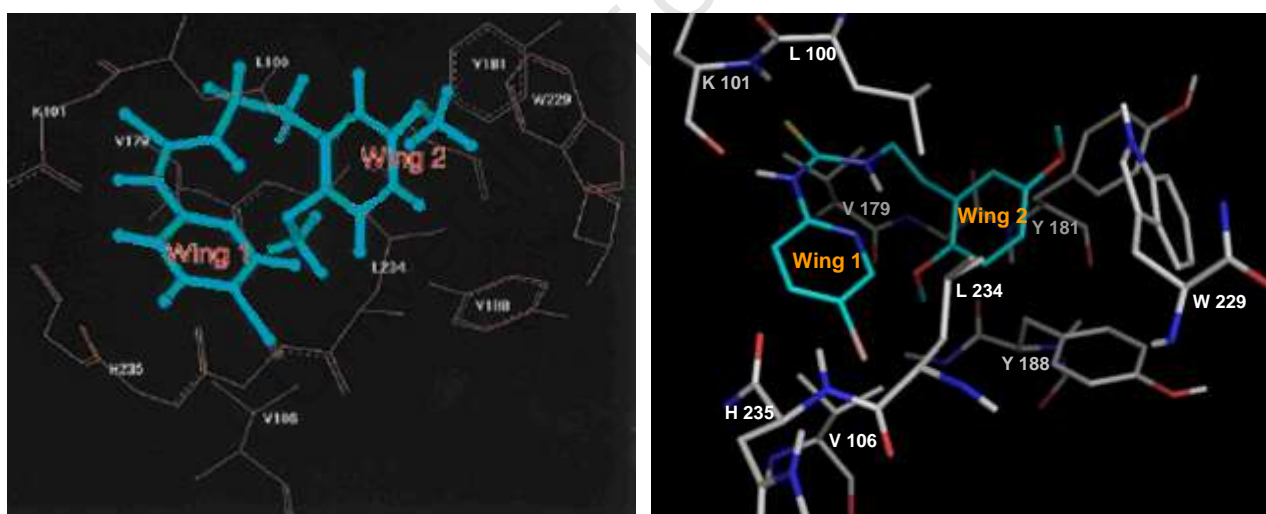


Figure 2.9 Structure of HI-236 showing the intramolecular hydrogen bond.

This protocol resulted in a strong preference for one low energy conformation that dominated 153 of the 250 possible conformations. HI-236 was docked first, and we were able to establish parity of result with that obtained by Uckun.^{102,105,107,152} The two structures are shown in Figure 2.10.



Uckun's HI-236 docked into the HIV pocket.

Our HI-236 docked by AutoDock 3.05.¹⁴⁸

Figure 2.10 HI-236 docked into the HIV pocket.

Thus, as established by Uckun, the inhibitor adopts the characteristic butterfly-shaped orientation with the thiourea moiety embedded in Wing 1 in which hydrogen bonding between the thiourea hydrogen on the *N*-pyridyl side and the carbonyl oxygen of K101 is clearly visible. Wing 2 accommodates the phenyl ring of HI-236 close to the Y181 and Y188 region with the 5-methoxy group interacting with W229. The 2-alkoxy substituent positions into a well containing residues Y181, Y188, F227, V106 and V179. This feature had significance for

the aims of this study. The only difference between our structure and that of Uckun's was the orientation of W229 relative to Y181. In Uckun's model, the six-membered ring of the indole of W229 overlapped Tyr181, whereas the model obtained from our calculations had the five-membered ring of the indole overlapping Tyr181. This could have been due to differences in the static protein structure used in our docking calculations as compared with the structure of the HIV-1 RT binding pocket used in the studies by Uckun.

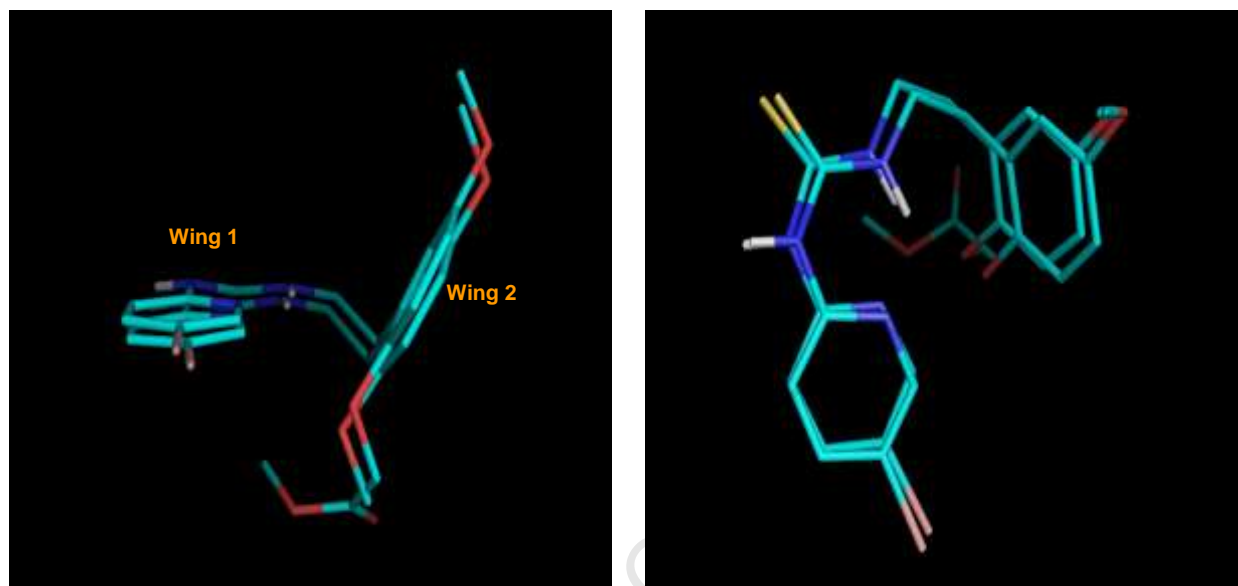


Figure 2.11 The similarities in orientation between the AutoDock models of HI-236 and **77g**.¹⁴⁸

Attention was then focused on docking two of the derivatives, chosen as the ester **77g** and the alcohol **77n**. The parity of **77g** and **77n** with our docked HI-236 in terms of overall topology in the pocket was first investigated, as illustrated in Figure 2.11 for **77g**. The elongation of the 2-alkoxy substituent can be seen but the positioning of the rest of the PEST structure essentially stayed the same, revealing that EC_{50} differences are likely to be based on interactions in the Wing 2 region as postulated. **77n** gave a similar result.

Examination of the way in which the 2-alkoxy substituents of **77g** and **77n** positioned themselves in the hydrophobic region of Wing 2 gave insights into the possible interactions responsible for fluctuation of biological activity as shown in Figures 2.12 and 2.13 taken from each end of the pocket for both cases.

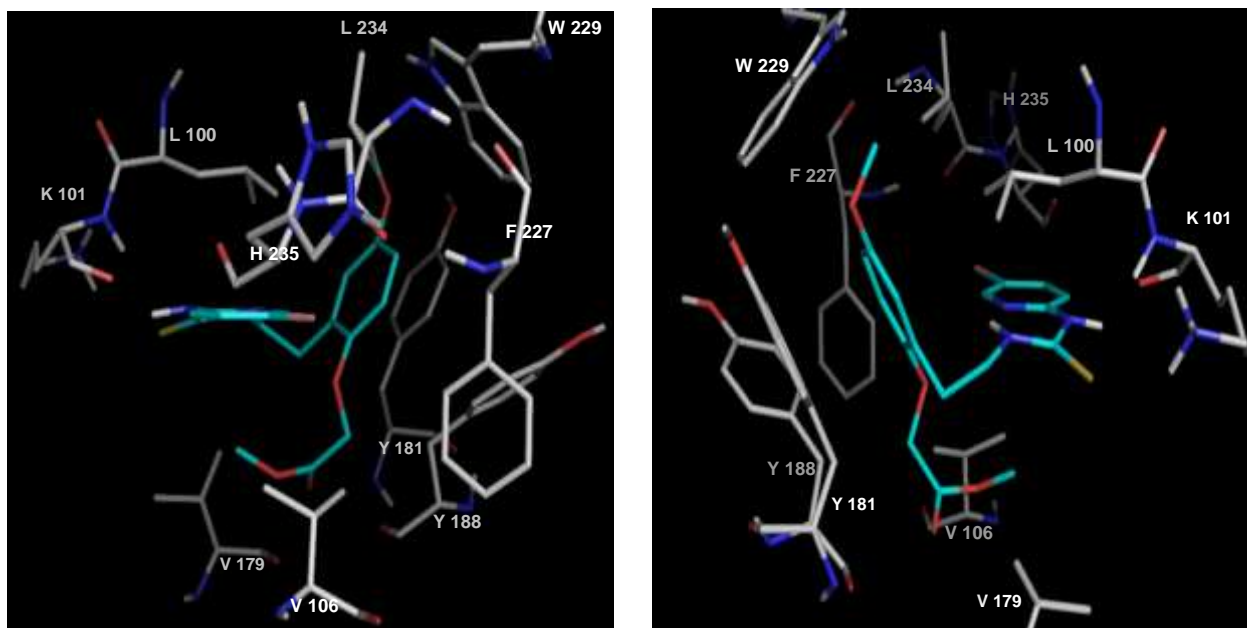


Figure 2.12 Docking of Ester **77g**.¹⁴⁸

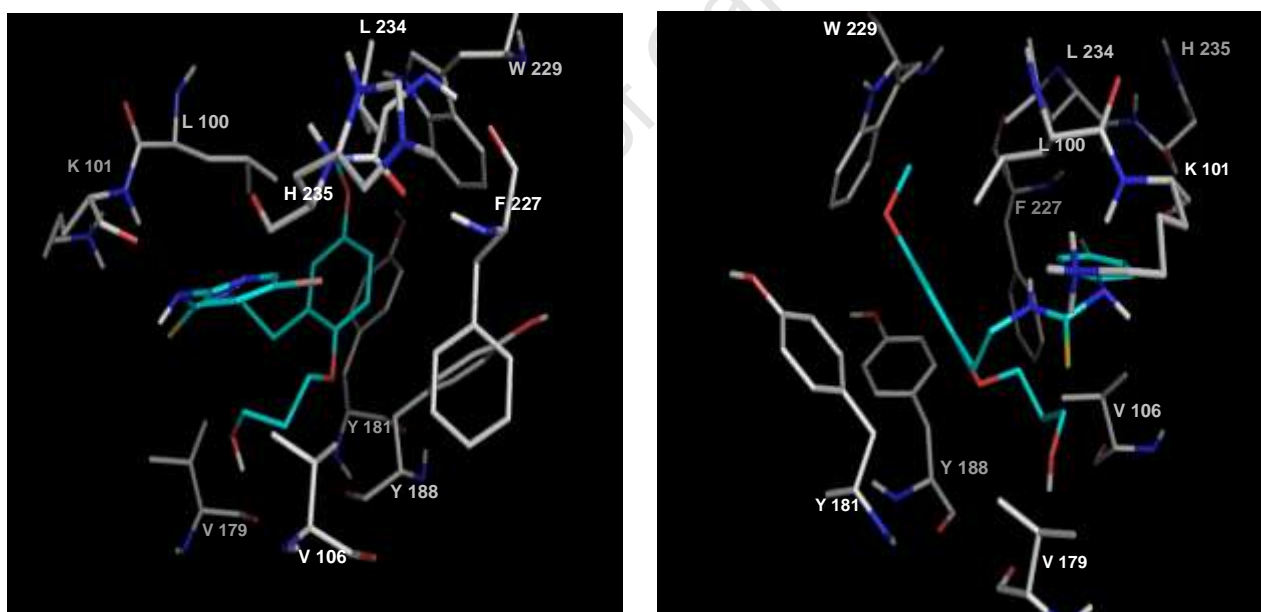


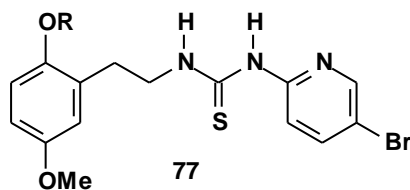
Figure 2.13 Docking of Alcohol **77n**.¹⁴⁸

Both structures suggest the possibility of interaction with V106 or, to a lesser extent V179, towards the floor of the pocket. A possible explanation of their vastly different activities may be that while alcohol **77n** might forge a hydrogen bond with a backbone valine carbonyl group, the ester moiety of **77g** presumably promotes unfavourable carbonyl-carbonyl group repulsion exacerbated by steric interactions between the ester methyl (methoxy) group and

the valine methyl groups. Furthermore, other conformations for **77g** involving swinging the ester group of **77g** away from the valine region, only result in promoting repulsive electrostatic interactions between the carbonyl group and the aromatic faces of Y181, Y188 and F227. A cooperative hydrogen bond for **77n** would nicely explain the much enhanced activity of alcohol **77m** ($EC_{50} = 0.012 \mu\text{M}$) with a shorter (two-carbon) chain, in which presumably the distance between hydrogen-bond donor and acceptor is optimal. **77m** returned an activity four times higher than HI-236 in our system, and presents as an interesting candidate for the problematic V106A mutation if the hydrogen bonding postulate is correct.

Similarly, for the alkyl and alkynyl compounds **77a-77f**, the results show that the hydrophobic pocket is accommodating but with the only significant cooperative interaction being with the triple bond. In this regard, the butynyl chain of **77c**, rather than the propargyl **77b** or pentynyl substituents **77d** appears to be optimal, with **77c** indicating a twofold increase in activity compared to HI-236. Although this classical force field does not include an explicit π - π term, the charge distribution on the aromatic rings mimics this fundamentally quantum effect surprisingly well. Therefore we suggest that the increased activity of **77c** is an optimal cooperative π - π face-to-face interaction between the aromatic residues of Y181, Y188 and the triple bond. It was thus interesting to test this derivative against the Y181C mutant. The PEG derivatives **77n-q** predictably returned lower activities, but not overly so given their bulk. Thus **77l**, with 10 atoms in the substituent, returned an activity of $0.39 \mu\text{M}$ as only eightfold less potent than HI-236. By comparison, the benzyl derivative **77j** is too apparently bulky to be satisfactorily accommodated ($IC_{50} = 2 \mu\text{M}$). Finally, the nitrile derivative **77i** indicated some level of cooperation in the pocket being as active as HI-236, in spite of its five-atom substituent. Once again, π - π and/or hydrogen bonding possibilities appear to be likely explanations.

In order to lend support that these HI-236 derivatives indeed act as NNRTIs, six of the derivatives (**77c**, **77d**, **77k**, **77g**, **77m** and **77n**) as the most (**77m**) to the least active (**77g**) were subjected to an in vitro steady-state RT inhibition assay (details given in Chapter 3), the results of which are shown in Table 2.9.

Table 2.9 Comparison of cell-culture versus *in vitro* RT inhibition (nM) for selected derivatives of **77**.¹⁴⁸

R	Cell-culture EC ₅₀ (nM)	RT assay IC ₅₀ (nM)	Cell-culture Y181C EC ₅₀ (nM)	Cell-culture Y181C IC ₅₀ (TI) (nM)
Me (HI-236)	48	28	1200	18000 (15)
$\equiv\text{---CH}_2\text{CH}_2$ 77c	26	3.8	<200	4000 (>20)
$\equiv\text{---CH}_2\text{CH}_2\text{CH}_2$ 77d	250	27		
$\equiv\text{---CH}_2\text{OCH}_2\text{CH}_2$ 77k	95	41		
$\text{MeO}-\text{C}(=\text{O})-\text{CH}_2$ 77g	12000	100		
$\text{HO}-\text{CH}_2\text{CH}_2$ 77m	12	19		
$\text{HO}-\text{CH}_2\text{CH}_2\text{CH}_2$ 77n	98	24		

The RT assay results present strong support for all the derivatives in this study to be acting as NNRTIs since the derivatives have no possibility of being phosphorylated for NRTI activity against RT. This is also in keeping with published findings on HI-236. The activities ranged from 3.8 to 100 nM, and as expected were superior to those from the cell-culture results except for **77m**, which was slightly poor. Such improvements likely reflect the lipophilicity of the derivatives and their poor solubility in the aqueous cell-culture medium.¹⁵³ Notably, the ester **77g**, which was effectively inactive in cell culture (12 μM), revealed a 120-fold improvement to 100 nM in the RT assay, possibly due to ester hydrolysis in the cell-culture

medium. Importantly, the alkyne **77c** returned a value of 3.8 nM in the RT assay, which was more active compared to that of alcohol **77m** (19 nM), in spite of the reverse being true in cell culture (26 nM vs 12 nM, respectively). The most active derivative **77c** was then evaluated in cell culture against the Y181C resistant strain and this retained activity much better than HI-236 (8-fold decrease against 25 for HI-236).

In summary, it is important to note that of the 17 compounds tested in cell-culture, two (**77c**, **77m**) were more active than HI-236 and two (**77b**, **77i**) were as active, while this picture improved in the RT assay in which of the six derivatives tested, two (**77c**, **77m**) were more active and two were as active as HI-236 (**77d**, **77n**). Such results endorse the conclusions drawn from the study by Uckun¹⁰⁷ that the PETT derivatives have unused available pocket volume with good potential for drug-development. Furthermore, they have identified tethered butynyl derivative **77c** as an advanced lead. Further fine-tuning is worthwhile pursuing on developing side chains that can cope with mutated residues contained in resistant strains,¹⁵⁴ and the modelling results suggest that this might be pursued by substituting at the C-3 position of the aromatic ring *ortho* to the C-2 O-tether. In addition, in view of the tethered PEGed derivatives (e.g **77l**) retaining appreciable activities, the study has generated support regarding the choice of the C-2 oxygen as the attachment point for the tether in the bifunctional compounds, and the likelihood of a tether at this position providing a route from the pocket to the NRTI binding site. This part of the Ph.D study just described effectively paved the way for a comprehensive study of elongated alkynylated bifunctional double-drugs to be carried out, which is the topic of the next Chapter.

CHAPTER 3: SYNTHESIS OF [d4U]-SPACER-[HI-236] DOUBLE-DRUGS

3.1 Introduction

Non-nucleoside reverse transcriptase inhibitors (NNRTIs) act allosterically by slowing down the chemical step catalysed by the HIV reverse transcriptase (RT) enzyme, and Anderson⁸⁵ has shown that this retardation still allows the two-step binding of the nucleoside analogues (NRTI) to come to equilibrium leading to a tighter binding of the nucleotide triphosphate. Thus, in such a case there is communication between the two sites, and the close proximity (10-15 Å) of the NRTI/NNRTI binding sites has inspired several groups to synthesize bifunctional heterodimers containing one of each class of drug separated by a spacer following an original suggestion by Arnold.¹¹⁶ In principle, such a bifunctional inhibitor might utilize the additive binding energies from the interactions at each site, translating into very tight binding. Based on results in Chapter 2, as well as the reasons given in the objectives regarding the attachment points of the drugs to the spacer, a family of flexible non-cleavable bifunctional systems [d4U]-spacer-[HI-236] **51**, **78**, **79**, **80** and the pro-drug **81** were initially identified as shown in Figure 3.1 to explore their ability to interact and thus (shut down) HIV-RT.

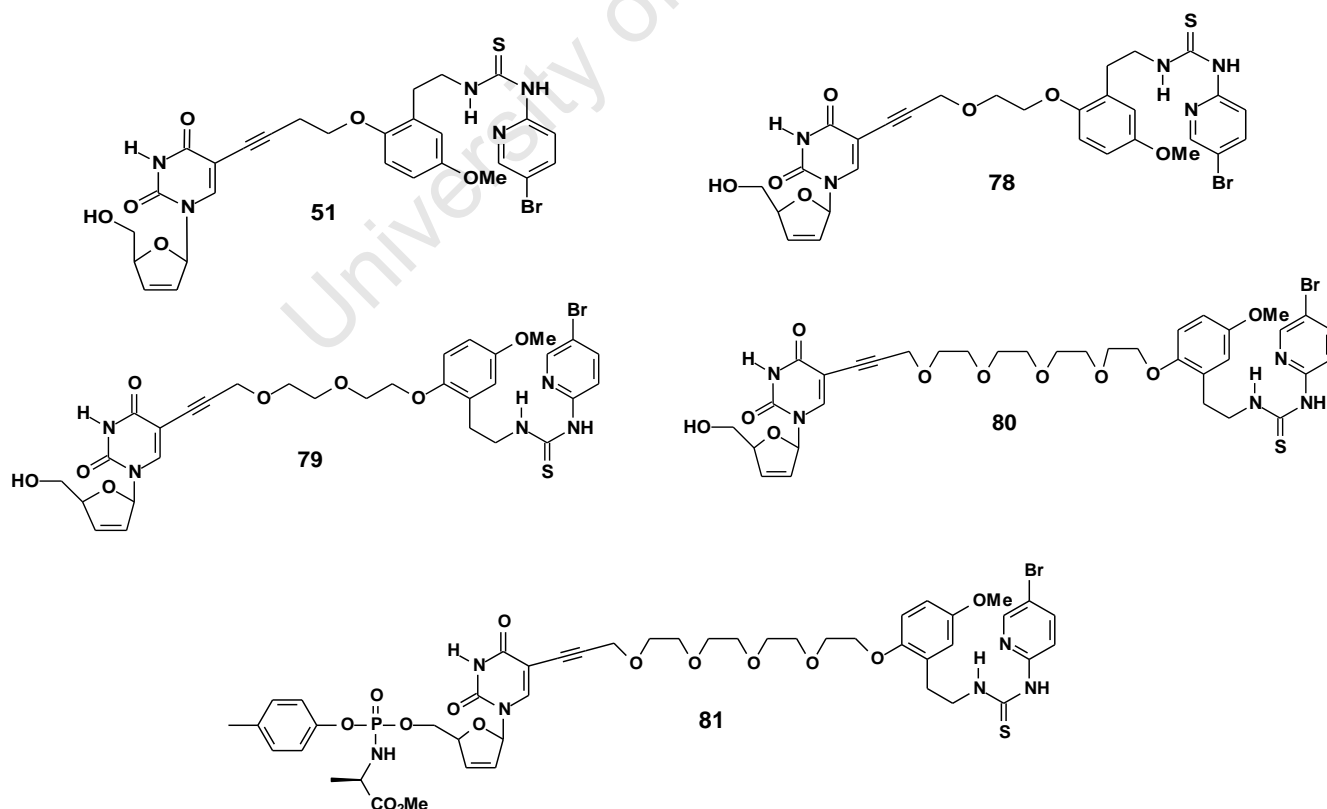


Figure 3.1 Structure of bifunctional target molecules.

Attachment of the linker to the C-5 position of the nucleoside was thought to be achievable via a palladium cross-coupling Sonogashira reaction of a terminal alkyne with a 5-iodo nucleoside. C-5 tethered heterodimers have been developed extensively by the Ladurée group^{129,130} in which a Sonogashira coupling¹⁵⁵ strategy has been demonstrated. Furthermore, C-5 substituted pyrimidine nucleosides constitute a class of biologically significant molecule in which the C-5 alkenyl and alkynyl substituted molecules have shown various antiviral activities. For example, (*E*)-5-(bromovinyl)-2'-deoxyuridine (BVDU) shown in Figure 3.2 is a highly potent and selective anti-Herpes agent that inhibits Herpes Simplex Virus type 1 (HSV-1) and which is currently in clinical use. Other C-5 substituted nucleosides in clinical use¹⁵⁶ include 5-iodo-2'-deoxyuridine (IDU) and 5-trifluoromethyl-2'-deoxyuridine (TFT) which are both administered as eye drops or ophthalmic cream in the treatment of herpes virus infection.¹⁵⁷

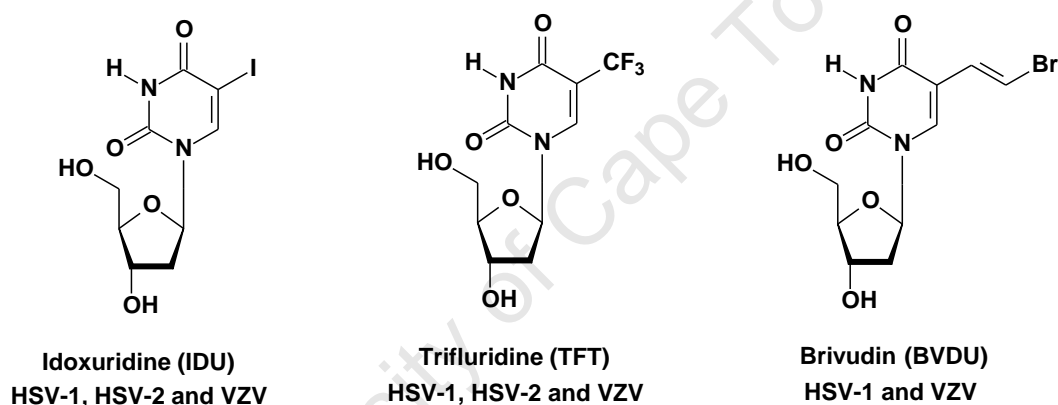
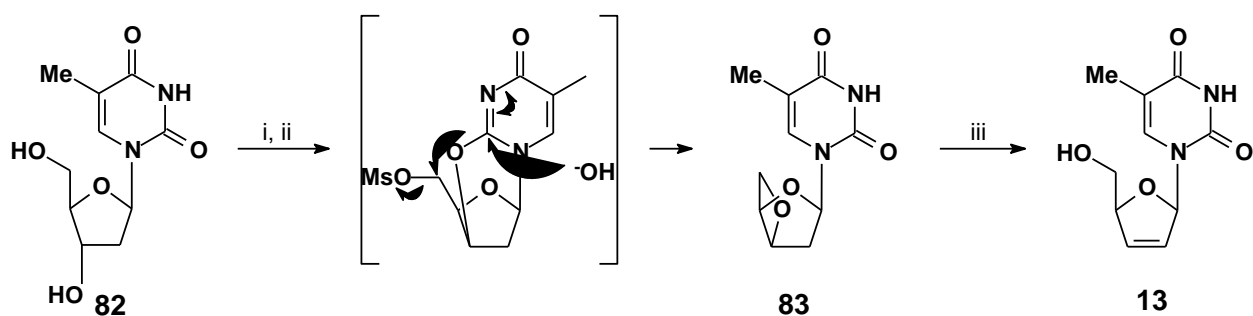


Figure 3.2 C-2 substituted nucleoside in clinical use.

3.2 Overview on the synthesis of d4T

Horwitz *et al.*¹⁵⁸ reported the first synthesis of d4T **13** in 1964 as a potentially novel anti-cancer drug. The strategy used involved conversion of 3',5'-anhydrothymidine **83** to d4T by a base-mediated elimination reaction. Thus, 2'-deoxythymidine **82** was readily converted into 1-(3',5'-anhydro-2-deoxy- β -D-threo-pentofuranosyl)-thymine **83** by converting it first into its 3',5'-di-*O*-mesyl derivative, and then by heating the crude product under reflux with an excess of aq. sodium hydroxide. Oxetane formation from the dimesylate of **82** proceeded via intermediacy of the pyrimidine base with the ring closing step as shown. Elimination of oxetane **83** to afford d4T **13** was achieved via treatment with *t*-BuOK in DMSO (Scheme 3.1).

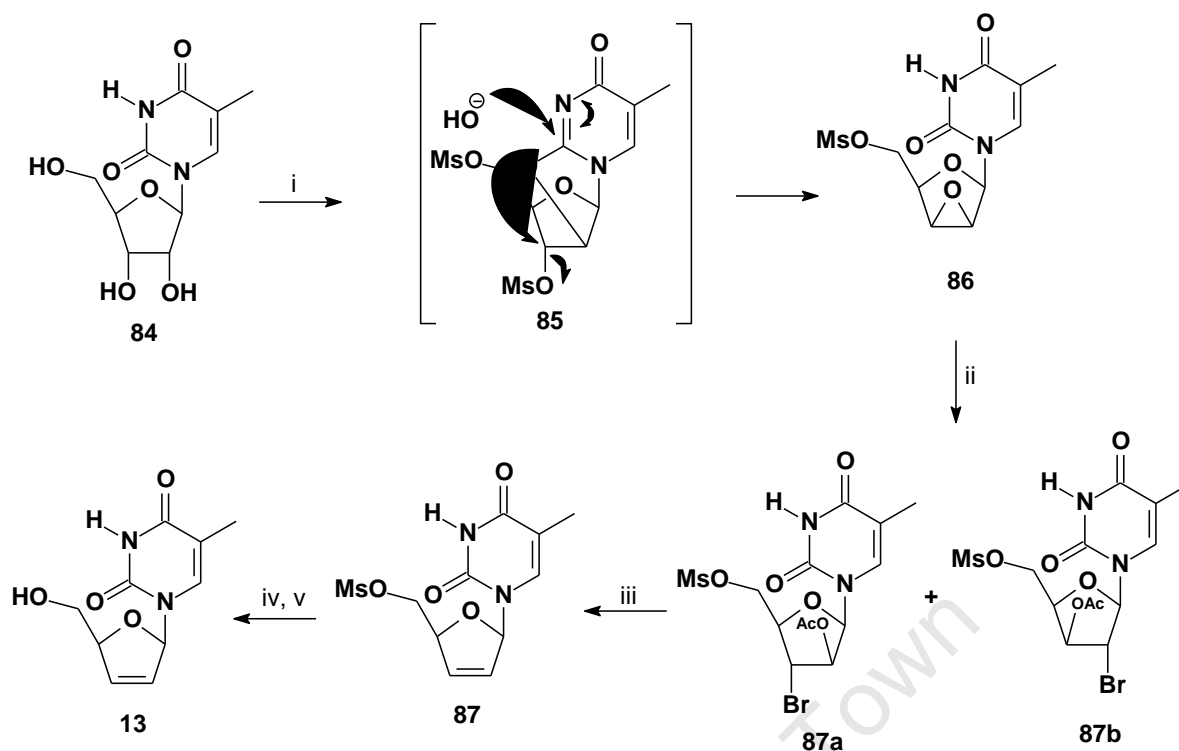


Scheme 3.1 Reagents and Conditions: (i) MeSO_2Cl (3eq), $\text{C}_6\text{H}_5\text{N}$; (ii) aq. NaOH , reflux; (iii) $t\text{-BuOK}$, DMSO; 57%.

Prolonged exposure of d4T to strong base at high temperatures led to its decomposition to give thymine as an undesired product thereby decreasing the overall yield.

3.2.1 Synthesis of d4T from 5-methyluridine

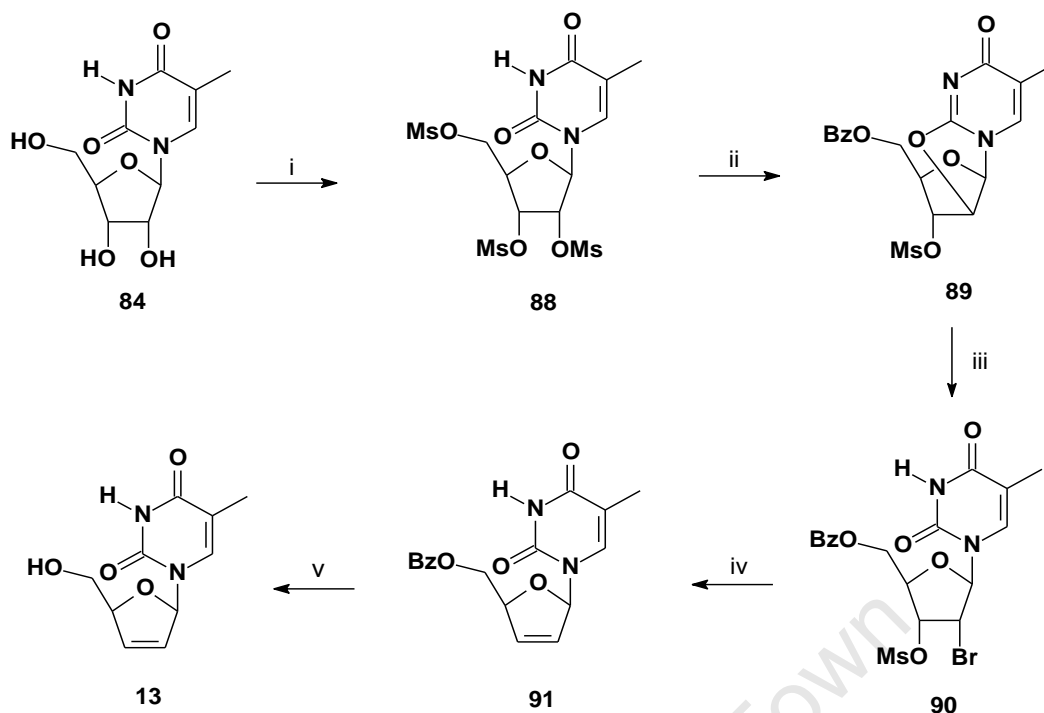
Chen *et al.*¹⁵⁹ (Scheme 3.2) from the Bristol-Myers Squibb group minimized extensive nucleoside bond cleavage by inverting the 2',3'-stereochemistry to proceed via a *trans* haloacetate. This was achieved by base-mediated conversion of the trimesylate of **84** into epoxide **86** via intermediate **85**. **86** opened with acetyl bromide to afford a regioisomeric mixture of *trans*-bromoacetates **87a,b**. β -Elimination with a Zn/Cu couple as before afforded 5'-mesyl d4T **87** under mild reductive elimination conditions, without significant nucleoside bond cleavage as a result of superior *trans* stereoelectronic alignment in the elimination step. **87** could then be transformed into d4T **13**.



Scheme 3.2 Reagents and Conditions: (i) (1) MsCl (3.0 eq), NMM, acetone; (2) 1N NaOH/H₂O, 82%; (ii) AcBr (5.0 eq), MeOH, 92%; (iii) Zn/Cu, MeOH, 88%; (iv) PhCO₂Na, Δ, DMF, 91%; (v) BuNH₂, 90%.

Alternatively, Bristol-Myers-Squibb also made use of a sulfonyl group at the 3'-position of 5-methyluridine instead of an acetyl group in the *syn*-bromomesylate **90** to completely avoid the undesired cleavage of the thymine base (Scheme 3.3). D4T was prepared employing this methodology in 75% overall yield starting from the readily available ribonucleoside 5-methyluridine.¹⁶⁰ The key step in the synthesis was the zinc-induced reductive elimination of bromomesylate **90**, which afforded d4T without nucleoside bond cleavage. Sodium benzoate acted as a base to form anhydro sugar **89** as well as acting as a nucleophile to displace the 5'-mesyl group, preparing the way for the final facile deprotection with butylamine.

Apart from the Bristol-Myers-Squibb synthesis, most of the other d4T syntheses are only amenable to producing research quantities of d4T and not for production purposes, owing to the involvement of protecting groups or convergent coupling of a silylated thymine to a suitably primed ribosugar.



Scheme 3.3 Reagents and Conditions: (i) MsCl, NMM, acetone, 97%; (ii) PhCO₂Na, CH₃CONH₂, 90%; (iii) AcBr, MeOH, EtOAc, 98%; (iv) Zn, EtOAc/MeOH, cat. AcOH, 97%; (v) BuNH₂, 70 °C, 90%.

3.3 Strategies for the synthesis of [d4U]-spacer-[HI-236]

Two divergent routes were envisioned for the synthesis of the target molecules **51**, **78-80**, with appropriate synthetic analysis using forward arrows depicted in Figure 3.3 starting from the useful synthon **69** explored at length in Chapter 2. These routes were developed in view of the failure initially to develop a convergent synthesis based on Pd (0) cross-coupling of the two drugs intact, in view of thiourea interference with cross-coupling. Later appraisal revealed this to be actually possible, albeit in low yield. The following points for the strategies used apply:

(1) Route (A) was used in the synthesis of compounds **51**, **78** and **79** involving a divergent approach via palladium cross-coupling reaction of an alkyne **a** with iodo-d4U **47** followed by deprotection of the Boc group and condensation of the resultant amine with thiourea derivative **49**. Subsequent deprotection of the benzoyl group furnished the target compounds **51**, **78** and **79**.

(2) Route (B), which involved deprotection of the alkyne **a** to amine **b**. Palladium cross-coupling reaction of amine **b** with iodo-d4U **47** followed by condensation with thiourea derivative **49** and deprotection would furnish **80**.

(3) Strategies for phosphoramidate **81** will be discussed in the text.

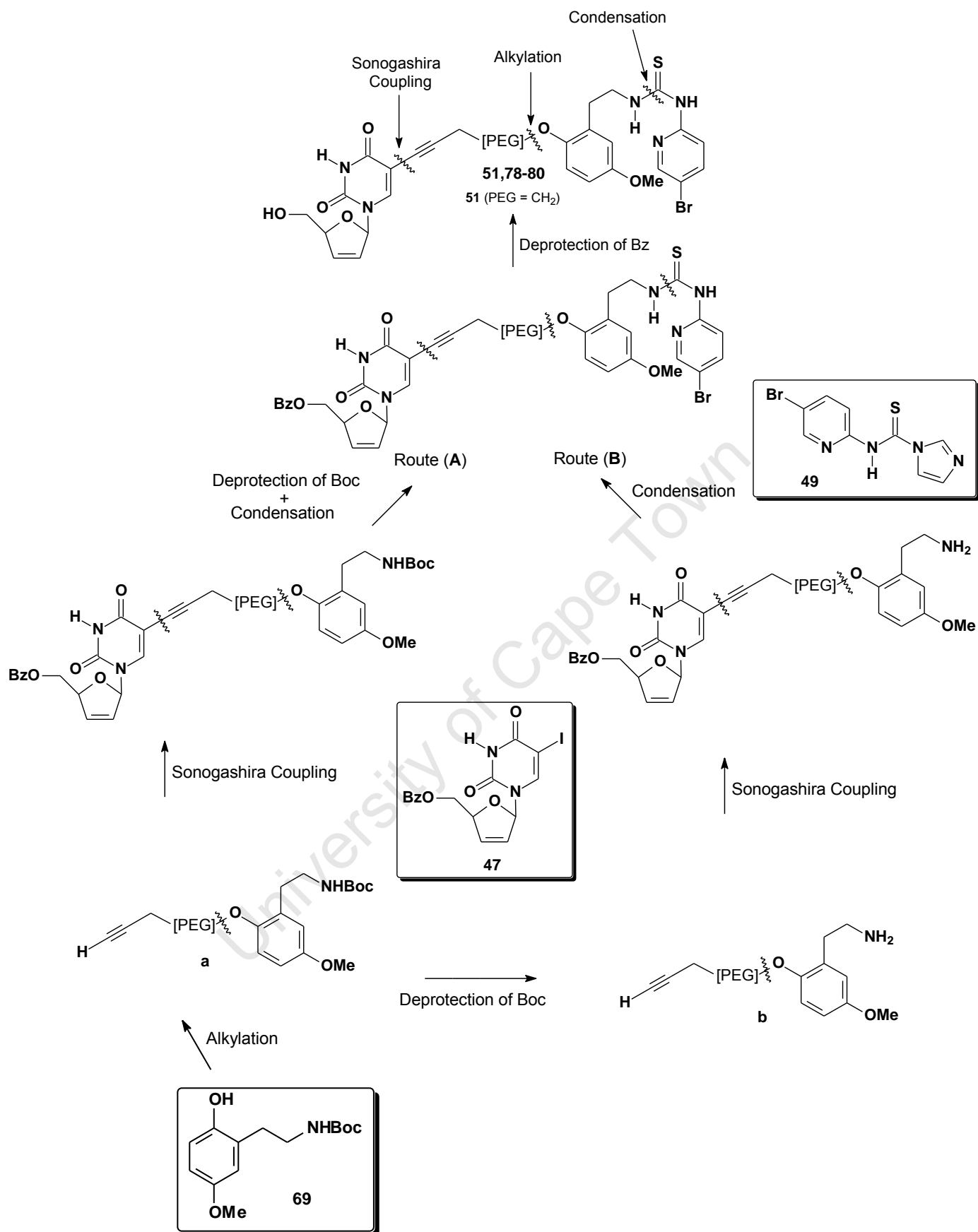
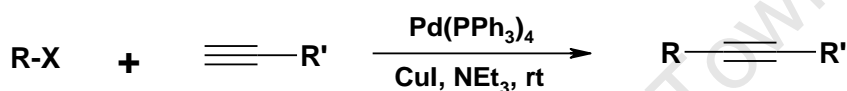


Figure 3.3 Synthetic analysis of target molecules **51, 78-80** using forward arrows.

The steps envisaged to present potential challenges in these syntheses were the Boc and benzoate deprotection steps in view of the unknown chemical stability of the nucleoside part of the molecule. Fortunately, protocols for these could be developed.

3.4 Overview on Sonogashira coupling

The Sonogashira coupling of 5-iodouridine with terminal alkynes has been extensively studied.¹⁶¹ The mechanism of this reaction involves firstly oxidative insertion of Pd(0) into the aryl-halide bond. CuI activates the alkyne by forming a copper acetylide, which undergoes transmetalation with the palladium complex to form an alkynyl-Pd-R intermediate. Reductive elimination of the Pd(0) leads to the coupled product (Fig. 3.4), with regeneration of the coordinatively unsaturated Pd(PPh₃)₂ (d14) catalyst.



General equation for Sonogashira coupling reaction

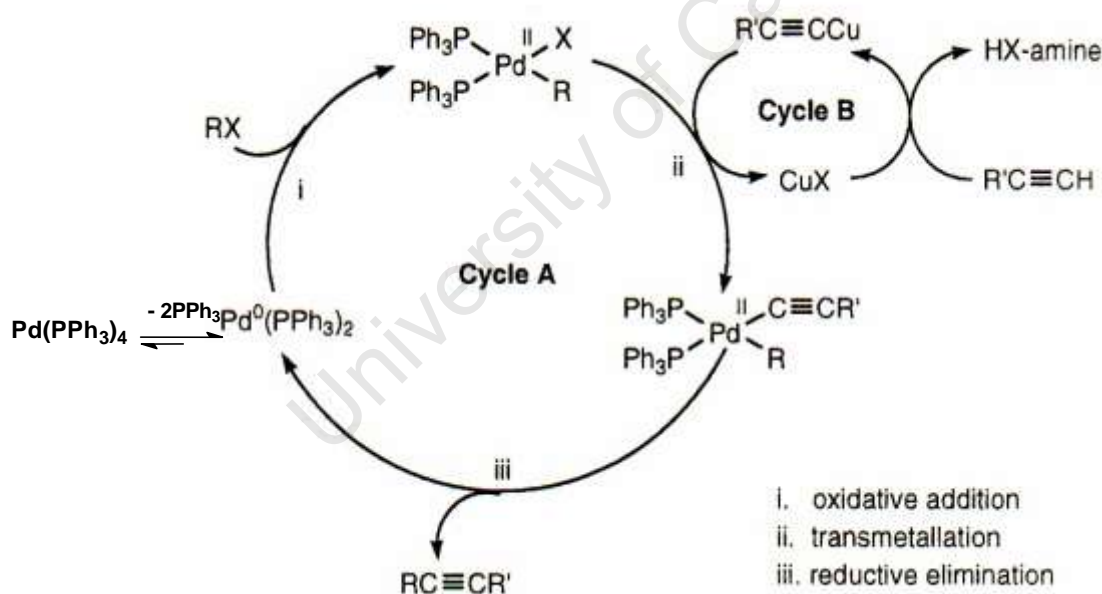
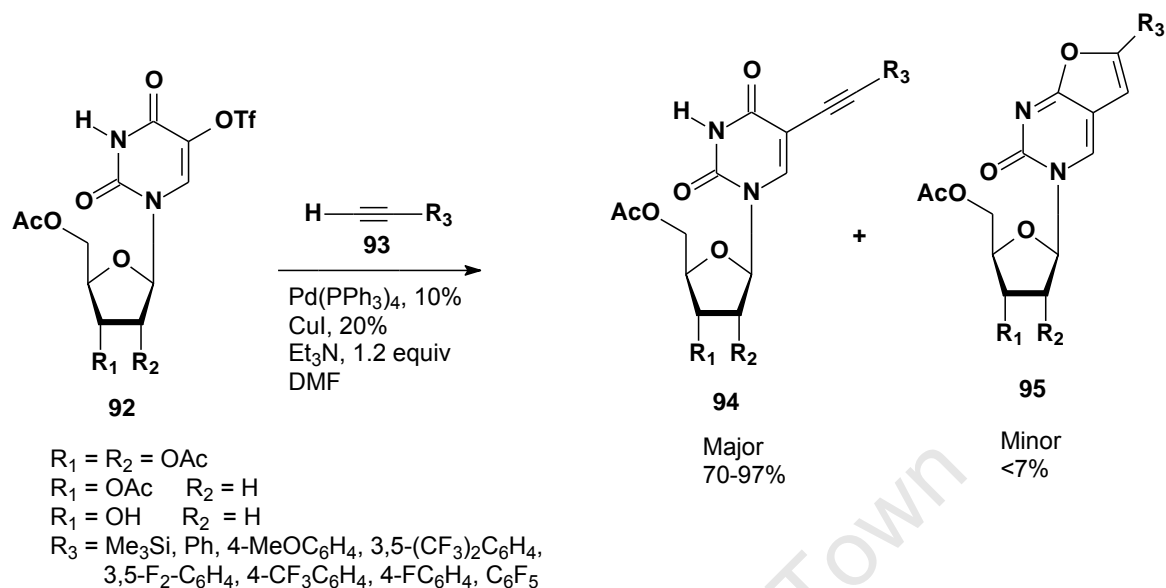


Figure 3.4: General equation and mechanism of Sonogashira coupling.

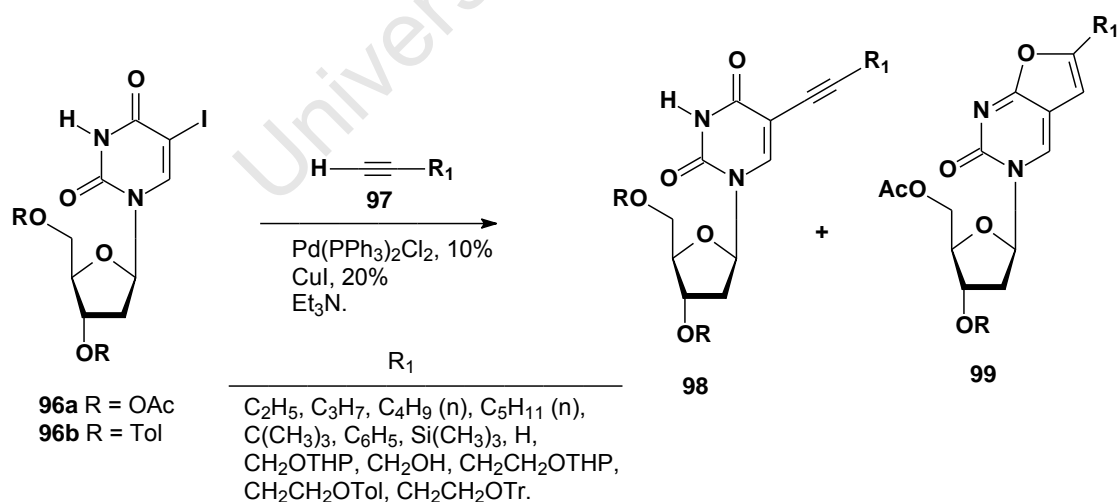
Regarding literature precedent for our approach on nucleosides, Crisp and Flynn¹⁶² have demonstrated that the C-5 alkynyl derivatives **94** could be obtained in high yield (70-90%) by cross-coupling of acetylated uridine triflate **92** with a range of terminal alkynes **93** (Scheme 3.4) using tetrakis(triphenylphosphine)palladium(0) as a catalyst. A slight elevation of

reaction temperature increased the rate of coupling. In this case, furanopyrimidine by-product **95**¹⁶³ was isolated in low yield (7%) to trace amounts.



Scheme 3.4

Similarly, Robins *et al.*¹⁶³ applied the Sonogashira reaction to couple protected 2'-deoxythymidine derivatives **96** with several alkynes **97** in triethylamine at 50 °C in the presence of *bis*(triphenylphosphine)palladium (II) chloride and copper (I) iodide (Scheme 3.5).

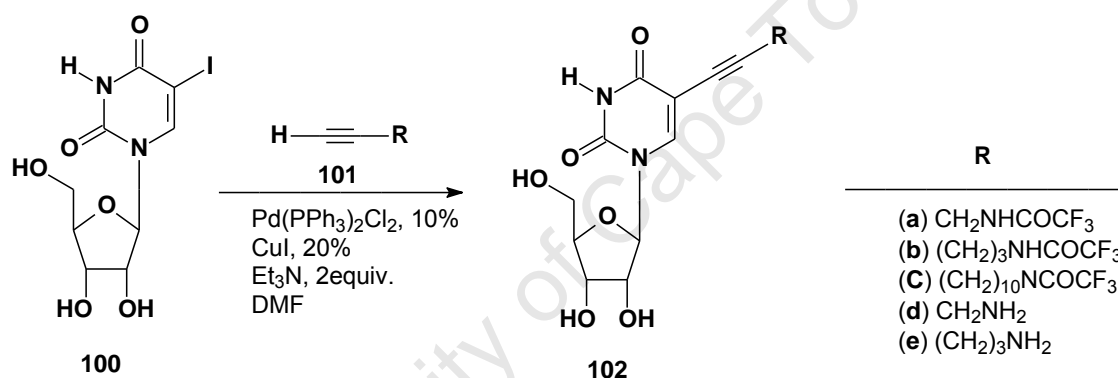


Scheme 3.5 Sonogashira reaction to couple protected 2'-deoxythymidine derivatives.

In this case, the extent of cyclization was dependent on the reactants. Thus, coupling of **96a** with (trimethylsilyl)acetylene gave the target product **98** in 80% yield, whereas the use of 1-hexyne, 4-(*p*-toluoyloxy)butyne, 4-(tetrahydropyranyloxy)butyne or 4-(trityloxy)butyne amongst

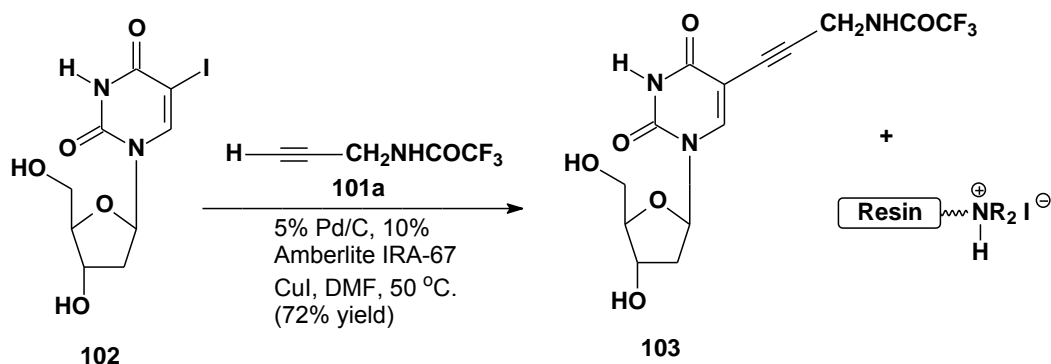
others, under the same conditions gave the cyclized furanopyrimidine compound **99** as the major product. Conversely, coupling reactions with the same range of alkynes but using the nucleoside protected as its *p*-toluyl ester proceeded smoothly with minimal formation of deiodinated and furanopyrimidine by-products.

Hobbs¹⁶⁴ (Scheme 3.6) attempted to use the conditions optimized by Robins *et al.*¹⁶⁵ to couple propargylamine **101** with unprotected 5-iodouridine **100** but failed owing to the nucleoside's insolubility in triethylamine. Successful coupling was achieved to form the products **102** in good yields (70-90%) by using DMF as a solvent and *tetrakis*(triphenylphosphine)palladium as a catalyst instead of the Pd(II) used by Robins. He concluded that the successful coupling was a result of using Pd(0) instead of Pd(II). A review of these conditions by Robins revealed that the use of DMF significantly improved the rate of coupling and not the Pd(0).



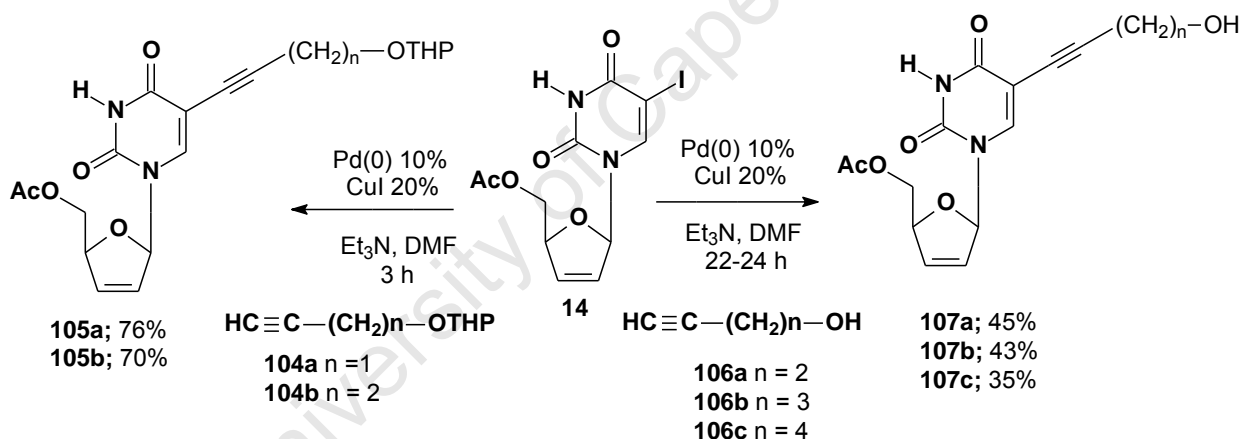
Scheme 3.6

Sonogashira coupling of protected propargylamine **101a** with 2'-deoxynucleoside **102** by the Robins group in the presence of triethylamine as a base furnished the target nucleoside **103** together with triethylammonium salts that were difficult to separate. To improve the purification of these nucleosides, Garg *et al.*¹⁶⁶ developed a heterogeneous protocol that employed a palladium-on-carbon catalyst and a resin-bound tertiary amine (Amberlite IR-67) as a base. These conditions furnished the coupled product **103** in good yield (Scheme 3.7). The study involved a cross-coupling reaction of the nucleoside **102** in the presence of Amberlite IR-67 and Pd(0) (10 mol%) which resulted in the coupled compound **103** in 79% yield after filtration of the reaction media and purification by column chromatography. The authors then substituted Pd(0) with a heterogeneous transition-metal catalyst (Pd/C) to further simplify the purification process.



Scheme 3.7

C-5 alkynylated d4U analogues **105** and **107** have been synthesized via the smooth and efficient coupling of alkynes **104** and **106** with 5'-O-acetyl-5-iodo d4U **14** in DMF under co-catalysis with Pd and CuI (Scheme 3.8). Reaction with unprotected alkynes **106** gave the coupling compounds **107** after 22-24 h in low yields (35-45%), whereas the protected alkynes **104** gave the target compounds in good yields (70-76%).



Scheme 3.8

In summary, the use of CuI as a co-catalyst has been shown to give better results. A mole ratio of 2:1 copper to palladium has been shown to offer the best coupling conditions for alkynes, as the production of side products (cyclic furanopyrimidine) is minimized. It is noteworthy that performing the reaction in the presence of CuI has also reported to increase the conversion rate of by-products. The solvent employed has been reported to be an important determinant for successful coupling of terminal alkynes with idonucleosides, with the use of DMF as a solvent having been shown to reduce the percentage of cyclic by-product formed.¹⁶⁵ A considerable percentage of this cyclized by-product was isolated when longer reaction times were employed or when an electron-withdrawing group on the nucleoside was present. Optimal conditions have been found to be 2.0-2.5 equiv of terminal

alkyne, 10% Pd(PPh₃)₄, 20% CuI and 1.2 equiv Et₃N in DMF. Pd(0) has been reported to give better results than Pd(II).¹⁶¹

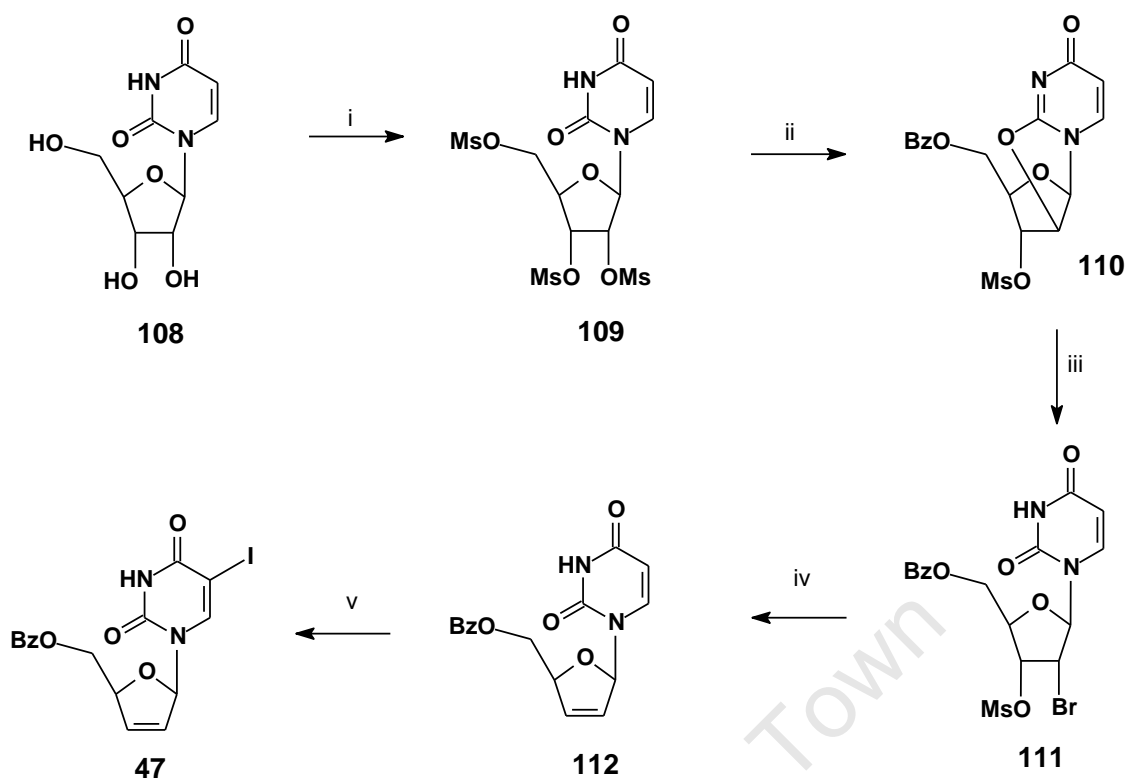
3.5 Route (A): Synthesis of target compounds 51, 78 and 79

3.5.1 Synthesis of [d4U]-butyne-[HI-236] 51

3.5.1.1 Synthesis of 5'-O-benzoyl iodo-d4U

The 5'-O-benzoyl d4U derivative **112**^{158c} was synthesized in four steps as outlined in Scheme 3.9 according to the Bristol-Mayers Squibb procedure for d4T.¹⁶⁰ Thus, reaction of uridine with methanesulfonyl chloride (4.5 eq.) in pyridine furnished trimesylate **109**¹⁸¹ in good yield. The product was isolated by adding the reaction mixture into ice-cold water, followed by filtration of the precipitate formed and washing the filter cake. Following extensive drying on the pump, the ¹H NMR spectrum of **109** revealed the presence of the three mesylate methyl singlets resonating at δ_{H} 3.35, δ_{H} 3.33 and δ_{H} 3.22, while its ¹³C NMR spectrum displayed resonances at δ_{C} 38.0, δ_{C} 37.9 and δ_{C} 36.9 for the methyl carbons.

The next step involved chemoselective transformation of the C-5' centre as well as preparation of C-2' for bromide substitution. Thus, the 2,2'-anhydrouridine **110**¹⁸¹ was synthesized by treatment of **109** with sodium benzoate in acetamide at 132 °C. After 2 h, the product was poured into ice-cold water, stirred at 0 °C for 15 min and the solid filtered to give the target compound as a very insoluble paste in 77% yield. The ¹H NMR spectrum of **110** displayed the absence of an NH singlet at δ_{H} 11.51 from **109** as well as the presence of additional resonances in the downfield region for the aromatic protons of the benzoyl group. Its ¹³C NMR spectrum displayed the appearance of a different carbonyl carbon at δ_{C} 170.5 as well as aromatic carbons, confirming the presence of a benzoyl group, which could be assigned to the C-5' position in view of the relative deshielding of the diastereotopic H-5' protons. There was also a significant downfield shift in the C-2' carbon from δ_{C} 76.0 in **109** to δ_{C} 86.0, thus suggesting that displacement of the mesylate and formation of the anhydro ring had taken place at this carbon. C-2' over C-3' attack by the pyrimidine base occurs in view of 5-*exo-tet* cyclization being faster than the 6-*exo-tet* process as well as the C-3' substitution forming a bridged compound.



Scheme 3.9 Reagents and Conditions: (i) MsCl (4.5 eq), pyridine, 0 °C, 5 h, 80%; (ii) PhCO₂Na (3.5 eq) CH₃CONH₂, 132 °C, 2 h, 77%; (iii) AcBr (4.0 eq), MeOH/EtOAc (1:10), reflux, 1 h, 86%; (iv) Zn (3.0 eq) MeOH, cat. (conc) H₂SO₄, rt, 15 min, 91%; (v) I₂ (0.6 eq), CAN (0.5 eq), CH₃CN, 35 °C, 4 h, 82%.

Acid-catalysed ring opening of **110** with nucleophilic attack by bromide ion at the 2'-position using acetyl bromide in MeOH/EtOAc (1:10) gave *cis*-bromomesylate **111**¹⁸² in 86% yield. Introduction of the bromine atom was evident in the ¹H NMR spectrum by virtue of an upfield shift in the H-2' protons from δ_H 5.69 in **110** to δ_H 4.77 in **111**. Similarly, the ¹³C NMR spectrum of **103** displayed an upfield shift of the C-2' resonance from δ_C 86.0 in **110** to δ_C 47.5 consistent with substitution by bromine. The mechanism of this reaction involves S_N2 displacement by bromide at C-2' with a protonated pyrimidine ring as a leaving group. The net result is inversion of configuration to afford the *syn* stereochemistry shown in **111**.

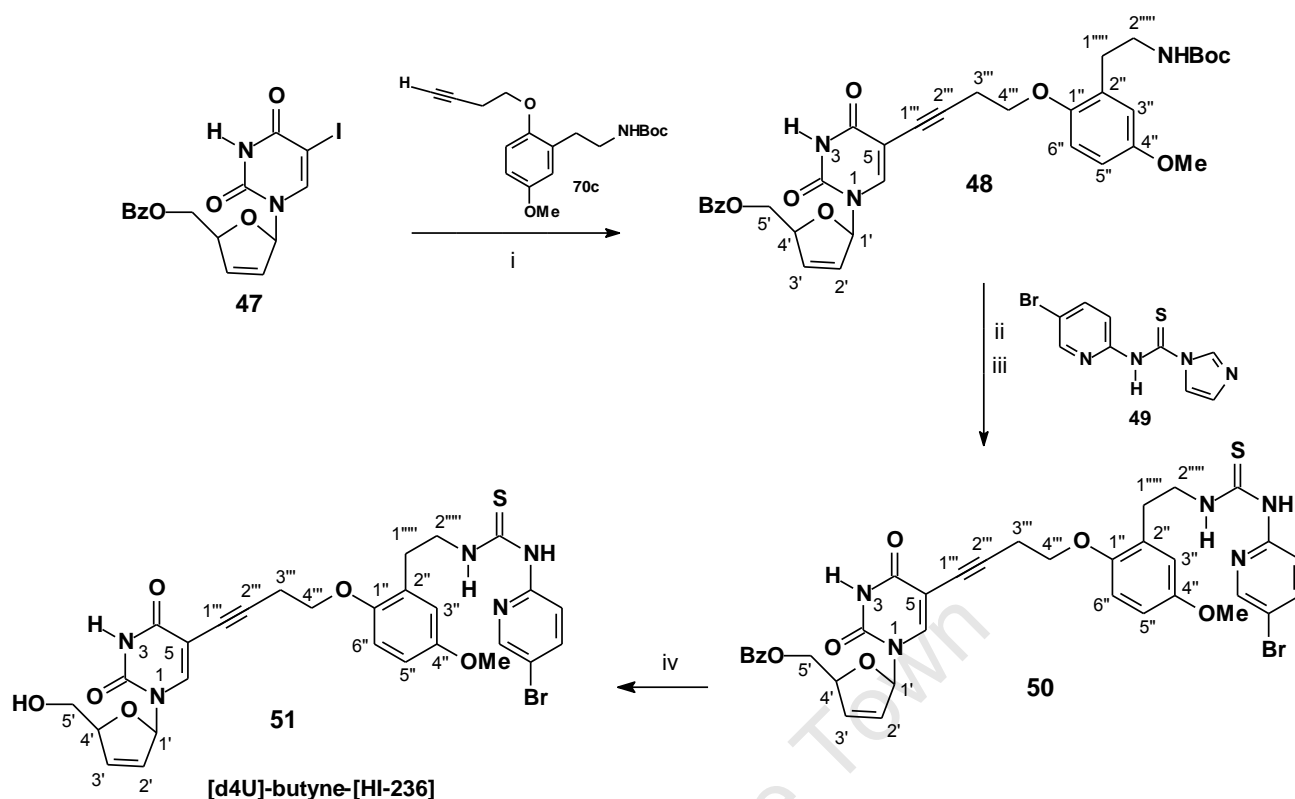
For the reductive elimination of bromomesylate **111**, zinc metal was employed in methanol. It was found that the reaction was accelerated by the addition of 2% (v/v) conc. HCl (15 min) compared to using acetic acid (3.5 h). This afforded the 5'-O-benzoate ester of d4U **112** in an excellent yield (91%) after chromatography, with no detectable cleavage of the nucleoside. The downfield shift of the C-2' and C-3' carbons in the ¹³C NMR spectrum of **112** from δ_C 47.5 and δ_C 75.7 in **111** to δ_C 127.1 and δ_C 133.5 respectively, confirmed the introduction of the double bond via elimination of bromine and mesylate groups. Elimination of the mesylate

was further confirmed by the absence of the mesylate methyl carbon at δ_C 38.7. Although *syn*-elimination is energetically more demanding than *anti*, undoubtedly the potent leaving ability of the sulfonyl group assisted the elimination over the alternative involving uracil.

The CAN-mediated C-5 halogenation of uracil derivatives was first reported by Asakura *et al.*¹⁶⁷ in 1990, in which molecular iodine as well as NaI and LiI were used as the iodine source. Ultimately in this work, iodination of **112** to its 5-iodo d4U **47**¹⁴² was effected using elemental iodine and CAN at 35 °C to afford the product in 82% yield. This reaction was found to be heavily dependent on time and temperature. Thus, higher temperature and long reaction times led to isolation of a by-product due to migration of the benzoyl group from the C-5'-hydroxyl to the pyrimidine nitrogen. Iodination was confirmed by the ¹H NMR spectrum which revealed the absence of a doublet at δ_H 5.32 for H-5 as well as a downfield shift in H-6 from δ_H 7.33 in **112** to δ_H 7.73. H-6 also appeared as a singlet in the ¹H NMR spectrum of **47**. The ¹³C NMR spectrum of **47** revealed that C-5 had shifted upfield from δ_C 102.6 in **112** to δ_C 69.6, consistent with the presence of iodine at C-5. The double bond resonances were still intact, confirming that iodination of the double bond had not taken place.

3.5.1.2 Sonogashira coupling, deprotection and condensation

Sonogashira coupling of 5-iodo-5'-O-benzoyl d4U **47** with alkyne **70c**, which had been successfully synthesized and already discussed (Figure 2.6, Chapter 2) yielded the desired coupled product **48** in 69% within 4 h at room temperature (Scheme 3.10). The conditions of using Pd(0) catalyst (10%), CuI (20%) and NEt₃ (2 eq) in DMF as already described were used throughout the project. The ¹H NMR spectral data for **48** revealed signals for both the alkynyl and d4U moieties in a ratio of 1:1. A successful coupling was further supported by the absence of an alkyne proton at around δ_H 2.04. The ¹³C NMR spectrum of **48** displayed diagnostic resonances at 141.6 (C-6), 150.5 (C-1''), 100.7 (C-2''), 91.3 (C-1'''), δ_C 90.1 (C-1'), 72.4 (C-5), 40.6 (C-2''''') and 1.40 (OC(CH₃)₃) confirmed by 2D NMR. The HMBC spectrum revealed a correlation between the methylene protons at δ_H 2.68 (H-3''') with the carbons at δ_C 100.7 (C-2''), 91.3 (C-1'''), 72.4 (C-5), 66.6 (C-4'') and 28.4 (OC(CH₃)₃). The mass spectroscopy data also confirmed that the coupling had taken place.



Scheme 3.10 *Reagents and Conditions:* (i) alkyne **70c**, (PPh₃)₄Pd (10%), CuI (50%), Et₃N (2 eq), DMF: THF (1: 2), rt, 4h, 69%; (ii) TFA, CH₂Cl₂, 0 °C; (iii) EtN(i-Pr)₂ followed by **49**, THF, rt, 18 h, (60% for 2 steps); (iv) NaOMe (cat), MeOH, 0 °C, 20 min, 51%.

With **48** in hand, the key condensation/deprotection steps required extensive optimization and the isolation conditions proved critical to ensure a reproducible result. Eventually, it was found that using trifluoroacetic acid in methylene chloride at 0 °C furnished the crude amine as a triflate salt. The reaction could be monitored by tlc to form a very polar primary amine spot ($R_f = 0.3$ in 5% MeOH in CH₂Cl₂). Since the product could not be extracted from water into an organic solvent, work-up involved adding Hünig's base to liberate the amine. The solvent was evaporated and dried on a vacuum pump. The crude amine was then condensed directly with thiocarbonyl derivative **49** in THF at rt for 20 h to afford the desired product **50** in 60% yield for the two steps. Interestingly, these conditions contrast with the much harsher ones reported by Bell¹⁰¹ of heating at 100 °C for 1 h in DMF. The ¹H NMR spectrum of **50** displayed diagnostic signals for two thiourea NH signals at δ_H 10.92 and δ_H 9.75, the H-3''' propargylic methylene diastereotopic protons at δ_H 3.03, δ_H 2.88 and the aromatic methoxy at δ_H 3.79. Its ¹³C NMR spectrum showed the presence of a thiocarbonyl carbon at δ_C 179.1 as well as C-Br at δ_C 111.1, C-6 at δ_C 141.2, OCH₃ at δ_C 55.5 and C-1'''' at δ_C 20.9. The IR spectrum also revealed the presence of a C=S stretch at 1461 cm⁻¹ and a C≡C stretch at 2254 cm⁻¹. High resolution mass spectrometry data also confirmed the molecular ion of **50**.

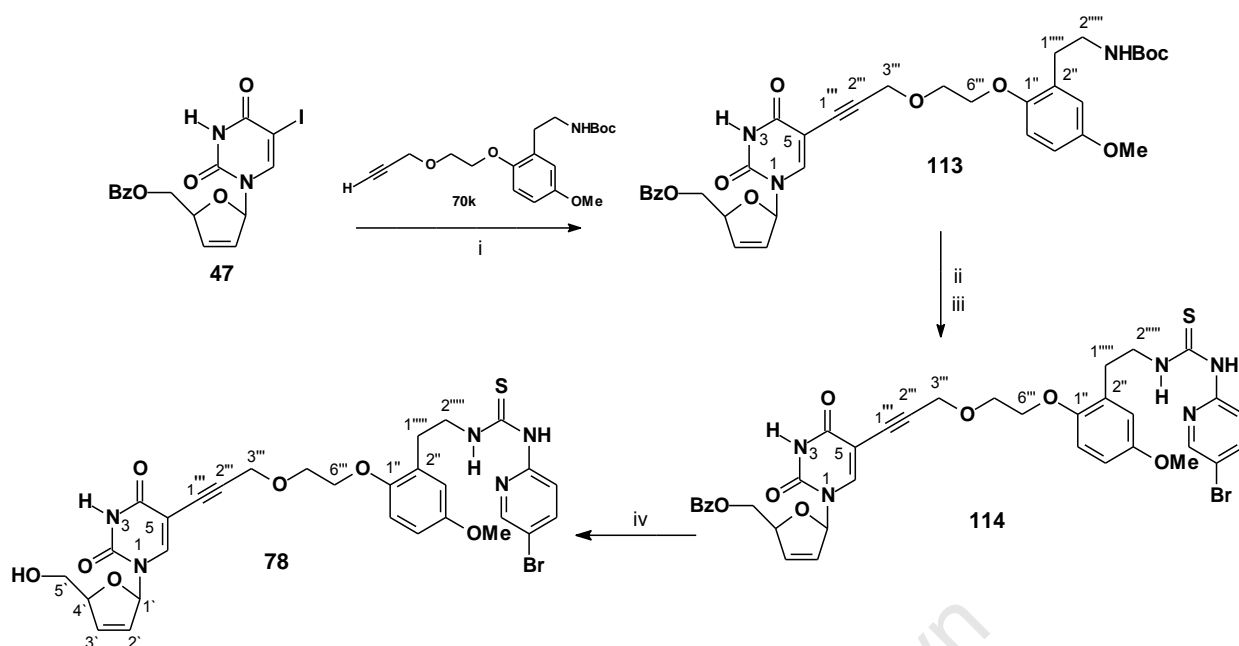
3.5.2.3 The end-game

The final step of the synthesis was deprotection of the benzoyl group to afford the target molecule **51**¹⁴². Considerable optimization of conditions was needed and the reaction was clearly sensitive to cleavage of the sugar residue. This could be monitored by ¹H NMR and integration of the two drug moieties. Unfortunately, the cleaved product eluted with **50**. However, eventually, efficient debenzoylation could be achieved in a satisfactory manner with sodium methoxide (cat) in methanol at 0 °C. The reaction was monitored carefully by tlc to reveal the formation of a polar spot (R_f = 0.4 in 10% MeOH in CH₂Cl₂). The reaction was quenched using a few drops of acetic acid, followed by solvent removal and direct flash chromatography in view of the nucleoside's solubility in water. Ultimately, this gave the deprotected compound **51** in 51% yield. The ¹H NMR resonance for **51** exhibited an expected upfield shift for the H-5' methylene protons to δ_{H} 3.80 as a result of a loss in the deshielding effect of the carbonyl group. Similarly, the ¹³C NMR spectrum of **51** displayed the absence of the carbonyl carbon at δ_{C} 166.3 and an upfield shift of C-5' from δ_{C} 65.3 in **50** to δ_{C} 62.9 in **51**. Otherwise, all of the other resonances were present in similar places to **50**, and the product structure was also confirmed by mass spectrometry.

3.5.2 Synthesis of [d4U]-monoPEG-propyne-[HI-236] **78**

For structure-activity purposes, it was decided to turn towards synthesizing a family of flexible bifunctional systems with longer spacers. A polyethylene (PEG) unit was chosen as the repeating unit in view of its synthetic accessibility as well as its promotion of water solubility.

Synthesis of [d4U]-monoPEG-propyne-[HI-236] **78** was accomplished using the methodology described for **51**. Specifically, palladium (0) cross-coupling of alkyne **70k** (described in Scheme 2.14, Chapter 2), with **47** afforded the coupled compound **113** in 76% yield after column chromatography (Scheme 3.11).



Scheme 3.11 Reagents and Conditions: (i) alkyne **70k**, $(\text{PPh}_3)_4\text{Pd}$ (10%), CuI (50%), Et_3N (2 eq), $\text{DMF}:\text{THF}$ (1: 2), rt, 4h; 76%; (ii) TFA, CH_2Cl_2 , 0 °C; (iii) $\text{EtN}(\text{i-Pr})_2$ followed by **49**, THF , rt, 18 h 60% (for 2 steps); (iv) NaOMe (cat), MeOH , 0 °C, 20 min, 69%.

The ^1H NMR spectrum of **113** revealed (see Figure 3.5) the disappearance of the alkyne proton at δ_{H} 2.45 in **70k**. Some of the resonances for **113** derived from **47** and **70k** included a singlet at δ_{H} 7.68 (1H, H-6), a multiplet for the anomeric sugar proton (1H, H-1') at δ_{H} 6.92, a singlet at δ_{H} 4.27 (2H, H-3'''), a singlet at δ_{H} 3.73 (3H, OCH_3) and a multiplet at δ_{H} 3.33 (2H, H-2'''). The ^{13}C NMR spectrum displayed diagnostic signals for the alkyne carbons at δ_{C} 90.0 for C-1'', δ_{C} 99.9 for C-2'', δ_{C} 55.6 for OCH_3 , δ_{C} 30.8 for C-1'''' and the anomeric carbon of the sugar (C-1') at δ_{C} 90.8.

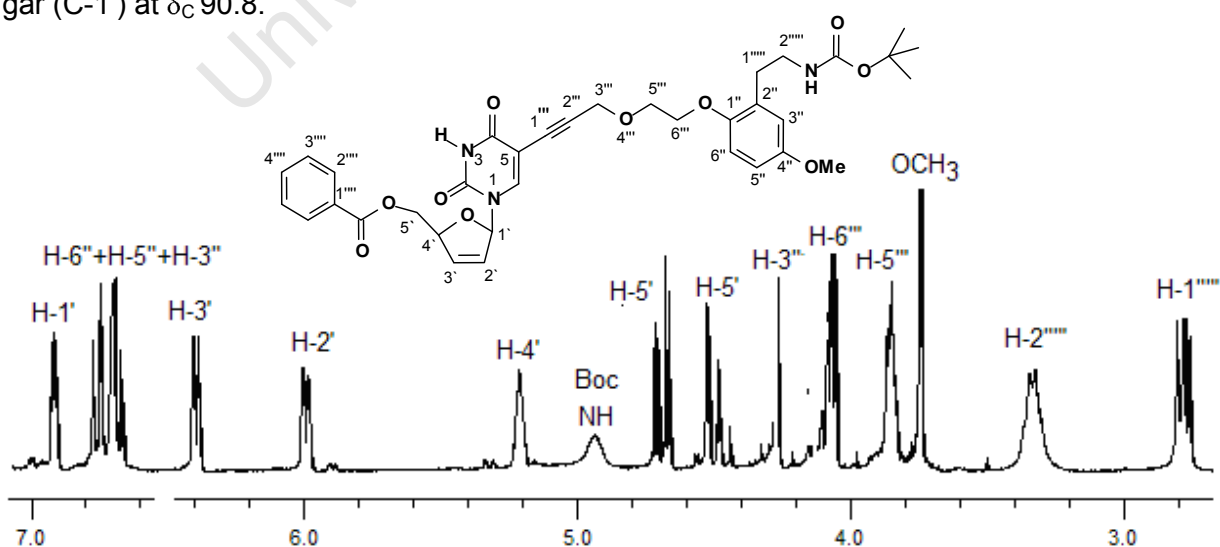


Figure 3.5 A portion of ^1H NMR (CDCl_3) spectrum of compound **113**.

The Boc group of **113** was deprotected employing trifluoroacetic acid in methylene chloride as before and the resultant amine condensed with thiourea derivative **49** in THF at rt to furnish **114** in 60% yield after chromatography for the two steps. The ^1H and ^{13}C NMR spectra of compound **114** revealed the absence of resonances for the Boc group. The ^1H NMR spectrum revealed the three desired NH peaks at δ_{H} 10.82, δ_{H} 9.00, and δ_{H} 8.84, the H-3' at δ_{H} 4.25, OCH_3 at δ_{H} 3.75, H-6'''' at δ_{H} 8.03 and δ_{H} 7.70 for H-6. The ^{13}C NMR spectrum confirmed the presence of a thiocarbonyl carbon at δ_{C} 179.2, C-Br at δ_{C} 112.5, C-6 at δ_{C} 142.6, OCH_3 at δ_{C} 55.6 and C-1'''' at δ_{C} 30.8. The parent ion was found to be 776.1379 ($\text{M}^+ + \text{H}$) correlating to a correct molecular formula of $\text{C}_{36}\text{H}_{35}\text{N}_5\text{O}_8\text{SBr}$, thus confirming the formation of **114**.

The benzoyl group on **114** was once again successfully deprotected using the standard established conditions of NaOMe (cat) in MeOH to give the target molecule **78** in 69% yield after purification by column chromatography. The structure of compound **78** was unequivocally assigned on the basis of its spectroscopic data, using a combination of both 1D and 2D ^1H and ^{13}C NMR as well as IR techniques and high-resolution mass spectrometry. The ^1H and ^{13}C NMR spectra of **78** revealed the absence of resonances for the benzoyl group. Interestingly H-6 shifted downfield in the free nucleoside suggesting shielding of it in benzoate **114** by the phenyl group. In addition, the ^1H NMR spectrum (see Figure 3.6) in CDCl_3 revealed that H-5' had moved upfield from δ_{H} 4.68 and δ_{H} 4.54 in **114** to between δ_{H} 4.06-3.78 in **78**, indicating that debenzoylation had taken place. The three NH resonances for the thiourea and imide were discernible downfield between 9 and 11 ppm. The appearance of a broad singlet at δ_{H} 3.36 corresponding to a hydroxyl group, supported the absence of a benzoate ester. Importantly, **78** showed a correct integration for the two drug fragments with no loss of sugar. Generally, the longer the spacer, the more stable the bifunctional became. Further evidence was given in the ^{13}C NMR spectrum, which displayed an upfield shift in the resonance of C-5' from δ_{C} 65.1 in **114** to δ_{C} 62.8 as well as the absence of the carbonyl carbon at δ_{C} 166.3. Overall, the carbon spectrum returned the correct number of resonances 29. Furthermore, the mass spectrometry data correlated with the molecular formula (HRMS (ES): m/z found 672.1139 ($\text{M}^+ + \text{H}$), $\text{C}_{29}\text{H}_{31}\text{N}_5\text{O}_7\text{SBr}$ requires ($\text{M}^+ + \text{H}$) 672.1128).

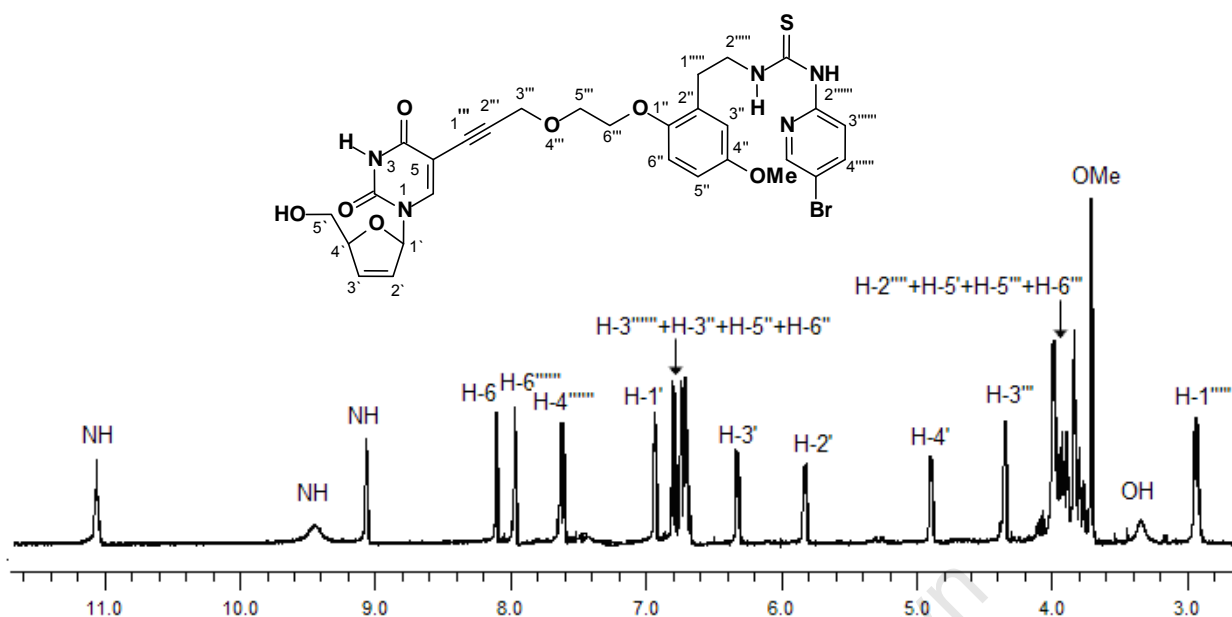
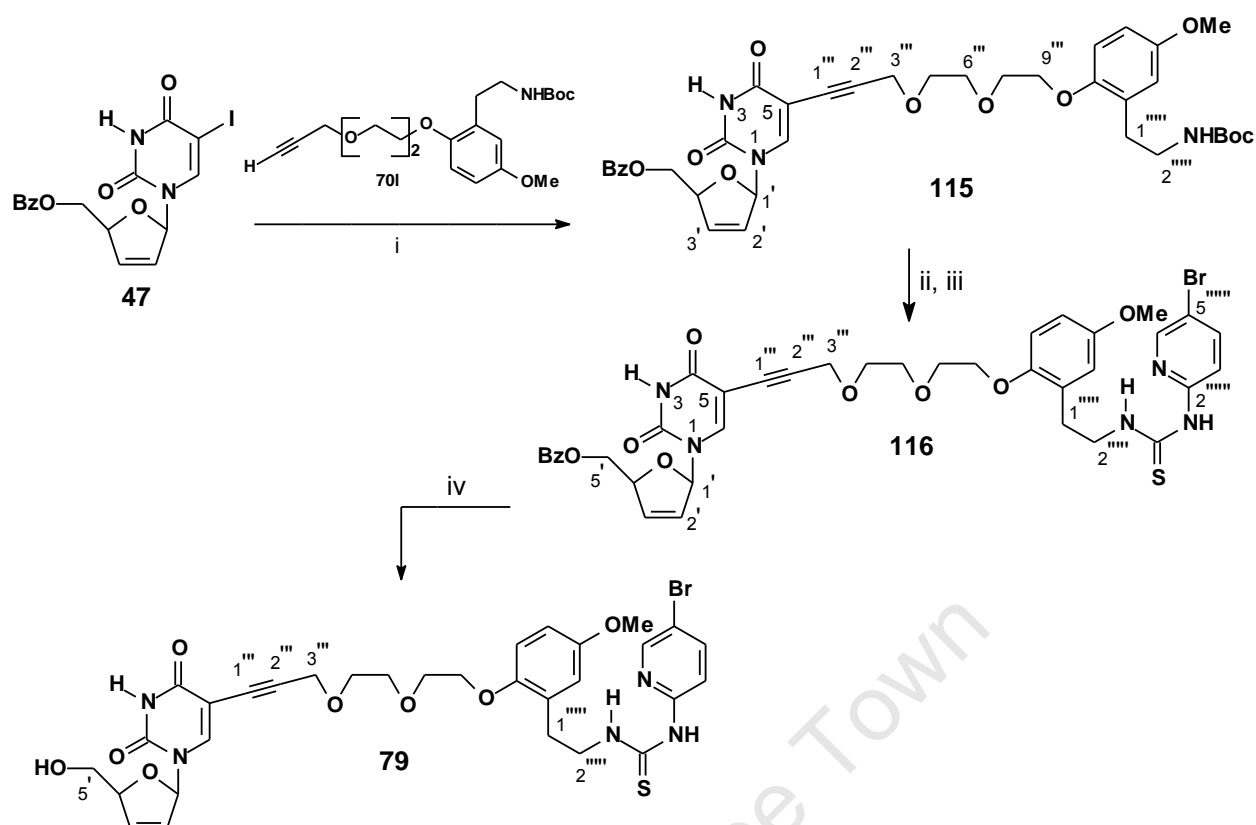


Figure 3.6 ^1H NMR (CDCl_3) spectrum for compound **78**.

3.5.3 Synthesis of [d4U]-diPEG-propyne-[HI-236] **79**

The synthesis of the next homologue as bifunctional [d4U]-diPEG-propyne-[HI-236] **79** was carried out using a similar procedure as described above (Scheme 3.11) for **78**. The Sonogashira coupling of **47** with alkyne **70I**, which was successfully synthesized before (Scheme 2.21, Chapter 2) yielded the desired coupling product **115** within 4 h at room temperature in 72% yield (Scheme 3.12). Tlc showed the product to be more polar than the previous product **113**, but the similar profile as before helped to follow the reaction.



Scheme 3.12 *Reagents and Conditions:* (i) alkyne **70I**, $(\text{PPh}_3)_4\text{Pd}$ (10%), CuI (50%), Et_3N (2 eq), $\text{DMF}:\text{THF}$ (1: 2), rt, 4h, 72%; (ii) TFA , CH_2Cl_2 , 0 °C; (iii) $\text{EtN}(\text{i-Pr})_2$ followed by thiourea **49**, THF , rt, 18 h, 63% (for 2 steps); (iv) NaOMe (cat), MeOH , 0 °C, 20 min, 54%.

The ^1H NMR spectral data for **115** (Fig. 3.7) as expected showed the lack of an alkyne proton at around δ_{H} 2.40. Some important resonances in the ^1H NMR spectrum of **115** included the peaks at δ_{H} 6.92 for H-1', δ_{H} 7.68 for H-6, δ_{H} 4.25 for H-3''', δ_{H} 3.75 for OCH_3 and δ_{H} 2.80 for H-1'''. A highfield singlet for the Boc *t*-butyl group could be clearly seen at δ_{H} 1.43. Similarly, its ^{13}C NMR spectrum displayed corresponding resonances at δ_{C} 90.7 for (C-1'), δ_{C} 142.2 for C-6, δ_{C} 58.9 for C-3''', δ_{C} 55.6 for OCH_3 and δ_{C} 31.0 for C-1'''. Importantly, no cleavage of the sugar moiety was observed in that the double bond protons H-2' and H-3' integrated relatively for one proton each.

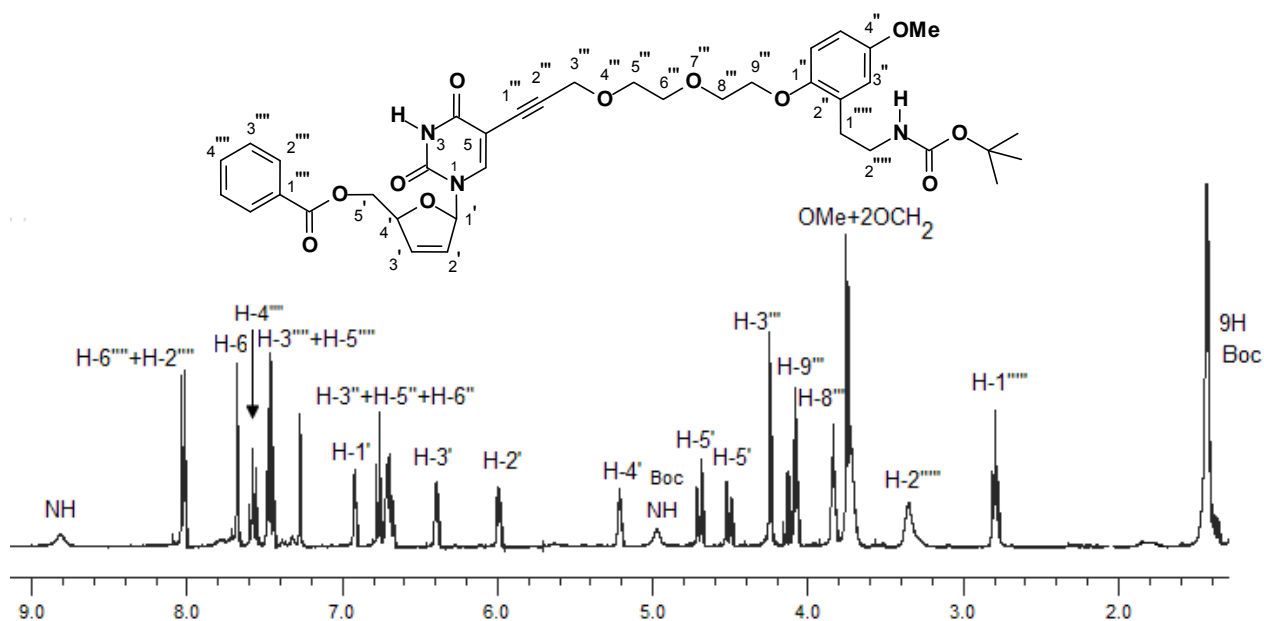


Figure 3.7 A full ^1H NMR (CDCl_3) spectrum for compound **115**.

Deprotection of the Boc group and condensation with thiourea derivative **49** (Scheme 3.12) was carried out for compound **115** using the standard procedure that was described before, to afford the desired product **116** in 63% yield over the two steps after column chromatography. Once again, the ^1H and ^{13}C NMR spectra of **116** were consistent with desired changes. The ^1H NMR spectrum (Fig. 3.8) showed resonances for the two new NH protons at δ_{H} 11.01 and δ_{H} 9.29 as well as δ_{H} 6.91 for H-1', δ_{H} 4.21 for H-3''', δ_{H} 3.74 for OCH_3 and δ_{H} 3.98 for H-2''''', with correct relative integrations. The individual six protons of both the pyridine and aromatic ring could be discerned. The pyrimidine proton H-6 appeared, as expected, relatively shielded by the benzoate phenyl group at δ_{H} 7.67 consistent with other cases.

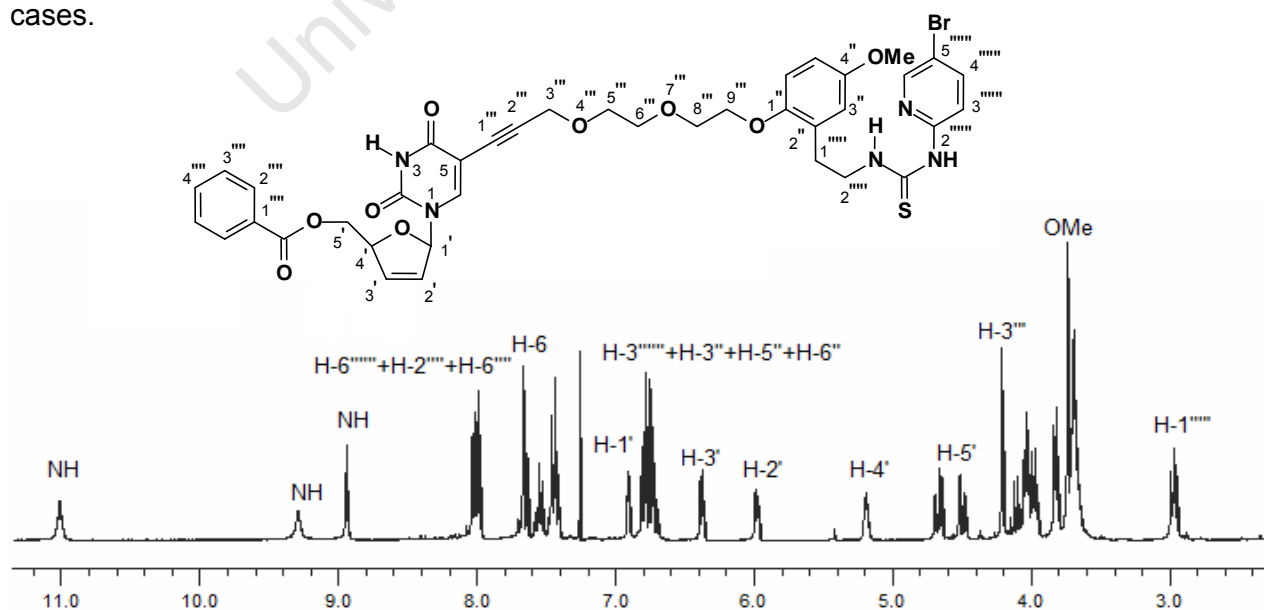


Figure 3.8 A full ^1H NMR (CDCl_3) spectrum for compound **116**.

The ^{13}C NMR spectrum for compound **116** revealed the presence of a thiocarbonyl carbon at δ_{C} 179.2, δ_{C} 112.5 for C-5''''', δ_{C} 55.5 for OCH₃, δ_{C} 90.8 for C-1' and δ_{C} 90.1 for C-1''' as well as four OCH₂ carbons as shown in Figure 3.9.

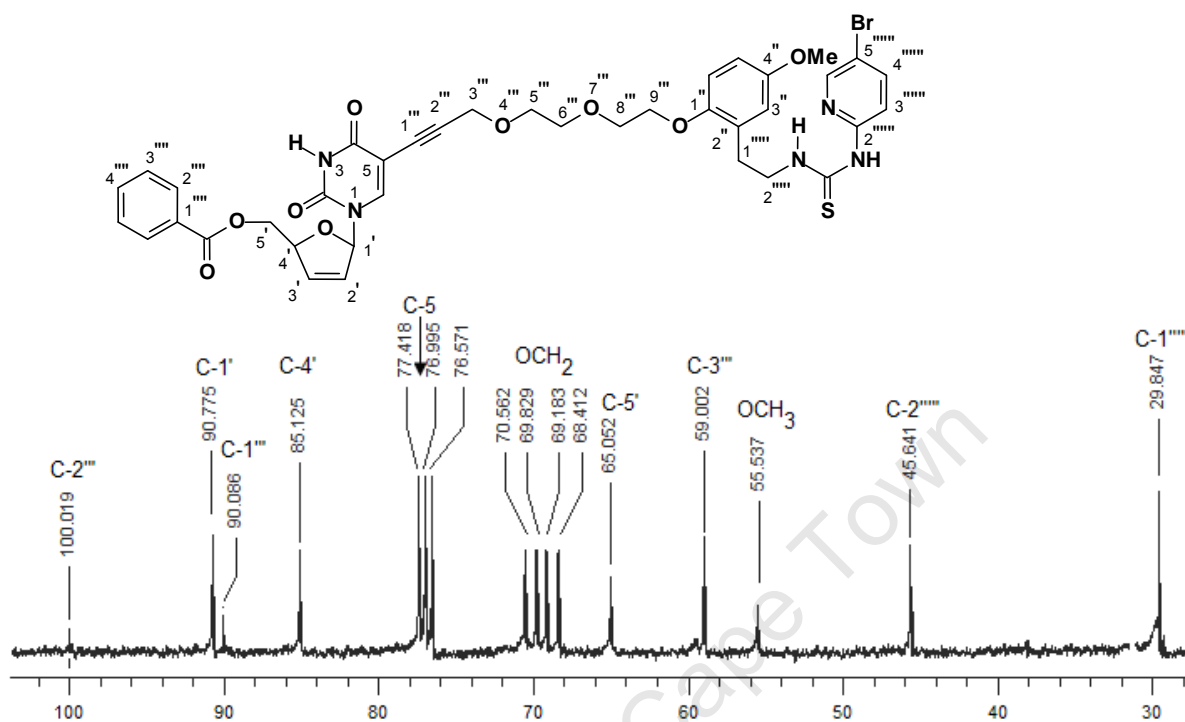


Figure 3.9 A portion of ^{13}C NMR (CDCl_3) spectrum for compound **116**.

With **116** in hand, only benzoyl deprotection remained for synthesis of the target molecule **79**, which was carried out using the same conditions as above (NaOMe (cat) in MeOH at 0 °C), to afford the target **79** with retention of the sugar moiety in 54% after column chromatography, as revealed by relative integration. The ^1H and ^{13}C NMR spectra of **79** revealed the disappearance of the benzoyl group, (Fig. 3.10) as well as an upfield shift for the diastereotopic protons H-5' from δ_{H} 4.67 and δ_{H} 4.50 in **116** to between δ_{H} 3.66-3.56 in **79**. The appearance of a triplet at δ_{H} 4.94 corresponding to a hydroxyl group confirmed the absence of a benzoate ester. H-6 of the pyrimidine ring now appeared downfield at δ_{H} 8.10 consistent with the benzoyl group shielding mentioned previously. As with the shorter pegged bifunctional **78**, the three NH resonances could be clearly discerned but even more downfield than before. The ^{13}C NMR spectrum displayed the absence of a carbonyl carbon at δ_{C} 166.2 as well as an upfield shift of the C-5' resonance from δ_{C} 65.1 in **116** to δ_{C} 61.7. Four methylene singlets 69.5 (OCH₂), 68.9 (OCH₂), 68.5 (OCH₂), 68.2 (OCH₂), could be seen for the peg. Further evidence was given by mass spectrometry data, HRMS (ES): 716.1389 (M^+ + H), which correlated with the molecular formula of $\text{C}_{31}\text{H}_{35}\text{N}_5\text{O}_8\text{SBr}$.

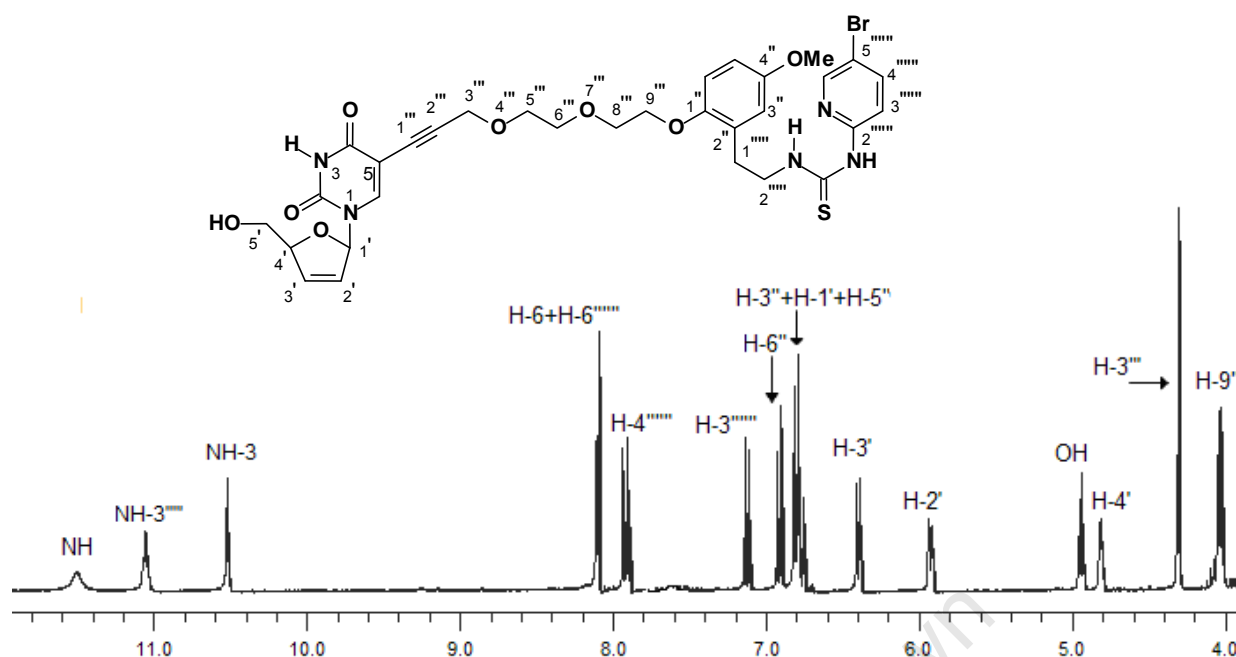


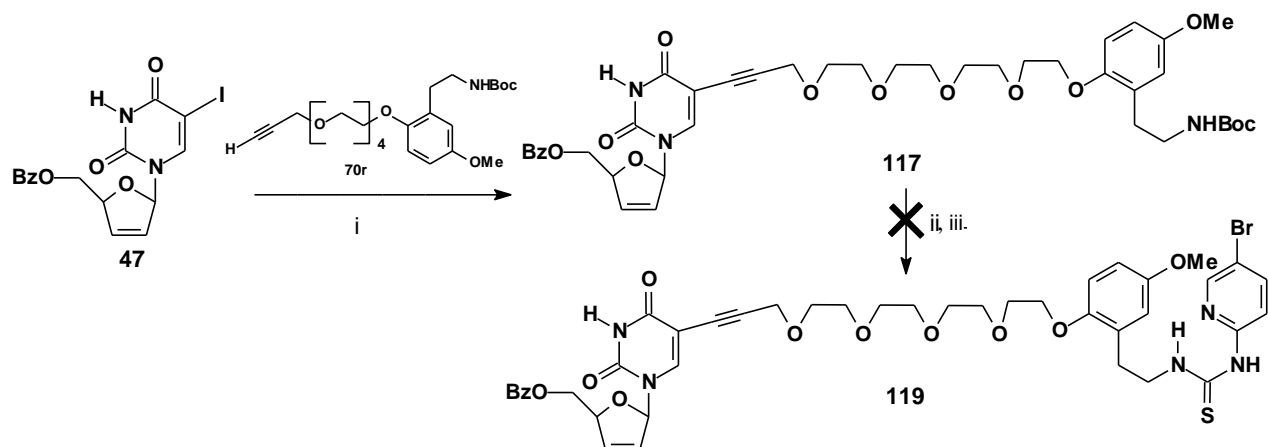
Figure 3.10 A portion of ^1H NMR (CDCl_3) spectrum of compound **79**.

3.6 Route (B): Synthesis of target compounds **80** and **81**

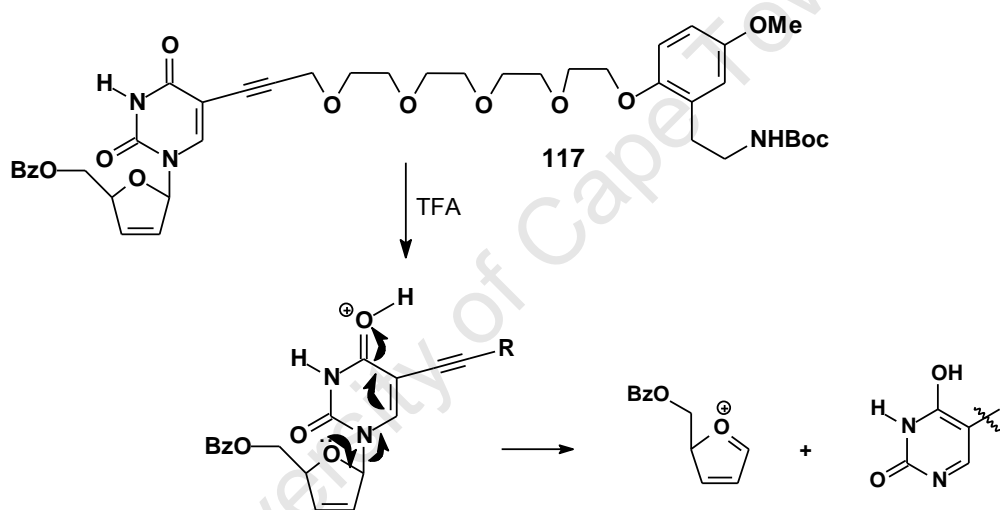
3.6.1 Synthesis of [d4U]-tetraPEG-propyne-[HI-236] **80**

Extending the sequence to the 4-PEG tether give the first signs of breakdown. Thus, the Sonogashira coupling of iodo-d4U **47** with alkyne **70r**, which had already been synthesized (Scheme 2.21, Chapter 2) gave the coupling product **117** in 70% yield (Scheme 3.13). Its structure was confirmed by ^1H NMR spectroscopy, which showed all the expected resonances in much the same position as the mono- and 2-PEG derivatives (**113** and **115**) except with the appearance of the additional signals for the extra PEG groups. The coupling product **117** was then subjected to the standard deprotection conditions of TFA in DCM followed by condensation with thiourea derivative **49** using the standard procedure. However, following product isolation, the ^1H NMR spectrum of the reaction product revealed the absence of the sugar moiety, indicating that cleavage of the sugar had taken place and that the product was not **119**. This step was extensively optimized in different way by minimizing trifluoroacetic acid equivalents and carrying out the reaction at various (lower) temperatures, but the cleavage persisted.

A plausible explanation for the cleavage relates to the leaving ability of a protonated pyrimidine base being favoured by the allylic bond resonance in the sugar ring helping to stabilize the resultant oxocarbenium ion as shown in Scheme 3.14. The cleavage was only observed for the 4-PEG derivative for reasons unknown.



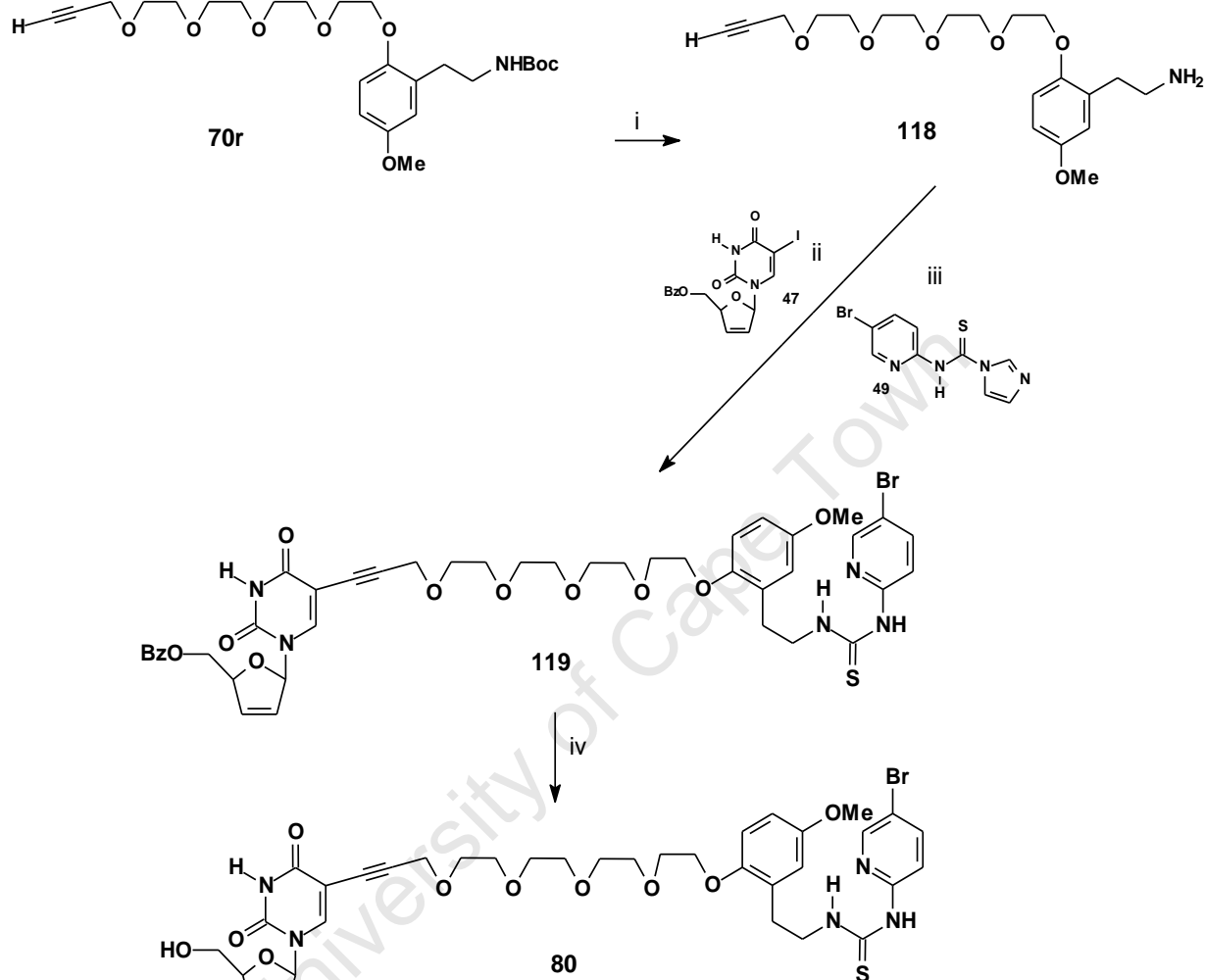
Scheme 3.13 Reagents and Conditions: (i) alkyne **70r**, $(\text{PPh}_3)_4\text{Pd}$ (10%) CuI (50%), Et_3N (2 eq), DMF: THF (1: 2), rt, 4h, 70%; (ii) TFA, CH_2Cl_2 , 0 °C; (iii) $\text{EtN}(\text{i-Pr})_2$ followed by thiourea **49**, THF, rt, 18 h.



Scheme 3.14 Plausible mechanism for degradation of **117**.

Since Sonogashira coupling reactions are documented to proceed in the presence of unprotected hydroxyl and amino groups,^{165,168} It was decided to deprotect the Boc group of **70r** to the amine first, and then react under Sonogashira coupling conditions. Condensation with thiourea derivative **49** followed by benzoyl deprotection would then afford the target product. To this end, deprotection of alkyne **70r** using trifluoroacetic acid in DCM at 0 °C gave a very polar primary amine spot ($R_f = 0.9$ in 10% MeOH in CH_2Cl_2). Since the product could not be extracted from water into an organic solvent, work-up involved adding anhydrous K_2CO_3 in MeOH, filtering and evaporating to liberate the crude amine **118**, which was used in the next step without further purification. Sonogashira coupling of iodo-d4U **47** with amine **118** carried out using the same conditions above yielded a coupling product according to tlc, which was subjected to column chromatography employing EtOAc / MeOH /

Et₃N (5 / 4 / 1). The amine product was then condensed with thiourea derivative **49** in THF at room temperature for 20 h. Following evaporation of solvent, the residue was subjected directly to column chromatography to afford the desired product **119** in 40% over the three steps (Scheme 3.15).



Scheme 3.15 Reagents and Conditions: (i) TFA, DCM, 0 °C, 2 h, K₂CO₃; (ii) **47**, (PPh₃)₄Pd (10%), CuI (50%) Et₃N (2 eq), DMF: THF (1: 2), rt, 4h; (iii) followed by thiourea **49**, THF, rt, 18 h, 40% (for the 3 steps); (iv) NaOMe (cat), MeOH, 0 °C, 20 min, 52%.

Given the spectral information on the other adducts already available, it was reasonably straightforward to confidently conclude that the desired product **119** had been formed. The ¹H and ¹³C spectra of **119** are shown in Figures 3.11 and 3.12, and pleasingly they reveal a very pure sample.

With **119** in hand, deprotection of the benzoyl group using the same conditions as described before (NaOMe (cat) in MeOH at 0 °C) was carried out to give the target molecule **80** in 52%

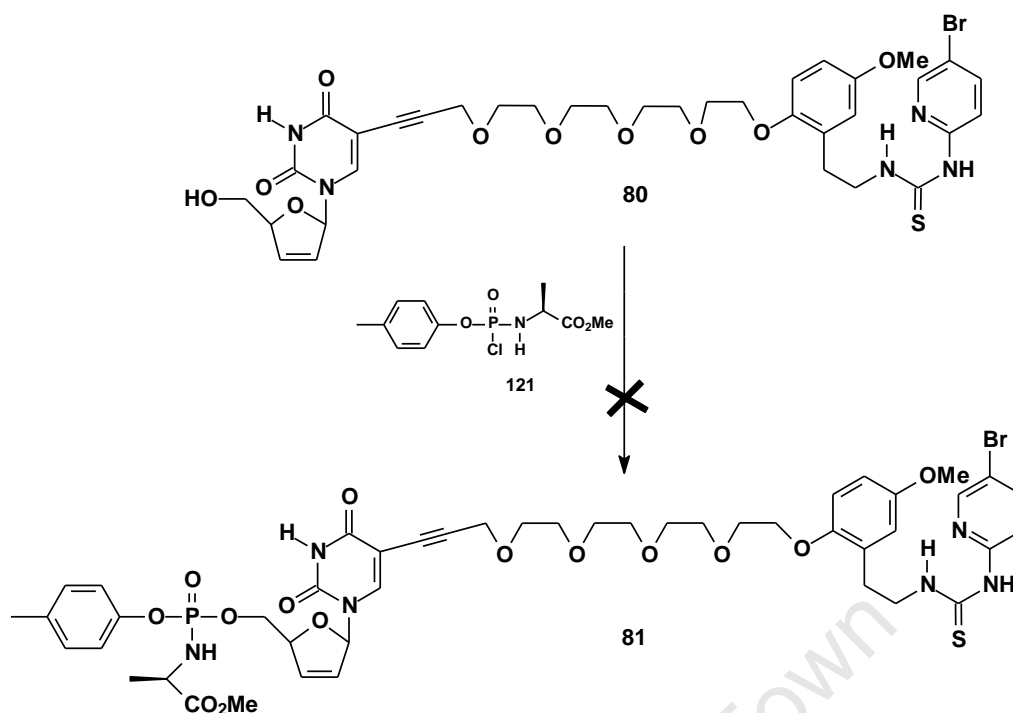
yield, with spectral data consistent with previous assignments. The structure of compound **80** was unequivocally assigned on the basis of its spectroscopic data using a combination of both 1D and 2D ^1H and ^{13}C NMR as well as IR techniques and high-resolution mass spectrometry. The ^1H and ^{13}C NMR spectra of **80** revealed the absence of resonances for the benzoyl group. The ^1H NMR spectrum in d_6 DMSO (Fig. 3.13) revealed an upfield shift for the H-5' protons from δ_{H} 4.70 and δ_{H} 4.52 in **119** to between δ_{H} 3.60-3.47, indicated that debenzoylation had taken place. The appearance of a triplet at δ_{H} 5.02 corresponding to the hydroxyl group supported the absence of a benzoate ester. As expected, the three pyridine ring signal were downfield to those for the aromatic ring. Integration of sugar signals to those for HI-236 confirmed a 1:1 ratio. The ^{13}C NMR spectrum (Fig. 3.14) displayed the absence of a carbonyl carbon at δ_{C} 166.2 as well as an upfield shift in the C-5' resonance from δ_{C} 65.0 in **119** to δ_{C} 61.7. For HRMS (ES), the parent ion was found to be 804.1932 ($M^+ + \text{H}$) correlating to the correct molecular formula of $\text{C}_{35}\text{H}_{43}\text{N}_5\text{O}_{10}\text{SBr}$ (requires ($M^+ + \text{H}$) 804.1914), thus confirming the formation of **80**.

3.6.2 Synthesis of [d4U-phosphoramidate]-tetraPEG-propyne-[HI-236] **81**

3.6.2.1 Synthesis of iodo-d4U-phosphoramidate.

It was decided to convert the [d4U]-tetraPEG-propyne-[HI-236] bifunctional molecule **80** into a phosphoramidate prodrug **81** in an attempt to improve inhibitory activity. The main idea as discussed in Chapter 1 was to bypass the rate-determining first step by virtue of having one phosphate in place, thus facilitating formation of the triphosphate *in vitro*.¹⁶⁹ A McGuigan-type phosphoramidate^{170,171} was chosen initially in view of its proven biological track-record as well as the prospect of realising it in a one-pot reaction in a straightforward manner via conditions compatible with the bifunctional. The 4-PEG derivative was the one chosen in view of its length being perceived as optimal for reaching the DNA site.

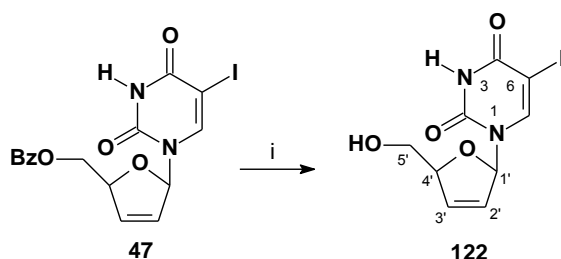
The first approach, therefore, involved attempting to directly phosphorylate bifunctional nucleoside **80** with phosphorochloridate **121**¹⁷², itself readily prepared from *p*-methylphenol and phosphorous oxychloride followed by substitution with L-alanine methyl hydrochloride ester according to McGuigan's original protocol.^{172,173} However, reaction of **121** with **80** failed to give the desired product **81** (Scheme 3.16) and only degradation of the starting material was observed on the tlc.



Scheme 3.16 Reagents and Conditions: (i) *N*-Methylimidazole, THF, rt, 24 h.

Thus, it was decided to pursue a synthesis involving a convergent Sonogashira coupling of an iodo-nucleotide as its phosphoramidate with an alkynylated version of HI-236. Given the problems of coupling with the thiourea moiety intact as well as a lack of confidence of Boc removal with TFA in the presence of the phosphoramidate, it was decided to use amine **118** in the strategy just described in Scheme 3.15.

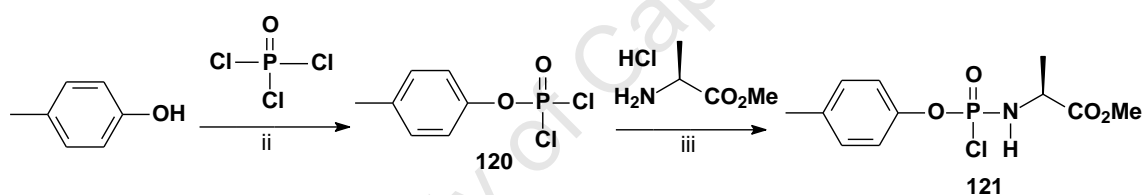
For the synthesis of the nucleotide coupling partner, deprotection of the benzoyl group of 5'-O-benzoyl iodo-d4U **47** using NaOMe (1.0 eq.) in MeOH was carried out to give the desired product **122**¹⁸³ in a good yield and as a more polar product on tlc Scheme 3.17. The ¹H and ¹³C NMR spectra of **122** displayed the absence of resonances for the benzoyl group, while its ¹H NMR spectrum displayed an upfield shift of H-5' from δ_{H} 4.52 in **47** to δ_{H} 3.62, indicating that debenzoylation had taken place. The appearance of a triplet at δ_{H} 5.01 corresponding to the hydroxyl group, supported the presence of a primary alcohol. Further evidence was given in the ¹³C NMR spectrum which displayed an upfield shift in the C-5' resonance from δ_{C} 65.3 in **47** to δ_{C} 61.5 as well as the disappearance of the ester carbonyl carbon at δ_{C} 165.5.



Scheme 3.17 Reagents and Conditions: (i) NaOMe (1.0 eq), MeOH, 0 °C-rt, 2 h, 74%.

Following the method described by McGuigan *et. al.*,^{172,173} *p*-methylphenol was reacted with phosphoryl chloride in diethyl ether and triethylamine to afford the aryl phosphorodichloridate **120**¹⁷² in 81% after vacuum distillation (bp 85-90 °C, 0.1 mmHg), (lit. bp 80-85 °C, 0.1 mmHg) as shown in Scheme 3.18. The product was also confirmed using ¹H and ³¹P NMR spectroscopy data which corresponded to that of the literature.¹⁷²

p-Methylphenyl phosphorodichloridate **120** was allowed to react with alanine methyl ester hydrochloride in dichloromethane in presence of triethylamine to give *p*-methylphenyl methoxyalaninyl phosphorochloridate **121** as a colourless oil in 100%, which was used in the next step without further purification (Scheme 3.18).



Scheme 3.18 Reagents and Conditions: (i) Et₃N (1 eq), Et₂O, 0 °C-rt, 17 h, 81%; (ii) DCM, Et₃N (2 eq), -78 °C-rt, 14 h, 100%.

Chloride **121** was then reacted with iodo-d4U **122** in THF in the presence of *N*-methylimidazole to give the desired compound **123** as a (1:1) mixture of diastereoisomers in a 54% yield after purification by column chromatography (Scheme 3.19). The ¹H NMR spectrum of **121** revealed split peaks at δ_H 6.38, 6.32 for (dt, H-3'), between δ_H 4.46-3.82 for (m, H-5'), at δ_H 3.72, 3.71 for (s, OCH₃) and at δ_H 1.41, 1.36 for (d, Ala-CH₃) due to diastereoisomers at the phosphoramidate centre. The additional aromatic resonance at δ_H 7.11 for the new phenyl ring also confirmed substitution. The ¹³C NMR spectrum also revealed split peaks due to diastereoisomers (starred) for (CO₂Me) 173.9*, (C-3'', C-5'') 133.0*, (C-5') 66.6*, (Ala-OCH₃) 52.4* and (ArCH₃) 20.8* (given as an average). Further evidence of substitution to **121** was provided by the ³¹P NMR spectrum which displayed two closely-spaced singlets at δ_P 3.7, 3.5 (1:1).

spectrometry. The ^1H and ^{13}C NMR spectra for compound **81** revealed that some peaks were split due to diastereoisomers as a result of stereogenicity at phosphorus as expected. Notably, some important ^1H NMR chemical shifts are shown in Table 3.1 and Figure 3.15. The ^{13}C NMR spectrum displayed resonances at 179.2 for C=S, 173.9* for CO_2Me , 66.7 for (d, $J_{\text{cp}} = 4.5$ Hz, C-5'), 99.9 for C-2''', 91.3* for C-1', 58.9 for C-3''', 55.6 for OCH_3 , 52.5 for CO_2CH_3 , 50.3* for Ala-CH, 29.8 C-1'''' and 20.7 Ph- CH_3 with starred peaks as an average for the diastereoisomers. The ^{31}P NMR spectrum revealed two closely-spaced singlets at δ_{P} 3.63 and 3.56 in 1:1 ratio (Fig. 3.16). The IR spectrum of **81** indicated a characteristic peak for C=S at 1462 cm^{-1} , for C=O at 1707 cm^{-1} and for P=O at 1259 cm^{-1} . Finally, a correct HRMS evaluation established in structure of **81** (m/z HRMS (ES) found 1059.2548 ($\text{M}^+ + \text{H}$), $\text{C}_{46}\text{H}_{57}\text{N}_6\text{O}_{14}\text{SBrP}$ requires ($\text{M}^+ + \text{H}$) 1059.2574). **81** is the second reported phosphoramidate of a bifunctional HIV inhibitor following those of Camarasa.¹³⁵

Table 3.1 Some Important split resonances in the ^1H NMR spectrum of **81**

δ_{H}	Multiplicity and Assignment	δ_{H}	Multiplicity and Assignment
7.79, 7.78	1H, s, H-6	5.91, 5.81	1H, dq, H-2'
7.66, 7.63	1H, dd, H-4''''	3.68, 3.67	3H, s, CO_2CH_3
6.96, 6.94	1H, m, H-1'	1.37, 1.33	3H, d, Ala- CH_3
6.37, 6.27	1H, dt, H-3'		

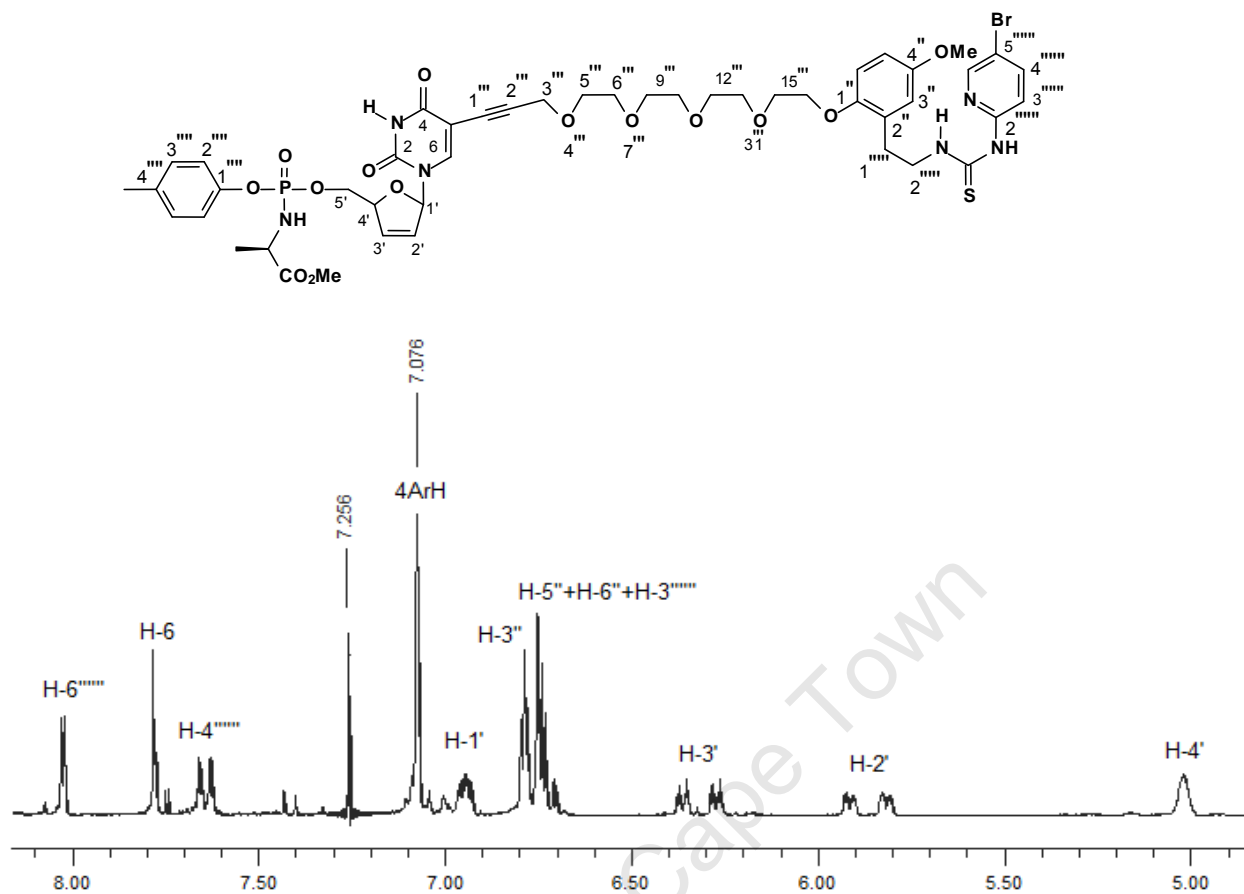


Figure 3.15 A portion ^1H NMR (CDCl₃) spectrum of compound 81.

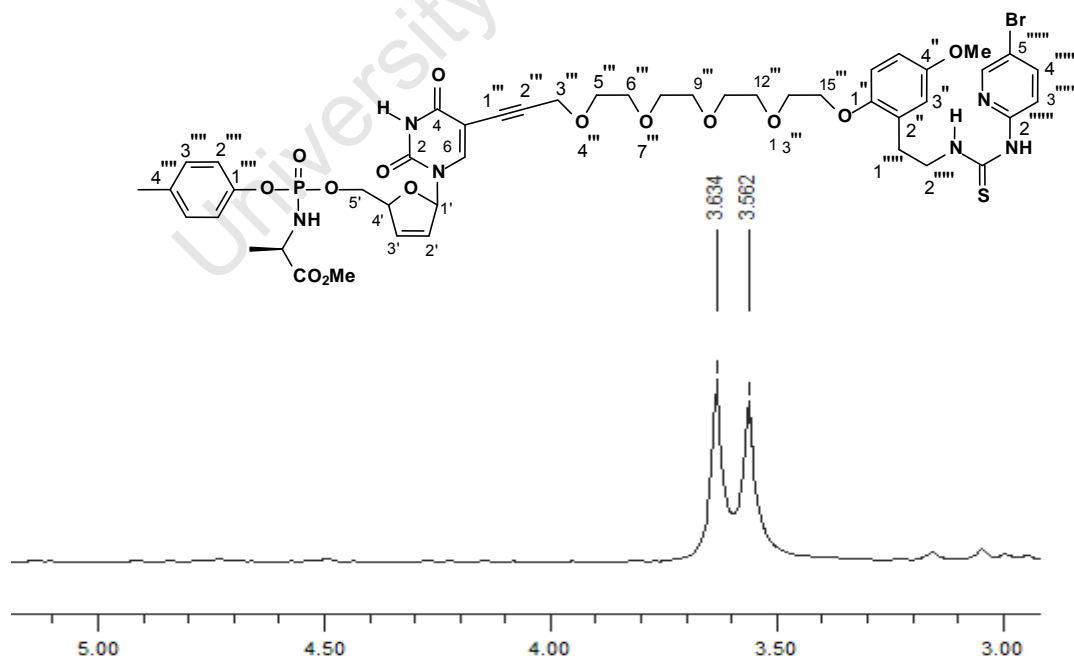


Figure 3.16 ^{31}P NMR (CDCl₃) spectrum of compound 81.

3.7 Biological results and rationale

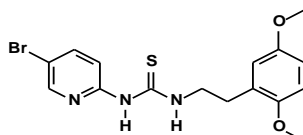
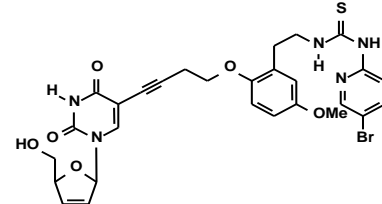
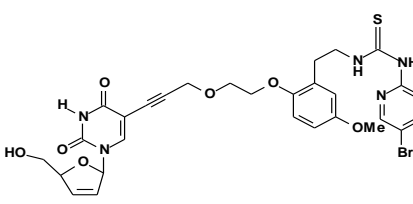
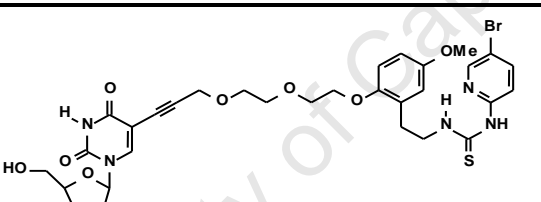
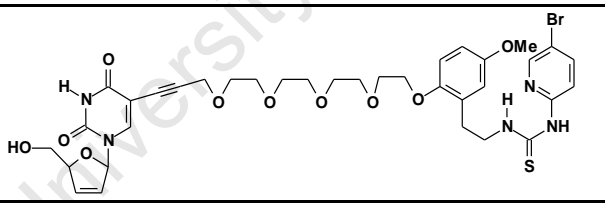
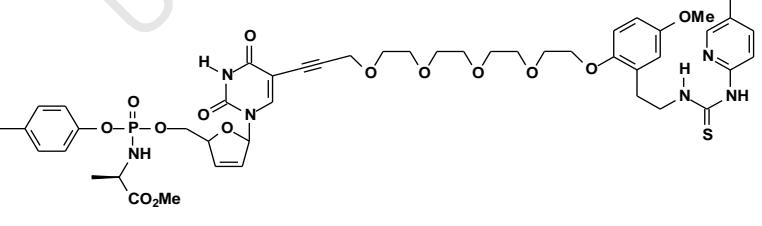
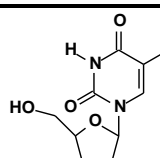
The following experimental applies for biological work carried out at Yale University. dTTP and dGTP were purchased from GE Biosciences. Oligonucleotide primers and template were synthesized at the Keck Facility at Yale University and were purified using 20% denaturing gel-electrophoresis. Primers and template used in this study are as follows: D23 (5'-TCA GGT CCC TGT TCG GGC GCC AC -3'), D24 (5'-TCA GGT CCC TGT TCG GGC GCC ACT-3'), and D36 (5'-TCT CTA GCA GTG GCG CCC GAA CAG GGA CCT GAA AGC-3'). Labeling and annealing of primer/templates were performed as described.¹⁷⁴

Expression and Purification of HIV-1 RT. C-terminal histidine tagged heterodimeric p66/p51 wild-type HIV-1 RT was expressed and purified as described previously¹⁷⁵ using a clone generously provided by Stephen Hughes, Paul Boyer, and Andrea Ferris (Fredrick Cancer Research and Development Center, Fredrick, MD).

IC₅₀ determination. 8 nM RT (active sites based on pre-steady state active site determination) was pre-incubated for at least 15 minutes with 1 μ M 5'-labeled primer/template prior to mixing with appropriate concentrations of inhibitor and allowed to incubate for a minimum of 15 additional minutes on ice. DMSO concentrations were kept constant at less than 2%. DMSO alone was added as a no inhibitor control for each set of experiments. Reactions were initiated with the addition of 5 μ M dNTP and 10 mM MgCl₂ and were quenched after 15 minutes at 37° C with 0.3 M EDTA. All concentrations represent final concentrations after mixing. Reaction products were subjected to 20% denaturing polyacrylamide gel-electrophoresis and quantitated on a Bio-Rad Molecular Imager FX. Product formation was plotted as a function of inhibitor concentration and fitted to a hyperbola to generate IC₅₀ curves. IC₅₀ values are defined as the concentration of inhibitor that inhibits steady-state single nucleotide incorporation by 50%.

The inhibitory activity of the bifunctional compounds **51**, **78**, **79**, **80** and **81** was explored against HIV-1 (IIIB) replication in MT-2 cell culture using an MTT assay. The results are shown in Table 3.2. HI-236 and d4T were also evaluated for comparison purposes. The bifunctional [d4U]-butyne-[HI-236] **51** showed a good inhibitory activity of EC₅₀ = 250 nM, which is eight times greater than d4T (EC₅₀ = 2 μ M), five times less active than HI-236 and thus between those of the two component drugs.

Table 3.2 Comparison of cell-culture versus in vivo RT inhibition (nM) for bifunctional compounds.

		Cell culture	RT Enzyme assay
HI-236		0.058 μ M	38 \pm 7 nM
51		0.25 μ M	61 \pm 15 nM
78		1.3 μ M	940 \pm 580 nM 575 \pm 137 nM
79		950 nM	850 \pm 140 nM
80		3.1 μ M	1.4 \pm 0.9 μ M 1.4 \pm 0.5 μ M
81		2.9 μ M	4.7 \pm 2.7 μ M 2.3 \pm 0.8 μ M
d4T		2 μ M	Not done

Lengthening the spacer resulted in a reduction in activity, perhaps as expected, except with the 2-PEG derivative **79** being more active than the 1-PEG derivative **78**. The 4-PEG derivative **80** still retained appreciable activity (3.1 μM), remarkably so for such a large molecule. Disappointingly, the phosphoramidate **81** showed no improvement, effectively indicating a promotion of triphosphate formation not to be operating, and hence the activity to be due to the NNRTI part only.

Similarly, the *in vitro* RT assay results are shown in Table 3.2. These experiments are based on following the inhibition of Th-TP (Thymidine triphosphate) incorporation by the bifunctional into a primer strand (D23) of a short dsDNA primer/template (D23/D36) against an A coding on the template strand, see Figure 3.17.

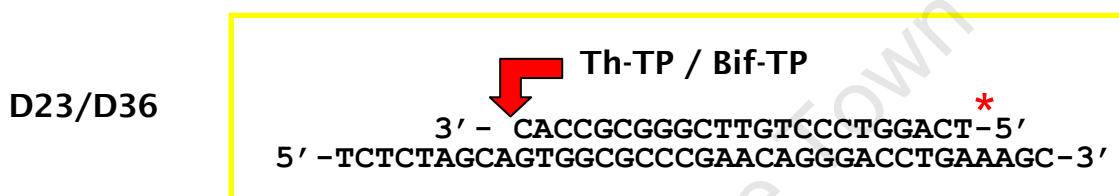


Figure 3.17 Schematic representation of correct base-pairing and incorporation experiments.

Certainly, the results in Table 3.2 from the enzyme assay support the expectation that the NRTI component of the bifunctional is being recognised as a “T” and getting incorporated in order to inhibit the incorporation of Th-TP. The *in vitro* RT inhibition results followed a similar trend, to those of the cell-culture except IC_{50} values (now directly on the enzyme) were generally indicative of greater potency compared to the cell-culture results. Once again, though, in spite of a large error factor in the results, phosphoramidate **81** proved to be no more active than its unphosphorylated precursor **80**.

In conclusion, the retention of activity in the double drugs suggests that one should view these inhibitors as substituted NNRTI's involving NNRTI binding with the tether exiting the pocket (maybe **51** can be completely in the pocket), leaving the NRTI in vicinity of the substrate binding site or somewhere between the two sites. NNRTI binding seems likely since d4T itself is only active at an EC_{50} of around 2 μM , and such a large “substituted NRTI” would be expected to be far less active based on NRTI activity alone. Furthermore, in the model study, HI-236 ester derivative **77g** was 12 μM as a much poorer but very much smaller binder suggesting these bifunctionals must be achieving binding in the NNRTI pocket. However, the phosphoramidate result for **81** suggests conversion to a triphosphate is not operating via a pronucleotide involvement and thus, no mixed-site inhibition is being realised. The NNRTI of such bifunctionals cannot go through the “back” of the pocket

because the molecules are not configured correctly, thus NNRTI binding must occur in the normal way through the “front” end.

However, bifunctional **51**, **78** and **78** compounds are much superior to the d4U dimers (with Troviridine) by Ladurée and co-workers,¹²⁸ which were inactive. Their results indicated an incorrect choice of attachment point of the NNRTI to the tether, and lend some credibility to our hypothesis that our HI-236 system can exit the pocket and still retain activity.

In view of the lack of success with the phosphoramidate **81**, at this point it was decided to change the NRTI to an acyclic nucleotide phosphonate, which is the topic of the final Chapter.

University of Cape Town

Similarly, the chiral centre in the side chain was omitted. Finally, a phosphate ester was chosen as the simplest option for a pro-drug,¹⁷⁶ but we were well aware of the possible need for better (cleavable) groups such as POM or POC. As before, a peg spacer was chosen for connection of the two drugs. Long spacers were chosen to probe flexibility.

4.1 Synthesis of [ANP]-*n*-PEG-propyne-[HI-236]: (*n* = 4 and 6)

4.1.1 Retrosynthetic analysis of [ANP]-*n*-PEG-propyne-[HI-236]

The synthesis of the ANP-incorporated bifunctionals **134** and **135** with medium-length (*n* = 4) and long spacers (*n* = 6) respectively was envisaged as being achievable *via* a condensation reaction between thiourea **49** and a convergently-derived Sonogashira coupling product from tethered amine **118** (or **133**) and pyrimidine-tethered phosphonate **132** as shown in Fig. 4.3.

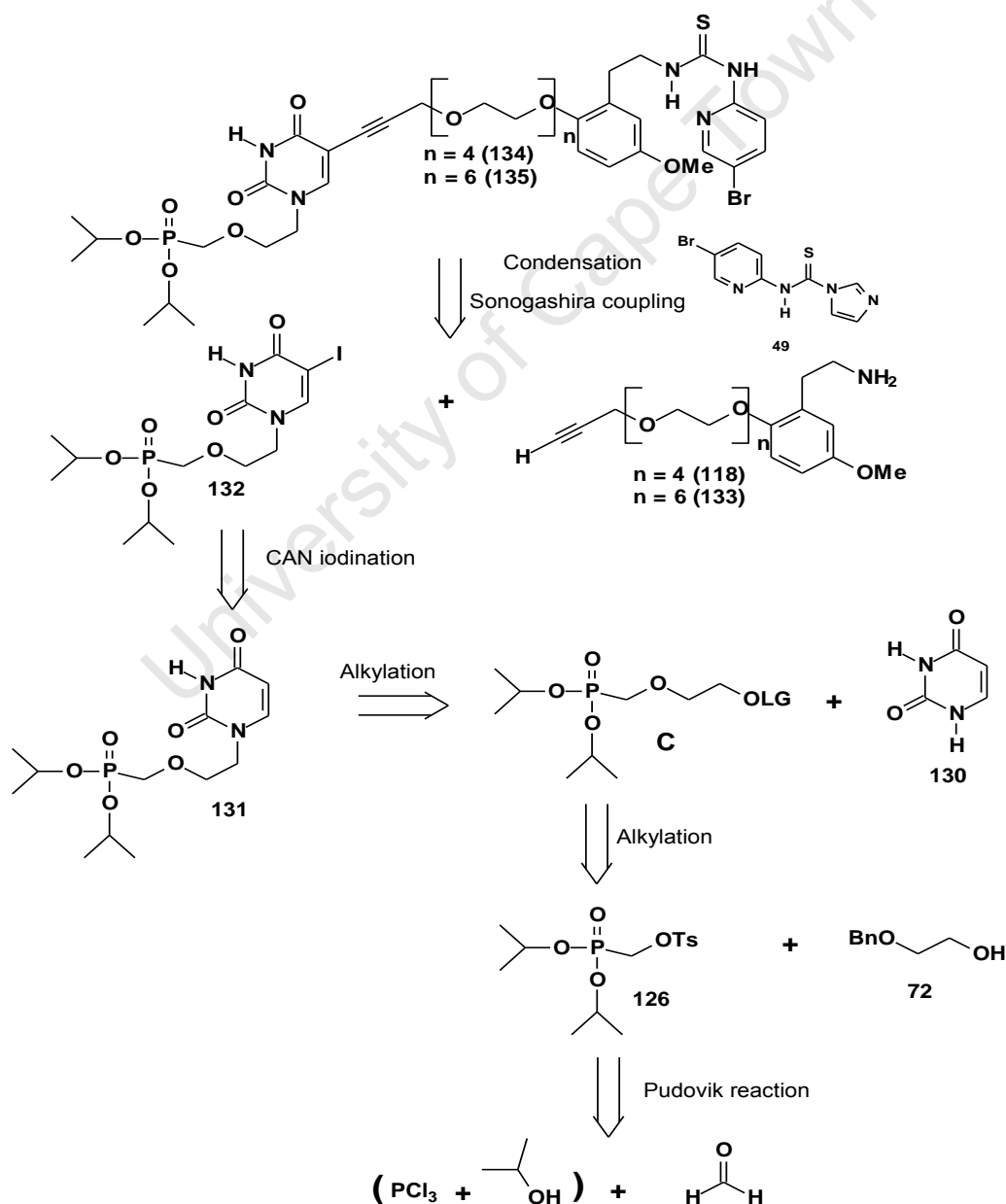
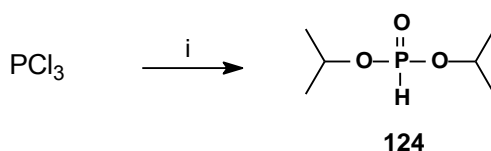


Figure 4.3 Retrosynthetic analysis of ANP incorporated bifunctionals **134** and **135**.

An amine-based Sonogashira coupling was preferred because the favored N-Boc-based coupling presented a potential problem with TFA deprotection regarding the phosphonate protecting groups. Phosphonate **132** would be generated from CAN iodination of **131**, which in turn would be prepared from ¹N-alkylation of unprotected uracil **130** by a modified two-carbon tethered phosphonate of type **C**. The latter was envisaged as available *via* alkylation of protected alcohol **73** by phosphonate **126**. Known chemistry in the form of the Pudovik reaction would be employed for the synthesis of **126**.

4.1.2 Synthesis of the ANP moiety

The synthesis towards 5-iodo-ANP **132** began with esterification of phosphorus trichloride with three equivalents of isopropanol (IPA) using two equivalents of sodium hydride in THF as outlined in a publication in 2004 by Fakhraian and co-workers¹⁷⁷ (Scheme 4.1). Diisopropyl hydrogen phosphonate **124**¹⁷⁷ was isolated in 98% yield after an aqueous work-up using ammonium chloride and evaporation of solvent, without the need for any column chromatography. The mechanism of the reaction (Fig. 4.4) reveals the importance of only adding two equivalents of base. Three equivalents of HCl are produced during the course of the reaction (step 1), of which only two equivalents can be neutralised up by the base. The remaining equivalent of HCl is used in the protonation of the phosphorus of the trialkylphosphite, which rearranges to a more stable pentavalent phosphorus in the form of the desired dialkyl hydrogen phosphonate (DAHP) *via* an Arbuzov-type dealkylation. In the case of adding three equivalents of base, no DAHP is produced. The reaction can also be performed under base-free conditions, but this means having to neutralize large quantities of HCl in the work-up. The ¹H NMR spectrum of **124** revealed the characteristically large P-H coupling for the hydrogen attached to phosphorus at δ_{H} 6.77 (1H, d, J_{HP} = 687.0 Hz), thus confirming an H-phosphonate structure rather than a hydroxyphosphite one.



Scheme 4.1 Reagents and conditions: (i) IPA (3eq), NaH (2eq), THF, r.t, 98%.

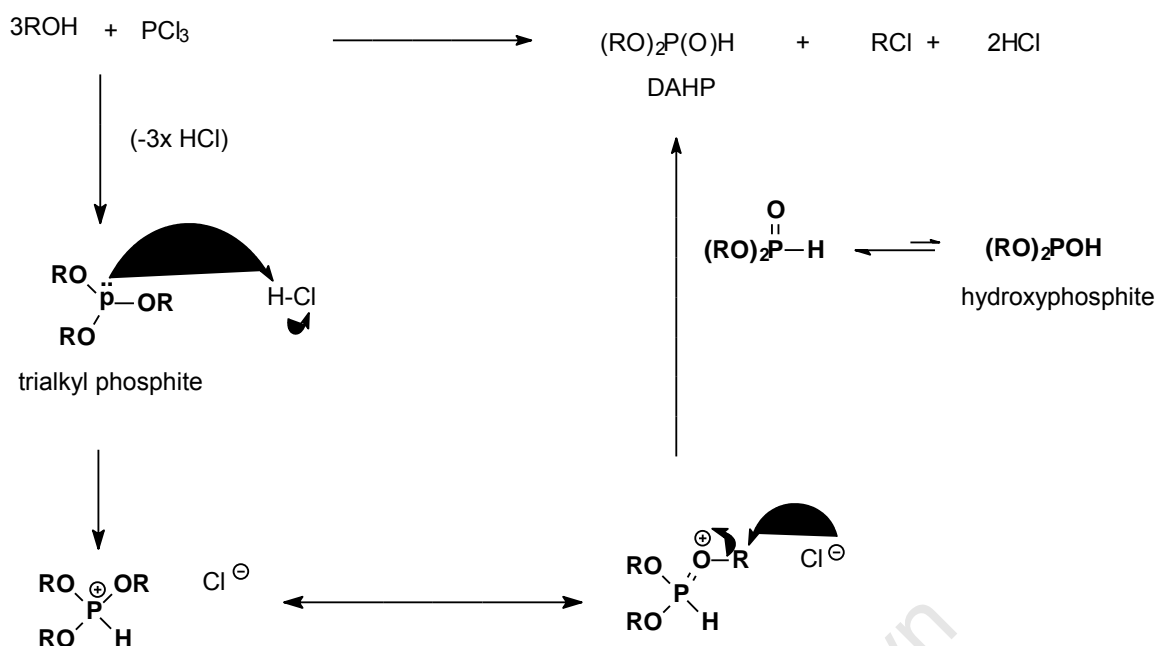
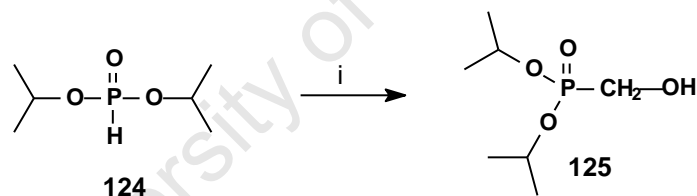


Figure 4.4 Mechanistic pathway proposed for production of DAHP.¹⁷⁷

Diisopropyl α -hydroxymethylphosphonate **125** was synthesized next by reacting **124** with paraformaldehyde and anhydrous potassium carbonate as a catalyst in IPA at 60 °C, (Scheme. 4.2) in a transformation better known as the Pudovik reaction^{178a} (Fig. 4.5).^{178b}



Scheme 4.2 Reagents and conditions: (i) $(\text{H}_2\text{CO})_n$, K_2CO_3 , IPA, 60 °C, 98%.

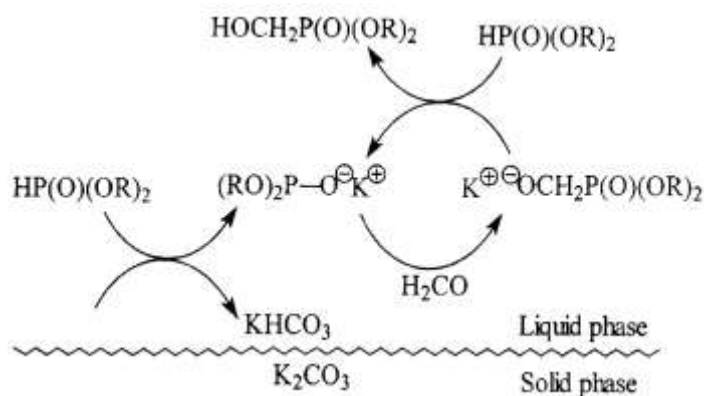
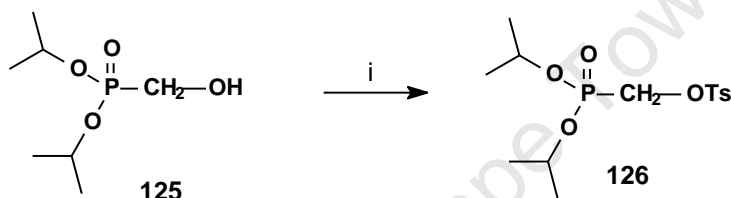


Figure 4.5 Proposed mechanism of the Pudovik reaction under heterogeneous conditions.¹⁷⁸

Carbonates are commonly used in heterogeneous phase as a non-nucleophilic solid 'soft' base because they are easy to handle, and to eliminate by filtration at the end of the reaction. Therefore, the α -hydroxymethylphosphonate **125** was isolated in 98% yield without the need for silica-gel chromatography.

The ^1H NMR spectrum of **125** revealed a diagnostic OH singlet at δ_{H} 2.15, as well as a methylene doublet at δ_{H} 3.82 (2H, d, $J_{\text{HP}} = 6.6$ Hz, CH_2P). Its ^{31}P NMR spectrum displayed a characteristic signal at δ_{P} 22.9, exactly as reported in the literature.¹⁷⁸

Subsequent tosylation of alcohol **125** using *p*-toluenesulfonyl chloride in the presence of triethylamine and a catalytic amount of DMAP in dichloromethane returned the desired tosylate **126** uneventfully in 92% yield after column chromatography as shown in Scheme 4.3.



Scheme 4.3 Reagents and conditions (iii) *p*-TsCl, NEt_3 , CH_2Cl_2 , DMAP (cat), r.t, 92%.

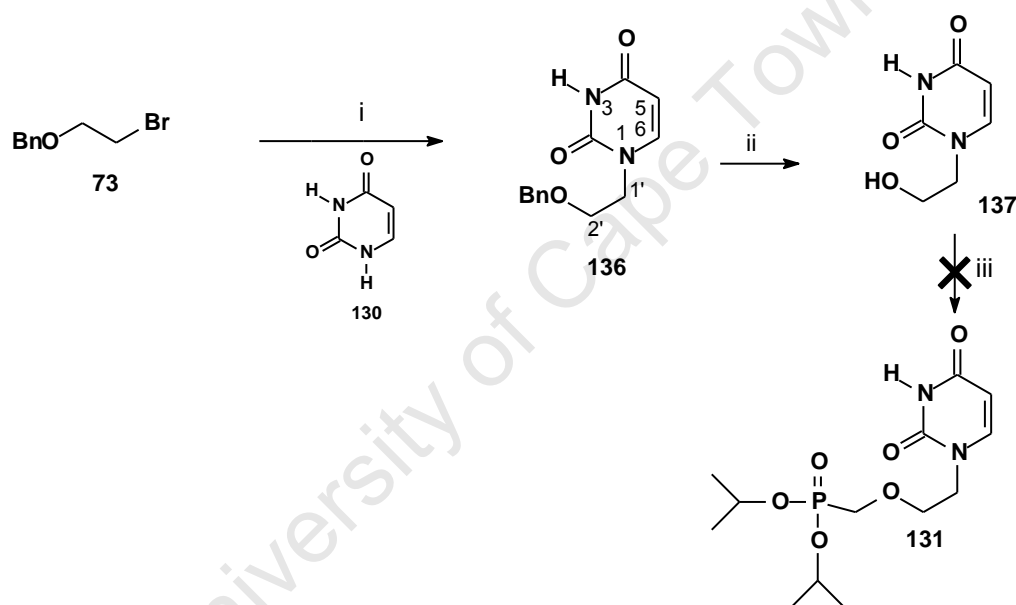
The ^1H NMR spectrum of **126** displayed a new set of aromatic protons as an AB pair ($J_{\text{AB}} = 8.0$ Hz) resonating at δ_{H} 7.36 and δ_{H} 7.80 as well as a methyl singlet at δ_{H} 2.46. The presence of additional aromatic signals in the ^{13}C NMR spectrum of **126** further confirmed the presence of a tosylate group.

With **126** now in hand, the next phase involved coupling of it to obtain 5-iodo-ANP **132**, which in the first strategy tried out began with nucleophilic substitution of bromide **73**, whose synthesis was mentioned previously (Scheme 2.10, Chapter 2). Thus uracil **130** was reacted with **73** in the presence of NaH as a base in DMF at 100 °C. The desired product **136** was obtained as the major product but in only 30% isolated yield after column chromatography (Scheme 4.4). The product was fully characterized using ^1H and ^{13}C NMR spectroscopy. Thus, apart from the correct integration of the two molecular fragments, ^1N -alkylation over ^3N -alkylation was supported by the disappearance of the ^1NH proton in the ^1H NMR spectrum as well as the retention of the ^3NH proton at around δ_{H} 9.07. HMBC connectivities were also used to reveal H-6 coupling to H-1'. This chemoselective alkylation is consistent with a literature report¹⁷⁶ describing the greater reactivity of the ^1N anion over the more stable ^3N anion. Thereafter, compound **136** was committed to hydrogenolytic debenzoylation using a

10% palladium-on-carbon catalyst in MeOH:THF (1:1) under hydrogen gas at rt for 6 h to afford alcohol **137** in 80%. The ^1H NMR of **137** confirmed the disappearance of aromatic protons as well as the benzyl methylene singlet. Under varying conditions of temperature, solvent and base (see Table 4.1), alcohol **137** was subjected to alkylation with tosyloxyphosphonate **126**, however the reaction failed to give the desired product **131**, as shown in Table 4.1. The TLC of the reaction showed only starting material and no conversion.

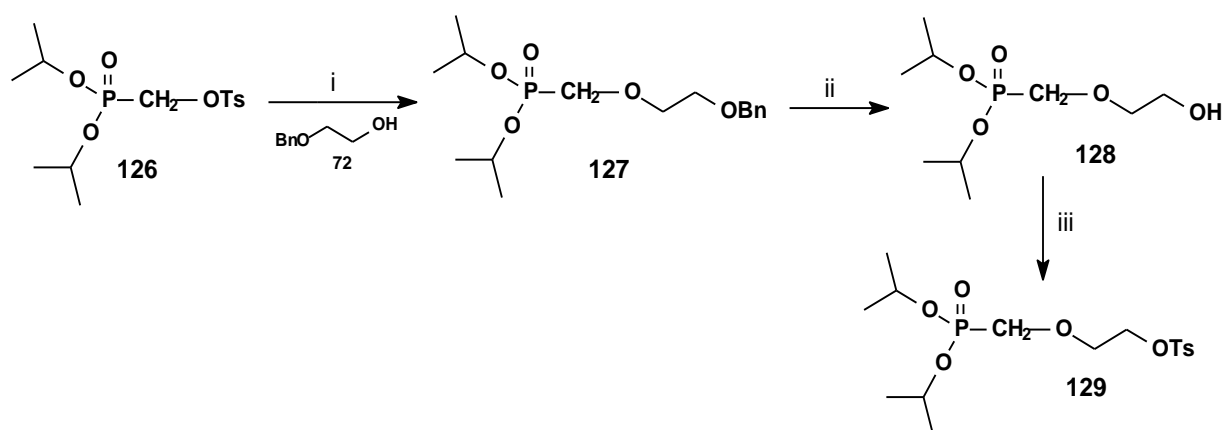
Table 4.1 Different reaction conditions for alkylation of alcohol **137** with tosyloxyphosphonate **126**.

Reaction	Solvent	Base	Time	Temperature	Observation
1	THF	NaH	18 h	70 °C	No product
2	CH ₃ CN	K ₂ CO ₃	20 h	80 °C	No product
3	DME	Cs ₂ CO ₃	24 h	100 °C	No product



Scheme 4.4 Reagents and conditions: (i) **130**, NaH, DMF, 100 °C, 30%; (ii) H₂, Pd/C, MeOH:THF (1:1), r.t., 6 h, 80%; (iii) **126**, various see Table 4.1.

The second strategy pursued was based on a more convergent approach involving substitution of a tethered phosphonate (Scheme 4.5). This was accomplished through alkylation of mono-benzyl ether **72** by tosylated phosphonate **126** using sodium hydride as base in THF at reflux, to obtain protected tethered phosphonate **124** in 72% yield after column purification. The ^1H NMR spectrum of **124** revealed an upfield shift of methylene protons α to phosphorus at δ_{H} 4.12 (d, $J_{\text{HP}} = 10.0$ Hz, CH₂P) for the tosylate **126** to δ_{H} 3.82 in **127**, as well as the presence of a new benzylic methylene singlet at δ_{H} 4.54. Its ^{31}P NMR spectrum returned a single peak at δ_{H} 19.7. Finally, a correct HRMS evaluation (m/z HRMS (ES) 331.16681 [M+H]⁺, C₁₆H₂₈O₅P requires m/z 331.1674 [M+H]⁺), confirmed the structure of **127**.



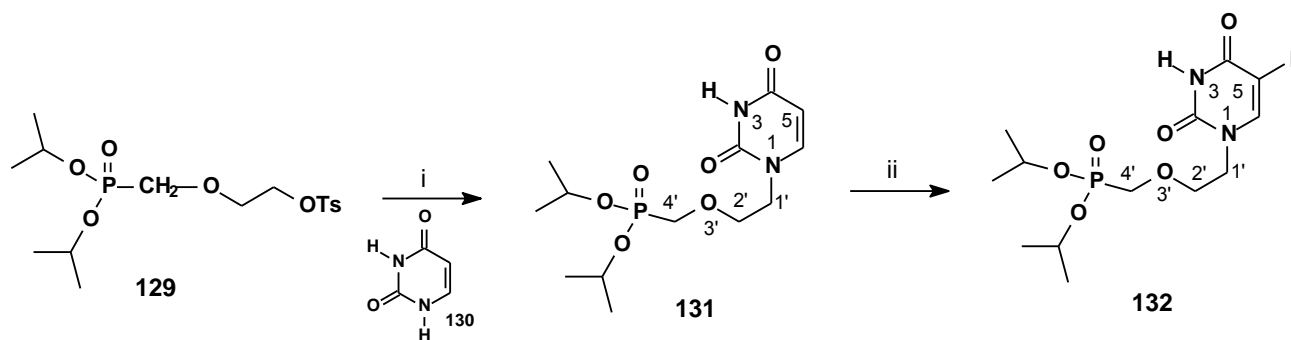
Scheme 4.5 Reagents and conditions: (i) **72**, NaH, THF, Δ , 72%; (ii) H₂, Pd/C, MeOH: THF (1:1), r.t. 77%; (iii) *p*-TsCl, NEt₃, CH₂Cl₂, DMAP (cat), r.t., 90%.

Catalytic hydrogenation of **127** to a more polar, non-uv active spot on tlc using a palladium-on-carbon catalyst in methanol/THF (1:1) furnished **128** in 77% yield (Scheme 4.5). The appearance of a hydroxyl proton as a broad singlet resonating at δ_{H} 2.52 and the absence of the characteristic benzylic methylene singlet at δ_{H} 4.54 for **128** provided evidence that debenylation had taken place.

The hydroxyl group of **128** was subsequently converted to tosylate **129** in 90% yield by reacting it with *p*-toluenesulfonyl chloride in the presence of triethylamine and a catalytic amount of DMAP in dichloromethane (Scheme 4.5). The ¹H NMR spectrum of **129** displayed aromatic protons with AB coupling ($J_{\text{AB}} = 8.3$ Hz) resonating at δ_{H} 7.33 and δ_{H} 7.78 as well as a methyl singlet at δ_{H} 2.43. The presence of additional aromatic signals in the ¹³C NMR spectrum further confirmed the presence of a tosylate group. The ³¹P NMR spectrum returned a singlet peak at δ_{P} 18.6 for the phosphonate.

The final part in the synthesis of the ANP involved coupling of the modified tethered phosphonate **129** (Scheme 4.6) via ¹N-alkylation of uracil **130** and was carried out using cesium carbonate in DMF at 100 °C. ANP **131** was isolated following aqueous work-up and purification by column chromatography in a modest 35% yield. Once again ¹N-chemoselectivity was observed based on alkylation of the more reactive anion. The ¹H NMR spectrum of **131** (Fig. 4.6) displayed two doublets at δ_{H} 5.64 (d, $J = 7.9$ Hz) and δ_{H} 7.36 (d, $J = 7.9$ Hz) for the H-5 and H-6 protons respectively. An upfield shift of the H-1' signal in the ¹H NMR spectrum from δ_{H} 4.14 in tosylate **129** to δ_{H} 3.94 in **131** supported the displacement of the tosylate. The ¹³C NMR spectrum of compound **131** displayed signals for the ANP at δ_{C} 66.2 (d, $J_{\text{C-P}} = 166.9$ Hz, H-4'), δ_{C} 48.3 (C-1'), δ_{C} 101.5 (C-5) and δ_{C} 145.8 (C-6). The diastereotopic methyl groups were observed as two sets of doublets (isopropoxy

groups enantiotopic). Its ^{31}P NMR spectrum displayed a diagnostic phosphonate singlet at δ_{P} 18.8.



Scheme 4.6 Reagents and conditions: (i) uracil **130**, Cs_2CO_3 , DMF, 100°C , 35%; (ii) I_2 , CAN, CH_3CN , 40°C , 4 hrs, 62%.

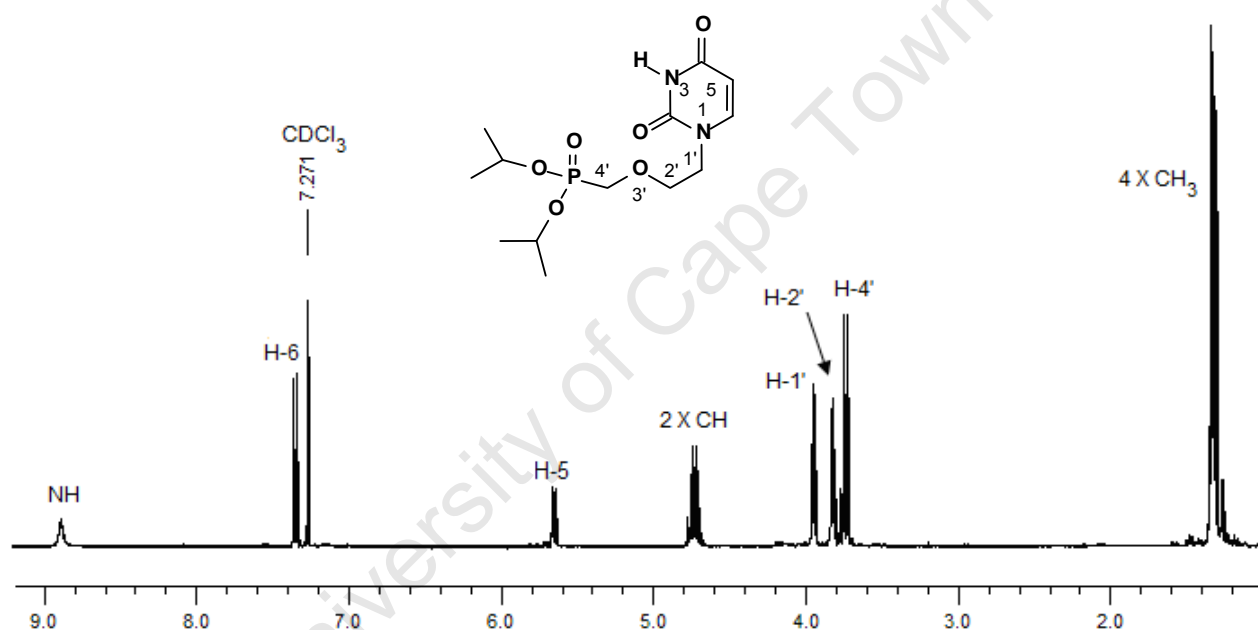
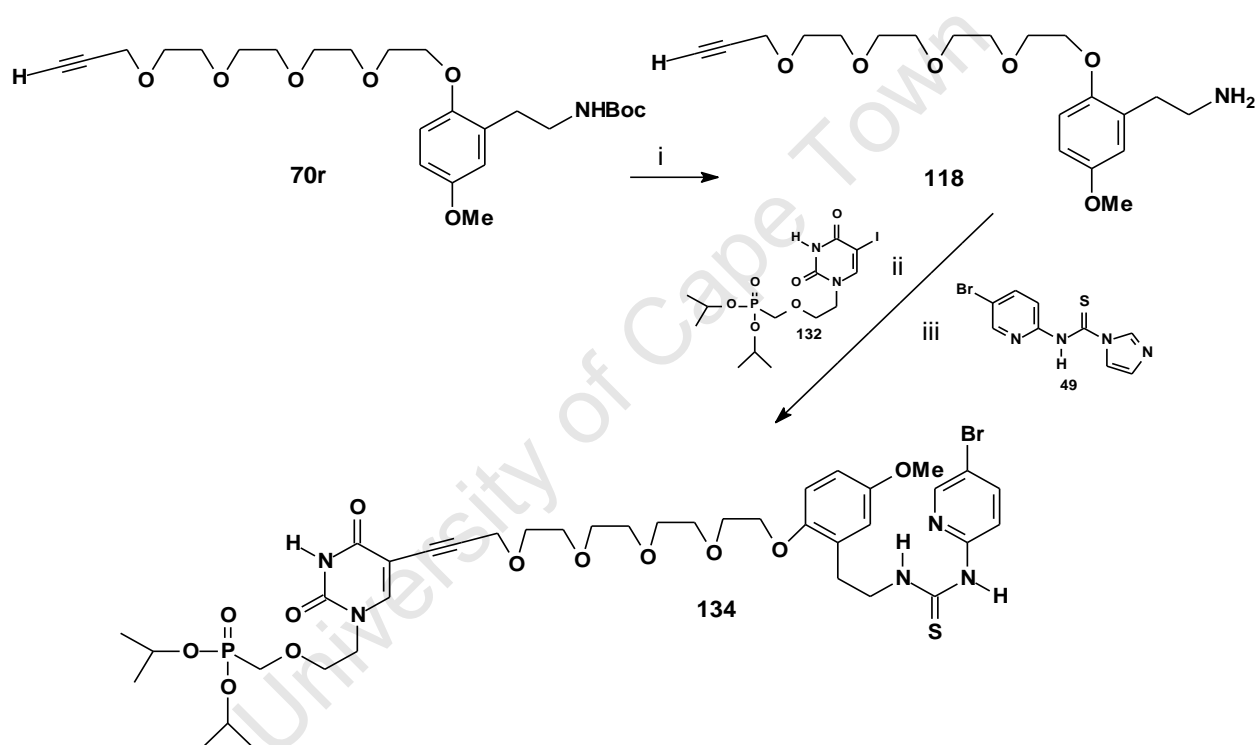


Figure 4.6 ^1H NMR (CDCl_3) spectrum of ANP **131**.

Finally, compound **131**¹⁷⁶ was iodinated (Scheme 4.6) using elemental iodine and cerium ammonium nitrate (IV) at 40°C . Tlc confirmed reaction completion after 4 hrs and **132** was obtained in 62% yield after column chromatography. The ^1H NMR spectrum of **132** supported iodination based on the change from an AB doublet pair in **131** to a singlet at δ_{H} 7.78 for H-6 in **132**. Its ^{13}C NMR spectrum also displayed a large upfield shift for C-5 from δ_{C} 101.5 in **131** to δ_{C} 67.2 in **132** consistent with the introduction of iodine. The ^{31}P NMR spectrum of **132** revealed a singlet at δ_{P} 18.7. The parent ion was found to be 461.0341 ($\text{M}^+ + \text{H}$) correlating to a correct molecular formula of $\text{C}_{13}\text{H}_{23}\text{N}_5\text{O}_6\text{PI}$, thus confirming that iodination had taken place.

4.1.3 Synthesis of [ANP]-tetraPEG-propyne-[HI-236] **134**

The target compound **134** was achieved by Sonogashira coupling of 5-iodo-ANP derivative **132** to 4-PEG amine **118** as the key step, following the same methodology as described before in Chapter 3. Thus the Boc group of alkyne **70r** was deprotected to amine **118** as described before using TFA (Chapter 3, Scheme 3.15). The amine was then coupled with phosphonate **132** without complications using the standard reaction conditions of Sonogashira coupling to afford the intermediate coupled amine, which was condensed directly with thiourea **49** in THF for 20 h at rt to afford the desired product **134** in 20% yield over the three steps after column chromatography Scheme 4.7.



Scheme 4.7 Reagents and conditions: (i) **70r**, TFA, DCM, 0 °C, 2 h, K₂CO₃; (ii) (PPh₃)₄Pd (10%), CuI (50%), Et₃N (2 eq), DMF:THF (1: 2), rt, 2 h; (iii) Thiourea **49**, THF, rt, 20 h, (20% over the 3 steps).

Key spectroscopic indicators in the ¹H NMR spectrum (Fig. 4.7) of **134** were the ANP uracil proton singlet (H-6) at δ_H 7.58, the absence of an alkyne signal at δ_H 2.40 as well as the characteristic aromatic signals for the HI-236 moiety. The two thiourea NH signals could be discerned downfield as usual, but the ANP imide proton was more upfield compared to the d4U series. The ¹³C NMR spectrum of **134** returned the correct number of resonances of 43. Its ³¹P NMR spectrum displayed the definitive phosphonate resonance at δ_P 18.7. Finally, a

correct HRMS evaluation (m/z HRMS (ES) 1016.3100 $[M+H]^+$, $C_{43}H_{64}N_5O_{14}PSBr$ requires m/z 1016.3091 $[M+H]^+$), confirmed the structure of **134**.

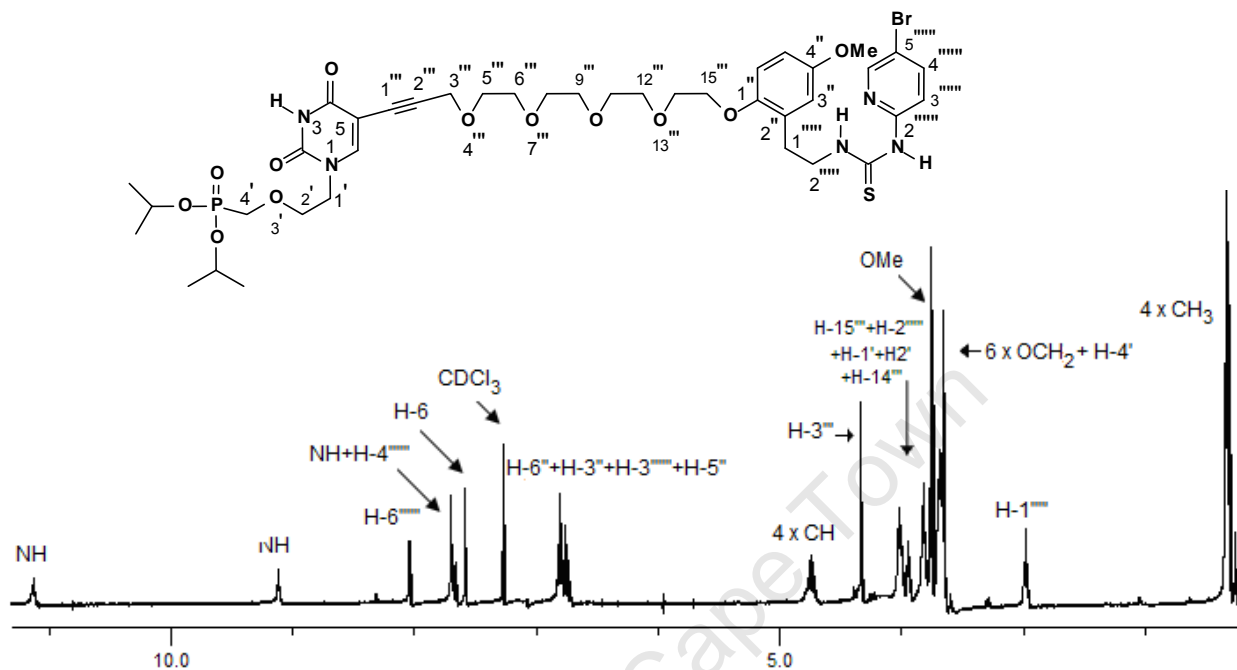
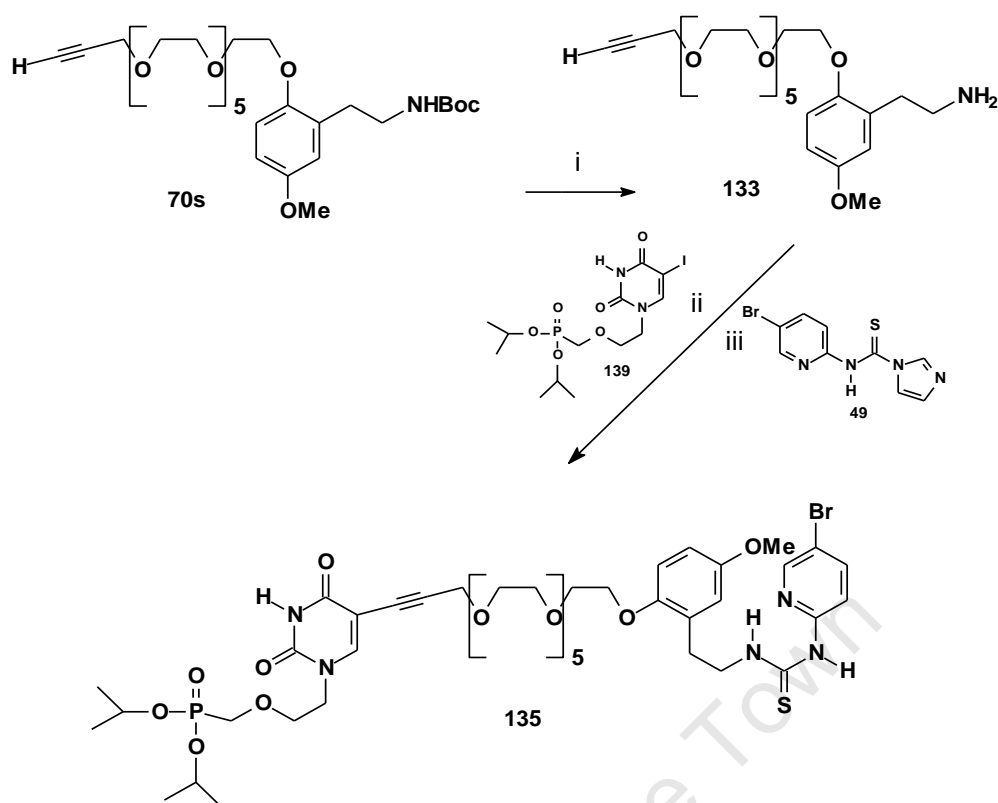


Figure 4.7 1H NMR ($CDCl_3$) spectrum of compound **134**.

4.1.4 Synthesis of [ANP]-hexaPEG-propyne-[HI-236] **135**

As an elongated variant of the prototype, the 6-PEG bifunctional **135** was synthesized using an identical sequence to that just described, except using alkyne **70s** from Chapter 3, Scheme 2.21 to afford the desired bifunctional **135** in a 15% yield over three steps after column chromatography as shown in Scheme 4.8.



Scheme 4.8 Reagents and conditions: (i) **70r**, TFA, DCM, 0 °C, 2 h, K₂CO₃; (ii) (PPh₃)₄Pd (10%), CuI (50%), Et₃N (2 eq), DMF: THF (1: 2), rt, 2 h; (iii) Thiourea **49**, THF, rt, 20 h, (15% over the 3 steps).

The ¹H NMR spectral data for **135** was very similar to that of the 4-PEG derivative **134** and revealed signals for both the HI-236 and 5-iodo-ANP moieties in a ratio of 1:1 (Fig. 4.8). The ¹³C NMR spectrum of **135** displayed diagnostic resonances at δ_C 66.2 (d, J_{CP} = 166.7 Hz, C-4'), δ_C 77.1 (C-5), δ_C 55.6 (OCH₃), and δ_C 179.3 (C=S), thus confirming the presence of both the nucleotide and the alkyne. The structure was further confirmed by 2D NMR. The IR spectrum of **135** indicated a characteristic peak for C=S at ν_{max} 1469 cm⁻¹, for C≡C at ν_{max} 2239 cm⁻¹ and for P=O at ν_{max} 1230 cm⁻¹. The parent ion was found to be 1016.3100 (M⁺ + H) correlating to a correct molecular formula of C₄₃H₆₄N₅O₁₄PSBr, thus confirming the formation of **135**. The two bifunctionals were both oils, hence the use of High resolution mass spectrometry (HRMS).

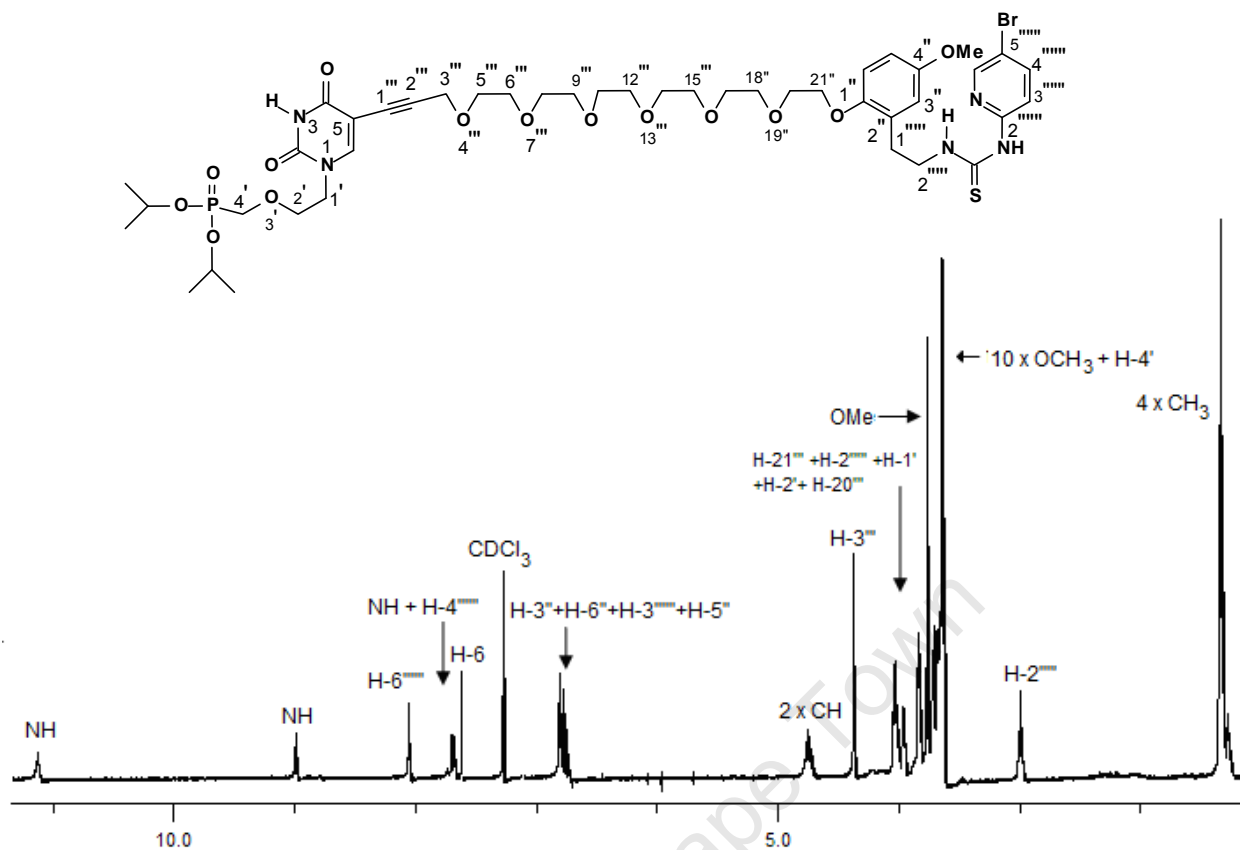
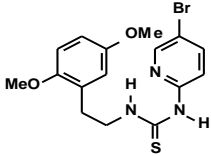
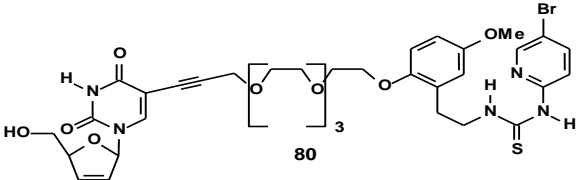
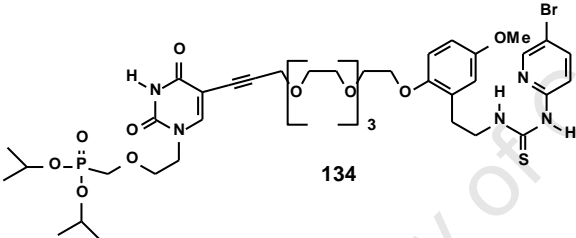
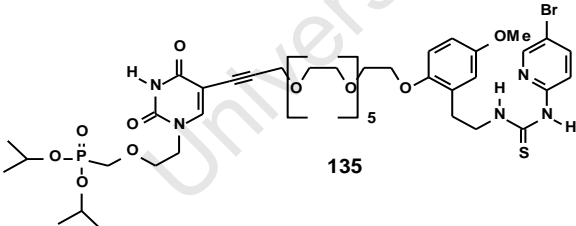


Figure 4.8 ¹H NMR (CDCl₃) spectrum of compound 135.

4.2 Biological results and rationale

The inhibition of viral replication in HIV-infected cells by the bifunctional targets **134** and **135** was measured for HIV-1 (IIIB) replication in MT-2 cell culture using an MTT assay (see Appendix). The results are summarized in Table 4.2, which includes the results for the 4-PEG d4U bifunctional **80** for comparison purpose. EC₅₀ represents the inhibitory potency, while CC₅₀ reflects cytotoxicity of the compounds towards untreated cells.

Table 4.2 *In vitro* anti-HIV and activity cytotoxicity of bifunctionals **134**, **135** and **80** in MT-4 cells.

Compound	EC ₅₀ ^a (μM)	CC ₅₀ ^b (μM)	T.I. ^c
 HI-236	0.012	> 0.1	> 10
 80	3.1	18	6
 134	3.1	16	5
 135	8.9	27	3

^a Effective concentration that inhibits viral-mediated T-cell death by 50% and as an average of three measurements.

^b Concentration that kills 50% of the T-cells and as an average of three results.

^c *In vitro* therapeutic index (IC₅₀ / EC₅₀).

The results in Table 4.2 reveal that the 4-PEG ANP prototype heterodimer **134** was 3-fold more potent than the 6-PEG analogue **135**. Furthermore, **no** evidence of an enhancement due to the phosphonate was provided as judged by comparing the d4U bifunctional **80** with the ANP one. This of course, could have also been due to changing from d4U to the ANP prototype chosen here. Given that the ANP in **134** is not based on a proven drug by comparison to the d4U bifunctional **80** result, the value for **134** is highly encouraging.

Together with results from the other bifunctional series, the following conclusions can be drawn:

(i) The activity in both series likely involves NNRTI pocket binding rather than just NRTI binding. The similarity of the results between the two different series (4-PEG) bears this out since changing d4U to ANP is quite a significant change and the ANP chosen here has no guarantee of binding by itself even if phosphorylated. Thus, to retain the same activity of 3.1 μM (**80** to **134**) should reflect the constancy due to the NNRTI component being the same in each case.

(ii) The tether-ANP or tether-d4U would then protrude from the cavity since these moieties are far too large to be accommodated completely in the cavity. The relatively high potencies (high nM range for the d4U series or low μM for the ANP) observed suggest a significant degree of cooperative binding outside the pocket, probably via H-bonding. Thus, these derivatives should be considered as elongated NNRTI's with some cooperative binding to residues outside the pocket, since the molecules are far too large to fit into the pocket completely. The degree to which the NRTI binding site is involved is unknown. Possibly there is none in which case the NRTI must have found a significant binding zone somewhere else.

(iii) No evidence exists for phosphorylation to an activated bifunctional in either series. This must be due to poor recognition by the kinases appropriate to each series.

(iv) A case exists for changing the presence ANP to a known one such as found in Cidofovir or Tenofovir, in order to fully evaluate the influence of changing from one proven NRTI to another (N^tRTI).

Future work could be carried out on more established ANP's like Tenofovir, and to vary the pro-drug groups as Cyclo-Sal, POC or POM, or a phosphoramidate. However, the issue of converting to a bifunctional triphosphate in vitro continues to be limiting. Finally, based on the possibility of exiting the back of the NNRTI pocket, it would be interesting to explore the C-5 oxygen of HI-236 as the tether attachment point on the NNRT.

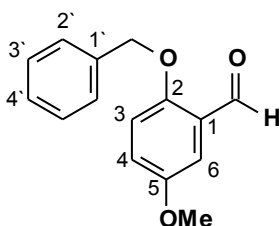
CHAPTER 5: EXPERIMENTAL SECTION

5.1 General procedures

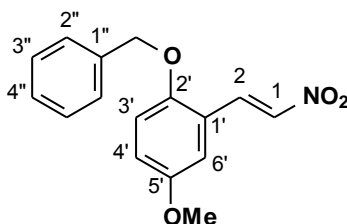
All reactions were performed in oven-dried glassware under an inert atmosphere of dry nitrogen. All starting materials were purchased from Sigma-Aldrich, South Africa except the solvents, acids and common salts. The following reaction solvents were distilled from the indicated drying agents: methylene chloride (P_2O_5), *N,N*-dimethylaniline (CaH_2), diethyl ether (P_2O_5), tetrahydrofuran (Na, benzophenone), methanol (Mg), acetonitrile (CaH_2), triethylamine (CaH_2), dimethoxyethane (Na, benzophenone).

1H NMR spectra were recorded on a Varian Mercury Spectrometer at 300 MHz or on a Varian Unity Spectrometer at 400 MHz. ^{13}C NMR spectra were recorded at 75 MHz on a Varian Mercury Spectrometer or at 100 MHz on a Varian Unity Spectrometer. The spectra were recorded in $CDCl_3$, Acetone- d_6 , CD_3OD-d_4 or $DMSO-d_6$ with tetramethylsilane as the internal standard. Chemical shifts are reported in ppm (δ); multiplicities are indicated by s (singlet), d (doublet), t (triplet), q (quartet), m (multiplet) and br (broad). Coupling constants, J , are reported in Hertz. High resolution mass spectra were recorded on a VG70 SEQ micromass spectrometer. Infrared (IR) absorptions were measured on a Perkin Elmer Spectrum One FT-IR spectrometer. Peaks are reported in cm^{-1} . Melting points were determined using a Reichert-Jung Thermovar hot-stage microscope and are uncorrected. Elemental analysis for C, H and N were carried out using a Fisons EA 110 CHN Elemental Analyser. Optical rotations were obtained using a Perkin Elmer 343 polarimeter at 20 °C. The concentration c refers to g/100 mL.

The reaction progress was monitored by TLC using Merck silica-gel 60 F_{254} . Visualisation was accomplished with UV light or spraying with anisaldehyde and/or cerium ammonium sulphate spray reagents and then heating at 150 °C. Column chromatography was performed with Merck silica-gel 60 (70-230 mesh).

2-Benzyloxy-5-methoxybenzaldehyde (62)^{146b}

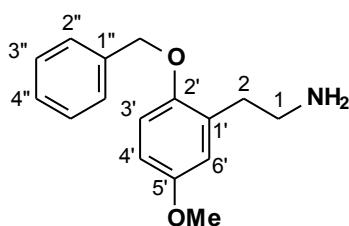
2-Hydroxy-5-methoxybenzaldehyde (5.00 mL, 40.10 mmol) was added to a stirring mixture of anhydrous potassium carbonate (16.63 g, 120.30 mmol) in ethanol (100 mL). Benzyl bromide (7.15 mL, 60.15 mmol) was added to the mixture which was refluxed for 16 h. The potassium carbonate was filtered from the mixture through Celite, washed with ethanol (50 mL), and the solvent was removed *in vacuo*. The filtrate was dissolved in diethyl ether (300 mL), washed with aqueous sodium chloride (2 × 100 mL), aqueous sodium hydroxide (100 mL) and water (2 × 50 mL). The organic layer was dried over MgSO₄, and the solvent was removed under reduced pressure. Recrystallization of the residue from ethanol gave colorless needles of the product **62** (9.10 g, 94%); mp: 44-46 °C; [lit. 47-48 °C]; IR (CHCl₃): ν_{\max} 3007, 2870 (C-H), 1682 (C=O), 1490 (C=C), 1223, 1158 (C-N) cm⁻¹; ¹H NMR (400 MHz, CDCl₃): δ 10.53 (1H, s, CHO), 7.43 (5H, m, ArH), 7.36 (1H, d, *J* = 3.3 Hz, H-6), 7.12 (1H, dd, *J* = 3.3, 9.1 Hz, H-4), 7.02 (1H, d, *J* = 9.1 Hz, H-3), 5.16 (2H, s, ArOCH₂), 3.81 (3H, s, OCH₃); ¹³C NMR (100 MHz, CDCl₃): δ 189.5 (HC=O), 155.9 (C-2), 154.0 (C-5), 136.3 (C-1'), 128.7 (C-3', C-5'), 128.3 (C-4'), 127.4 (C-2', C-6'), 125.7 (C-1), 123.4 (C-6), 115.2 (C-3), 110.4 (C-4), 71.4 (ArCH₂O), 55.8 (OCH₃); HRMS (EI): *m/z* found 242.09699 (M⁺). C₁₅H₁₄O₃ (M⁺) requires 242.09429; Found C, 74.35; H, 5.81. C₁₅H₁₄O₃ requires C, 74.36; H, 5.82

2-(2-Benzyloxy-5-methoxyphenyl)-1-nitroethene (65)¹⁴⁷

2-Benzyloxy-5-methoxybenzaldehyde **62** (6.50 g, 26.85 mmol) dissolved in nitromethane (80 mL) and ammonium acetate (2.07 g, 26.85 mmol) was heated at 70 °C for 14 h. The solution was diluted with dichloromethane (200 mL), washed with sodium chloride (2 X 200 mL) and water (200 mL). The organic layer was dried over MgSO₄ and the solvent removed under reduced pressure to give a residue which was recrystallized from hot ethanol to afford yellow crystals of **65** (6.10 g, 80%); mp: 112-114 °C, [lit. 114-116 °C]; IR (CHCl₃): ν_{\max} 3022, 2949

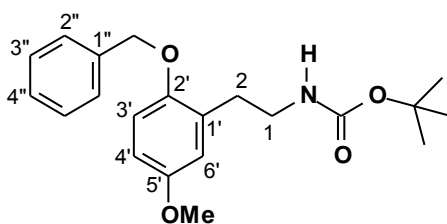
(C-H), 1577, 1498 (C=C), 1498, 1342 (N-O) 1216 (C-N) cm^{-1} ; ^1H NMR (400 MHz, CDCl_3): δ 8.17 (1H, d, $J = 13.6$ Hz, H-2), 7.83 (1H, d, $J = 13.6$ Hz, H-1), 7.43 (5H, m, ArH), 6.99 (3H, m, H-3', H-4', H-6'), 5.17 (2H, s, ArCH_2O), 3.81 (3H, s, OCH_3); ^{13}C NMR (100 MHz, CDCl_3): δ 153.8 (C-2'), 153.0 (C-5'), 138.6 (C-1), 136.1 (C-1''), 135.1 (C-2), 128.8 (C-2'', C-6''), 128.4 (C-4''), 127.4 (C-3'', C-5''), 120.1 (C-1'), 119.2 (C-6'), 116.1 (C-4'), 114.3 (C-3'), 71.4 (ArCH_2O), 55.9 (OCH_3); EI HRMS: m/z found 285.09932. $\text{C}_{16}\text{H}_{15}\text{NO}_4$ requires (M^+) 285.10011; Found C, 67.37; H, 5.27; N, 5.00. $\text{C}_{16}\text{H}_{15}\text{NO}_4$ requires C, 67.36; H, 5.30; N 4.91.

2-(2-Benzyloxy-5-methoxyphenyl)-ethanamine (66)



A compound of nitroethene **65** (5.00 g, 17.74 mmol), dissolved in THF (50 mL) and was added dropwise over 2 h to a stirred and refluxing suspension of lithium aluminium hydride (2.66 g, 70.16 mmol) in THF (100 mL). The mixture was refluxed for 4 h, cooled to 0 °C and quenched with water (2 mL) and 5% sodium hydroxide solution (2 mL). The mixture was stirred for an additional 30 min. The precipitate formed, was filtered through a pad of celite and washed with MeOH (3 × 50 mL). The filtrate was reduced under pressure to give crude product **66** (4.10 g, 91%). Compound **3** was carried to the next reaction without further purification.

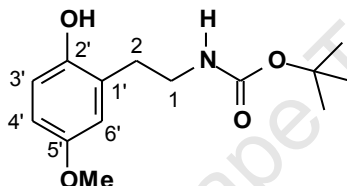
N-[2-(2-Benzyloxy-5-methoxyphenyl)ethyl]-*tert*-butylcarbamate (68)



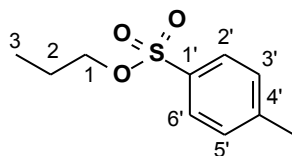
To a solution of crude amine **66** (4.10 g, 15.95 mmol) in acetonitrile (50 mL) and di-*tert*-butyldicarbonate (5.22 g, 23.93 mmol) in acetonitrile (6 mL) was added, the reaction mixture was stirred at rt for 20 h. The mixture was diluted with EtOAc (100 mL), which was washed with aqueous NH_4Cl (50 mL), water (50 mL) and dried over MgSO_4 . The solvent was evaporated under reduced pressure and the crude product was subject to column chromatography employing EtOAc / petroleum ether (15 / 85) to give product **68** as

colourless crystals (5.00 g, 88%); mp: 102-104 °C; IR (CHCl₃): ν_{\max} 3449 (NH), 3007, 2935 (C-H), 1703 (C=O), 1501 (C=C), 1165 (C-N) cm⁻¹; ¹H NMR (400 MHz, CDCl₃): δ 7.45-7.34 (5H, m, ArH), 6.85 (1H, d, J = 8.8 Hz, H-3'), 6.76 (1H, d, J = 2.8 Hz, H-6'), 6.72 (1H, dd, J = 2.8, 8.8 Hz, H-4'), 5.04 (2H, s, ArCH₂O), 4.70 (1H, brs, NH), 3.78 (3H, s, OCH₃), 3.40 (2H, q, J = 6.4 Hz, H-1), 2.85 (2H, t, J = 6.4 Hz, H-2), 1.44 (9H, s, OC(CH₃)₃); ¹³C NMR (75 MHz, CDCl₃): δ 155.9 (C=O), 153.8 (C-5'), 150.9 (C-2'), 137.4 (C-1''), 129.2 (C-1'), 128.5 (C-3'', C-5''), 127.8 (C-4''), 127.2 (C-2'', C-6''), 116.8 (C-6'), 113.0 (C-4'), 112.0 (C-3'), 79.0 (OC(CH₃)₃), 70.8 (ArCH₂O), 55.7 (OCH₃), 40.8 (C-1), 30.9 (C-2), 28.4 (OC(CH₃)₃); HRMS (EI): m/z found 301.13383 [(M⁺ - *t*-butyl) + H]. C₂₁H₂₇NO₄ requires 301.13409 [(M⁺ - *t*-butyl) + H]; Found C, 70.50; H, 7.62; N, 3.86. C₂₁H₂₇NO₄ requires C, 70.56; H, 7.61; N, 3.92.

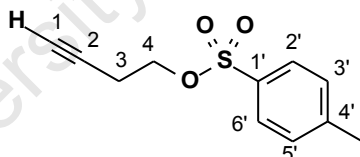
[2-(2-Hydroxy-5-methoxyphenyl)ethyl]-*tert*-butylcarbamate (69)



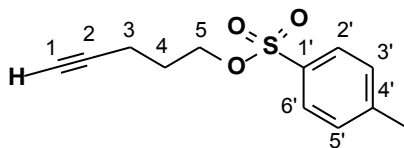
The carbamate **68** (4.50 g, 12.61 mmol) was added to 10% palladium on carbon (0.22 g, 1.26 mmol) in ethanol. Hydrogen gas was introduced to the reaction at rt for 5 h. The palladium was filtered from the solution through Celite and the precipitate was washed with ethanol (3 × 100 mL). The solvent was removed under reduced pressure and the residue was subjected to column chromatography using EtOAc / petroleum ether (4 / 6) to give a white solid **69** (2.50 g, 74%); mp: 115-117 °C; IR (CHCl₃): ν_{\max} 3457, 3326 (NH, OH), 1686 (C=O), 1508 (C=C), 1210, 1166 (C-N) cm⁻¹; ¹H NMR (400 MHz, CDCl₃): δ 6.99 (1H, brs, OH), 6.79 (1H, d, J = 8.4 Hz, H-3'), 6.67 (1H, d, J = 2.8 Hz, H-6'), 6.65 (1H, m, H-4'), 5.00 (1H, brs, NH), 3.75 (3H, s, OCH₃), 3.33 (2H, q, J = 7.1 Hz, H-1), 2.81 (2H, t, J = 7.1 Hz, H-2), 1.46 (9H, s, OC(CH₃)₃); ¹³C NMR (100 MHz, CDCl₃): δ 157.0 (C=O), 153.2 (C-5'), 148.8 (C-2'), 126.0 (C-1'), 116.5 (C-3'), 116.2 (C-6'), 112.8 (C-4'), 80.0 (OC(CH₃)₃), 55.8 (OCH₃), 41.0 (C-1), 31.4 (C-2), 28.4 (OC(CH₃)₃); HRMS (EI): m/z found 267.14329 (M⁺) C₁₄H₂₁NO₄ (M⁺) requires 267.14706; Found C, 62.82; H, 7.92; N, 5.16. C₁₄H₂₁NO₄ requires C, 62.94; H, 7.92; N, 5.24.

1-Propyl *p*-toluenesulfonate (138)

Triethylamine (5.00 mL, 40.00 mmol) and *p*-toluenesulfonyl chloride (7.00 g, 40.00 mmol) were added to a solution of 1-propanol (2.00 g, 33.30 mmol) in dry CH₂Cl₂ (30 mL) at 0 °C, followed by a catalytic amount of DMAP (20 mg). The reaction mixture was stirred at rt for 16 h, diluted with aq. NH₄Cl (40 mL) and extracted with CH₂Cl₂ (3 × 30 mL). Following drying over MgSO₄, filtering and solvent evaporation under reduced pressure, the crude was purified by column chromatography using EtOAc / pet ether (15 / 85) to give product **138** as a colourless oil (6.50 g, 91%). ¹H NMR (400 MHz, CDCl₃): δ 7.78 (2H, d, *J* = 8.1 Hz, H-2', H-6'), 7.33 (2H, d, *J* = 8.1 Hz, H-3', H-5'), 3.98 (2H, t, *J* = 7.0 Hz, H-1), 2.43 (3H, s, ArCH₃), 1.66 (2H, sextet, *J* = 7.0 Hz, H-2), 0.88 (3H, t, *J* = 7.0 Hz, H-3); ¹³C NMR (100 MHz, CDCl₃): δ 144.6 (C-1'), 133.3 (C-4'), 129.8 (C-2', C-6'), 127.8 (C-3', C-5'), 72.1 (C-1), 22.3 (ArCH₃), 21.6 (C-2), 9.9 (C-3).

1-But-3-ynyl *p*-toluenesulfonate (139)

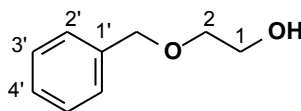
p-Toluenesulfonyl chloride (4.54 g, 23.80 mmol) in CH₂Cl₂ (10 mL) was added dropwise to a solution of but-3-yn-1-ol (1.50 mL, 19.80 mmol) containing triethylamine (3.14 mL, 23.80 mmol) and DMAP (20 mg) in CH₂Cl₂ (20 mL) at 0 °C. The mixture was stirred at rt for 16 h, diluted with aq. NH₄Cl (30 mL) and extracted with CH₂Cl₂ (3 × 25 mL). Following drying over MgSO₄, filtering and solvent evaporation under reduced pressure, the crude was purified by column chromatography using ethyl acetate / petroleum ether (15 / 85) to give a colourless oil **139** (4.44 g, 100%); ¹H NMR (300 MHz, CDCl₃): δ 7.75 (2H, d, *J* = 7.4 Hz, H-2', H-6'), 7.31 (2H, d, *J* = 7.4 Hz, H-3', H-5'), 4.06 (2H, t, *J* = 7.0 Hz, H-4), 2.50 (2H, td, *J* = 2.7, 7.0 Hz, H-3), 2.40 (3H, s, CH₃), 1.95 (1H, t, *J* = 2.7 Hz, H-1); ¹³C NMR (75 MHz, CDCl₃): δ 144.9 (C-1'), 132.6 (C-4'), 129.7 (C-2'), 127.7 (C-3'), 78.3 (C-2), 70.6 (C-1), 67.3 (C-4), 21.4 (C-3), 19.2 (CH₃).

1-Penta-4-ynyl *p*-toluenesulfonate (140)

To a solution of pen-4-yn-1-ol (1.11 mL, 11.90 mmol) in dry CH_2Cl_2 (15 mL), were added triethylamine (2.00 mL, 14.30 mmol) and *p*-toluenesulfonyl chloride (2.72 g, 14.30 mmol) at 0 °C, followed by a catalytic amount of DMAP (20 mg). The reaction mixture was stirred at rt for 16 h, diluted with aq. NH_4Cl (50 mL) and extracted with CH_2Cl_2 (100 mL). The organic extracts were dried over MgSO_4 and the solvent removed under reduced pressure to give a crude product, which was purified by silica-gel column chromatography EtOAc / pet ether (15 / 85) to give **140** as a colourless oil (2.70 g, 96%); ^1H NMR (400 MHz, CDCl_3): δ 7.78 (2H, d, $J = 8.2$ Hz, H-2', H-6'), 7.33 (2H, d, $J = 8.2$ Hz, H-3', H-5'), 4.14 (2H, t, $J = 6.2$ Hz, H-5), 2.44 (3H, s, ArCH_3), 2.25 (2H, td, $J = 2.8$ Hz, H-3), 1.87 (1H, t, $J = 2.8$ Hz, H-1), 1.85 (2H, m, H-4); ^{13}C NMR (100 MHz, CDCl_3): δ 144.7 (C-1'), 133.0 (C-4'), 129.8 (C-2', C-6'), 127.9 (C-3', C-5'), 82.1 (C-2), 69.4 (C-1), 68.7 (C-5), 27.7 (C-3), 21.6 (C-4), 14.6 (ArCH_3).

General Procedure for the monobenylation of the glycol (GP1)

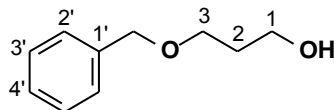
The glycol (1.00 mmol) was added dropwise to a suspension of NaH (60% in mineral oil, 1.00 mmol) in THF at 0 °C and the mixture was stirred for 30 min. Benzyl bromide (1.00 mmol) was added dropwise over 1 h. The reaction mixture refluxed for 20 h. The crude mixture was diluted with EtOAc (100 mL), washed with aq NH_4Cl (50 mL), water (2 × 50 mL), dried over Mg_2SO_4 , filtered and the solvent removed *in vacuo*. The crude product was purified by distillation or column chromatography.

2-Benzyloxyethanol (72)¹⁴⁹

According to GP1: Ethylene glycol (4.50 mL, 80.60 mmol), NaH (60% in mineral oil, 3.22 g, 80.60 mmol) in THF (50 mL) and benzyl bromide (9.58 mL, 80.60 mmol). A distillation of the mixture (bp: 98-103 °C/0.7 mm Hg); [lit. 90-95 °C/0.7 mm Hg] afforded **72** as a colourless oil (6.00 g, 49%); ^1H NMR (300 MHz, CDCl_3): δ 7.36 (5H, m, ArH), 4.56 (2H, s, ArCH_2O), 3.73 (2H, t, $J = 4.7$ Hz, H-2), 3.58 (2H, t, $J = 4.7$ Hz, H-1), 2.58 (1H, brs, OH); ^{13}C NMR (100

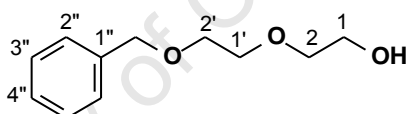
CDCl_3): δ 138.0 (C-1'), 128.5 (C-2', C-6'), 127.9 (C-4'), 127.8 (C-3', C-5'), 73.3 (ArCH_2O), 71.5 (CH_2O), 61.8 (C-1).

3-Benzyloxypropan-1-ol (72a)



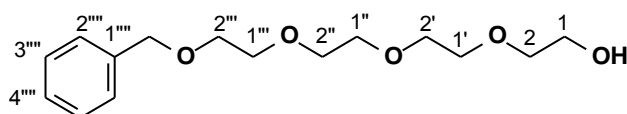
According to GP1: Propane-1,3-diol (3.00 g, 39.42 mmol), NaH (60% in mineral oil, 1.58 g, 39.42 mmol) in THF (50 mL) and benzyl bromide (4.69 mL, 39.42 mmol). Purification by column chromatography using EtOAc / pet ether (3 / 7) afforded **72a** as a colourless oil (2.4 g, 37%); ^1H NMR (400 MHz, CDCl_3): δ 7.33 (5H, m, ArH), 4.51 (2H, s, ArCH_2O), 3.76 (2H, m, H-3), 3.65 (2H, t, $J = 5.9$ Hz, H-1), 2.56 (1H, brs, OH), 1.86 (2H, quin, $J = 5.9$ Hz, H-2); ^{13}C NMR (75 MHz, CDCl_3): δ 138.0 (C-1'), 128.3 (C-2', C-6'), 127.6 (C-4'), 127.6 (C-3', C-5'), 73.1 (ArCH_2O), 69.0 (C-3), 61.4 (C-1), 32.1 (C-2).

2-(2-Benzyloxyethoxy)ethanol (72b)¹⁷⁹



According to GP1: Diethylene glycol (4.46 mL, 47.12 mmol), NaH (60% in mineral oil, 1.88 g, 47.12 mmol) in THF (50 mL) and benzyl bromide (5.60 mL, 47.12 mmol). A distillation (bp: 98-103 °C/0.7 mm Hg); [lit. 90-95 °C/0.7 mm Hg] afforded **72b** as a colourless oil (4.10 g, 44%); ^1H NMR (400 MHz, CDCl_3): δ 7.34 (5H, m, ArH), 4.57 (2H, s, ArCH_2O), 3.65 (8H, m, 4 \times CH_2O), 2.91 (1H, brs, OH); ^{13}C NMR (100 MHz, CDCl_3): δ 137.9 (C-1''), 128.3 (C-2'', C-6''), 127.7 (C-3'', C-5''), 127.6 (C-4''), 73.2 (ArCH_2O), 72.5 (CH_2O), 70.3 (CH_2O), 69.3 (CH_2O), 61.6 (C-1).

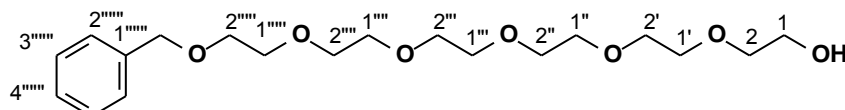
2-{2-[2-(2-Benzyloxy-ethoxy)-ethoxy]-ethoxy}-ethanol (72c)



According to GP1: Tetraethylene glycol (4.44 mL, 25.74 mmol), NaH (60% in mineral oil, 1.03 g, 25.74 mmol) in THF (50 mL) and benzyl bromide (3.06 mL, 25.74 mmol). Purification by

column chromatography using EtOAc / pet ether (9 / 1) afforded **72c** as a colourless oil (2.88 g, 39%); $^1\text{H NMR}$ (400 MHz, CDCl_3): δ 7.34 (5H, m, ArH), 4.56 (2H, s, ArCH_2O), 3.66 (14H, m, $7 \times \text{CH}_2\text{O}$), 3.58 (2H, t, $J = 4.8$ Hz, H-1), 2.80 (1H, brs, OH); $^{13}\text{C NMR}$ (100 MHz, CDCl_3): δ 138.2 (C-1'''), 128.2 (C-2''', C-6'''), 127.6 (C-3''', C-5'''), 127.4 (C-4'''), 73.1 (ArCH_2O), 72.4 (CH_2O), 70.5 ($2 \times \text{CH}_2\text{O}$), 70.5 ($2 \times \text{CH}_2\text{O}$), 70.2 (CH_2O), 69.3 (CH_2O), 61.6 (C-1).

2-[2-(2-{2-[2-(2-Benzyloxy-ethoxy)-ethoxy]-ethoxy}-ethoxy)-ethoxy]-ethanol (72d)

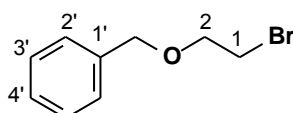


According to GP1: Hexaethylene glycol (3.56 mL, 14.17 mmol), NaH (60% in mineral oil, 0.57 g, 14.17 mmol) in THF (35 mL) and benzyl bromide (1.69 mL, 14.17 mmol). Purification by using column chromatography using EtOAc / MeOH (9 / 1) afforded **72d** as a colourless oil (2.02 g, 38%); $^1\text{H NMR}$ (300 MHz, CDCl_3): δ 7.28 (5H, m, ArH), 4.52 (2H, s, ArCH_2O), 4.18 (2H, m, CH_2O), 3.61 (22H, m, $12 \times \text{CH}_2\text{O}$), 2.85 (1H, brs, OH); $^{13}\text{C NMR}$ (75 MHz, CDCl_3): δ 138.2 (C-1'''''), 128.2 (C-2''''', C-6'''''), 127.6 (C-3''''', C-5'''''), 127.4 (C-4'''''), 73.0 (ArCH_2O), 72.4 (CH_2O), 70.4 ($3 \times \text{CH}_2\text{O}$), 70.4 ($3 \times \text{CH}_2\text{O}$), 70.2 (CH_2O), 69.3 (CH_2O), 69.0 (CH_2O), 63.4 (CH_2O), 61.5 (C-1).

General Procedure for the bromination of alcohol (GP2)

To a solution of alcohol (1.00 mmol) in CH_2Cl_2 at 0 °C were added PPh_3 (1.20 mmol) and CBr_4 (1.20 mmol) at 0 °C, and the mixture stirred at rt for 30 min. The solvent was removed *in vacuo*. The crude product was purified directly by column chromatography using EtOAc / pet ether or CH_2Cl_2 / pet ether mixtures to give the product as a colourless oil.

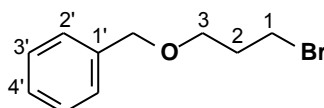
1-Benzyloxy-2-bromoethane (**73**)¹⁸⁰



According to GP2: Benzyloxyalcohol **72** (4.00 g, 26.28 mmol) in CH_2Cl_2 (30 mL), PPh_3 (8.27 g, 31.54 mmol) and CBr_4 (10.46 g, 31.54 mmol). The crude product was purified by column

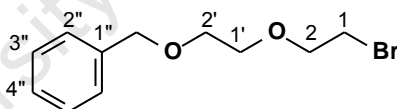
chromatography using pet ether / CH₂Cl₂ (95 / 5) to give **73** as a colourless oil (5.20 g, 92%); ¹H NMR (300 MHz, CDCl₃): δ 7.38 (5H, m, ArH), 4.61 (2H, s, ArCH₂O), 3.79 (2H, t, *J* = 6.2 Hz, H-2), 3.51 (2H, t, *J* = 6.2 Hz, H-1); ¹³C NMR (100 MHz, CDCl₃): δ 137.7 (C-1'), 128.4 (C-2', C-6'), 127.8 (C-4'), 127.7 (C-3', C-5'), 73.1 (ArCH₂O), 70.0 (C-2), 30.4 (C-1).

1-Benzyloxy-3-bromopropane (**73a**)

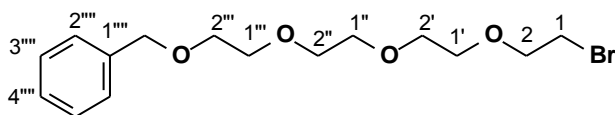


According to GP2: Benzyloxyalcohol **72a** (2.80 g, 16.85 mmol) in CH₂Cl₂ (20 mL), PPh₃ (5.30 g, 20.22 mmol) and CBr₄ (6.71 g, 20.22 mmol). The crude product was purified by column chromatography using EtOAc / pet ether (10 / 90) to give **73a** as a colourless oil (3.51 g, 91%); ¹H NMR (300 MHz, CDCl₃): δ 7.36 (5H, m, ArH), 4.54 (2H, s, ArCH₂O), 3.63 (2H, t, *J* = 6.0 Hz, H-3), 3.55 (2H, t, *J* = 6.0 Hz, H-1), 2.16 (2H, quin, *J* = 6.0 Hz, H-2); ¹³C NMR (100 MHz, CDCl₃): δ 138.3 (C-1'), 128.4 (C-2', C-6'), 127.6 (C-4'), 127.6 (C-3', C-5'), 73.2 (ArCH₂O), 67.7 (C-3), 33.0 (C-1), 30.6 (C-2).

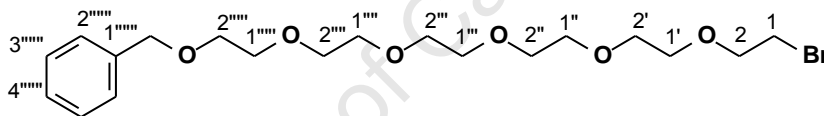
2-(2-Benzyloxy)ethoxy-1-bromoethane (**73b**)



According to GP2: Benzyloxyalcohol **72b** (4.00 g, 20.38 mmol) in CH₂Cl₂ (40 mL), PPh₃ (6.42 g, 24.46 mmol) and CBr₄ (8.11 g, 24.46 mmol). The crude product was purified by column chromatography using EtOAc / pet ether (2 / 8) to give **73b** as a colourless oil (4.81 g, 91%); ¹H NMR (400 MHz, CDCl₃): δ 7.33 (4H, m, ArH), 7.28 (1H, m, ArH), 4.56 (2H, s, ArCH₂O), 3.79 (2H, t, *J* = 6.3 Hz, CH₂O), 3.67 (2H, m, CH₂O), 3.62 (2H, m, CH₂O), 3.45 (2H, t, *J* = 6.3 Hz, H-1); ¹³C NMR (100 MHz, CDCl₃): δ 138.2 (C-1''), 128.4 (C-2'', C-6''), 127.8 (C-3'', C-5''), 127.7 (C-4''), 73.3 (ArCH₂O), 71.3 (CH₂O), 70.7 (CH₂O), 69.5 (CH₂O), 30.4 (C-1).

2-{2-[2-(2-Benzyloxy-ethoxy)-ethoxy]-ethoxy}-1-bromoethane (73c)

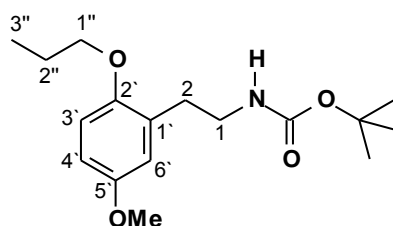
According to GP2: Benzyloxyalcohol **72c** (2.50 g, 8.79 mmol) in CH_2Cl_2 (20 mL), PPh_3 (2.77 g, 10.55 mmol) and CBr_4 (3.50 g, 10.55 mmol). The crude product was purified by column chromatography using EtOAc / pet ether (6 / 4) to give **73c** as a colourless oil (2.69 g, 88%); ^1H NMR (400 MHz, CDCl_3): δ 7.35 (4H, m, ArH), 7.28 (1H, m, ArH), 4.57 (2H, s, ArCH_2O), 3.80 (2H, t, $J = 6.3$ Hz, CH_2O), 3.67 (12H, m, $6 \times \text{CH}_2\text{O}$), 3.45 (2H, t, $J = 6.3$ Hz, H-1); ^{13}C NMR (100 MHz, CDCl_3): δ 138.2 (C-1'''), 128.2 (C-2''', C-6'''), 127.6 (C-3''', C-5'''), 127.5 (C-4'''), 73.1 (ArCH_2O), 71.1 (CH_2O), 70.6 ($2 \times \text{CH}_2\text{O}$), 70.5 ($2 \times \text{CH}_2\text{O}$), 70.4 (CH_2O), 69.4 (CH_2O), 30.2 (C-1).

2-[2-(2-[2-(2-[2-(2-Benzyloxy-ethoxy)-ethoxy]-ethoxy)-ethoxy]-ethoxy)-ethoxy]-1-bromoethane (73d)

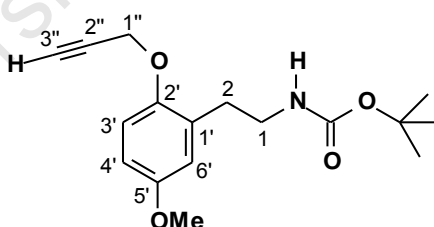
According to GP2: Benzyloxyalcohol **72d** (1.5 g, 4.03 mmol) in CH_2Cl_2 (15 mL), PPh_3 (1.27 g, 4.84 mmol) and CBr_4 (1.61 g, 4.84 mmol). The crude product was purified by column chromatography using EtOAc to give a colourless oil **73d** (2.94 g, 77%); ^1H NMR (400 MHz, CDCl_3): δ 7.36 (5H, m, ArH), 4.59 (2H, s, ArCH_2O), 3.81 (2H, m, CH_2O), 3.68 (20H, m, $10 \times \text{CH}_2\text{O}$), 3.44 (2H, m, H-1).

General Procedure for the *N*-Boc O-alkylated derivatives (GP3)

The alkylating agent as a tosylate or bromide (2.00 mmol) in dry acetonitrile (5 mL) was added dropwise over 1h to a refluxing and stirring mixture of the phenol **69** (1.00 mmol) and anhydrous potassium carbonate (4.00 mmol) in dry acetonitrile (15 mL). The reaction was refluxed for 20 h. The mixture was filtered, the acetonitrile evaporated and the residue subjected to silica-gel column chromatography (10% EtOAc / pet ether) to afford the product generally as a colourless solid.

***N*-(*tert*-Butoxycarbonyl)-2-(5-methoxy-2-propoxyphenyl)ethylamine (70a)**

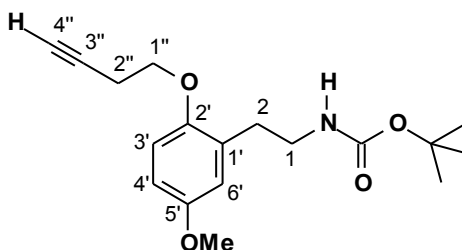
According to GP3: The tosylate **138** (0.32 g, 1.50 mmol), phenol **69** (0.20 g, 0.75 mmol) and anhydrous potassium carbonate (0.42 g, 3.00 mmol) afforded a colourless solid **70a** (0.22 g, 95%): mp 52-54 °C; IR (CHCl₃): ν_{\max} 3684, 3452 (NH), 3002, 2977 (C-H), 1706 (C=O), 1502 (C=C) cm⁻¹; ¹H NMR (400 MHz, CDCl₃): δ 6.76 (1H, d, J = 9.2 Hz, H-3'), 6.70 (2H, m, H-4', H-6'), 4.78 (1H, brs, NH), 3.88 (2H, t, J = 6.4 Hz, H-1''), 3.75 (3H, s, OCH₃), 3.35 (2H, q, J = 6.6 Hz, H-1), 2.78 (2H, t, J = 6.6 Hz, H-2), 1.80 (2H, m, H-2''), 1.42 (9H, s, OC(CH₃)₃), 1.04 (3H, t, J = 7.4 Hz, H-3''); ¹³C NMR (100 MHz, CDCl₃): δ 155.9 (C=O), 153.5 (C-5'), 151.3 (C-2'), 129.5 (C-1'), 116.8 (C-6'), 112.3 (C-3'), 112.0 (C-4'), 79.8 (OC(CH₃)₃), 70.2 (C-1''), 55.7 (OCH₃), 40.9 (C-1), 30.9 (C-2), 28.4 (OC(CH₃)₃), 22.8 (C-2''), 10.7 (C-3''); HRMS (EI): m/z found 309.19401 (M⁺). C₁₇H₂₇NO₄ (M⁺) requires 309.19400; Anal. Found: C, 66.13; H, 8.80; N, 3.91. C₁₇H₂₇NO₄ requires; C, 65.99; H, 8.80; N, 4.53.

***N*-(*tert*-Butoxycarbonyl)-2-(5-methoxy-2-propargyloxy-phenyl)ethylamine (70b)**

According to GP3: Propargyl bromide (0.40 mL, 6.74 mmol), phenol **69** (0.90 g, 3.37 mmol) and anhydrous potassium carbonate (1.87 g, 13.50 mmol) to give **70b** as colourless needles (0.77 g, 75%); m.p: 49-50 °C; IR (CHCl₃): ν_{\max} 3691, 3454 (NH), 3308 (\equiv CH), 2124 (C \equiv C), 1707 (C=O), 1501 (C=C) cm⁻¹; ¹H NMR (300 MHz, CDCl₃): δ 6.90 (1H, d, J = 9.3 Hz, H-3'), 6.72 (2H, m, H-4', H-6'), 4.65 (3H, d, J = 2.4 Hz, H-1'', NH), 3.75 (3H, s, OCH₃), 3.35 (2H, q, J = 6.8 Hz, H-1), 2.79 (2H, t, J = 6.8 Hz, H-2), 2.47 (1H, t, J = 2.4 Hz, H-3'''), 1.42 (9H, s, OC(CH₃)₃); ¹³C NMR (75 MHz, CDCl₃): δ 155.9 (C=O), 154.3 (C-5'), 149.8 (C-2'), 129.6 (C-1'), 116.7 (C-6'), 113.6 (C-3'), 112.0 (C-4'), 79.0 (C-2''), 79.0 (OC(CH₃)₃), 75.2 (C-3'''), 56.7 (C-1''), 55.6 (OCH₃), 40.6 (C-1), 30.9 (C-2), 28.4 (OC(CH₃)₃); HRMS (EI): m/z found

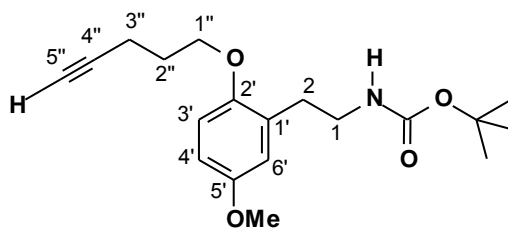
305.16244 (M^+). $C_{17}H_{23}NO_4$ (M^+) requires 305.16271; Anal. Found: C, 66.90; H, 7.54; N, 4.54. $C_{17}H_{23}NO_4$ requires C, 66.86; H, 7.59; N, 4.59.

***N*-(*tert*-Butoxycarbonyl)-2-[2-(3-butynyl-1-oxy)-5-methoxyphenyl]ethylamine (70c)**



According to GP3: The tosylate **139** (1.34 g, 6.00 mmol), phenol **69** (0.80 g, 3.00 mmol) and anhydrous potassium carbonate (1.70 g, 12.0 mmol) to give **70c** as colourless needles (0.57 g, 61%); mp: 76-77 °C; IR ($CHCl_3$): ν_{max} 3455 (NH), 3309 ($\equiv CH$), 2413 ($C\equiv C$), 1707 ($C=O$), 1602 ($C=C$) cm^{-1} ; 1H NMR (300 MHz, $CDCl_3$): δ 6.75 (3H, m, H-3', H-4', H-6'), 4.70 (1H, brs, NH), 4.05 (2H, t, $J = 6.8$ Hz, H-1''), 3.75 (3H, s, OCH_3), 3.36 (2H, q, $J = 6.6$ Hz, H-1), 2.79 (2H, t, $J = 6.6$ Hz, H-2), 2.66 (2H, dt, $J = 2.7, 6.8$ Hz, H-2''), 2.03 (1H, t, $J = 2.7$ Hz, H-4''), 1.42 (9H, s, $OC(CH_3)_3$); ^{13}C NMR (75 MHz, $CDCl_3$): δ 155.9 ($C=O$), 153.9 (C-5'), 150.6 (C-2'), 129.3 (C-1'), 116.8 (C-6'), 112.8 (C-3'), 112.0 (C-4'), 80.7 (C-3''), 78.9 ($OC(CH_3)_3$), 69.8 (C-4''), 66.8 (C-1''), 55.6 (OCH_3), 40.7 (C-1), 30.9 (C-2), 28.4 ($OC(CH_3)_3$), 19.7 (C-2''); HRMS (EI): m/z found 319.17756 (M^+). $C_{18}H_{25}NO_4$ (M^+) requires 319.17836. Found: C, 67.10; H, 7.66; N, 3.67. $C_{18}H_{25}NO_4$ requires C, 67.89; H, 7.89; N, 4.39.

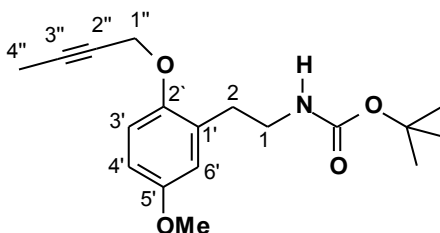
***N*-(*tert*-Butoxycarbonyl)-2-[5-methoxy-2-(4-pentynyl-1-oxy)phenyl]ethylamine (70d)**



According to GP3: The tosylate **140** (1.43 g, 6.00 mmol), phenol **69** (0.80 g, 3.00 mmol) and anhydrous potassium carbonate (1.70 g, 12.0 mmol) to give **70d** as colourless needles (0.93 g, 93%); m.p.: 69-71 °C; IR ($CHCl_3$): ν_{max} 3696, 3452 (NH), 3307 ($\equiv CH$), 2980, 2344 ($C\equiv C$), 1707 ($C=O$), 1502 ($C=C$), 1218, 1164 (C-N) cm^{-1} ; 1H NMR (300 MHz, $CDCl_3$): δ 6.79 (1H, d, $J = 9.6$ Hz, H-3'), 6.70 (2H, m, H-4', H-6'), 4.72 (1H, brs, NH), 4.02 (2H, t, $J = 6.5$ Hz, H-1''), 3.75 (3H, s, OCH_3), 3.34 (2H, q, $J = 6.5$ Hz, H-1), 2.78 (2H, t, $J = 6.5$ Hz, H-2), 2.41 (2H, td, J

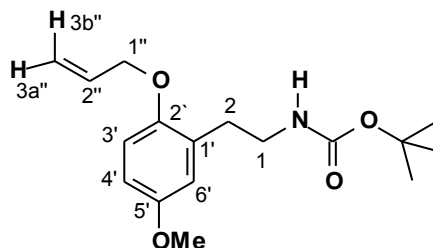
= 2.7 Hz, 6.5 Hz, H-3''), 1.99 (2H, m, H-2''), 1.96 (1H, t, $J = 2.7$ Hz, H-5''), 1.43 (9H, s, $\text{OC}(\text{CH}_3)_3$); ^{13}C NMR (75 MHz, CDCl_3): δ 155.9 (C=O), 153.7 (C-5'), 151.0 (C-2'), 129.0 (C-1'), 116.7 (C-6'), 112.5 (C-3'), 112.0 (C-4'), 83.4 (C-4''), 79.3 ($\text{OC}(\text{CH}_3)_3$), 68.9 (C-5''), 66.9 (C-1''), 55.7 (OCH_3), 40.8 (C-1), 30.9 (C-2), 28.4 ($\text{OC}(\text{CH}_3)_3$), 28.4 (C-3''), 15.4 (C-2''); Anal. Found: C, 68.44; H, 8.16; N, 4.20 $\text{C}_{19}\text{H}_{27}\text{NO}_4$ requires; C, 68.53; H, 8.28; N, 3.87.

***N*-(*tert*-Butoxycarbonyl)-2-[2-(2-butynyl-oxy)-5-methoxyphenyl]ethylamine (70e)**



According to GP3: 1-Bromo-2-butyne (0.19 g, 1.50 mmol), phenol **69** (0.20 g, 0.75 mmol) and anhydrous potassium carbonate (0.42 g, 3.00 mmol) to give colourless crystals **70e** (0.22 g, 92%); m.p: 53–55 °C; IR (CHCl_3): ν_{max} 3681, 3449 (NH), 3014, 2246 ($\text{C}\equiv\text{C}$), 1703 (C=O), 1501 (C=C), 1205 (C-N) cm^{-1} ; ^1H NMR (300 MHz, CDCl_3): δ 6.90 (1H, d, $J = 9.6$ Hz, H-3'), 6.71 (2H, m, H-4', H-6'), 4.65 (1H, brs, NH), 4.60 (2H, q, $J = 2.3$ Hz, H-1''), 3.76 (3H, s, OCH_3), 3.35 (2H, q, $J = 6.0$ Hz, H-1), 2.79 (2H, t, $J = 6.0$ Hz, H-2), 1.83 (3H, t, $J = 2.3$ Hz, H-4''), 1.43 (9H, s, $\text{OC}(\text{CH}_3)_3$); ^{13}C NMR (75 MHz, CDCl_3): δ 155.9 (C=O), 154.0 (C-5'), 150.1 (C-2'), 129.4 (C-1'), 116.5 (C-6'), 113.6 (C-3'), 111.9 (C-4'), 83.3 (C-2''), 78.6 ($\text{OC}(\text{CH}_3)_3$), 74.5 (C-3''), 57.3 (C-1''), 55.6 (OCH_3), 40.6 (C-1), 30.6 (C-2), 28.4 ($\text{OC}(\text{CH}_3)_3$), 3.6 (C-4''); Anal. Found: C, 67.39; H, 7.97; N, 4.12 $\text{C}_{18}\text{H}_{25}\text{NO}_4$ requires C, 67.69; H, 7.89; N, 4.23.

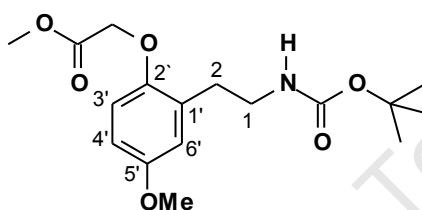
***N*-(*tert*-Butoxycarbonyl)-2-(2-allyloxy-5-methoxyphenyl)ethylamine (70f)**



According to GP3: Allyl bromide (0.24 mL, 2.24 mmol), phenol **69** (0.30 g, 1.12 mmol), anhydrous potassium carbonate (0.62 g, 4.50 mmol) to afford **70f** as a fine white powder (0.34 g, 99%); m.p: 54–56 °C; IR (CHCl_3): ν_{max} 3682, 3449 (NH), 3201 C-H), 1502 (C=C), 1703 (C=O), 1210 (C-N) cm^{-1} ; ^1H NMR (300 MHz, CDCl_3): δ 6.68 (1H, d, $J = 9.0$ Hz, H-3'),

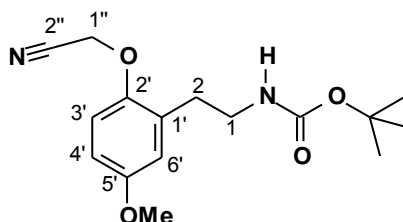
6.71 (3H, m, H-4', H-6'), 6.05 (1H, ddt, $J = 5.1$ Hz, 10.5 Hz, 17.3 Hz, H-2''), 5.39 (1H, dq, $J = 1.6$ Hz, 17.3 Hz, H-3b''), 5.26 (1H, dq, $J = 1.6$ Hz, 10.5 Hz, H-3a''), 4.71 (1H, brs, NH), 4.50 (2H, dt, $J = 1.6$ Hz, 5.1 Hz, H-1''), 3.76 (3H, s, OCH₃), 3.40 (2H, q, $J = 6.5$ Hz, H-1), 2.80 (2H, t, $J = 6.5$ Hz, H-2), 1.43 (9H, s, OCH₃); ¹³C NMR (75 MHz, CDCl₃): δ 156.0 (C=O), 153.7 (C-5'), 150.8 (C-2'), 133.6 (C-2''), 129.2 (C-1'), 117.1 (C-3''), 116.7 (C-6'), 112.9 (C-3'), 112.0 (C-4'), 79.0 (OC(CH₃)₃), 69.5 (C-1''), 55.7 (OCH₃), 40.8 (C-1), 30.9 (C-2), 28.4 (OC(CH₃)₃); Anal. Found C, 66.41; H, 8.21; N, 4.40 C₁₇H₂₅NO₄ requires C, 66.43; H, 8.20; N, 4.56.

***N*-(*tert*-Butoxycarbonyl)-2-(2-methoxycarbonylmethoxy-5-methoxyphenyl)ethylamine (70g)**



According to GP3: Methyl chloracetate (0.25 mL, 2.24 mmol), phenol **69** (0.30 g, 1.12 mmol), and anhydrous potassium carbonate (0.62 g, 4.50 mmol) to afford **70g** as a fine white powder (0.37 g, 98%); m.p 66-68 °C; IR (CHCl₃): ν_{\max} 3681, 3449 (NH), 1758, 1704 (C=O), 1501 (C=C), 1227 (C-N) cm⁻¹; ¹H NMR (300 MHz, CDCl₃): δ 6.67 (3H, m, H-3', H-4', H-6'), 4.84 (1H, brs, NH), 4.61 (2H, s, ArOCH₂), 3.78 (3H, s, CO₂CH₃), 3.74 (3H, s, ArOCH₃), 3.40 (2H, q, $J = 6.5$ Hz, H-1), 2.90 (2H, t, $J = 6.5$ Hz, H-2), 1.41 (9H, s, OC(CH₃)₃); ¹³C NMR (75 MHz, CDCl₃): δ 169.6 (OC=O), 156.0 (HNC=O), 154.3 (C-5'), 150.1 (C-2'), 129.5 (C-1'), 116.9 (C-6'), 112.4 (C-3'), 112.0 (C-4'), 78.8 (OC(CH₃)₃), 66.0 (ArOCH₂), 55.6 (OCH₃), 52.1 (CO₂CH₃), 40.7 (C-1), 30.9 (C-2), 28.4 (OC(CH₃)₃); Anal. Found C, 60.37; H, 7.36; N, 3.91 C₁₇H₂₅NO₆ requires C, 60.16; H, 7.42; N, 4.13.

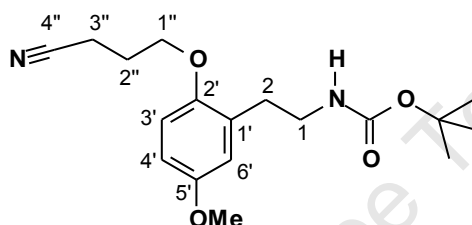
***N*-(*tert*-Butoxycarbonyl)-2-(2-cyanomethoxy-5-methoxyphenyl)ethylamine (70h)**



According to GP3: Bromoacetonitrile (0.17 g, 1.50 mmol), phenol **69** (0.20 g, 0.75 mmol) and anhydrous potassium carbonate (0.42 g, 3.00 mmol) to give colourless crystals **70h** (0.22 g, 96%); m.p: 98–102 °C; IR (CHCl₃): ν_{\max} 3681, 3449 (NH), 2240 (C≡N), 1703 (C=O), 1501

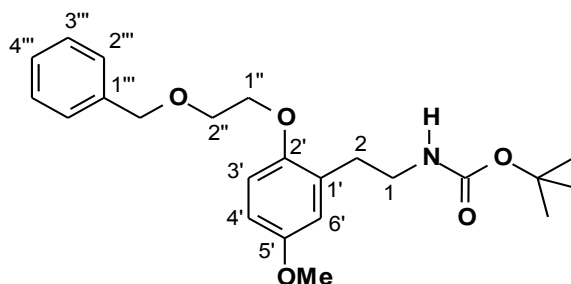
(C=C), 1226 (C-N) cm^{-1} ; ^1H NMR (300 MHz, CDCl_3): δ 6.89 (1H, d, J = 9.6 Hz, H-3'), 6.74 (2H, m, H-4', H-6'), 4.73 (2H, s, H-1''), 4.61 (1H, brs, NH), 3.76 (3H, s, OCH_3), 3.35 (2H, q, J = 6.8 Hz, H-1), 2.80 (2H, t, J = 6.8 Hz, H-2), 1.43 (9H, s, $\text{OC}(\text{CH}_3)_3$); ^{13}C NMR (75 MHz, CDCl_3): δ 155.9 (C=O), 155.4 (C-5'), 148.9 (C-2'), 130.1 (C-1'), 117.1 (C-6'), 115.4 (C-2''), 112.8 (C-3'), 112.2 (C-4'), 79.2 ($\text{OC}(\text{CH}_3)_3$), 55.6 (OCH_3), 54.9 (C-1''), 40.5 (C-1), 31.4 (C-2), 28.4 ($\text{OC}(\text{CH}_3)_3$); Anal. Found: C, 62.87; H, 7.09; N, 8.30; $\text{C}_{16}\text{H}_{22}\text{N}_2\text{O}_4$ requires C, 62.73; H, 7.24; N, 9.14.

***N*-(*tert*-Butoxycarbonyl)-2-[2-(3-cyanoprop-1-yloxy)-5-methoxyphenyl]ethylamine (70i)**



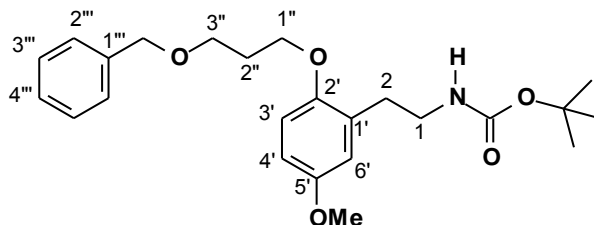
According to GP3: 4-Bromobutyronitrile (0.15 g, 0.74 mmol), phenol **69** (0.10 g, 0.37 mmol) and anhydrous potassium carbonate (0.20 g, 1.48 mmol) to give the title compound **70i** as a colourless solid (0.12 g, 96%); m.p: 69–71 °C; IR (CHCl_3): ν_{max} 3681, 3449 (NH), 3014 (C-H), 2246 ($\text{C}\equiv\text{N}$), 1703 (C=O) cm^{-1} ; ^1H NMR (300 MHz, CDCl_3): δ 6.74 (3H, m, H-3', H-4', H-6'), 4.73 (1H, brs, NH), 4.03 (2H, t, J = 5.8 Hz, H-1''), 3.75 (3H, s, OCH_3), 3.32 (2H, q, J = 6.8 Hz, H-1), 2.77 (2H, t, J = 6.8 Hz, H-2), 2.60 (2H, t, J = 7.0 Hz, H-3''), 2.14 (2H, m, H-2''), 1.42 (9H, s, $\text{OC}(\text{CH}_3)_3$); ^{13}C NMR (75 MHz, CDCl_3): δ 155.9 (C=O), 154.0 (C-5'), 150.6 (C-2'), 128.9 (C-1'), 119.3 (C-4''), 116.8 (C-6'), 112.5 (C-3'), 112.0 (C-4'), 79.5 ($\text{OC}(\text{CH}_3)_3$), 66.3 (C-1''), 55.7 (OCH_3), 40.8 (C-1), 31.2 (C-2), 28.4 ($\text{OC}(\text{CH}_3)_3$), 25.7 (C-3''), 14.4 (C-2''); HRMS (EI): m/z found 334.1924 (M^+). $\text{C}_{18}\text{H}_{26}\text{N}_2\text{O}_4$ (M^+) requires 334.1893; Anal. Found: C, 63.62; H, 7.82; N, 8.06 $\text{C}_{18}\text{H}_{26}\text{N}_2\text{O}_4$ requires C, 64.65; H, 7.84; N, 8.38.

***N*-(*tert*-Butoxycarbonyl)-2-[2-(2-benzyloxyeth-1-yloxy)-5-methoxyphenyl]ethylamine (70j)**



According to GP3: 2-Benzyloxy-1-bromoethane **73** (0.69 g, 3.00 mmol), phenol **69** (0.40 g, 1.50 mmol) and anhydrous potassium carbonate (0.83 g, 6.00 mmol) to afford **70j** as a colourless solid (0.53 g, 85%); m.p: 56-58 °C; IR (CHCl₃): ν_{\max} 3673, 3449 (NH), 3000, 2398 (C-H), 1701 (C=O), 1501 (C=C) cm⁻¹; ¹H NMR (300 MHz, CDCl₃): δ 7.40 (5H, m, ArH), 6.79 (1H, d, *J* = 8.8 Hz, H-3'), 6.70 (2H, m, H-4', H-6'), 4.78 (1H, brs, NH), 4.63 (2H, s, ArCH₂O), 4.10 (2H, t, *J* = 4.8 Hz, H-1''), 3.82 (2H, t, *J* = 4.8 Hz, H-2''), 3.75 (3H, s, OCH₃), 3.37 (2H, q, *J* = 6.5 Hz, H-1), 2.80 (2H, t, *J* = 6.5 Hz, H-2), 1.42 (9H, s, OC(CH₃)₃); ¹³C NMR (75 MHz, CDCl₃): δ 155.9 (C=O), 153.7 (C-5'), 151.0 (C-2'), 138.1 (C-1'''), 129.2 (C-1'), 128.4 (C-2'', C-6'''), 127.7 (C-4'''), 127.6 (C-3'', C-5'''), 116.6 (C-6'), 112.9 (C-3'), 111.9 (C-4'), 78.7 (OC(CH₃)₃), 73.2 (ArCH₂O), 68.7 (C-1''), 68.4 (C-2''), 55.5 (OCH₃), 40.7 (C-1), 30.9 (C-2), 28.4 (OC(CH₃)₃); HRMS (EI): *m/z* found 401.22044 (M⁺). C₂₃H₃₁NO₅ (M⁺) requires 401.22022; Anal. Found C, 68.90; H, 7.80; N, 3.37. C₂₃H₃₁NO₅ requires C, 68.80; H, 7.78; N, 3.49.

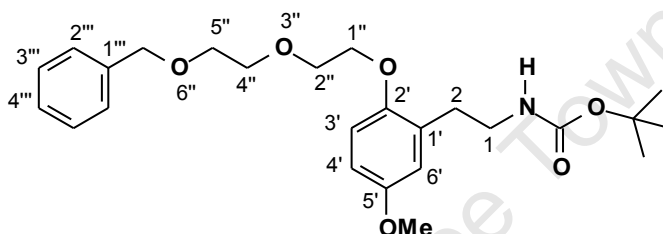
***N*-(*tert*-Butoxycarbonyl)-2-[2-(3-benzyloxypropan-1-yloxy)-5-methoxyphenyl]ethylamine (75)**



According to GP3: Bromide **73** (0.72 g, 3.14 mmol), phenol **69** (0.42 g, 1.57 mmol) and anhydrous potassium carbonate (0.87 g, 6.28 mmol) to give **75** as a white solid (0.65 g, 100%); mp: 44-46 °C; IR (CHCl₃): ν_{\max} 3681 (NH), 3015 (C-H), 1704 (C=O), 1516 (C=C) cm⁻¹; ¹H NMR (300 MHz, CDCl₃): δ 7.29 (5H, m, ArH), 6.78 (1H, d, *J* = 9.7 Hz, H-3'), 6.71 (2H, m, H-4', H-6'), 4.69 (1H, brs, NH), 4.53 (2H, s, ArCH₂O), 4.04 (2H, t, *J* = 6.2 Hz, H-1''), 3.76 (3H,

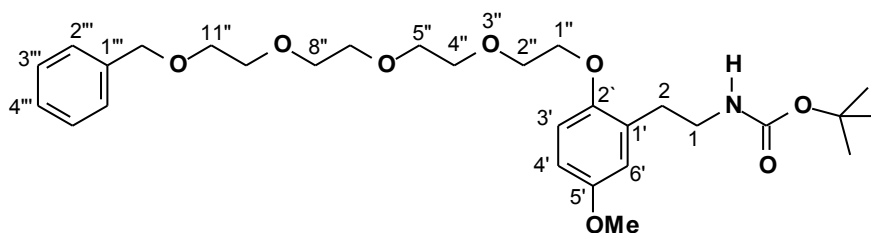
s, OCH₃), 3.67 (2H, t, $J = 6.2$ Hz, H-3''), 3.32 (2H, q, $J = 6.4$ Hz, H-1), 2.73 (2H, t, $J = 6.4$ Hz, H-2), 2.10 (2H, quin, $J = 6.2$, H-2''), 1.43 (9H, s, OC(CH₃)₃); ¹³C NMR (100 MHz, CDCl₃): δ 155.9 (C=O), 153.6 (C-5'), 151.1 (C-2'), 138.4 (C-1'''), 128.9 (C-1'), 128.4, (C-2''', C-6'''), 127.6, (C-4'''), 127.5 (C-3''', C-5'''), 116.8 (C-6'), 112.4 (C-3'), 112.0 (C-4'), 73.0 (ArCH₂O), 79.0 (OC(CH₃)₃), 66.9 (CH₂O), 65.6 (CH₂O), 55.7 (OCH₃), 40.7 (C-1), 31.0 (C-2), 29.9 (C-2''), 28.4 (OC(CH₃)₃); Anal. Found C, 70.35; H, 7.01; N, 3.30; C₂₄H₃₃N₃O₅ requires C, 69.37; H, 8.00; N, 3.37.

***N*-(*tert*-Butoxycarbonyl)-2-[2-(5-benzyloxy-3-oxapent-1-yloxy)-5-methoxyphenyl]ethylamine (75a)**



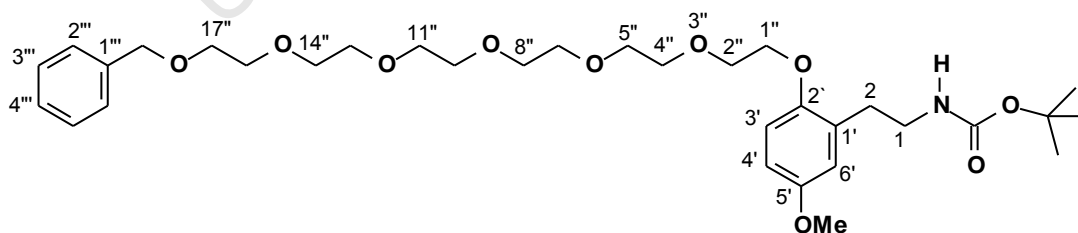
According to GP3: Bromide **73b** (0.87 g, 3.36 mmol), phenol **69** (0.45 g, 1.68 mmol) and anhydrous potassium carbonate (0.93 g, 6.70 mmol) to give **75a** as a colourless oil (0.61 g, 81%.); IR (CHCl₃): ν_{\max} 3442, 3377 (NH, OH), 3007, 2928 (C-H), 1697 (C=O), 1501 (C=O), 1227 (C-N) cm⁻¹; ¹H NMR (400 MHz, CDCl₃): δ 7.31 (4H, m, ArH), 7.21 (1H, m, ArH), 6.76 (1H, d, $J = 8.7$ Hz, H-3'), 6.70 (1H, d, $J = 2.8$ Hz, H-6'), 6.68 (1H, dd, $J = 2.8, 8.7$ Hz, H-4'), 4.83 (1H, brs, NH), 4.55 (2H, s, ArCH₂O), 4.06 (2H, t, $J = 4.8$ Hz, H-1''), 3.82 (2H, t, $J = 4.8$ Hz, CH₂O), 3.72 (3H, s, OCH₃), 3.70 (2H, m, CH₂O), 3.62 (2H, m, CH₂O), 3.31 (2H, q, $J = 6.5$ Hz, H-1), 2.76 (2H, t, $J = 6.5$ Hz, H-2), 1.38 (9H, s, OC(CH₃)₃); ¹³C NMR (100 MHz, CDCl₃): δ 156.0 (C=O), 153.8 (C-5'), 151.0 (C-2'), 138.2 (C-1'''), 129.4 (C-1'), 128.4 (C-2''', C-6'''), 127.7 (C-4'''), 127.6 (C-3''', C-5'''), 116.6 (C-6'), 113.1 (C-3'), 112.0 (C-4'), 78.8 (OC(CH₃)₃), 73.3 (ArCH₂), 70.8 (CH₂O), 69.9 (CH₂O), 69.5 (CH₂O), 68.5 (CH₂O), 55.6 (OCH₃), 40.7 (C-1), 31.0 (C-2), 28.4 (OC(CH₃)₃); HRMS (EI): m/z found 445.24814 (M⁺). C₂₅H₃₅NO₆ (M⁺) requires 445.24644.

***N*-(*tert*-Butoxycarbonyl)-2-{2-[2-(2-(2-(2-benzyloxyethoxy)-ethoxy)-ethoxy)ethoxy]-5-methoxyphenyl}ethylamine (75b)**



According to GP3: Bromide **73c** (0.91 g, 2.62 mmol), phenol **69** (0.35 g, 1.31 mmol) and anhydrous potassium carbonate (0.72 g, 5.20 mmol) to give **75b** as a colourless oil (0.56 g, 80%); IR (CHCl₃): ν_{\max} 3681, 3449 (N-H), 3021, 2913 (C-H), 1700 (C=O), 1501 (C=C) cm⁻¹; ¹H NMR (400 MHz, CDCl₃): δ 7.34 (4H, m, ArH), 7.21 (1H, m, ArH), 6.78 (1H, d, J = 8.8 Hz, H-3'), 6.72 (1H, d, J = 3.0 Hz, H-6'), 6.70 (1H, dd, J = 3.0 Hz, 8.8 Hz, H-4'), 4.90 (1H, brs, NH), 4.57 (2H, s, ArCH₂O), 4.08 (2H, t, J = 4.9 Hz, H-1''), 3.83 (2H, t, J = 4.9 Hz, CH₂O), 3.76 (3H, s, OCH₃), 3.72–3.68 (10H, m, 5 × CH₂O), 3.64 (2H, m, CH₂O), 3.35 (2H, q, J = 6.7 Hz, H-1), 2.80 (2H, t, J = 6.7 Hz, H-2), 1.43 (9H, s, OC(CH₃)₃); ¹³C NMR (100 MHz, CDCl₃): δ 155.9 (C=O), 153.7 (C-5'), 151.0 (C-2'), 138.3 (C-1'''), 129.3 (C-1'), 128.3 (C-2'', C-6'''), 127.6 (C-4'''), 127.5 (C-3'', C-5'''), 116.6 (C-6'), 113.0 (C-3'), 111.9 (C-4'), 78.7 (OC(CH₃)₃), 73.1 (ArCH₂), 78.7 (2 × CH₂O), 70.6 (2 × CH₂O), 70.6 (CH₂O), 69.8 (CH₂O), 69.4 (CH₂O), 68.4 (CH₂O), 55.6 (OCH₃), 40.6 (C-1), 31.0 (C-2), 28.4 (OC(CH₃)₃); HRMS (ES): m/z found 534.3036 (M⁺ + H), C₂₉H₄₄NO₈ requires (M⁺ + H) 534.3067.

***N*-(*tert*-Butoxycarbonyl)-2-{2-[2-(2-(2-(2-(2-(2-benzyloxyethoxy)-ethoxy)-ethoxy)ethoxy)ethoxy)ethoxy]-5-methoxyphenyl}ethylamine (75c)**



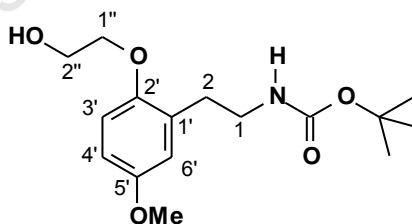
According to GP3: Bromide **73d** (0.82 g, 1.88 mmol), phenol **69** (0.25 g, 0.94 mmol) and anhydrous potassium carbonate (0.52 g, 3.76 mmol) to give **75c** as a colourless oil (0.46 g, 79%); IR (CHCl₃): ν_{\max} 3449 (NH), 3007, 2913 (C-H), 1703 (C=O), 1501 (C=C), 1230 (C-N) cm⁻¹; ¹H NMR (400 MHz, CDCl₃): δ 7.35–7.28 (5H, m, ArH), 6.78 (1H, d, J = 8.8 Hz, H-3'), 6.70 (2H, m, H-4', H-6'), 4.89 (1H, brs, NH), 4.57 (2H, s, ArCH₂O), 4.08 (2H, t, J = 4.8 Hz, H-1''), 3.83 (2H, t, J = 4.8 Hz, CH₂O), 3.76 (3H, s, OCH₃), 3.71 (2H, m, CH₂O), 3.65 (18H, m, 9

× CH₂O), 3.36 (2H, m, H-1), 2.80 (2H, t, *J* = 7.0 Hz, H-2), 1.43 (9H, s, OC(CH₃)₃); ¹³C NMR (100 MHz, CDCl₃): δ 156.0 (C=O), 153.8 (C-5'), 151.0 (C-2'), 138.3 (C-1'''), 129.3 (C-1'), 128.3 (C-2'', C-6'''), 127.7 (C-3''', C-5'''), 127.5 (C-4'''), 116.6 (C-6'), 113.0 (C-3'), 112.0 (C-4'), 78.7 (OC(CH₃)₃), 73.2 (ArCH₂), 70.7 (CH₂O), 70.6 (4 × CH₂O), 70.5 (4 × CH₂O), 69.8 (CH₂O), 69.4 (CH₂O), 68.4 (CH₂O), 55.6 (OCH₃), 40.6 (C-1), 31.0 (C-2), 28.4 (OC(CH₃)₃); HRMS (ES): *m/z* found (M⁺ + H), 622.3610, C₃₃H₅₂NO₁₀ requires (M⁺ + H) 622.3591.

General Procedure for hydrogenolysis of the benzyl group (GP4)

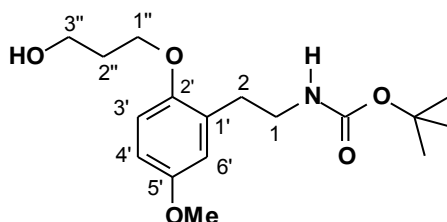
Hydrogen gas was introduced at atmospheric pressure to the carbamate **70j**, **75** and **75a-c** (1.00 mmol) and a suspension of 10% palladium-on-carbon (10 mol%) in ethanol (20 mL). The mixture was stirred at room temperature for 18 h. The catalyst was filtered through a pad of Celite, washed with EtOAc (3 × 15 mL) and the filtrate evaporated in *vacuo*. The crude product was purified by column chromatography using EtOAc / pet ether (8 / 2) to give the product.

N-(*tert*-Butoxycarbonyl)-2-[2-(2-hydroxyethoxy)-5-methoxyphenyl]ethylamine (**70m**)



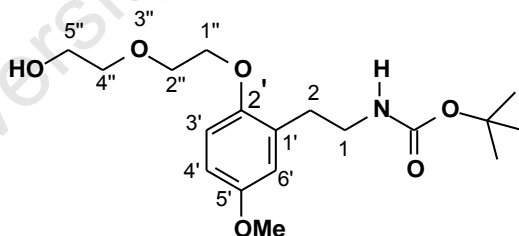
Compound **70m**, colourless crystals (0.33 g, 93%); m.p.: 90–91 °C; IR (CHCl₃): ν_{\max} 3681, 3615, 3449 (NH, OH), 3021, 2405 (C-H), 1700 (C=O), 1501 (C=C), 1165 (C-N) cm⁻¹; ¹H NMR (400 MHz, CDCl₃) δ : 6.74 (3H, m, H-3', H-5', H-6'), 4.87 (1H, brs, NH), 4.00 (4H, m, H-1'', H-2''), 3.75 (3H, s, OCH₃), 3.31 (2H, q, *J* = 6.7 Hz, H-1), 2.78 (2H, t, *J* = 6.7 Hz, H-2), 1.42 (9H, s, OC(CH₃)₃), 1.25 (1H, brs, OH); ¹³C NMR (100 MHz, CDCl₃): δ 156.5 (C=O), 153.9 (C-5'), 151.4 (C-2'), 128.9 (C-1'), 117.1 (C-6'), 112.6 (C-3'), 112.0 (C-4'), 79.7 (OC(CH₃)₃), 70.6 (C-1''), 61.6 (C-2''), 55.9 (OCH₃), 41.0 (C-2), 32.6 (C-1), 28.6 (OC(CH₃)₃); HRMS (EI): *m/z* found 311.17278 (M⁺). C₁₆H₂₅NO₅ (M⁺) requires 311.17327; Anal. Found: C, 61.70; H, 8.03; N, 4.14. C₁₆H₂₅NO₅ requires C, 61.72; H, 8.09; N, 4.50.

***N*-(*tert*-Butoxycarbonyl)-2-[2-(3-hydroxyprop-1-yloxy)-5-methoxyphenyl]ethylamine (70n)**



Compound **70n**, colourless crystals (0.45 g, 95%); mp: 44-46 °C; IR (CHCl₃): ν_{\max} 3681, 3623, 3449 (NH, OH), 2399 (C-H), 1700 (C=O), 1505 (C=C), 1205 (C-N) cm⁻¹; ¹H NMR (300 MHz, CDCl₃): δ 6.80 (1H, d, J = 9.6 Hz, H-3'), 6.70 (2H, m, H-4', H-6'), 4.78 (1H, brs, NH), 4.06 (2H, t, J = 5.9 Hz, H-1''), 3.87 (2H, t, J = 5.9 Hz, H-3''), 3.75 (3H, s, OCH₃), 3.34 (2H, q, J = 6.6 Hz, H-1), 2.76 (2H, t, J = 6.6 Hz, H-2), 2.37 (1H, brs, OH), 2.03 (2H, quin, J = 5.9 Hz, H-2''), 1.41 (9H, s, OC(CH₃)₃); ¹³C NMR (100 MHz, CDCl₃): δ 155.9 (C=O), 153.6 (C-5'), 151.1 (C-2'), 128.9 (C-1'), 116.8 (C-6'), 112.4 (C-3'), 112.0 (C-4'), 79.0 (OC(CH₃)₃), 66.9 (C-1''), 65.9 (C-3''), 55.7 (OCH₃), 40.7 (C-1), 31.0 (C-2), 29.9 (C-2''), 28.4 (OC(CH₃)₃); Anal. Found C, 62.97; H, 8.35; N, 4.13 C₁₇H₂₇NO₄ requires C, 62.75; H, 8.36; N, 4.30.

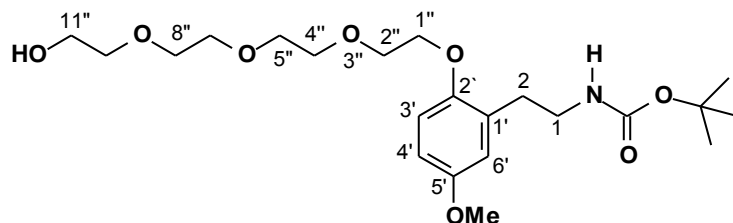
***N*-(*tert*-Butoxycarbonyl)-2-{2-[2-(2-hydroxyethoxy)ethoxy]-5-methoxyphenyl}ethylamine (70o)**



Compound **70o**, as a colourless oil (0.41 g, 93%); IR (CHCl₃): ν_{\max} 3667, 3457, 3384 (NH, OH), 3007, 2928 (C-H), 1700 (C=O), 1501 (C=C), 1223 (C-N) cm⁻¹; ¹H NMR (400 MHz, CDCl₃): δ 6.74 (1H, d, J = 8.4 Hz, H-3'), 6.68 (1H, d, J = 2.8 Hz, H-6'), 6.65 (1H, dd, J = 2.8, 8.4 Hz, H-4'), 4.88 (1H, brs, NH), 4.07 (2H, t, J = 4.6 Hz, CH₂O), 3.82 (2H, t, J = 4.6 Hz, CH₂O), 3.71 (5H, m, OCH₃, CH₂O), 3.62 (2H, t, J = 4.6 Hz, CH₂O), 3.32 (2H, m, H-1), 2.76 (2H, t, J = 6.8 Hz, H-2), 2.51 (1H, brs, OH), 1.36 (9H, s, OC(CH₃)₃); ¹³C NMR (100 MHz, CDCl₃): δ 156.0 (C=O), 153.9 (C-5'), 151.0 (C-2'), 129.3 (C-1'), 116.7 (C-6'), 113.0 (C-3'), 112.0 (C-4'), 79.0 (OC(CH₃)₃), 72.6 (C-1''), 69.8 (CH₂O), 68.4 (CH₂O), 61.7 (C-5''), 55.6

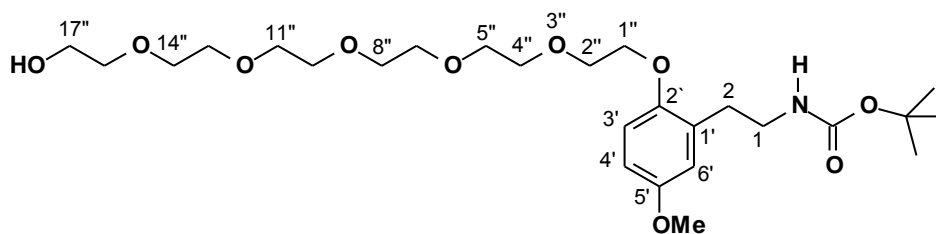
(OCH₃), 40.7 (C-1), 30.8 (C-2), 28.4 (OC(CH₃)₃); HRMS (EI): *m/z* found 355.19828 (M⁺). C₁₈H₂₉O₆N (M⁺) requires 355.19949

***N*-(*tert*-Butoxycarbonyl)-2-{2-[2-(2-(2-(2-hydroxyethoxy)ethoxy)ethoxy)-ethoxy]-ethoxy}ethoxy]-5-methoxyphenyl}ethylamine (70p)**



Compound **70p**, as a colourless oil (0.38 g, 90%); IR (CHCl₃) ν_{\max} 3667, 3449 (NH, OH), 3007, 2928 (C-H), 1700 (C=O), 1501 (C=C), 1220 (C-N) cm⁻¹; ¹H NMR (400 MHz, CDCl₃): δ 6.78 (1H, d, *J* = 8.8 Hz, H-3'), 6.72 (1H, d, *J* = 3.0 Hz, H-6'), 6.69 (1H, dd, *J* = 3.0 Hz, 8.8 Hz, H-4'), 5.01 (1H, brs, NH), 4.08 (2H, t, *J* = 4.8 Hz, H-1''), 3.83 (2H, t, *J* = 4.8 Hz, CH₂O), 3.75 (3H, s, OCH₃), 3.72–3.66 (10H, m, 5 × CH₂O), 3.60 (2H, m, CH₂O), 3.34 (2H, m, H-1), 2.80 (2H, t, *J* = 7.0 Hz, H-2), 1.42 (9H, s, OC(CH₃)₃); ¹³C NMR (100 MHz, CDCl₃): δ 156.0 (C=O), 153.8 (C-5'), 150.9 (C-2'), 129.3 (C-1'), 116.6 (C-6'), 113.0 (C-3'), 112.0 (C-4'), 78.7 (OC(CH₃)₃), 72.5 (C-1''), 70.7 (CH₂O), 70.6 (2 × CH₂O), 70.4 (CH₂O), 69.8 (CH₂O), 68.4 (CH₂O), 61.6 (CH₂O), 55.6 (OCH₃), 40.6 (C-1), 31.0 (C-2), 28.4 (OC(CH₃)₃); HRMS (ES): *m/z* found 444.2610 (M⁺ + H), C₂₂H₃₈NO₈ requires (M⁺ + H) 444.2597.

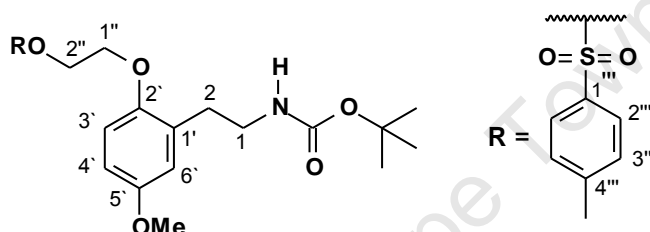
***N*-(*tert*-Butoxycarbonyl)-2-{2-[2-(2-(2-(2-(2-(2-hydroxyethoxy)ethoxy)ethoxy)-ethoxy)-ethoxy)-ethoxy]-ethoxy}ethoxy]-5-methoxyphenyl}ethylamine (70q)**



Compound **70q**, as a colourless oil (0.31 g, 91%); IR (CHCl₃): ν_{\max} 3652, 3449 (NH, OH), 3007, 2884 (C-H), 1700 (C=O), 1501 (C=C), 1227, 1100 (C-N) cm⁻¹; ¹H NMR (400 MHz, CDCl₃): δ 6.78 (1H, d, *J* = 8.8 Hz, H-3'), 6.71 (1H, d, *J* = 2.8 Hz, H-6'), 6.69 (1H, dd, *J* = 2.8, 8.8 Hz, H-4'), 4.96 (1H, brs, NH), 4.08 (2H, t, *J* = 4.6 Hz, H-1''), 3.83 (2H, t, *J* = 4.6 Hz,

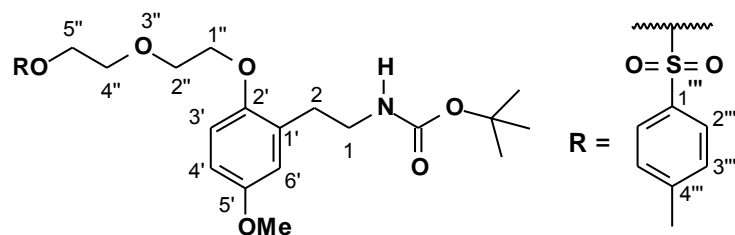
CH₂O), 3.75 (3H, s, OCH₃), 3.70 (2H, t, $J = 4.6$ Hz, CH₂O), 3.64 (16H, m, 8 × CH₂O), 3.59 (2H, t, $J = 4.6$ Hz, CH₂O), 3.34 (2H, q, $J = 6.5$ Hz, H-1), 2.79 (2H, t, $J = 6.5$ Hz, H-2), 1.41 (9H, s, OC(CH₃)₃); ¹³C NMR (100 MHz, CDCl₃): δ 156.0 (C=O), 153.8 (C-5'), 151.0 (C-2'), 129.3 (C-1'), 116.6 (C-6'), 113.0 (C-3'), 112.0 (C-4'), 78.8 (OC(CH₃)₃), 72.6 (C-1''), 70.7 (CH₂O), 70.6 (CH₂O), 70.5 (4 × CH₂O), 70.4 (CH₂O), 70.2 (CH₂O), 69.8 (CH₂O), 68.4 (CH₂O), 61.6 (C-17''), 55.6 (OCH₃), 40.6 (C-1), 31.0 (C-2), 28.4 (OC(CH₃)₃); HRMS (ES): m/z found 532.3112 (M⁺ + H), C₂₆H₄₆NO₁₀ requires (M⁺ + H) 532.3122.

***N*-(*tert*-Butoxycarbonyl)-2-[5-methoxy-2-(2-*p*-toluenesulfonyloxyethoxy)phenyl]ethylamine (74)**



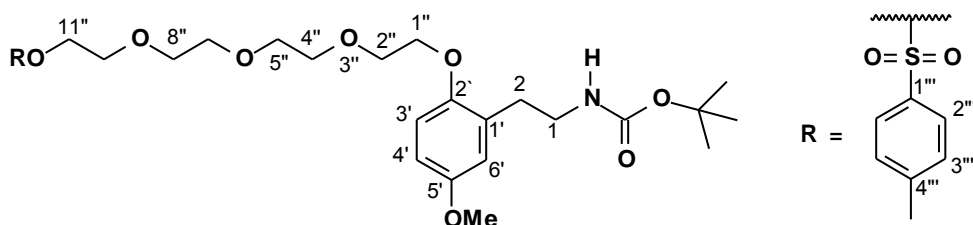
Triethylamine (0.31 mL, 2.39 mmol) and *p*-toluenesulfonyl chloride (0.46 g, 2.39 mmol) were added to a solution of alcohol **70m** (0.62 g, 1.99 mmol) in dry CH₂Cl₂ (15 mL) at 0 °C, followed by a catalytic amount of DMAP (20 mg). The reaction mixture was stirred at rt for 16 h. The crude was diluted with CH₂Cl₂ (60 mL), washed with aq NH₄Cl (20 mL), water (30 mL), and the organic extracts dried over MgSO₄ and the solvent removed under reduced pressure. The crude product was purified by silica-gel column chromatography using EtOAc in light petroleum (2 / 8) to give **74** as a colourless oil (0.72 g, 77%); IR (CHCl₃): ν_{\max} 3659, 3442 (NH), 3007, 2934 (C-H), 1703 (C=O), 1501 (C=C), 1176 (-SO₂-O) cm⁻¹; ¹H NMR (300 MHz, CDCl₃): δ 7.80 (2H, d, $J = 8.2$ Hz, H-2''', H-6'''), 7.34 (2H, d, $J = 8.2$ Hz, H-3''', H-5'''), 6.68 (3H, m, H-3', H-4', H-6'), 4.69 (1H, brs, NH), 4.35 (2H, t, $J = 4.7$ Hz, H-2''), 4.10 (2H, t, $J = 4.7$ Hz, H-1''), 3.73 (3H, s, OCH₃), 3.25 (2H, q, $J = 6.8$ Hz, H-1), 2.69 (2H, t, $J = 6.8$ Hz, H-2), 2.43 (3H, s, ArCH₃), 1.39 (9H, s, OC(CH₃)₃); ¹³C NMR (75 MHz, CDCl₃): δ 155.9 (C=O), 154.1 (C-5'), 150.2 (C-2'), 145.0 (C-1'''), 133.0 (C-4'''), 129.9 (C-3''', C-5'''), 129.3 (C-1'), 127.9 (C-2''', C-6'''), 116.7 (C-6'), 112.9 (C-3'), 112.0 (C-4'), 78.9 (OC(CH₃)₃), 68.3 (C-1''), 66.4 (C-2''), 55.6 (OCH₃), 40.5 (C-2), 30.9 (C-1), 28.4 (OC(CH₃)₃), 21.6 (ArCH₃); HRMS (EI): m/z found 465.18130 (M⁺). C₂₃H₃₁NO₇S (M⁺) requires 465.18212.

***N*-(*tert*-Butoxycarbonyl)-2-{5-methoxy-2-[2-(2-*p*-toluenesulphonyloxyethoxy)ethoxy]phenyl}ethylamine (74a)**



To a solution of alcohol **70o** (0.56 g, 1.58 mmol) in dry CH_2Cl_2 (15 mL), triethylamine (0.25 mL, 1.90 mmol) and *p*-toluenesulfonyl chloride (0.36 g, 1.90 mmol) were added at 0 °C, followed by a catalytic amount of DMAP (20 mg). The reaction mixture was stirred at rt for 16 h. The mixture was diluted with CH_2Cl_2 (70 mL), washed with aq NH_4Cl (30 mL), water (30 mL), dried over MgSO_4 and solvent was removed under reduced pressure. Purification by column chromatography EtOAc in light petroleum (4 / 6) gave **74a** as a colorless oil (0.64 g, 80%); IR (CHCl_3): ν_{max} 3406 (NH), 3007, 2928 (C-H), 1704 (C=O), 1501 (C=C), 1223 (C-N), 1176 (O-SO_2) cm^{-1} ; ^1H NMR (300 MHz, CDCl_3): δ 7.78 (2H, d, $J = 8.4$ Hz, H-2''', H-6'''), 7.30 (2H, d, $J = 8.4$ Hz, H-3''', H-5'''), 6.73 (3H m, H-3', H-4', H-6'), 4.79 (1H, brs, NH), 4.18 (2H, t, $J = 4.7$ Hz, H-5''), 4.01 (2H, t, $J = 4.7$ Hz, CH_2O), 3.77 (4H, m, $2 \times \text{CH}_2\text{O}$), 3.75 (3H, s, OCH_3), 3.30 (2H, q, $J = 6.6$ Hz, H-1), 2.75 (2H, t, $J = 6.6$ Hz, H-2), 2.41 (3H, s, ArCH_3), 1.40 (9H, s, $\text{OC}(\text{CH}_3)_3$); ^{13}C NMR (75 MHz, CDCl_3): δ 150.9 (C=O), 153.8 (C-5'), 150.9 (C-2'), 144.8 (C-1'''), 133.0 (C-4'''), 129.8 (C-3''', C-5'''), 129.3 (C-1'), 127.9 (C-2''', C-6'''), 116.6 (C-6'), 12.9 (C-3'), 111.9 (C-4'), 78.8 ($\text{OC}(\text{CH}_3)_3$), 70.0 (CH_2O), 69.2 (CH_2O), 68.8 (CH_2O), 68.3 (CH_2O), 55.6 (OCH_3), 40.6 (C-1), 31.0 (C-2), 28.4 ($\text{OC}(\text{CH}_3)_3$), 21.5 (ArCH_3); HRMS (EI): m/z found 509.20675 (M^+). $\text{C}_{25}\text{H}_{35}\text{NO}_8\text{S}$ (M^+) requires 509.20834.

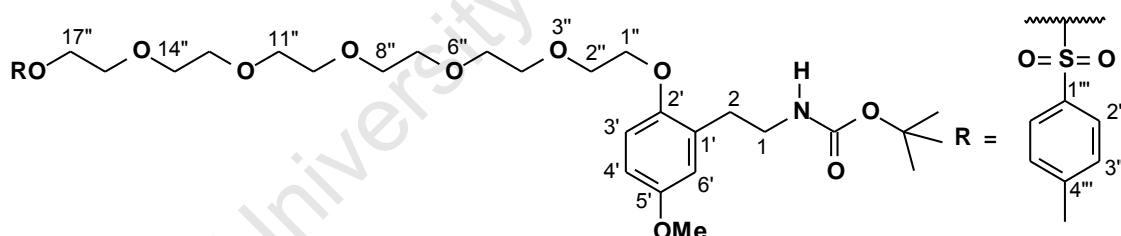
***N*-(*tert*-Butoxycarbonyl)-2-{5-methoxy-2-[2-(2-(2-(2-*p*-toluenesulphonyloxyethoxy)ethoxy)ethoxy)ethoxy]phenyl}ethylamine (74b)**



p-Toluenesulfonyl chloride (0.26 g, 1.36 mmol) was added to a stirring solution of the alcohol **70p** (0.50 g, 1.13 mmol) containing triethylamine (0.18 mL, 1.36 mmol), and a catalytic

amount of DMAP (20 mg) in dry CH_2Cl_2 (15 mL) at 0 °C. The reaction mixture was stirred at rt for 16 h. The mixture was diluted with CH_2Cl_2 (80 mL), the organic extracts washed with aq NH_4Cl (25 mL), water (30 mL), dried over MgSO_4 and the solvent removed under reduced pressure. Purification by column chromatography EtOAc in petroleum ether (8 / 2) gave **74b** as a colorless oil (0.58 g, 84%); IR (CHCl_3): ν_{max} 3377 (NH), 2928 (C-H), 1707 (C=O), 1501 (C=C), 1223 (C-N), 1176 (O-SO₂-) cm^{-1} ; ¹H NMR (300 MHz, CDCl_3): δ 7.77 (2H, d, J = 8.4 Hz, H-2''', H-6'''), 7.31 (2H, d, J = 8.4 Hz, H-3''', H-5'''), 6.76 (1H, d, J = 9.2 Hz, H-3'), 6.68 (2H, m, H-4', H-6'), 4.85 (1H, brs, NH), 4.14 (2H, t, J = 4.8 Hz, H-11''), 4.06 (2H, t, J = 4.8 Hz, CH₂O), 3.81 (2H, t, J = 4.8 Hz, CH₂O), 3.73 (3H, s, OCH₃), 3.69–3.57 (10H, m, 5 × CH₂O), 3.32 (2H, q, J = 6.5 Hz, H-1), 2.77 (2H, t, J = 6.5 Hz, H-2), 2.42 (3H, s, ArCH₃), 1.40 (9H, s, OC(CH₃)₃); ¹³C NMR (75 MHz, CDCl_3): δ 155.9 (C=O), 153.8 (C-5'), 151.0 (C-2'), 144.7 (C-1'''), 133.0 (C-4'''), 129.7 (C-3''', C-5'''), 129.3 (C-1'), 127.9 (C-2'', C-6'''), 116.6 (C-6'), 113.0 (C-3'), 111.9 (C-4'), 78.8 (OC(CH₃)₃), 70.7 (3 × CH₂O), 70.5 (CH₂O), 69.8 (CH₂O), 69.2 (CH₂O), 68.6 (CH₂O), 68.4 (CH₂O), 55.6 (OCH₃), 40.6 (C-1), 31.0 (C-2), 28.4 (OC(CH₃)₃), 21.5 (ArCH₃); HRMS (ES): m/z found 598.2673 (M^+ + H), C₂₉H₄₄NO₁₀S requires (M^+ + H) 598.2686.

***N*-(*tert*-Butoxycarbonyl)-2-{5-methoxy-2-[2-(2-(2-(2-(2-(2-*p*-toluenesulphonyloxyethoxy)ethoxy)ethoxy)ethoxy)ethoxy)ethoxy]phenyl}ethylamine (**74c**)**



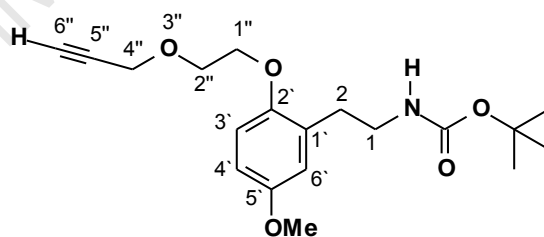
To a solution of alcohol **70q** (0.35 g, 0.66 mmol) in dry CH_2Cl_2 (10 mL), triethylamine (0.11 mL, 0.79 mmol) and *p*-toluenesulfonyl chloride (0.15 g, 0.79 mmol) were added at 0 °C, followed by a catalytic amount of DMAP (20 mg). The reaction mixture was stirred at rt for 16 h. The mixture was diluted with CH_2Cl_2 (50 mL), washed with aq NH_4Cl (20 mL), water (20 mL), dried over MgSO_4 and the solvent removed under reduced pressure. Purification by column chromatography EtOAc in light petroleum (8 / 2) gave **74c** as a colorless oil (0.42 g, 93%); IR (CHCl_3): ν_{max} 3449 (NH), 3007, 2913 (C-H), 1704 (C=O), 1501 (C=C), 1176 (O-SO₂-) cm^{-1} ; ¹H NMR (300 MHz, CDCl_3): δ 7.78 (2H, d, J = 8.2 Hz, H-2''', H-6'''), 7.32 (2H, d, J = 8.2 Hz, H-3''', H-5'''), 6.77 (1H, d, J = 9.2 Hz, H-3'), 6.68 (2H, m, H-4', H-6'), 4.87 (1H, brs, NH), 4.14 (2H, t, J = 4.9 Hz, CH₂O), 4.07 (2H, t, J = 4.9 Hz, CH₂O), 3.82 (2H, t, J = 4.9 Hz, CH₂O),

2.41 (3H, s, ArCH₃), 3.74 (3H, s, OCH₃), 3.70-3.56 (18H, m, 9 × CH₂O), 3.34 (2H, q, *J* = 6.6 Hz, H-1), 2.78 (2H, t, *J* = 6.6 Hz, H-2), 2.41 (3H, s, ArCH₃), 1.41 (9H, s, OCH₃); ¹³C NMR (100 MHz, CDCl₃): δ 156.0 (C=O), 153.8 (C-5'), 151.0 (C-2'), 144.7 (C-1'''), 133.1 (C-4'''), 129.8 (C-3''', C-5'''), 129.3 (C-1'), 127.9 (C-2''', C-6'''), 116.6 (C-6'), 113.0 (C-3'), 112.0 (C-4'), 78.8 (OC(CH₃)₃), 70.7 (CH₂O), 70.7 (CH₂O), 70.6 (CH₂O), 70.5 (2 × CH₂O), 70.5 (2 × CH₂O), 70.5 (CH₂O), 69.8 (CH₂O), 69.2 (CH₂O), 68.7 (CH₂O), 68.4 (CH₂O), 55.6 (OCH₃), 40.6 (C-1), 31.0 (C-2), 28.4 (OC(CH₃)₃), 21.6 (ArCH₃); HRMS (ES): *m/z* found 686.3192 (M⁺ + H), C₃₃H₅₂NO₁₂S requires (M⁺ + H) 686.3210.

General Procedure for O-alkylation of propargyl alcohol (GP5)

To a stirred suspension of NaH (60% in mineral oil, 4.00 mmol) in THF at 0 °C was added propargyl alcohol dropwise (6.00 mmol). The mixture was refluxed for 30 min and the solution of tosylate *N*-Boc carbamate **74**, **74a-c** (1.00 mmol) in THF (10 mL) then added dropwise. After refluxing for 20 h, the crude product was diluted with EtOAc (70 mL), washed with a solution of NH₄Cl (20 mL) and water (2 × 20 mL). The organic extracts were dried over MgSO₄, filtered and the solvent evaporated under reduced pressure to afford a residue, which was purified by column chromatography (15% EtOAc in petroleum ether) to afford the following products as colourless oils.

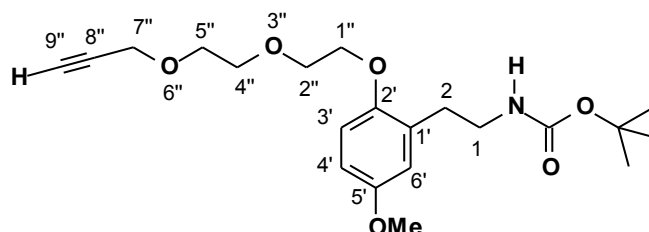
N-(*tert*-Butoxycarbonyl)-2-[5-methoxy-2-(2-propargyloxyethoxy)phenyl]ethylamine (**70k**)



Compound **70k** (0.27 g, 73%); IR (CHCl₃): ν_{\max} 3667, 3449 (NH), 3304 (\equiv C-H), 3007, 2935 (C-H), 2123 (C \equiv C), 1703 (C=O), 1227 (C-N) cm⁻¹; ¹H NMR (300 MHz, CDCl₃): δ 6.77 (1H, d, *J* = 7.8 Hz, H-3'), 6.70 (2H, m, H-4', H-6'), 4.80 (1H, brs, NH), 4.25 (2H, d, *J* = 2.5 Hz, H-4''), 4.10 (2H, m, H-1''), 3.88 (2H, m, H-2''), 3.74 (3H, s, OCH₃), 3.35 (2H, q, *J* = 6.7 Hz, H-1), 2.80 (2H, t, *J* = 6.7 Hz, H-2), 2.45 (1H, t, *J* = 2.5 Hz, H-6''), 1.41 (9H, s, OC(CH₃)₃); ¹³C NMR (75 MHz, CDCl₃): δ 156.0 (C=O), 153.9 (C-5'), 150.9 (C-2'), 129.4 (C-1'), 116.6 (C-6'), 113.0 (C-3'), 112.0 (C-4'), 79.5 (C-5''), 78.9 (OC(CH₃)₃), 74.7 (C-6''), 68.3 (CH₂O), 68.2 (CH₂O), 58.4

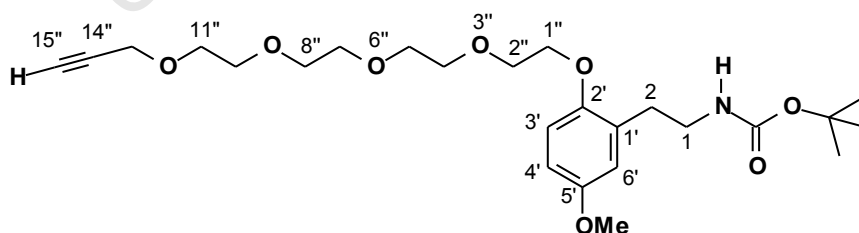
(C-4''), 55.6 (OCH₃), 40.7 (C-1), 30.9 (C-2), 28.4 (OC(CH₃)₃); HRMS (EI): *m/z* found 349.18937 (M⁺). C₁₉H₂₇NO₅ (M⁺) requires 349.18892.

***N*-(*tert*-Butoxycarbonyl)-2-[5-methoxy-2-[2-(2-propargyloxyethoxy)ethoxy]phenyl]ethylamine (70l)**



Compound **70l** (0.39 g, 90%); IR (CHCl₃): ν_{\max} 3449 (NH), 3304 (\equiv CH), 3000, 2906 (C-H), 2116 (C \equiv C), 1733, 1704 (C=O), 1501 (C=C) cm⁻¹; ¹H NMR (400 MHz, CDCl₃): δ 6.75 (1H, d, *J* = 9.2 Hz, H-3'), 6.67 (2H, m, H-4', H-6'), 4.83 (1H, brs, NH), 4.18 (2H, d, *J* = 2.4 Hz, H-7''), 4.06 (2H, t, *J* = 4.9 Hz, CH₂O), 3.80 (2H, t, *J* = 4.9 Hz, CH₂O), 3.72 (3H, s, OCH₃), 3.69 (4H, m, 2 \times CH₂O), 3.32 (2H, q, *J* = 6.6 Hz, H-1), 2.76 (2H, t, *J* = 6.6 Hz, H-2), 2.40 (1H, t, *J* = 2.4 Hz, H-9''), 1.39 (9H, s, OC(CH₃)₃); ¹³C NMR (100 MHz, CDCl₃): δ 156.0 (C=O), 153.9 (C-5'), 151.0 (C-2'), 129.4 (C-1'), 116.6 (C-6'), 113.1 (C-3'), 112.0 (C-4'), 79.6 (C-8''), 78.8 (OC(CH₃)₃), 74.6 (C-9''), 70.6 (CH₂O), 69.9 (CH₂O), 69.2 (CH₂O), 68.5 (CH₂O), 58.4 (C-7''), 55.7 (OCH₃), 40.7 (C-2), 31.1 (C-1), 28.4 (OC(CH₃)₃); HRMS (EI): *m/z* found 393.21448 (M⁺), C₂₁H₃₁NO₆ (M⁺) requires 393.21514.

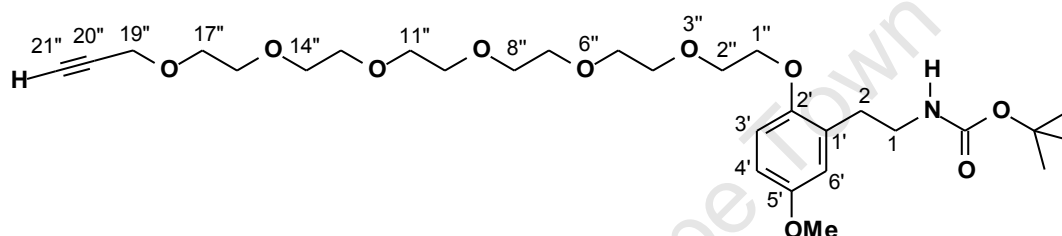
***N*-(*tert*-Butoxycarbonyl)-2-[5-methoxy-2-[2-(2-(2-(2-propargyloxyethoxy)ethoxy)ethoxy)ethoxy]phenyl]ethylamine (70r)**



Compound **70r** (0.29 g, 83%); IR (CHCl₃): ν_{\max} 3449 (NH), 3304 (\equiv CH), 3007, 2920 (C-H), 2116 (C \equiv C), 1703 (C=O), 1501 (C=C), 1227 (C-N) cm⁻¹; ¹H NMR (300 MHz, CDCl₃): δ 6.77 (1H, d, *J* = 8.8 Hz, H-3'), 6.68 (2H, m, H-4', H-6'), 4.88 (1H, brs, NH), 4.18 (2H, d, *J* = 2.1 Hz, H-13''), 4.07 (2H, t, *J* = 4.8 Hz, H-1''), 3.82 (2H, t, *J* = 4.8 Hz, CH₂O), 3.74 (3H, s, OCH₃), 3.72–3.64 (12H, m,

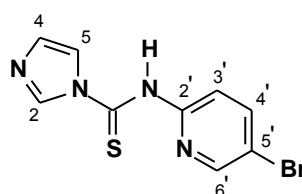
6 × CH₂O), 3.34 (2H, q, *J* = 6.5 Hz, H-1), 2.78 (2H, t, *J* = 6.5 Hz, H-2), 2.40 (1H, t, *J* = 2.1 Hz, H-15''), 1.41 (9H, s, OC(CH₃)₃); ¹³C NMR (100 MHz, CDCl₃): δ 156.0 (C=O), 153.8 (C-5'), 151.0 (C-2'), 129.3 (C-1'), 116.6 (C-6'), 113.0 (C-3'), 112.0 (C-4'), 79.7 (C-14''), 78.8 (OC(CH₃)₃), 74.4 (C-15''), 70.8 (CH₂O), 70.7 (CH₂O), 70.6 (2 × CH₂O), 70.4 (CH₂O), 69.9 (CH₂O), 69.1 (CH₂O), 68.5 (CH₂O), 58.3 (C-13''), 55.6 (OCH₃), 40.6 (C-2), 31.0 (C-1), 28.4 (OC(CH₃)₃); HRMS (ES): *m/z* found 482.2732 (M⁺ + H), C₂₅H₄₀NO₈ requires (M⁺ + H) 482.2754.

***N*-(*tert*-Butoxycarbonyl)-2-{5-methoxy-2-[2-(2-(2-(2-(2-(2-propargyloxyethoxy)ethoxy)ethoxy)ethoxy)ethoxy)ethoxy]phenyl}ethylamine (70s)**



Compound **70s** (0.21 g, 80%); IR (CHCl₃): ν_{\max} 3362 (NH), 3246 (\equiv CH), 2870 (C-H), 2116 (C \equiv C), 1707 (C=O), 1501 (C=C), 1223 (C-N) cm⁻¹; ¹H NMR (300 MHz, CDCl₃): δ 6.77 (1H, *J* = 9.2 Hz, H-3'), 6.68 (2H, m, H-4', H-6'), 4.87 (1H, brs, NH), 4.18 (2H, d, *J* = 2.4 Hz, H-19''), 4.07 (2H, t, *J* = 4.9 Hz, H-1''), 3.82 (2H, t, *J* = 4.9 Hz, CH₂O), 3.74 (3H, s, OCH₃), 3.71-3.62 (20H, m, 10 × CH₂O), 3.34 (2H, q, *J* = 6.6 Hz, H-1), 2.78 (2H, t, *J* = 6.6 Hz, H-2), 2.41 (2H, t, *J* = 2.4 Hz, H-21''), 1.41 (9H, s, OC(CH₃)₃); ¹³C NMR (75 MHz, CDCl₃): δ 156.0 (C=O), 153.8 (C-5'), 151.0 (C-2'), 129.3 (C-1'), 116.6 (C-6'), 113.0 (C-3'), 112.0 (C-4'), 79.7 (C-20''), 78.8 (OC(CH₃)₃), 74.5 (C-21''), 70.8 (2 × CH₂O), 70.6 (2 × CH₂O), 70.6 (3 × CH₂O), 70.4 (CH₂O), 69.8 (CH₂O), 69.1 (CH₂O), 68.4 (2 × CH₂O), 58.4 (C-19''), 55.6 (OCH₃), 40.6 (C-2), 31.0 (C-1), 28.4 (OC(CH₃)₃); HRMS (ES): *m/z* found 570.3289 (M⁺ + H), C₂₉H₄₈NO₁₀ requires (M⁺ + H) 570.3278.

***N*-(5-Bromo-2-pyridinyl)-1*H*-imidazole-1-carbothioamide (49)¹⁰¹**



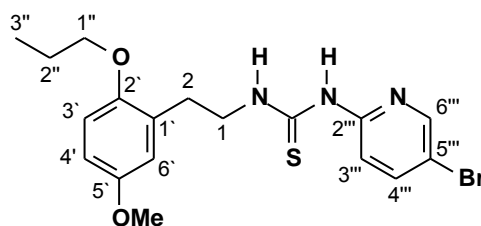
1, 1'-Thiocarbonyldiimidazole (1.26 g, 7.07 mmol) was added to 2-amino-5-bromopyridine (1.22 g, 7.07 mmol) in dry CH₃CN (20 mL) and the solution was stirred for 20 h at rt. The

precipitate was filtered and washed with cold CH₃CN (10 mL) to yield **49** as a white solid (1.83 g, 92%); ¹H NMR (300 MHz, CDCl₃): δ 10.19 (1H, brs, NH), 8.49 (1H, d, *J* = 2.4 Hz, H-6'), 8.16 (2H, m, H-2', H-3'), 7.79 (1H, s, H-2), 7.09 (2H, m, H-4, H-5); ¹³C NMR (75 MHz, CDCl₃): δ 176.8 (C=S), 151.2 (C-2'), 147.3 (C-6'), 140.7 (C-4'), 134.9 (C-2), 121.3 (C-4, C-5), 116.2 (C-3'), 113.8 (C-5').

General Procedure for the Synthesis of Thioureas (GP6)

Trifluoroacetic acid (0.20 mL) was added to a solution of the *N*-Boc carbamate **70a-q** (1.00 mmol) in CH₂Cl₂ (2 mL) at 0 °C, and the solution stirred for 2 h. Diisopropylethylamine (0.40 mL) was added, the solvent evaporated *in vacuo* and the crude amine dried under vacuum for 1 h. Thiocarbonyl reagent **49** (1.30 mmol) was added to the crude amine in DMF (5 mL) and the mixture stirred at 100 °C for 16 h. The mixture was then poured into ice-cold water (5 mL) and stirred for 30 min. The precipitate formed was filtered and washed with cold water (2 × 5 mL) or alternatively extracted into ethyl acetate/ light petroleum mixtures as eluent. Alternatively, the condensation reaction with **49** could be carried out in THF (5 mL) at room temperature for 20 h. Following evaporation of the solvent, the residue was subjected directly to column chromatography to afford the desired thioureas.

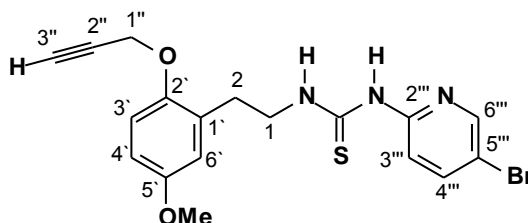
N-(5-Bromo-2-pyridinyl)-*N'*-[2-(5-methoxy-2-prop-1-yloxyphenyl)ethyl]-thiourea (**77a**)



Using THF/ rt, gave compound **77a** (0.13 g, 65%); mp: 162-163 °C; IR (CHCl₃): ν_{\max} 3696, 3413 (NH), 3167, 2963 (C-H), 1512 (C=C), 1472 (C=S), 1212 (C-N) cm⁻¹; ¹H NMR (400 MHz, CDCl₃): δ 11.18 (1H, brs, NH), 8.95 (1H, brs, NH), 8.08 (1H, d, *J* = 2.4 Hz, H-6'''), 7.67 (1H, dd, *J* = 2.4 Hz, 8.8 Hz, H-4'''), 6.81 (1H, d, *J* = 3.2 Hz, H-6'), 6.78 (1H, d, *J* = 8.8 Hz, H-3'), 6.74 (1H, dd, *J* = 3.2, 8.8 Hz, H-4'), 6.72 (1H, d, *J* = 8.8 Hz, H-3'''), 4.02 (2H, m, H-1''), 3.87 (2H, t, *J* = 6.4 Hz, H-1), 3.75 (3H, s, OCH₃), 2.99 (2H, t, *J* = 6.4 Hz, H-2), 1.80 (2H, m, H-2''), 1.04 (3H, t, *J* = 7.4 Hz, H-3''); ¹³C NMR (100 MHz, CDCl₃): δ 179.0 (C=S), 153.3 (C-5'), 151.7 (C-2'''), 151.5 (C-2'), 146.8 (C-6'''), 141.1 (C-4'''), 128.5 (C-1'), 117.7 (C-6'), 113.2 (C-3'), 112.6 (C-3'''), 112.2 (C-5'''), 111.5 (C-4'), 70.2 (C-1''), 55.6 (OCH₃), 45.8 (C-1), 30.0 (C-2),

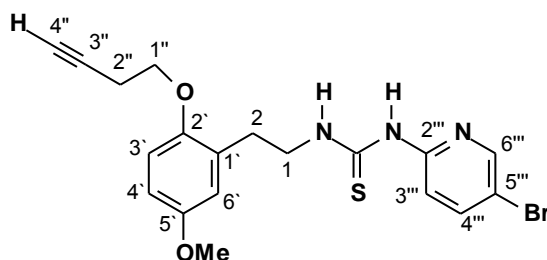
22.8 (C-2''), 10.7 (C-3''); Anal. Found: C, 50.77; H, 5.21; N, 9.50; S, 7.14. C₁₈H₂₂BrN₃O₂S requires C, 50.95; H, 5.23; N, 9.90; S, 7.55.

***N*-(5-Bromo-2-pyridinyl)-*N'*-[2-(5-methoxy-2-propargyloxyphenyl)ethyl]-thiourea (77b)**



Using DMF/ 100 °C, gave compound **77b** (80 mg, 17%); mp: 121-122 °C; IR (CHCl₃): ν_{\max} 3691 (NH), 3307, 3174 (\equiv CH), 1602 (C=C), 1137 (C-N) cm⁻¹; ¹H NMR (400 MHz, CDCl₃): δ 11.13 (1H, brs, NH), 8.29 (1H, brs, NH), 8.12 (1H, d, J = 2.4 Hz, H-6'''), 7.69 (1H, dd, J = 2.4 Hz, 8.8 Hz, H-4'''), 6.95 (1H, d, J = 8.8 Hz, H-3'''), 6.82 (1H, d, J = 3.1 Hz, H-6'), 6.76 (1H, dd, J = 3.2 Hz, 8.8 Hz, H-4'), 6.59 (1H, d, J = 8.8 Hz, H-3'), 4.67 (2H, d, J = 2.2 Hz, H-1''), 4.01 (2H, q, J = 6.8 Hz, H-1), 3.76 (3H, s, OCH₃), 3.01 (2H, t, J = 6.7 Hz, H-2), 2.47 (1H, t, J = 2.2 Hz, H-3''); ¹³C NMR (75 MHz, CDCl₃): δ 179.1 (C=S), 154.2 (C-5'), 151.7 (C-2''), 150.0 (C-2'), 146.7 (C-6'''), 141.1 (C-4'''), 129.2 (C-1'), 117.6 (C-6'), 113.5 (C-3'), 113.3 (C-3'''), 112.6 (C-5'''), 111.5 (C-4'), 79.0 (C-2''), 75.3 (C-3''), 56.8 (C-1'), 55.5 (OCH₃), 45.7 (C-1), 29.8 (C-2); Anal. Found: C, 51.23; H, 4.50; N, 8.62 C₁₈H₁₈BrN₃O₂S requires C, 51.44; H, 4.32; N, 10.00.

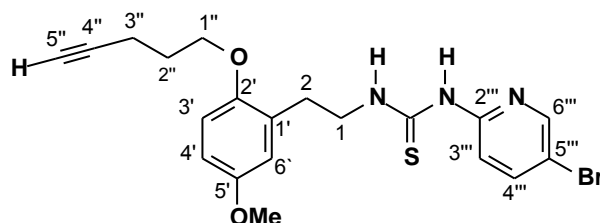
***N*-(5-Bromo-2-pyridinyl)-*N'*-{2-[2-(3-butynyl-1-oxy)-5-methoxyphenyl]ethyl}-thiourea (77c)**



Using DMF/ 100 °C, gave compound **77c** (33 mg, 25%); mp: 155-156 °C; IR (CHCl₃): ν_{\max} 3691, 3415 (NH), 3308 (\equiv CH), 3152, 3018, 2956 (C-H), 2245 (C \equiv C), 1591 (C=C), 1511 (C=S), 1138 (C-N) cm⁻¹; ¹H NMR (300 MHz, CDCl₃): δ 11.13 (1H, brs, NH), 8.44 (1H, brs, NH), 8.10 (1H, d, J = 2.4 Hz, H-6'''), 7.68 (1H, dd, J = 2.4, 8.7 Hz, H-4'''), 6.76 (3H, m, H-3''', H-4', H-6'), 6.61 (1H, d, J = 8.7 Hz, H-3'''), 4.03 (4H, m, H-1, H-1''), 3.75 (3H, s, OCH₃), 3.00 (2H, t, J = 6.6 Hz, H-2), 2.68 (2H, td, J = 2.6, 6.9 Hz, H-2''), 2.04 (1H, t, J = 2.6 Hz, H-4''); ¹³C NMR (75 MHz, CDCl₃): δ 179.2 (C=S), 153.8 (C-5'), 151.6 (C-2'), 150.9 (C-2'''), 146.9 (C-6'''),

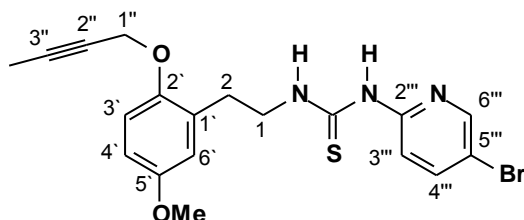
141.2 (C-4''), 128.9 (C-1'), 117.8 (C-6'), 113.1 (C-3'''), 112.8 (C-3'), 112.7 (C-5'''), 111.6 (C-4'), 80.8 (C-4'') 69.9 (C-3''), 66.9 (C-1''), 55.6 (OCH₃), 45.8 (C-1), 30.0 (C-2), 19.8 (C-2'''); Found: C, 52.01; H, 4.46; N, 9.00. C₁₉H₂₀BrN₃O₂S requires C, 52.54; H, 4.64; N, 9.67.

***N*-(5-Bromo-2-pyridinyl)-*N'*-(2-[5-methoxy-2-(4-pentynyl-1-yloxy)phenyl]ethyl)-thiourea (77d)**



Using THF/ rt, gave compound **77d** (0.18 g, 69%); mp: 140-141 °C; IR (CHCl₃): ν_{\max} 3684, 3415 (NH), 3308 (C≡CH), 3152, 3018, 2956 (C-H), 2245 (C≡C), 1512 (C=C), 1468 (C=S), 1226 (C-N) cm⁻¹; ¹H NMR (400 MHz, CDCl₃): δ 11.18 (1H, brs, NH), 8.83 (1H, brs, NH), 8.10 (1H, d, J = 2.4 Hz, H-6'''), 7.68 (1H, dd, J = 2.4 Hz, 8.8 Hz, H-4'''), 6.81 (1H, d, J = 9.0 Hz, H-3'), 6.81 (1H, d, J = 3.0 Hz, H-6'), 6.75 (1H, dd, J = 3.0, 9.0 Hz, H-4'), 6.70 (1H, d, J = 8.8 Hz, H-3'''), 4.01 (4H, m, H-1, H-1''), 3.75 (3H, s, OCH₃), 2.98 (2H, t, J = 6.8 Hz, H-2), 2.41 (2H, td, J = 2.4, 6.8 Hz, H-3''), 2.02 (2H, m, H-2''), 1.96 (1H, t, J = 2.4 Hz, H-5''); ¹³C NMR (100 MHz, CDCl₃): δ 179.1 (C=S), 153.5 (C-5'), 151.7 (C-2'''), 151.2 (C-2'), 146.7 (C-6'''), 141.1 (C-4'''), 128.5 (C-1'), 117.7 (C-6'), 113.2 (C-3'), 112.6 (C-3'''), 112.3 (C-5'''), 111.5 (C-4'), 83.5 (C-4''), 68.9 (C-5''), 66.9 (C-1''), 55.6 (OCH₃), 45.7 (C-1), 30.0 (C-2), 28.4 (C-3''), 15.4 (C-2''); Anal. Found: C, 53.54; H, 4.78; N, 7.81; S, 5.62%. C₂₀H₂₂BrN₃O₂S requires C, 53.58; H, 4.95; N, 9.37; S, 7.15.

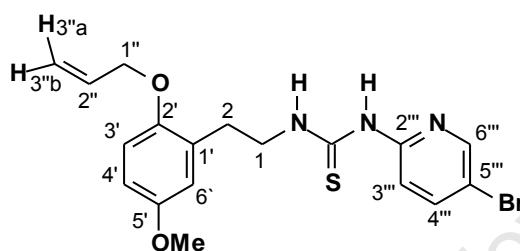
***N*-(5-Bromo-2-pyridinyl)-*N'*-(2-[2-(2-butynyloxy)-5-methoxyphenyl]ethyl)-thiourea (77e)**



Using THF/ rt, gave compound **77e** (0.12 g, 60%); mp: 149-150 °C; IR (CHCl₃): ν_{\max} 3690, 3410 (NH), 3018 (C-H), 2239 (≡CH), 1510 (C=C), 1469 (C=S), 1207 (C-N) cm⁻¹; ¹H NMR (400 MHz, CDCl₃): δ 11.12 (1H, brs, NH), 8.58 (1H, brs, NH), 8.11 (1H, d, J = 2.4 Hz, H-6'''), 7.68 (1H, dd, J = 2.4 Hz, 8.8 Hz, H-4'''), 6.93 (1H, d, J = 8.8 Hz, H-3'), 6.81 (1H, d, J = 3.2 Hz, H-6'), 6.75 (1H, dd, J = 3.2 Hz, 8.8 Hz, H-4'), 6.65 (1H, d, J = 8.8 Hz, H-3'''), 4.61 (2H, q, J =

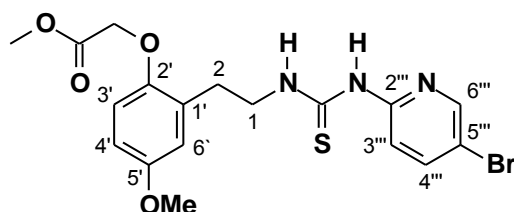
2.4 Hz, H-1''), 4.01 (2H, q, $J = 6.8$ Hz, H-1), 3.75 (3H, s, OCH₃), 3.00 (2H, t, $J = 6.8$ Hz, H-2), 1.83 (3H, t, $J = 2.4$ Hz, CH₃); ¹³C NMR (100 MHz, CDCl₃): δ 179.1 (C=S), 153.9 (C-5'), 151.6 (C-2''), 150.4 (C-2'), 146.8 (C-6'''), 141.1 (C-4'''), 129.1 (C-1'), 117.5 (C-6'), 113.6 (C-3'), 113.1 (C-3'''), 112.6 (C-5'''), 111.6 (C-4'), 83.4 (C-2''), 74.5 (C-3''), 57.5 (C-1''), 55.6 (OCH₃), 45.8 (C-1), 29.8 (C-2), 3.7 (CH₃); Anal. Found: C, 52.51; H, 4.53; N, 8.95; S, 6.31. C₁₉H₂₀BrN₃O₂S requires C, 52.54; H, 4.64; N, 9.67; S, 7.38.

***N*-(5-Bromo-2-pyridinyl)-*N'*-[2-(2-allyloxy-5-methoxy-phenyl)ethyl]-thiourea (77f)**



Using THF/ rt, gave compound **77f** (65 mg, 67%); mp: 153-154 °C; IR (CHCl₃): ν_{\max} 3681, 3413 (N-H), 3041 (C-H), 1509 (C=C), 1422 (C=S), 1212 (C-N) cm⁻¹; ¹H NMR (400 MHz, CDCl₃): δ 11.11 (1H, brs, NH), 8.13 (1H, brs, NH), 8.10 (1H, d, $J = 2.4$ Hz, H-6'''), 7.69 (1H, dd, $J = 2.4, 8.7$ Hz, H-4'''), 6.82 (1H, d, $J = 2.9$ Hz, H-6'), 6.80 (1H, d, $J = 9.0$ Hz, H-3'), 6.74 (1H, dd, $J = 2.9, 9.0$ Hz, H-4'), 6.55 (1H, d, $J = 8.7$ Hz, H-3'''), 6.05 (1H, ddt, $J = 5.1, 10.5, 17.3$ Hz, H-2''), 5.39 (1H, dq, $J = 1.6, 17.3$ Hz, H-3''a), 5.26 (1H, dq, $J = 1.6, 10.5$ Hz, H-3''b), 4.49 (2H, dt, $J = 1.6, 5.1$ Hz, H-1''), 4.01 (2H, m, H-1), 3.76 (3H, s, OCH₃), 3.01 (2H, t, $J = 6.6$ Hz, H-2); ¹³C NMR (100 MHz, CDCl₃): δ 179.1 (C=S), 153.5 (C-5'), 151.5 (C-2''), 151.0 (C-2'), 146.9 (C-6'''), 141.1 (C-4'''), 133.6 (C-2''), 128.7 (C-1'), 117.7 (C-6'), 117.0 (C-3'), 113.0 (C-3'), 112.8 (C-3'''), 112.6 (C-5'''), 111.5 (C-4'), 69.5 (C-1''), 55.6 (OCH₃), 45.8 (C-1), 30.0 (C-2); Anal. Found: C, 51.32; H, 4.62; N, 9.56. C₁₈H₂₀BrN₃O₂S requires C, 51.18; H, 4.78; N, 9.95.

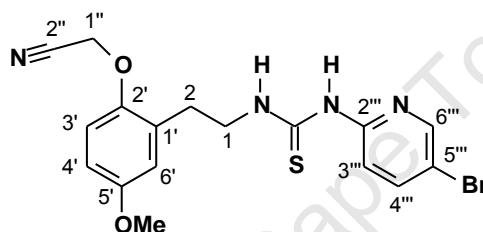
***N*-(5-Bromo-2-pyridinyl)-*N'*-[2-(2-methoxycarbonylmethoxy-5-methoxyphenyl)ethyl]-thiourea (77g)**



Using THF/ rt, gave compound **77g** (23 mg, 50%); mp: 161-164 °C; IR (CHCl₃): ν_{\max} 3681 (N-H), 3015 (C-H), 1519 (C=C), 1469 (C=S), 1212 (C-N) cm⁻¹; ¹H NMR (400 MHz, CDCl₃): δ

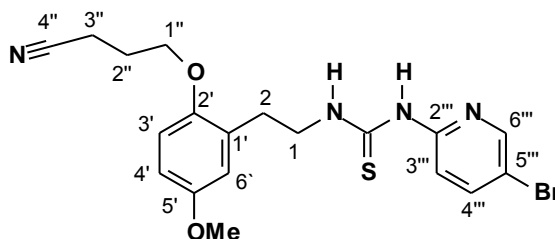
11.12 (1H, br s, NH), 8.32 (1H, br s, NH), 8.11 (1H, d, $J = 2.4$ Hz, H-6'''), 7.69 (1H, dd, $J = 2.4, 9.1$ Hz, H-4'''), 6.83 (1H, d, $J = 2.4$ Hz, H-6'), 6.71 (2H, m, H-4', H-3'), 6.61 (1H, d, $J = 9.1$ Hz, H-3'''), 4.62 (2H, s, ArOCH₂), 4.05 (2H, m, H-1), 3.78 (3H, s, ArOCH₃), 3.74 (3H, s, COCH₃), 3.06 (2H, t, $J = 6.8$ Hz, H-2); ¹³C NMR (100 MHz, CDCl₃): δ 179.2 (C=S), 169.6 (OC=O), 154.2 (C-5'), 151.5 (C-2'''), 150.3 (C-2'), 146.9 (C-6'''), 141.2 (C-4'''), 129.2 (C-1'), 117.8 (C-6'), 113.0 (C-3'), 112.7 (C-3'''), 112.6 (C-5'''), 111.6 (C-4'), 66.3 (ArOCH₂), 55.5 (ArOCH₃), 52.2 (CO₂CH₃), 45.7 (C-1), 29.9 (C-2); HRMS (EI): m/z found ($M^+ + H$), 454.0437 C₁₈H₂₁BrN₃O₄S requires ($M^+ + H$) 454.0436.

***N*-(5-Bromo-2-pyridinyl)-*N'*-[2-(2-cyanomethoxy-5-methoxyphenyl)ethyl]-thiourea (77h)**



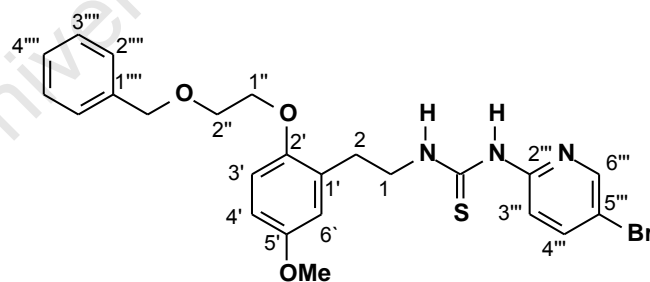
Using THF/ rt, gave compound **77h** (0.13 g, 68%); mp: 155-156 °C; IR (CHCl₃): ν_{\max} 3681, 3413, 3022 (NH), 2239 (C≡N), 1505 (C=C), 1469 (C=S), 1216 (C-N) cm⁻¹; ¹H NMR (400 MHz, CDCl₃) δ : 11.20 (1H, brs, NH), 8.72 (1H, brs, NH), 8.10 (1H, d, $J = 2.4$ Hz, H-6'''), 7.70 (1H, dd, $J = 2.4$ Hz, 8.8 Hz, H-4'''), 6.92 (1H, d, $J = 8.8$ Hz, H-3'), 6.85 (1H, d, $J = 3.2$ Hz, H-6'), 6.78 (1H, dd, $J = 3.2$ Hz, 8.8 Hz, H-4'), 6.69 (1H, d, $J = 8.8$ Hz, H-3'''), 4.75 (2H, s, H-1''), 3.99 (2H, q, $J = 6.8$ Hz, H-1), 3.76 (3H, s, OCH₃), 3.01 (2H, t, $J = 6.8$ Hz, H-2); ¹³C NMR (100 MHz, CDCl₃) δ : 179.4 (C=S), 155.4 (C-5'), 151.6 (C-2'''), 149.0 (C-2'), 146.7 (C-6'''), 141.3 (C-4'''), 129.8 (C-1'), 117.9 (C-6'), 115.4 (C-2''), 114.0 (C-3'), 113.3 (C-3'''), 112.8 (C-5'''), 111.9 (C-4'), 55.6 (OCH₃), 54.9 (C-1''), 45.6 (C-1), 29.6 (C-2); Anal. Found: C, 48.38; H, 4.04; N, 12.38; S, 6.76%. C₁₇H₁₇BrN₄O₂S requires C, 48.46; H, 4.07; N, 13.30; S, 7.61.

***N*-(5-Bromo-2-pyridinyl)]-*N'*-(2-[2-(3-cyanopropyl-1-oxy)-5-methoxyphenyl]ethyl)-thiourea (77i)**



Using THF/ rt, gave compound **77i** (70 mg, 53%); mp: 165-166 °C; IR (CHCl₃): ν_{\max} 3413 (NH), 3167, 2964 (C-H), 2246 (C≡N), 1505 (C=C), 1465 (C=S), 1239 (C-N) cm⁻¹; ¹H NMR (400 MHz, CDCl₃): δ 11.26 (1H, brs, NH), 9.34 (1H, brs, NH), 8.08 (1H, d, *J* = 2.4 Hz, H-6'''), 7.67 (1H, dd, *J* = 2.4 Hz, 8.8 Hz, H-4'''), 6.82 (1H, d, *J* = 3.2 Hz, H-6'), 6.81 (1H, d, *J* = 8.8 Hz, H-3'), 6.77 (1H, d, *J* = 8.8 Hz, H-3'''), 6.74 (1H, dd, *J* = 3.2 Hz, 8.8 Hz, H-4'), 3.99 (4H, m, H-1'', H-1), 3.74 (3H, s, OCH₃), 2.98 (2H, t, *J* = 6.8 Hz, H-3''), 2.62 (2H, t, *J* = 7.0 Hz, H-2), 2.14 (2H, m, H-2''); ¹³C NMR (75 MHz, CDCl₃): δ 179.0 (C=S), 153.7 (C-5'), 151.7 (C-2'''), 150.6 (C-2'), 146.5 (C-6'''), 141.1 (C-4'''), 128.4 (C-1'), 119.2 (C-4''), 117.7 (C-6'), 113.4 (C-3'), 112.7 (C-3'''), 112.2 (C-5'''), 111.5 (C-4'), 66.0 (C-1''), 55.5 (OCH₃), 45.6 (C-1), 29.9 (C-2), 25.6 (C-3''), 14.4 (C-2''); Anal. Found: C, 50.61; H, 4.78; N, 12.37; S, 6.92; C₁₉H₂₁BrN₄O₂S requires C, 50.78; H, 4.71; N, 12.47; S, 7.13.

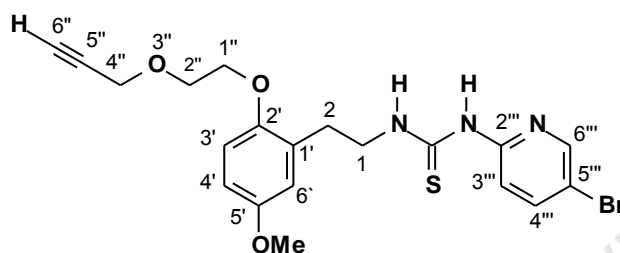
***N*-(5-Bromo-2-pyridinyl)]-*N'*-(2-[2-(2-Benzyloxyethoxy)-5-methoxyphenyl]ethyl)-thiourea (77j)**



Using THF/ rt, gave compound **77j** (70 mg, 58% yield); mp 110-111 °C; IR (CHCl₃): ν_{\max} 3692, 3416 (NH), 3175, 3016, (C-H), 1506 (C=C), 1475 (C=S) cm⁻¹; ¹H NMR (400 MHz, CDCl₃): δ 11.09 (1H, brs, NH), 8.38 (1H, brs, NH), 8.04 (1H, d, *J* = 2.4 Hz, H-6'''), 7.66 (1H, dd, *J* = 2.4 Hz, 8.8 Hz, H-4'''), 7.31 (5H, m, ArH), 6.81 (1H, d, *J* = 8.8 Hz, H-3'), 6.80 (1H, d, *J* = 3.2 Hz, H-6'), 6.74 (1H, dd, *J* = 3.2 Hz, 8.8 Hz, H-4'), 6.58 (1H, d, *J* = 8.8 Hz, H-3'''), 4.63 (2H, s, OCH₂), 4.11 (2H, t, *J* = 4.8 Hz, H-1''), 4.03 (2H, m, H-1), 3.84 (2H, t, *J* = 4.8 Hz, H-2''), 3.75 (3H, s, OCH₃), 3.01 (2H, t, *J* = 6.6 Hz, H-2); ¹³C NMR (100 MHz, CDCl₃): δ 179.0 (C=S), 153.6 (C-5'), 151.8 (C-2'''), 151.3 (C-2'), 146.6 (C-6'''), 141.0 (C-4'''), 138.1 (C-1'''), 128.8 (C-

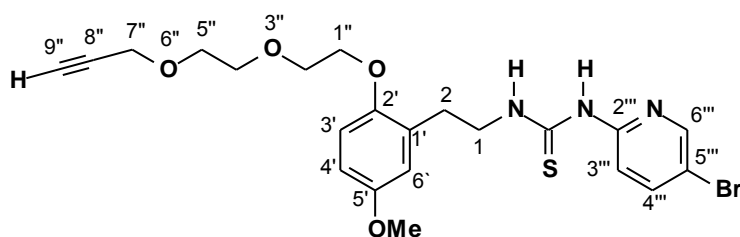
1'), 128.5 (C-2'''), C-6'''), 127.7 (C-4'''), 127.7 (C-3'''), C-5'''), 117.7 (C-6'), 113.4 (C-3'), 112.8 (C-3'''), 112.9 (C-5'''), 111.6 (C-4'), 73.4 (ArOCH₂), 68.9 (OCH₂), 68.5 (OCH₂), 55.6 (OCH₃), 45.7 (C-1), 30.0 (C-2); Anal. Found: C, 56.07; H, 4.86; N, 7.37; S, 5.80; C₂₄H₂₆BrN₃O₃S requires C, 55.82; H, 5.07; N, 8.14; S, 6.21.

***N*-(5-Bromo-2-pyridinyl)-*N'*-(2-[5-methoxy-2-(2-propargyloxyethoxy)phenyl]ethyl)-thiourea (77k)**



Using DMF/ 100 °C, gave compound **77k** (42 mg, 62%); mp: 128-130 °C; IR (CHCl₃): ν_{\max} 3693, 3416 (NH), 3307 (\equiv CH), 3165, 2961 (C-H), 1506 (C=C), 1475 (C=S), 1223 (C-N) cm⁻¹; ¹H NMR (300 MHz, CDCl₃): δ 11.19 (1H, brs, NH), 9.24 (1H, brs, NH), 8.07 (1H, d, J = 2.6 Hz, H-6'''), 7.66 (1H, dd, J = 2.6, 8.7 Hz, H-4'''), 6.81-6.77 (3H, m, H-3''', H-3', H-6'), 6.72 (1H, dd, J = 2.9, 9.2 Hz, H-4'), 4.25 (2H, d, J = 2.4 Hz, H-4''), 4.09 (2H, t, J = 4.8 Hz, H-1''), 4.01 (2H, q, J = 6.6 Hz, H-1), 3.88 (2H, t, J = 4.8 Hz, H-2''), 3.74 (3H, s, OCH₃), 2.99 (2H, t, J = 6.6 Hz, H-2), 2.45 (1H, t, J = 2.4 Hz, H-6''); ¹³C NMR (75 MHz, CDCl₃): δ 178.9 (C=S), 153.6 (C-5'), 151.7 (C-2'''), 151.1 (C-2'), 146.6 (C-6'''), 141.0 (C-4'''), 128.8 (C-1'), 117.6 (C-6'), 113.4 (C-3'), 112.9 (C-3'''), 112.6 (C-5'''), 111.5 (C-4'), 79.5 (C-5''), 74.7 (C-6''), 68.4 (CH₂O), 68.2 (CH₂O), 58.5 (C-4''), 55.5 (OCH₃), 45.6 (C-1), 29.9 (C-2); HRMS (EI): m/z found (M⁺), 463.0578 C₂₀H₂₂BrN₃O₃S requires (M⁺) 463.0565; Anal. Found: C, 51.76; H, 4.72; N, 8.66; S, 6.86; C₂₀H₂₂BrN₃O₃S requires C, 51.73; H, 4.78; N, 9.05; S, 6.91.

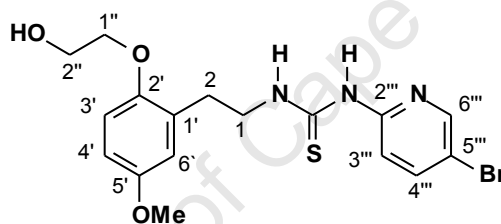
***N*-(5-Bromo-2-pyridinyl)-*N'*-(2-[5-methoxy-2-(2-(2-propargyloxyethoxy)ethoxy)phenyl]ethyl)-thiourea (77l)**



Using DMF/ 100 °C, gave compound **77l** (53 mg, 60%); mp: 91-92 °C; IR (CHCl₃): ν_{\max} 3691, 3416 (NH), 3307 (\equiv CH), 3166, 2935 (C-H), 1506 (C=C), 1475 (C=S), 1266 (C-N) cm⁻¹; ¹H

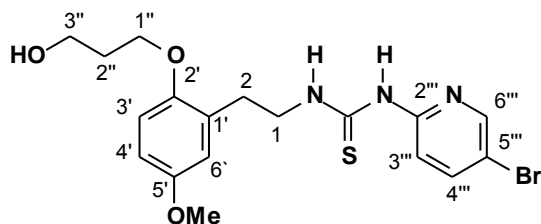
NMR (300 MHz, CDCl₃): δ 11.11 (1H, brs, NH), 8.67 (1H, brs, NH), 8.07 (1H, d, J = 2.4 Hz, H-6'''), 7.67 (1H, dd, J = 2.4, 8.7 Hz, H-4'''), 6.81-6.78 (2H, m, H-3', H-6'), 6.73 (1H, dd, J = 3.0, 8.7 Hz, H-4'), 6.67 (1H, d, J = 8.7 Hz, H-3'''), 4.21 (2H, d, J = 2.1 Hz, H-6''), 4.07 (2H, t, J = 4.9 Hz, H-1''), 4.01 (2H, q, J = 6.6 Hz, H-1), 3.85 (2H, t, J = 4.9 Hz, H-2''), 3.73 (7H, m, OCH₃, H-4'', H-5''), 2.99 (2H, t, J = 6.6 Hz, H-2), 2.42 (1H, t, J = 2.1 Hz, H-9''); ¹³C NMR (75 MHz, CDCl₃): δ 179.1 (C=S), 153.6 (C-5'), 151.6 (C-2'''), 151.2 (C-2'), 146.8 (C-6'''), 141.1 (C-4'''), 128.8 (C-1'), 117.7 (C-6'), 113.2 (C-3'), 112.8 (C-3'''), 112.6 (C-5'''), 111.5 (C-4'), 79.6 (C-8''), 74.6 (C-9''), 70.6 (CH₂O), 70.0 (CH₂O), 69.2 (CH₂O), 68.4 (CH₂O), 58.5 (C-7'''), 55.6 (OCH₃), 45.7 (C-1), 30.0 (C-2); HRMS (EI): m/z found (M^+), 507.0821 C₂₂H₂₆BrN₃O₄S requires (M^+) 507.0827; Anal. Found: C, 52.02; H, 4.10; N, 7.87; S, 6.24; C₂₂H₂₆BrN₃O₄S requires C, 51.97; H, 5.15; N, 8.26; S, 6.31.

***N*-(5-Bromo-2-pyridinyl)-*N'*-(2-[2-(2-hydroxyethoxy)-5-methoxyphenyl]ethyl)-thiourea (77m)**



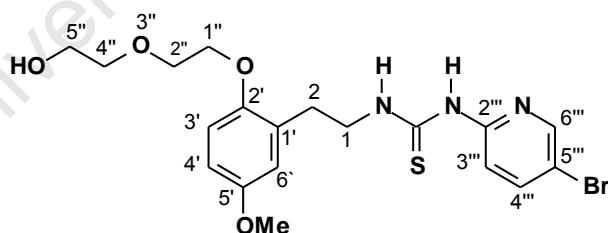
Using THF/ rt, gave compound **77m** (120 mg, 65%); mp 162-163 °C; IR (CHCl₃): ν_{\max} 3623, 3413, 3181 (NH, OH), 2928, 1505 (C=C), 1472 (C=S) 1227 (C-N) cm⁻¹; ¹H NMR (400 MHz, CDCl₃): δ 11.16 (1H, brs, NH), 8.47 (1H, brs, NH), 8.12 (1H, d, J = 2.4 Hz, H-6'''), 7.70 (1H, dd, J = 2.4 Hz, 8.8 Hz, H-4'''), 6.81 (1H, d, J = 2.8 Hz, H-6'), 6.77 (1H, d, J = 8.8 Hz, H-3'), 6.73 (1H, dd, J = 2.8 Hz, 8.8 Hz, H-4'), 6.66 (1H, d, J = 8.8 Hz, H-3'''), 3.99 (6H, m, H-1'', H-2''. H-1), 3.77 (3H, s, OCH₃), 3.03 (2H, t, J = 7.2 Hz, H-2), 2.66 (1H, brs, OH); ¹³C NMR (75 MHz, CDCl₃): δ 179.4 (C=S), 153.7 (C-5'), 151.6 (C-2'''), 151.3 (C-2'), 146.7 (C-6'''), 141.3 (C-4'''), 128.3 (C-1'), 117.4 (C-6'), 113.4 (C-3'), 112.8 (C-3'''), 112.5 (C-5'''), 111.7 (C-4'), 70.3 (C-1''), 61.5 (C-2''), 55.6 (OCH₃), 45.7 (C-1), 30.3 (C-2); Anal. Found: C, 47.96; H, 4.61; N, 9.77; S, 7.01; C₁₇H₂₀BrN₃O₃S requires C, 47.89; H, 4.75; N, 9.86; S, 7.52.

***N*-(5-Bromo-2-pyridinyl)]-*N'*-(2-[2-(3-hydroxypropoxy)-5-methoxyphenyl]ethyl)-thiourea (77n)**



Using THF/ rt, gave compound **77n** (48 mg, 51%); mp 163-165 °C; IR (CHCl₃): ν_{\max} 3681(N-H), 3406 (O-H) 3014 (C-H), 1509, 1472 (C=S), 1216 (C-N) cm⁻¹; ¹H NMR (400 MHz, CDCl₃): δ 11.15 (1H, brs, NH), 8.46 (1H, brs, NH), 8.10 (1H, d, J = 2.4 Hz, H-6'''), 7.68 (1H, dd, J = 2.4, 8.8 Hz, H-4'''), 6.81 (1H, d, J = 8.8 Hz, H-3'), 6.81 (1H, d, J = 2.9 Hz, H-6'), 6.74 (1H, dd, J = 2.9, 8.8 Hz, H-4'), 6.62 (1H, d, J = 8.8 Hz, H-3'''), 4.05 (2H, t, J = 5.9 Hz, H-1''), 4.00 (2H, m, H-1), 3.87 (2H, q, J = 5.9 Hz, H-3''), 3.76 (3H, s, OCH₃), 2.98 (2H, t, J = 6.6 Hz, H-2), 2.05 (2H, quin, J = 5.9 Hz, H-2''), 2.04 (1H, brs, OH); ¹³C NMR (100 MHz, CDCl₃): δ 179.1 (C=S), 153.5 (C-5'), 151.6 (C-2'''), 151.3 (C-2'), 146.8 (C-6'''), 141.2 (C-4'''), 128.4 (C-1'), 117.7 (C-6'), 113.2 (C-3'), 112.7 (C-3'''), 112.4 (C-5'''), 111.6 (C-4'), 65.9 (C-1''), 60.1 (C-3''), 55.6 (OCH₃), 45.8 (C-1), 32.3 (C-2''), 30.0 (C-2); Anal. Found: C, 49.37; H, 4.88; N, 9.08; S, 6.60. C₁₈H₂₂BrN₃O₄S requires C, 49.09; H, 5.04; N, 9.54; S, 7.28.

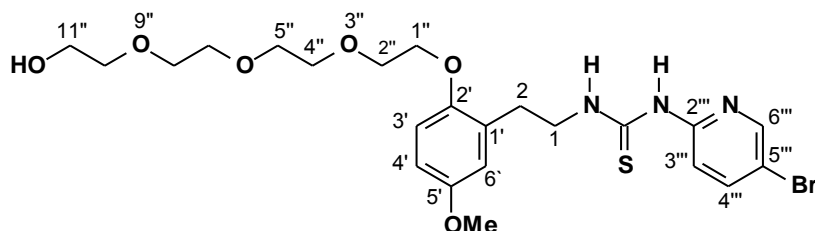
***N*-(5-Bromo-2-pyridinyl)]-*N'*-(2-[2-(2-(2-hydroxyethoxy)ethoxy)ethoxy]-5-methoxyphenyl]ethyl)-thiourea (77o)**



Using THF/ rt, gave compound **77o** (150 mg, 62%); mp: 97-98 °C; IR (CHCl₃): ν_{\max} 3652, 3413 (NH), 3007, 2942 (C-H), 1591, 1501 (C=C), 1469 (C=S), 1230 (C-N) cm⁻¹; ¹H NMR (300 MHz, CDCl₃): δ 11.34 (1H, t, J = 4.6 Hz, NH), 9.09 (1H, brs, NH), 8.06 (1H, d, J = 2.4 Hz, H-6'''), 7.66 (1H, dd, J = 2.4, 8.8 Hz, H-4'''), 6.80 (1H, d, J = 2.7 Hz, H-6'), 6.76 (1H, d, J = 8.8 Hz, H-3'), 6.74 (1H, d, J = 8.8 Hz, H-3'''), 6.72 (1H, dd, J = 2.7, 8.8 Hz, H-4'), 4.02 (4H, m, H-1'', H-1), 3.84 (2H, t, J = 4.6 Hz, CH₂O), 3.76 (5H, m, OCH₃, CH₂O), 3.66 (2H, t, J = 4.6 Hz, CH₂O), 2.98 (2H, t, J = 6.5 Hz, H-2), 2.54 (1H, brs, OH); ¹³C NMR (75 MHz, CDCl₃): δ 179.0 (C=O), 153.6 (C-5'), 151.7 (C-2'''), 151.2 (C-2'), 146.6 (C-6'''), 141.0 (C-4'''), 128.7 (C-1'), 117.7 (C-6'), 113.4 (C-3'), 112.7 (C-3'''), 112.6 (C-5'''), 111.5 (C-4'), 72.6 (C-1''), 69.8 (CH₂O),

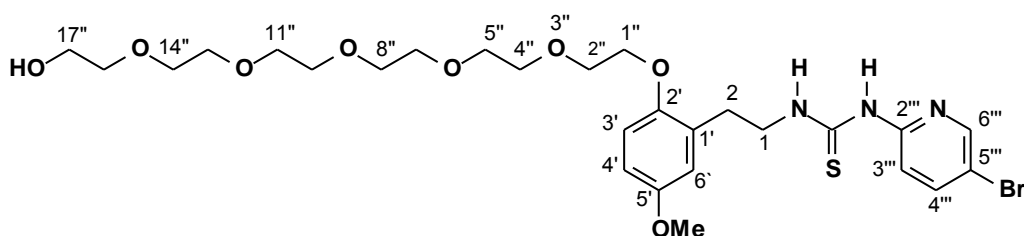
68.3 (CH₂O), 61.8 (C-5''), 55.5 (OCH₃), 45.7 (C-1), 29.9 (C-2); HRMS (ES): *m/z* found (M⁺ + H), 470.0749 C₁₉H₂₅BrN₃O₄S requires (M⁺ + H) 470.0741.

***N*-(5-Bromo-2-pyridinyl)]-*N'*-{2-[2-(2-(2-(2-(2-hydroxyethoxy)ethoxy)ethoxy)ethoxy)ethoxy)-5-methoxyphenyl]ethyl}-thiourea (77p)**



Using THF/ rt, gave compound **77p** (110 mg, 63 %); mp: 44-45 °C; IR (CHCl₃): ν_{\max} 3616, 3413 (NH, OH), 3007, 2935 (C-H), 1501 (C=C), 1469 (C=S), 1227 (C-N) cm⁻¹; ¹H NMR (400 MHz, CDCl₃): δ 10.51 (1H, brs, NH), 8.89 (1H, brs, NH), 8.06 (1H, d, *J* = 2.4 Hz, H-6'''), 7.67 (1H, dd, *J* = 2.4, 8.8 Hz, H-4'''), 6.80 (1H, d, *J* = 2.8 Hz, H-6'), 6.78 (1H, d, *J* = 8.8 Hz, H-3'), 6.74 (1H, dd, *J* = 2.8, 8.8 Hz, H-4'), 6.72 (1H, d, *J* = 8.8 Hz, H-3'''), 4.04 (4H, m, H-1'', H-1), 3.84 (2H, t, *J* = 4.8 Hz, CH₂O), 3.76 (3H, s, OCH₃), 3.74-3.69 (10H, m, 5 × CH₂O), 3.62 (2H, m, CH₂O), 2.99 (2H, t, *J* = 6.6 Hz, H-2), 2.98 (1H, brs, OH); ¹³C NMR (100 MHz, CDCl₃): δ 179.1 (C=S), 153.6 (C-5'), 151.7 (C-2'''), 151.2 (C-2'), 146.6 (C-6'''), 141.0 (C-4'''), 128.8 (C-1), 117.6 (C-6'), 113.4 (C-3'), 112.8 (C-3'''), 112.5 (C-5'''), 111.5 (C-4'), 72.5 (C-1''), 70.8 (CH₂O), 70.6 (2 × CH₂O), 70.3 (CH₂O), 69.9 (CH₂O), 68.4 (CH₂O), 61.7 (C-11''), 55.5 (OCH₃), 45.8 (C-1), 29.9 (C-2); HRMS (ES): *m/z* found (M⁺ + H), 558.1273 C₂₃H₃₃BrN₃O₆S requires (M⁺ + H) 558.1296.

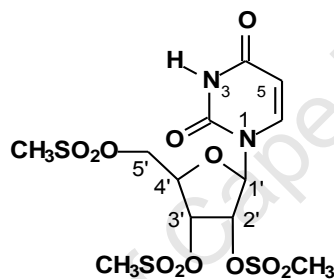
***N*-(5-Bromo-2-pyridinyl)]-*N'*-{2-[2-(2-(2-(2-(2-(2-hydroxyethoxy)ethoxy)ethoxy)ethoxy)ethoxy)ethoxy)-5-methoxyphenyl]ethyl}-thiourea (77q)**



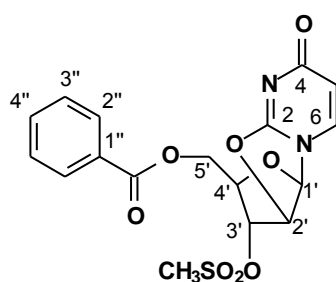
Using THF/ rt, gave compound **77q** as a colourless oil (33 mg, 52%); IR (CHCl₃): ν_{\max} 3652, 3413 (NH, OH), 3007, 2913 (C-H), 1501 (C=C), 1469 (C=S), 1227 (C-N) cm⁻¹; ¹H NMR (300

MHz, CDCl₃): δ 11.07 (1H, t, *J* = 4.7 Hz, NH), 8.56 (1H, brs, NH), 8.04 (1H, d, *J* = 2.4 Hz, H-6''), 7.67 (1H, dd, *J* = 2.4, 8.8 Hz, H-4''), 6.80 (1H, d, *J* = 2.9 Hz, H-6'), 6.78 (1H, d, *J* = 8.8 Hz, H-3'), 6.73 (1H, dd, *J* = 2.9, 8.8 Hz, H-4'), 6.67 (1H, d, *J* = 8.8 Hz, H-3''), 4.02 (4H, m, H-1'', H-1), 3.82 (2H, t, *J* = 4.9 Hz, CH₂O), 3.75 (3H, s, OCH₃), 3.71-3.58 (20H, m, 10 × CH₂O), 2.98 (2H, t, *J* = 6.5 Hz, H-2), 2.90 (1H, brs, OH); ¹³C NMR (75 MHz, CDCl₃): δ 179.3 (C=S), 153.6 (C-5'), 151.6 (C-2''), 151.3 (C-2'), 146.7 (C-6''), 141.0 (C-4''), 128.8 (C-1'), 117.5 (C-6'), 113.3 (C-3'), 112.7 (C-3''), 112.6 (C-5''), 111.5 (C-4'), 72.6 (C-1''), 70.8 (CH₂O), 70.7 (2 × CH₂O), 70.6 (CH₂O), 70.5 (CH₂O), 70.3 (CH₂O), 69.9 (CH₂O), 69.7 (CH₂O), 68.6 (CH₂O), 68.4 (CH₂O), 61.7 (C-17''), 55.6 (OCH₃), 45.9 (C-1), 29.8 (C-2); HRMS (ES): *m/z* found (*M*⁺ + H), 646.1799 C₂₇H₄₁BrN₃O₈S requires (*M*⁺ + H) 646.1798.

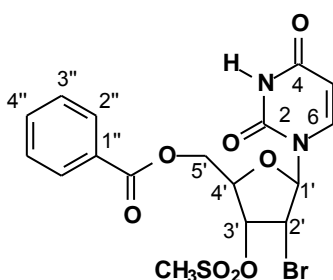
Uridine-2',3',5'-trimesylate (**109**)¹⁸¹



Methanesulfonyl chloride (28.54 mL, 368.58 mmol) was slowly added to a stirred solution of uridine (20.00 g, 81.90 mmol) in pyridine (120 mL) at 0 °C. The reaction was stirred for 5h at 0 °C. The reaction mixture was poured into an ice-water mixture (500 mL) with rapid stirring and the product precipitated. The precipitate was collected by filtration, washed with water (3 × 200 mL) and dried over P₂O₅ to give the product **109** as a white solid (39.11 g, 80%); mp: 180-183 °C; (lit. 184-186 °C); ¹H NMR (400 MHz, DMSO-d₆): δ 11.51 (1H, brs, NH), 7.70 (1H, d, *J* = 8.4 Hz, H-6), 5.98 (1H, d, *J* = 5.6 Hz, H-1'), 5.69 (1H, d, *J* = 8.4 Hz, H-5), 5.61 (1H, t, *J* = 5.6 Hz, H-2'), 5.35 (1H, t, *J* = 5.6 Hz, H-3'), 4.56 (1H, m, H-4'), 4.46 (2H, m, H-5'), 3.35 (3H, s, O₃SCH₃), 3.33 (3H, s, O₃SCH₃), 3.22 (3H, s, O₃SCH₃); ¹³C NMR (100 MHz, DMSO-d₆): δ 163.0 (C-4), 150.3 (C-2), 141.5 (C-6), 102.4 (C-5), 88.6 (C-1'), 78.5 (C-4'), 76.0 (C-2'), 74.0 (C-3'), 67.3 (C-5'), 38.0 (O₃SCH₃), 37.9 (O₃SCH₃), 36.9 (O₃SCH₃).

5'-O-Benzoyl-3'-O-methanesulfonyl-2,2'-anhydrouridine (110)¹⁸¹

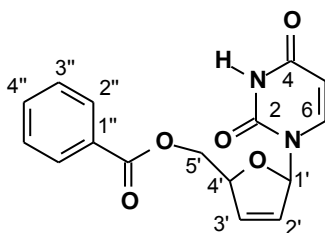
Trimesylate **109** (38.80 g, 81.10 mmol) was added to a stirred slurry of sodium benzoate (40.88 g, 283.86 mmol) in acetamide (180 g). The reaction was stirred at 132 °C for 2 h. The reaction mixture was poured into ice-water (500 mL) with rapid stirring and the product precipitated. The precipitate was collected by filtration, washed with water (3 × 200 mL) and dried over P₂O₅ to give the product **110** as a white solid (25.64 g, 77%); mp: 218-219 °C, (lit. 226-227 °C); ¹H NMR (400 MHz, DMSO-d₆): δ 7.89 (3H, m, H-2'', H-6'', H-6), 7.64 (1H, m, H-4''), 7.50 (2H, t, *J* = 7.6 Hz, H-3'', H-5''), 6.45 (1H, d, *J* = 5.6 Hz, H-1'), 5.86 (1H, d, *J* = 7.6 Hz, H-5), 5.69 (1H, d, *J* = 5.6 Hz, H-2'), 5.63 (1H, d, *J* = 2.8 Hz, H-3'), 4.78 (1H, m, H-4'), 4.32 (1H, dd, *J* = 5.0, 12.3 Hz, H-5'), 4.22 (1H, dd, *J* = 7.2, 12.3 Hz, H-5''), 3.43 (3H, s, O₃SCH₃); ¹³C NMR (100 MHz, DMSO-d₆): δ 170.5 (C=O), 165.1 (C-4), 159.1 (C-2), 136.5 (C-6), 133.5 (C-4''), 129.2 (C-2'', C-6''), 128.9 (C-1''), 128.7 (C-3'', C-5''), 109.0 (C-5), 89.6 (C-1'), 86.0 (C-2'), 82.1 (C-4'), 80.9 (C-3'), 62.5 (C-5'), 37.5 (O₃SCH₃).

5'-O-Benzoyl-2'-bromo-3'-O-methanesulfonyl-2'-deoxyuridine (111)¹⁸²

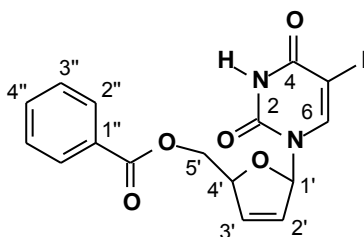
Acetyl bromide (18.46 mL, 249.72 mmol) was added to a stirring solution of 5'-benzoyl-3'-O-methanesulfonyl-2,2'-anhydrouridine **110** (25.49 g, 62.43 mmol) in EtOAc (90 mL) and MeOH (10 mL). The reaction mixture was refluxed at 80 °C for 1 h and then the solvent was reduced under vacuum. The crude residue was diluted with aq. NaHCO₃ (200 mL) and extracted with EtOAc (3 × 250 mL). The organic layer was dried over MgSO₄ and the solvent reduced under vacuum. Purification by chromatography using a silica-gel column employing EtOAc / pet ether (7 / 3) afforded compound **111** as a white solid (26.22 g, 86%); mp. 52-58 °C, (lit. 90-

140 °C); ^1H NMR (400 MHz, CDCl_3): δ 9.78 (1H, brs, NH), 8.02 (2H, d, $J = 7.5$ Hz, H-2'', H-6''), 7.61 (1H, d, $J = 7.5$ Hz, H-4''), 7.47 (2H, t, $J = 7.5$ Hz, H-3'', H-5''), 7.34 (1H, d, $J = 8.2$ Hz, H-6), 6.13 (1H, d, $J = 5.6$ Hz, H-1'), 5.62 (1H, d, $J = 8.2$ Hz, H-5), 5.29 (1H, t, $J = 5.3$ Hz, H-3'), 4.77 (1H, d, $J = 5.3$ Hz, H-2'), 4.74-4.61 (3H, m, H-4', H-5'), 3.19 (3H, s, O_3SCH_3); ^{13}C NMR (100 MHz, CDCl_3): δ 165.9 (C=O), 163.0 (C-4), 150.0 (C-2), 139.7 (C-6), 133.7 (C-4''), 129.6 (C-2'', C-6''), 129.0 (C-1''), 128.7 (C-3'', C-5''), 103.4 (C-5), 91.8 (C-1'), 80.6 (C-4'), 75.7 (C-3'), 62.2 (C-5'), 47.5 (C-2'), 38.7 (O_3SCH_3).

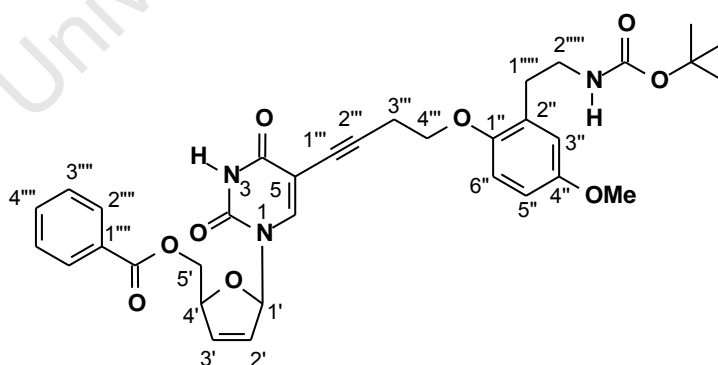
5'-Benzoyl-2',3'-didehydro-2',3'-dideoxyuridine (**112**)^{158c}



To a solution of 5'-O-benzoyl-2'-bromo-3'-O-methanesulfonyl-2'-deoxyuridine **111** (20.17 g, 41.22 mmol) in MeOH (120 mL), was added zinc dust (8.09 g, 123.66 mmol) followed by addition of conc HCl (2 mL). The reaction mixture was stirred at room temperature for 15 min. The excess zinc was then removed by filtration through celite and the solvent reduced under vacuum. The crude residue was diluted with NaHCO_3 (200 mL) and the product extracted with EtOAc (3 x 250 mL). The organic layer was dried over MgSO_4 , filtered and the solvent was removed under reduced pressure to afford pure compound **112** as a white solid (11.82 g, 91%): mp: 135-138 °C; (lit. 138.5-139 °C); ^1H NMR (300 MHz, CDCl_3): δ 9.61 (1H, brs, NH), 7.97 (2H, d, $J = 7.4$ Hz, H-2'', H-6''), 7.58 (1H, m, H-4''), 7.45 (2H, t, $J = 7.4$ Hz, H-3'', H-5''), 7.33 (1H, d, $J = 8.2$ Hz, H-6), 7.00 (1H, m, H-1'), 6.37 (1H, dt, $J = 1.7, 6.2$ Hz, H-3'), 5.88 (1H, dq, $J = 1.5, 6.2$ Hz, H-2'), 5.32 (1H, d, $J = 8.2$ Hz, H-5), 5.14 (1H, m, H-4'), 4.68 (1H, dd, $J = 3.5, 12.5$ Hz, H-5'), 4.52 (1H, dd, $J = 2.9, 12.5$ Hz, H-5'); ^{13}C NMR (75 MHz, CDCl_3): δ 166.0 (C=O), 163.3 (C-4), 150.7 (C-2), 139.8 (C-6), 133.5 (C-4''), 133.5 (C-3'), 129.5 (C-2'', C-6''), 129.2 (C-1''), 128.6 (C-3'', C-5''), 127.1 (C-2'), 102.6 (C-5), 89.7 (C-1'), 84.8 (C-4') 64.6 (C-5').

5'-Benzoyl-2',3'-didehydro-2',3'-dideoxy-5-iodouridine (47)¹⁴²

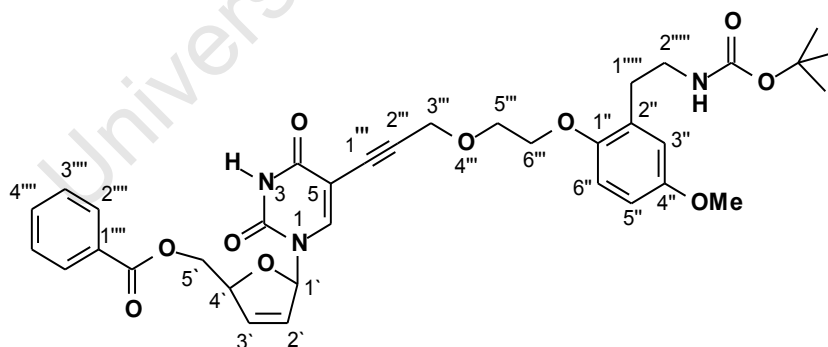
To a solution of 5'-O-benzoyl-2'-bromo-3'-O-methanesulfonyl-2'-deoxyuridine **112** (2.00 g, 6.36 mmol) in CH₃CN (30 mL), were added cerium ammonium (IV) nitrate (1.74 g, 3.18 mmol) and iodine (0.49 g, 1.93 mmol). The mixture was stirred at 35 °C for 4 h. The crude residue was diluted with a solution of sodium thiocyanate (100 mL) and extracted with EtOAc (3 x 200 mL). The organic layer was dried over MgSO₄ and the solvent reduced under vacuum. Purification by chromatography using a silica-gel column using EtOAc / pet ether (6 / 4) gave compound **47** as a white solid (2.30 g, 82%); mp: 168-170 °C; ¹H NMR (300 MHz, CDCl₃): δ 11.78 (1H, brs, NH), 7.96 (2H, d, *J* = 7.9 Hz, H-2'', H-6''), 7.73 (1H, s, H-6), 7.67 (1H, m, H-4''), 7.55 (2H, t, *J* = 7.9 Hz, H-3'', H-5''), 6.76 (1H, m, H-1'), 6.54 (1H, dt, *J* = 1.7, 6.0 Hz, H-3'), 6.12 (1H, dq, *J* = 1.5, 6.0 Hz, H-2'), 5.18 (1H, m, H-4'), 4.52 (2H, m, H-5'); ¹³C NMR (75 MHz, CDCl₃): δ 165.5 (C=O), 160.2 (C-4), 150.1 (C-2), 144.0 (C-6), 133.5 (C-4''), 133.3 (C-3'), 129.2 (C-2'', C-6''), 129.0 (C-1''), 128.7 (C-3'', C-5''), 126.5 (C-2'), 90.0 (C-1'), 84.0 (C-4'), 69.6 (C-5), 65.3 (C-5').

5-{4-[2-(2-*tert*-Butoxycarbonylaminoethyl)-4-methoxyphenoxy]but-1-ynyl}-5'-O-benzoyl-2',3'-didehydro-2',3'-dideoxyuridine (48)

A solution of 5'-benzoyl-5-iodouridine **47** (70 mg, 0.20 mmol) in dry DMF (2.5 mL) was added to a stirred solution of triethylamine (0.05 mL, 0.30 mmol) and alkyne **70c** (0.10 g, 0.30 mmol) in THF (4 mL). The mixture was thoroughly degassed with nitrogen for 1h. CuI (20 mg, 0.10 mmol) and Pd(PPh₃)₄ (20 mg, 0.02 mmol) were added to the degassed solution under a nitrogen atmosphere. The mixture was left stirring at rt for 4h. The crude mixture was

dissolved in CHCl_3 (20 mL) which was washed with portions (2 x 15 mL) of 5% aq disodium EDTA, water (15 mL) and dried over MgSO_4 . Following filtration and solvent evaporation under reduced pressure, the crude product was purified by column chromatography employing 50% EtOAc in pet ether to give **48** as a yellow oil (95 mg, 94%): $[\alpha]_D -14.4^\circ$ (c 1.60, CHCl_3); IR (CHCl_3): ν_{max} 3692, 3606, 3451 (NH), 3011, 2934 (C-H), 2243 ($\text{C}\equiv\text{C}$), 1707 (C=O), 1502 (C=C) cm^{-1} ; ^1H NMR (300 MHz, CDCl_3): δ 8.79 (1H, brs, NH), 8.00 (2H, d, $J = 7.7$ Hz, H-2''', H-6'''), 7.61 (1H, s, H-6), 7.53 (1H, t, $J = 7.7$ Hz, H-4'''), 7.42 (2H, t, $J = 7.7$ Hz, H-3''', H-5'''), 6.91 (1H, m, H-1'), 6.70 (3H, m, H-3'', H-5'', H-6''), 6.39 (1H, dt, $J = 1.7, 5.8$ Hz, H-3'), 5.99 (1H, dq, $J = 1.4, 5.8$ Hz, H-2'), 5.20 (1H, m, H-4'), 4.83 (1H, brs, NH), 4.64 (1H, dd, $J = 4.3, 12.5$ Hz, H-5'), 4.50 (1H, dd, $J = 3.0, 12.5$ Hz, H-5'), 3.94 (2H, t, $J = 6.8$ Hz, H-4'''), 3.74 (3H, s, OCH_3), 3.32 (2H, m, H-2''''), 2.77 (2H, t, $J = 6.9$ Hz, H-1''''), 2.68 (2H, t, $J = 6.8$ Hz, H-3'''), 1.40 (9H, s, $\text{OC}(\text{CH}_3)_3$); ^{13}C NMR (75 MHz, CDCl_3): δ 166.2 (PhCO_2), 161.4 (C-4), 153.9 (NHCO), 153.9 (C-4''), 150.5 (C-1''), 149.4 (C-2), 141.6 (C-6), 133.5 (C-4'''), 133.3 (C-3'), 132.0 (C-1''), 129.7 (C-2'', C-6''), 129.2 (C-2''), 128.6 (C-3'', C-5''), 127.0 (C-2'), 116.7 (C-3''), 112.9 (C-6''), 112.0 (C-5''), 100.7 (C-2''), 91.3 (C-1''), 90.7 (C-1'), 85.0 (C-4'), 78.8 ($\text{O}_2\text{C}(\text{CH}_3)_3$), 72.4 (C-5), 66.7 (C-4'''), 65.1 (C-5'), 55.6 (OCH_3), 40.6 (C-2''''), 31.0 (C-1''''), 28.4 ($\text{OC}(\text{CH}_3)_3$), 20.8 (C-3'''); FABHRMS: m/z found 654.24300 $[\text{M}+\text{Na}]^+$. $\text{C}_{34}\text{H}_{37}\text{N}_3\text{O}_9$ $[\text{M}+\text{Na}]^+$ requires 654.24274.

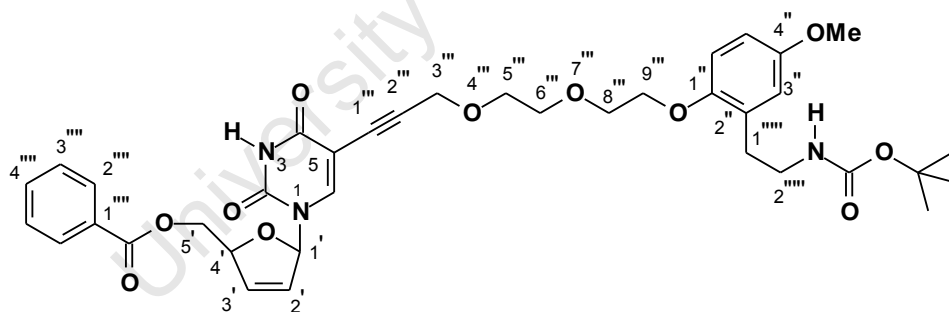
5-{6-[2-(2-*tert*-Butoxycarbonylaminoethyl)-4-methoxyphenoxy]hexa-4-oxa-1-ynyl}-5'-O-benzoyl-2', 3'-didehydro-2', 3'-dideoxyuridine (113)



A solution of 5'-O-Benzoyl-2',3'-didehydro-2',3'-dideoxy-5-iodouridine **47** (0.30 g, 0.68 mmol) in dry DMF (3 mL) was added to a stirred solution of triethylamine (0.19 mL, 1.36 mmol) and alkyne **70k** (0.26 g, 0.75 mmol) in THF (4 mL). The mixture was thoroughly degassed with nitrogen for 1h. CuI (65 mg, 0.34 mmol) and $\text{Pd}(\text{PPh}_3)_4$ (79 mg, 0.07 mmol) were added to the degassed solution under a nitrogen atmosphere. The mixture was left stirring at rt for 4h. The crude was dissolved in CHCl_3 (30 mL) which was washed with portions (2 x 15 mL) of 5% aq disodium EDTA, water (20 mL) and dried over MgSO_4 . Following filtration and solvent

evaporation under reduced pressure, the crude product was purified by column chromatography employing 60% EtOAc in pet ether to give **113** as a yellow oil (0.34 g, 76%): $[\alpha]_D +16.2^\circ$ (c 1.0, CHCl_3); IR (CHCl_3): ν_{max} 3449, 3384 (NH), 3007, 2928 (C-H), 2246 ($\text{C}\equiv\text{C}$), 1711 (C=O), 1501 (C=C), 1169 (C-N) cm^{-1} ; ^1H NMR (300 MHz, CDCl_3): δ 8.42 (1H, brs, NH), 8.01 (2H, d, $J = 7.5$ Hz, H-2''', H-6'''), 7.68 (1H, s, H-6), 7.56 (1H, m, H-4'''), 7.45 (2H, t, $J = 7.5$ Hz, H-3''', H-5'''), 6.92 (1H, m, H-1'), 6.76 (1H, d, $J = 8.7$ Hz, H-6''), 6.68 (2H, m, H-3'', H-5''), 6.40 (1H, dt, $J = 1.7, 6.0$ Hz, H-3'), 6.00 (1H, dq, $J = 1.3, 6.0$ Hz, H-2'), 5.21 (1H, m, H-4'), 4.94 (1H, brs, NH), 4.69 (1H, dd, $J = 4.2, 12.5$ Hz, H-5'), 4.50 (1H, dd, $J = 3.0, 12.5$ Hz, H-5'), 4.27 (2H, s, H-3'''), 4.07 (2H, t, $J = 4.5$ Hz, H-6'''), 3.85 (2H, m, H-5'''), 3.74 (3H, s, OCH_3), 3.33 (2H, m, H-2'''''), 2.78 (2H, t, $J = 6.9$ Hz, H-1'''''), 1.42 (9H, s, $\text{OC}(\text{CH}_3)_3$); ^{13}C NMR (75 MHz, CDCl_3): δ 166.2 ($\text{C}_6\text{H}_5\text{OCO}$), 161.3 (C-4), 156.0 (NHCO), 153.8 (C-4''), 151.0 (C-1''), 149.4 (C-2), 142.2 (C-6), 133.6 (C-4'''), 133.5 (C-3'), 129.7 (C-2''', C-6'''), 129.3 (C-1'''), 129.2 (C-2''), 128.6 (C-3''', C-5'''), 127.0 (C-2'), 116.5 (C-3''), 113.0 (C-6''), 111.9 (C-5''), 99.9 (C-2''), 90.8 (C-1'), 90.0 (C-1'''), 85.1 (C-4'), 78.8 ($\text{OC}(\text{CH}_3)_3$), 77.2 (C-5), 68.4 (OCH_2), 68.2 (OCH_2), 65.0 (C-5'), 59.0 (C-3''), 55.6 (OCH_3), 40.6 (C-2'''''), 30.8 (C-1'''''), 28.4 ($\text{OC}(\text{CH}_3)_3$); HRMS (ES): m/z found 662.2698 ($\text{M}^+ + 2\text{H}$), $\text{C}_{35}\text{H}_{40}\text{N}_3\text{O}_{10}$ requires ($\text{M}^+ + 2\text{H}$) 662.2714.

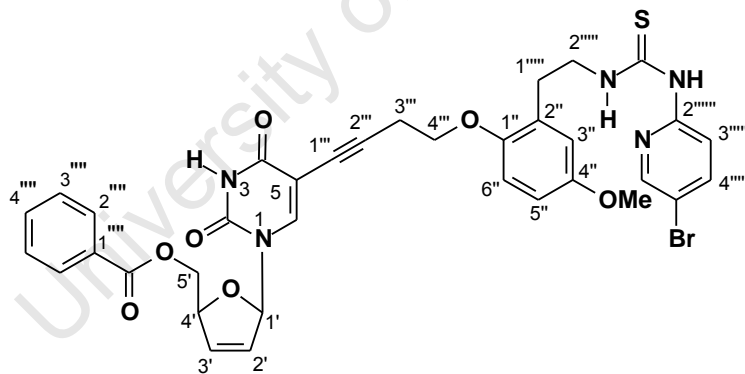
5-{9-[2-(2-*tert*-Butoxycarbonylaminoethyl)-4-methoxyphenoxy]nona-4, 7-dioxo-1-ynyl}-5'-O-benzoyl-2', 3'-didehydro-2', 3'-dideoxyuridine (**115**)



A solution of 5'-O-Benzoyl-2',3'-didehydro-2',3'-dideoxy-5-iodouridine **47** (0.20 g, 0.46 mmol) in dry DMF (2 mL) was added to stirred solution of triethylamine (0.13 mL, 0.92 mmol) alkyne **70I** (0.20 g, 0.51 mmol) in THF (3 mL). The mixture was thoroughly degassed with nitrogen for 1h. CuI (44 mg, 0.23 mmol) and $\text{Pd}(\text{PPh}_3)_4$ (53 mg, 0.05 mmol) were added to the degassed solution under a nitrogen atmosphere. The mixture was left stirring at rt for 4h. The crude was dissolved in CHCl_3 (20 mL) which was washed with portions of (2 x 10 mL) 5% aq disodium EDTA, water (15 mL) and dried over MgSO_4 . Filtration and solvent removal under reduced pressure gave a crude product, which was purified by column chromatography employing EtOAc in pet ether (7 / 3) to give compound **115** as a yellow oil (0.23 g, 72%): $[\alpha]_D$

+32.1 ° (c 1.0, CHCl₃); IR (CHCl₃): ν_{\max} 3674, 3377 (NH), 3014 (C-H), 2225 (C≡C), 1711 (C=O), 1501 (C=C), 1212 (C-N) cm⁻¹; ¹H NMR (400 MHz, CDCl₃): δ 8.82 (1H, brs, NH), 8.02 (2H, d, *J* = 7.6 Hz, H-2''', H-6'''), 7.68 (1H, s, H-6), 7.56 (1H, m, H-4'''), 7.46 (2H, t, *J* = 7.6 Hz, H-3''', H-5'''), 6.92 (1H, m, H-1'), 6.77 (1H, d, *J* = 8.8 Hz, H-6''), 6.69 (2H, m, H-3'', H-5''), 6.39 (1H, dt, *J* = 1.5, 6.0 Hz, H-3'), 5.99 (1H, dq, *J* = 1.3, 6.0 Hz, H-2'), 5.21 (1H, m, H-4'), 4.97 (1H, brs, NH), 4.70 (1H, dd, *J* = 4.2, 12.4 Hz, H-5'), 4.51 (1H, dd, *J* = 2.9, 12.4 Hz, H-5''), 4.25 (2H, s, H-3'''), 4.08 (2H, t, *J* = 4.9 Hz, H-9'''), 3.84 (2H, t, *J* = 4.9 Hz, H-8'''), 3.75 (3H, m, OCH₃), 3.73 (4H, m, 2 × OCH₂), 3.35 (2H, m, H-2'''''), 2.80 (2H, t, *J* = 6.9 Hz, H-1'''''), 1.43 (9H, s, OC(CH₃)₃); ¹³C NMR (75 MHz, CDCl₃): δ 166.2 (PhOCO), 161.1 (C-4), 156.0 (NHCO), 153.7 (C-4''), 151.0 (C-1''), 149.4 (C-2), 142.2 (C-6), 133.5 (C-4'''), 133.4 (C-3'), 129.7 (C-2''', C-6'''), 129.3 (C-1'''), 129.2 (C-2''), 128.6 (C-3''', C-5'''), 127.0 (C-2'), 116.5 (C-3''), 113.0 (C-6''), 112.0 (C-5''), 99.9 (C-2'''), 90.7 (C-1'), 90.1 (C-1'''), 85.1 (C-4'), 78.9 (OC(CH₃)₃), 77.2 (C-5), 70.5 (OCH₂), 69.8 (OCH₂), 69.1 (OCH₂), 68.4 (OCH₂), 65.0 (C-5'), 58.9 (C-3'''), 55.6 (OCH₃), 40.6 (C-2'''''), 31.0 (C-1'''''), 28.4 (OC(CH₃)₃); HRMS (ES): *m/z* found 706.2958 (M⁺ + H), C₃₇H₄₄N₃O₁₁ requires (M⁺ + H) 706.2976.

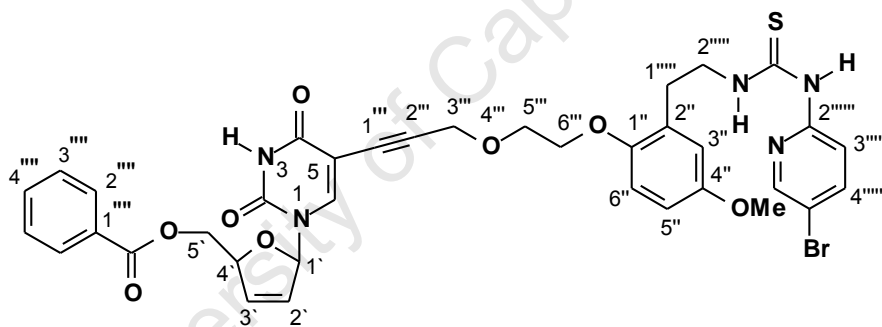
5-{4-[2-(2-(5-Bromo-2-pyridinyl)amino thiocarbonylamino)ethyl]-4-methoxyphenoxy]but-1-ynyl}-5'-O-benzoyl-2',3'-dideoxy-2',3'-dideoxyuridine (50)



Trifluoroacetic acid (0.20 mL) was added to a solution of compound **48** (0.10 g, 0.16 mmol) in CH₂Cl₂ (3 mL) at 0 °C, and the solution stirred for 2 h. Diisopropylethylamine (0.30 mL) was added, the solvent evaporated *in vacuo* and the crude amine dried under vacuum for 1 h. Thiourea **49** (0.54 mg, 0.19 mmol) was added to the crude amine in THF (5 mL) and the reaction mixture was stirred at room temperature for 20 h. Following evaporation of the solvent, the residue was subjected directly to column chromatography using (70% EtOAc in pet ether) to give **50** as a yellow solid (72 mg, 60%): mp: 95-97 °C; [α]_D - 9.9 ° (c 0.8, CHCl₃); IR (CHCl₃): ν_{\max} 3934, 3681 (NH), 2297 (C≡C), 1714 (C=O), 1602 (C=C), 1418 (C=S), 1212 (C-N) cm⁻¹; ¹H NMR (400 MHz, CDCl₃): δ 10.92 (1H, t, *J* = 2.7 Hz, NH), 9.75 (1H, brs, NH),

9.13 (1H, s, NH), 8.03 (2H, m, H-2''', H-6'''), 7.91 (1H, d, $J = 2.3$ Hz, H-6'''''), 7.61 (1H, s, H-6), 7.56 (1H, m, H-4''), 7.45 (2H, m, H-3''', H-5'''), 7.28 (1H, dd, $J = 2.3, 8.8$ Hz, H-4'''''), 6.96 (1H, m, H-1'), 6.80 (1H, m, H-3''), 6.76 (2H, m, H-5'', H-6''), 6.62 (1H, d, $J = 8.8$ Hz, H-3'''''), 6.37 (1H, dt, $J = 1.6, 6.0$ Hz, H-3'), 6.09 (1H, m, H-2'), 5.19 (1H, m, H-4'), 4.65 (1H, dd, $J = 4.2, 12.3$ Hz, H-5'), 4.53 (1H, dd, $J = 3.8, 12.3$ Hz, H-5'), 3.97 (4H, m, H-4''', H-2'''''), 3.79 (3H, s, OCH₃), 3.03 (1H, m, H-3'''), 2.88 (1H, m, H-3'''), 2.71 (2H, t, $J = 6.3$ Hz, H-1'''''); ¹³C NMR (100 MHz, CDCl₃): δ 179.1 (C=S), 162.2 (C-4), 153.6 (C-2'''''), 151.6 (C-1''), 150.9 (C-4''), 149.3 (C-2), 141.8 (C-6'''''), 141.2 (C-6), 140.6 (C-4'''''), 133.3 (C-4'''), 133.3 (C-3'), 129.7 (C-2''', C-6'''), 129.3 (C-1'''), 128.9 (C-2''), 128.6 (C-3''', C-5'''), 127.7 (C-2'), 118.3 (C-3''), 113.3 (C-3'''''), 112.0 (C-6''), 111.1 (C-5'''''), 100.6 (C-2''), 91.3 (C-1''), 90.7 (C-1'), 84.9 (C-4'), 72.6 (C-5), 66.5 (C-4'''), 65.3 (C-5'), 55.5 (OCH₃), 45.4 (C-2'''''), 30.3 (C-3'''), 20.9 (C-1'''''); HRMS (ES): m/z found 746.1262 ($M^+ + H$), C₃₅H₃₃N₅O₇BrS requires ($M^+ + H$) 746.1284.

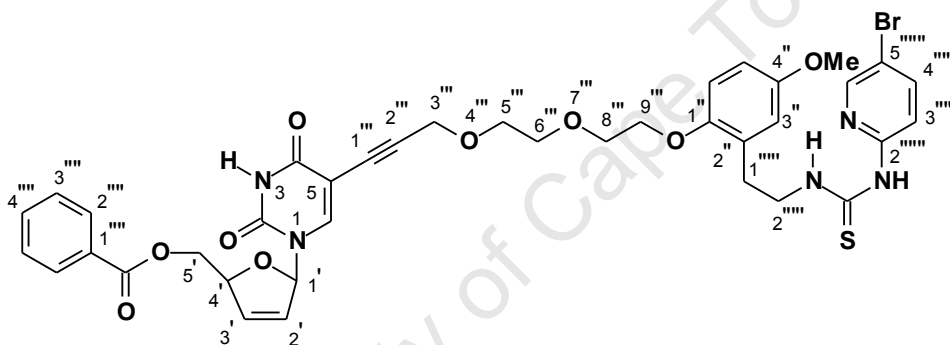
5-{6-[2-(2-(5-Bromo-2-pyridinylaminothiocarbonylamino)ethyl)-4-methoxyphenoxy]hexa-4-oxa-1-ynyl}-5'-O-benzoyl-2',3'-dideoxyuridine (114)



Trifluoroacetic acid (0.20 mL) was added to a solution of compound **113** (0.20 g, 0.30 mmol) in CH₂Cl₂ (3 mL) at 0 °C, and the solution stirred for 2 h. Diisopropylethylamine (0.30 mL) was added, the solvent evaporated *in vacuo* and the crude amine dried under vacuum for 1 h. Thiourea **49** (0.11 g, 0.39 mmol) was added to the crude amine in THF (5 mL) and the reaction mixture was stirred at room temperature for 20 h. Following evaporation of the solvent, the residue was subjected directly to column chromatography using (70% EtOAc in pet ether) to give **114** as a yellow solid (0.13 g, 60%): mp: 73-76 °C; [α]_D - 20.2 ° (c 1.0, CHCl₃); IR (CHCl₃): ν_{\max} 3601, 3391 (NH), 2957 (C-H), 2254 (-C≡C-), 1718 (C=O), 1501 (C=C), 1462 (C=S) cm⁻¹; ¹H NMR (300 MHz, CDCl₃): δ 10.82 (1H, m, NH), 9.00 (1H, brs, NH), 8.84 (1H, brs, NH), 8.03 (1H, d, $J = 2.4$ Hz, H-6'''''), 8.00 (2H, m, H-2''', H-6'''), 7.70 (1H, s, H-6), 7.65 (1H, dd, $J = 2.4, 8.8$ Hz, H-4'''''), 7.56 (1H, m, H-4'''), 7.45 (2H, m, H-3''', H-5'''), 6.93 (1H, m, H-1'), 6.87 (1H, d, $J = 8.8$ Hz, H-3'''''), 6.79 (1H, d, $J = 2.8$ Hz, H-3''), 6.77 (1H, d, $J = 8.8$ Hz, H-6''), 6.73 (1H, dd, $J = 2.8, 8.8$ Hz, H-5''), 6.40 (1H, dt, $J = 1.7, 6.0$ Hz, H-3'), 6.02 (1H, dq, $J = 1.4, 6.0$ Hz, H-2'), 5.21 (1H, m, H-4'), 4.68 (1H, dd, $J = 4.3, 12.5$ Hz, H-5'),

4.54 (1H, dd, $J = 2.9, 12.5$ Hz, H-5'), 4.25 (2H, s, H-3'''), 4.00 (4H, m, H-2''''', H-6'''''), 3.83 (2H, m, H-5'''), 3.75 (3H, s, OCH₃), 2.98 (2H, m, H-1'''''); ¹³C NMR (100 MHz, CDCl₃): δ 179.2 (C=S), 166.3 (PhCO₂), 161.6 (C-4), 153.7 (C-4''), 151.8 (C-2'''''), 151.2 (C-1''), 149.4 (C-2), 146.6 (C-6'''''), 142.6 (C-6), 141.0 (C-4'''''), 133.6 (C-4'''''), 133.4 (C-3'), 129.7 (C-2''', C-6'''''), 129.2 (C-1'''), 128.9 (C-2''), 128.7 (C-3''', C-5'''), 127.0 (C-2'), 117.5 (C-3''), 113.6 (C-3'''''), 112.8 (C-6''), 112.5 (C-5'''''), 111.6 (C-5''), 100.0 (C-2''), 90.9 (C-1'), 90.0 (C-1'''), 85.2 (C-4'), 77.2 (C-5), 68.5 (OCH₂), 68.3 (OCH₂), 65.1 (C-5'), 59.2 (C-3'''), 55.6 (OCH₃), 45.7 (C-2'''''), 29.9 (C-1'''''); HRMS (ES): m/z found 776.1379 (M⁺ + H), C₃₆H₃₅N₅O₈SBr requires (M⁺ + H) 776.1390.

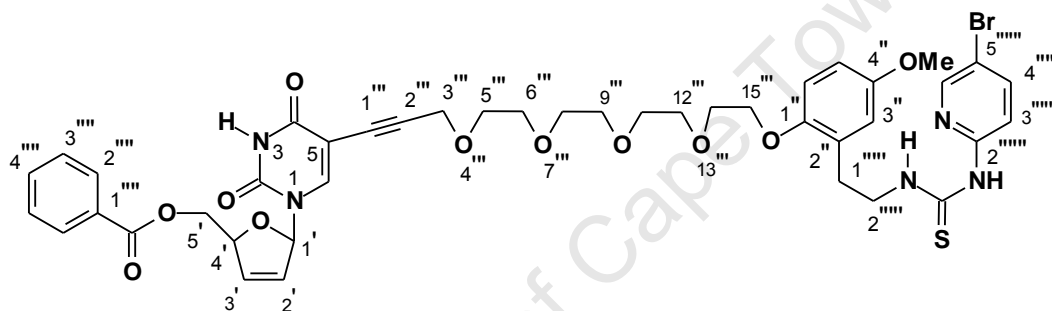
5-{9-[2-(2-(5-Bromo-2-pyridinylaminothiocarbonylamino)ethyl)-4-methoxyphenoxy]nona-4,7-dioxa-1-ynyl}-5'-O-benzoyl-2',3'-dideoxyuridine (116)



To a solution of compound **115** (0.15 g, 0.21 mmol) in CH₂Cl₂ (3 mL), trifluoroacetic acid (0.20 mL) was added at 0 °C, and the solution stirred for 2 h. Diisopropylethylamine (0.40 mL) was added, the solvent evaporated *in vacuo* and the crude amine dried under vacuum for 1 h. Thiourea **49** (76 mg, 0.27 mmol) was added to the crude amine in THF (5 mL) and the reaction mixture was stirred at room temperature for 20 h. Following evaporation of the solvent, the residue was subjected directly to column chromatography using EtOAc/ pet ether (8 / 2) to give **116** as a yellow solid (0.10 g, 63%): m.p: 88-91 °C; [α]_D -18.5 ° (c 1.0, CHCl₃); IR (CHCl₃): ν_{\max} 3406 (NH), 3029, 2949 (C-H), 2152 (-C≡C-), 1718, 1671 (C=O), 1501 (C=C), 1469 (C=S), 1126 (C-N) cm⁻¹; ¹H NMR (300 MHz, CDCl₃): δ 11.01 (1H, t, $J = 4.8$ Hz, NH), 9.29 (1H, brs, NH), 8.94 (1H, brs, NH), 8.04 (1H, d, $J = 2.4$ Hz, H-6'''''), 8.00 (2H, d, $J = 7.4$ Hz, H-2''', H-6'''''), 7.67 (1H, s, H-6), 7.65 (1H, dd, $J = 2.4, 8.8$ Hz, H-4'''''), 7.56 (1H, m, H-4'''''), 7.43 (2H, t, $J = 7.4$ Hz, H-3''', H-5'''''), 6.91 (1H, m, H-1'), 6.80 (1H, d, $J = 9.2$ Hz, H-6''), 6.79 (1H, d, $J = 2.9$ Hz, H-3''), 6.77 (1H, d, $J = 8.8$ Hz, H-3'''''), 6.73 (1H, dd, $J = 2.9, 9.2$ Hz, H-5'''), 6.38 (1H, dt, $J = 1.6, 6.0$ Hz, H-3'), 5.98 (1H, m, H-2'), 5.19 (1H, m, H-4'), 4.67 (1H, dd, $J = 4.3, 12.5$ Hz, H-5'), 4.50 (1H, dd, $J = 3.0, 12.5$ Hz, H-5'), 4.21 (2H, s, H-3'''), 4.03 (2H, t, $J = 4.7$ Hz, H-9'''), 3.98 (2H, q, $J = 6.6$ Hz, H-2'''''), 3.82 (2H, t, $J = 4.7$ Hz, H-8'''), 3.74 (3H, s,

OCH₃), 3.71-3.64 (4H, m, 2 × OCH₂), 2.97 (2H, t, *J* = 6.6 Hz, H-1'''''); ¹³C (75 MHz, CDCl₃): δ 179.2 (C=S), 166.2 (PhCO₂), 161.4 (C-4), 153.6 (C-4'''), 151.7 (C-2'''''), 151.2 (C-1'''), 149.5 (C-2), 146.6 (C-6'''''), 142.5 (C-6), 141.0 (C-4'''''), 133.5 (C-4'''''), 133.4 (C-3'''), 129.7 (C-2''''', C-6'''''), 129.2 (C-1'''''), 128.8 (C-2'''), 128.6 (C-3''''', C-5'''''), 127.0 (C-2'), 117.5 (C-3'''), 113.5 (C-3'''''), 112.7 (C-6'''), 112.5 (C-5'''''), 111.5 (C-5'''), 100.0 (C-2'''), 90.8 (C-1'), 90.1 (C-1'''), 85.1 (C-4'), 77.0 (C-5), 70.6 (OCH₂), 69.8 (OCH₂), 69.2 (OCH₂), 68.4 (OCH₂), 65.1 (C-5'), 59.0 (C-3'''), 55.5 (OCH₃), 45.6 (C-2'''''), 29.8 (C-1'''''); HRMS (ES): *m/z* found 820.1638 (M⁺ + H), C₃₈H₃₉N₅O₉SBr requires (M⁺ + H) 820.1652.

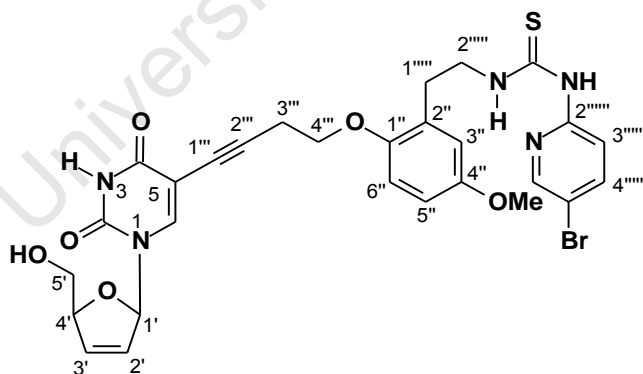
5-{15-[2-(2-(5-Bromo-2-pyridinylaminothiocarbonylamino)ethyl)-4-methoxyphenoxy]pentadeca-4,7,10,13-tetraoxa-1-ynyl}-5'-O-benzoyl-2',3'-dideoxy-2',3'-dideoxyuridine (119)



Trifluoroacetic acid (0.20 mL) was added to a solution of alkyne **70r** (0.12 g, 0.25 mmol) in CH₂Cl₂ (3 mL) at 0 °C, and the solution stirred for 2 h. Anhydrous K₂CO₃ (0.10 g, 0.75 mmol) was added, the mixture stirred for a further 15 min then filtered through Celite, the solvent evaporated *in vacuo* and the crude amine dried under vacuum for 1 h. The crude amine was dissolved in dry THF (4 mL), DMF (2 mL), and 5'-O-Benzoyl-2',3'-dideoxy-5-iodouridine **47** (0.10 g, 0.23 mmol) and triethylamine (0.06 mL, 0.46 mmol) were added. The mixture was thoroughly degassed with nitrogen for 1h. CuI (23 mg, 0.12 mmol) and Pd(PPh₃)₄ (27 mg, 0.02 mmol) were added to the degassed solution under a nitrogen atmosphere. The mixture was left stirring at rt for 4h. The reaction mixture was then dissolved in MeOH: CHCl₃ (1: 4) (30 mL), which was washed with portions (15 mL) of 5% aq disodium EDTA, water (10 mL) and dried over MgSO₄. Filtration and solvent removal under reduced pressure gave a crude product, which was subjected to column chromatography employing EtOAc / MeOH / Et₃N (5 / 4 / 1). The amine product was dissolved in dry THF (5 mL), thiourea **49** (85 mg, 0.30 mmol) was added and the mixture was stirred at room temperature for 20 h. Following evaporation of solvent, the residue was subjected directly to column chromatography using EtOAc / pet ether (9 / 1) to afford the title compound **119** as a solid (76 mg, 40% over the 3 steps):

m.p: 112-115 °C; $[\alpha]_D - 24.1^\circ$ (c 1.0, CHCl₃); IR (CHCl₃): ν_{\max} 3377, 3217 (NH), 3007, 2920 (C-H), 2239 (-C≡C-), 1722, 1675 (C=O), 1501 (C=C), 1465 (C=S), 1227 (C-N) cm⁻¹; ¹H NMR (400 MHz, CDCl₃): δ 11.09 (1H, t, *J* = 5.1 Hz, NH), 8.88 (1H, brs, NH), 8.76 (1H, brs, NH), 8.05 (1H, d, *J* = 2.4 Hz, H-6'''''), 8.02 (2H, d, *J* = 7.6 Hz, H-2''', H-6'''), 7.68 (1H, s, H-6), 7.68 (1H, dd, *J* = 2.4, 8.8 Hz, H-4'''''), 7.58 (1H, m, H-4'''), 7.46 (2H, t, *J* = 7.6 Hz, H-3''', H-5'''), 6.93 (1H, m, H-1') 6.81 (1H, d, *J* = 2.8 Hz, H-3''), 6.78 (1H, d, *J* = 8.8 Hz, H-6''), 6.75 (1H, dd, *J* = 2.8, 8.8 Hz, H-5''), 6.74 (1H, d, *J* = 8.8 Hz, H-3'''''), 6.41 (1H, dt, *J* = 1.7, 6.0 Hz, H-3'), 6.00 (1H, dq, *J* = 1.2, 6.0 Hz, H-2'), 5.22 (1H, m, H-4'), 4.70 (1H, dd, *J* = 4.2, 12.5 Hz, H-5'), 4.52 (1H, dd, *J* = 3.0, 12.5 Hz, H-5'), 4.21 (2H, s, H-3'''), 4.02 (4H, m, H-2''''', H-15'''), 3.83 (2H, t, *J* = 5.8 Hz, OCH₂), 3.77 (3H, s, OCH₃), 3.71-3.64 (12H, m, 6 × OCH₂), 2.99 (2H, t, *J* = 6.6 Hz, H-1'''''); ¹³C NMR (75 MHz, CDCl₃): δ 179.1 (C=S), 166.2 (PhOCO), 161.3 (C-4), 153.5 (C-4''), 151.8 (C-2'''''), 151.2 (C-1''), 149.5 (C-2), 146.4 (C-6'''''), 142.3 (C-6), 141.0 (C-4'''''), 133.5 (C-4'''), 133.4 (C-3'), 129.6 (C-2''', C-6'''), 129.1 (C-1'''), 128.8 (C-2''), 128.6 (C-3''', C-5'''), 126.9 (C-2'), 117.5 (C-3''), 113.6 (C-3'''''), 112.7 (C-6''), 112.4 (C-5'''''), 111.5 (C-5''), 100.0 (C-2'''), 90.7 (C-1'), 90.1 (C-1'''), 85.1 (C-4'), 76.9 (C-5), 70.8 (OCH₂), 70.6 (OCH₂), 70.5 (2 × OCH₂), 70.3 (OCH₂), 69.8 (OCH₂), 69.1 (OCH₂), 68.4 (OCH₂), 65.0 (C-5'), 58.9 (C-3'''), 55.5 (OCH₃), 45.7 (C-2'''''), 29.8 (C-1'''''); HRMS (ES): *m/z* found 908.2178 (M⁺ + H), C₄₂H₄₇N₅O₁₁SBr requires (M⁺ + H) 908.2176.

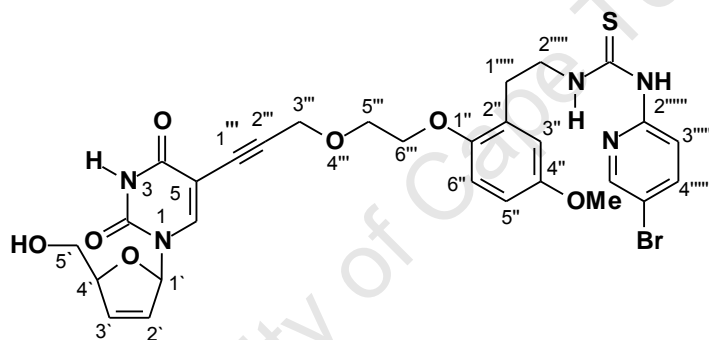
5-{4-[2-(2-(5-Bromo-2-pyridinylaminothiocarbonylamino)ethyl)-4-methoxyphenoxy]but-1-ynyl}-2',3'-dideoxyuridine (51)¹⁴²



A solution of NaOMe in methanol (0.01 mL, 2M, 0.01 mmol), was added to a solution of the nucleoside **50** (83 mg, 0.11 mmol) in MeOH (2 mL) at 0 °C. The mixture was stirred for 30 min, then acetic acid (0.05 mL) was added, and the crude mixture was diluted with CH₂Cl₂ (1 mL) and subjected to column chromatography employing MeOH/ CH₂Cl₂ (2 / 8) to give the title product **51** as a pale yellow solid (43 mg, 60%): mp: 121-122 °C; $[\alpha]_D +22.4^\circ$ (c 1.10, CHCl₃); IR (CHCl₃): ν_{\max} 3934, 3688 (NH), 2304 (-C≡C-), 1696 (C=O), 1606 (C=C), 1425 (C=S) cm⁻¹; ¹H NMR (400 MHz, CDCl₃): δ 11.05 (1H, t, *J* = 4.2 Hz, NH), 8.70

(1H, brs, NH), 9.13 7.99 (1H, d, $J = 2.6$ Hz, H-6'''''), 7.97 (1H, s, H-6), 7.56 (1H, dd, $J = 2.6$, 8.8 Hz, H-4'''''), 6.97 (1H, m, H-1'), 6.80 (1H, m, H-3'''), 6.77 (2H, m, H-5'', H-6''), 6.66 (1H, d, $J = 8.8$ Hz, H-3'''''), 6.37 (1H, dt, $J = 1.5$, 5.8 Hz, H-3'), 5.86 (1H, m, H-2'), 4.93 (1H, m, H-4'), 4.05 (2H, t, $J = 5.9$ Hz, H-4'''), 3.95 (2H, m, H-2'''''), 3.80 (2H, m, H-5'), 3.78 (3H, s, OCH₃), 2.98 (2H, m, H-3'''), 2.84 (2H, t, $J = 5.8$ Hz, H-1'''''); ¹³C NMR (100 MHz, CDCl₃): δ 178.9 (C=S), 162.2 (C-4), 153.4 (C-4''), 151.5 (C-2'''''), 150.9 (C-1''), 149.1 (C-2), 146.6 (C-6'''''), 143.6 (C-6), 140.8 (C-4'''''), 135.6 (C-3'), 129.3 (C-2''), 128.9 (C-2'), 118.0 (C-3''), 113.4 (C-3'''''), 112.8 (C-6''), 111.4 (C-5''), 110.8 (C-5'''''), 100.3 (C-2''), 91.3 (C-1''), 90.4 (C-1'), 87.7 (C-4'), 72.5 (C-5), 66.8 (C-4'''), 62.9 (C-5'), 55.6 (OCH₃) 45.7 (C-2'''''), 30.2 (C-1'''''), 21.0 (C-3'''); HRMS (ES): m/z found 642.1008 ($M^+ + H$), C₂₈H₂₉N₅O₆BrS requires ($M^+ + H$) 642.1022.

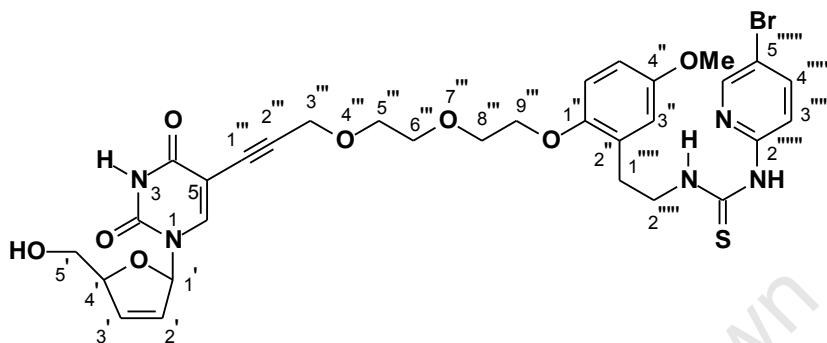
5-{6-[2-(2-(5-Bromo-2-pyridinylaminothiocarbonylamino)ethyl)-4-methoxyphenoxy]hexa-4-oxa-1-ynyl}-2',3'-didehydro-2',3'-dideoxyuridine (78)



A solution of NaOMe in methanol (0.03 mL, 2M, 0.06 mmol), was added to a solution of the nucleoside **114** (100 mg, 0.14 mmol) in MeOH (2 mL) at 0 °C. The mixture was stirred for 30 min, then acetic acid (0.05 mL) was added, and the crude mixture was diluted with CH₂Cl₂ (1 mL) and subjected to column chromatography employing EtOAc / pet ether (8 / 2) to give the title product **78** as a pale yellow solid (59 mg, 69%): m.p: 76-79 °C; [α]_D +49.1 ° (c 1.0, CHCl₃); IR (CHCl₃): ν_{\max} 3681, 3594, 3391 (NH, OH), 3022, 2928 (C-H), 2239 (-C≡C-), 1715, 1697 (C=O), 1501 (C=C), 1465 (C=S), 1216 (C-N) cm⁻¹; ¹H NMR (300 MHz, CDCl₃): δ 11.09 (1H, t, $J = 5.1$ Hz, NH), 9.44 (1H, brs, NH), 9.09 (1H, brs, NH), 8.14 (1H, s, H-6), 8.00 (1H, d, $J = 2.4$ Hz, H-6'''''), 7.65 (1H, dd, $J = 2.4$, 8.7 Hz, H-4'''''), 6.97 (1H, m, H-1'), 6.83 (1H, d, $J = 8.7$ Hz, H-3'''''), 6.75 (3H, m, H-3'', H-5'', H-6''), 6.35 (1H, dt, $J = 1.7$, 6.0 Hz, H-3'), 5.85 (1H, m, H-2'), 4.93 (1H, m, H-4'), 4.38 (2H, s, H-3'''), 4.06–3.78 (8H, m, H-2''''', H-5', H-5''''', H-6'''), 3.75 (3H, s, OCH₃), 3.36 (1H, brs, OH), 2.97 (2H, t, $J = 6.6$ Hz, H-1'''''); ¹³C NMR (100 MHz, CDCl₃): δ 178.8 (C=S), 161.8 (C-4), 153.7 (C-4''), 151.8 (C-2'''''), 151.1 (C-1''), 149.9 (C-2), 146.4 (C-6'''''), 144.7 (C-6), 141.0 (C-4'''''), 135.1 (C-3'), 128.9 (C-2''), 126.0 (C-2'), 117.5 (C-3''), 113.8 (C-3'''''), 112.9 (C-6''), 112.6 (C-5'''''), 111.6 (C-5''), 99.3 (C-

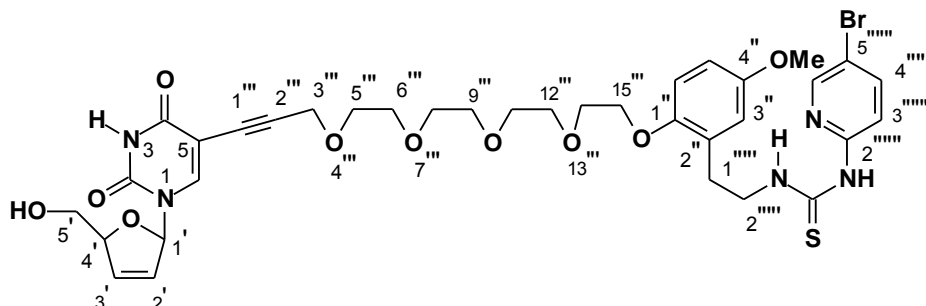
2'''), 90.3 (C-1'''), 89.4 (C-1'), 87.7 (C-4'), 77.5 (C-5), 68.4 (2 × OCH₂), 62.8 (C-5'), 59.3 (C-3'''), 55.6 (OCH₃), 45.8 (C-2'''''), 30.0 (C-1'''''); HRMS (ES): *m/z* found 672.1139 (M⁺ + H), C₂₉H₃₁N₅O₇SBr requires (M⁺ + H) 672.1128.

5-{9-[2-(2-(5-Bromo-2-pyridinylaminothiocarbonylamino)ethyl)-4-methoxyphenoxy]nona-4,7-dioxa-1-ynyl}-2',3'-didehydro-2',3'-dideoxyuridine (79)

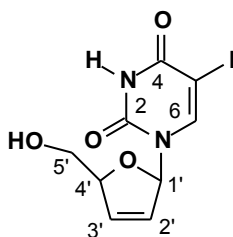


A solution of NaOMe in methanol (0.03 mL, 2M, 0.06 mmol), was added to a solution of the nucleoside **116** (80 mg, 0.11 mmol) in MeOH (2 mL) at 0 °C. The mixture was stirred for 30 min, then acetic acid (0.05 mL) was added, and the crude product was subjected to column chromatography employing EtOAc to give the product **79** as a white solid (37 mg, 54%): m.p: 130-134 °C; [α]_D + 41.1 ° (c 1.0, DMSO); IR (DMSO): ν_{max} 3442, 3260 (NH, OH), 2928 (C-H), 2246, 2123 (-C≡C-), 1700 (C=O), 1462 (C=S), 1223 (C-N) cm⁻¹; ¹H NMR (300 MHz, DMSO-d₆): δ 11.50 (1H, brs, NH), 11.05 (1H, t, *J* = 5.0 Hz, NH), 10.52 (1H, brs, NH), 8.11 (1H, d, *J* = 2.6 Hz, H-6'''''), 8.10 (1H, s, H-6), 7.93 (1H, dd, *J* = 2.6, 8.7 Hz, H-4'''''), 7.12 (1H, d, *J* = 8.7 Hz, H-3'''''), 6.92 (1H, d, *J* = 8.7 Hz, H-6''), 6.82 (1H, d, *J* = 3.0 Hz, H-3'), 6.80 (1H, m, H-1'), 6.77 (1H, dd, *J* = 3.0, 8.7 Hz, H-5''), 6.40 (1H, dt, *J* = 1.7, 6.0 Hz, H-3'), 5.93 (1H, dq, *J* = 1.4 Hz, 6.0 Hz, H-2'), 4.94 (1H, t, *J* = 5.0 Hz, OH), 4.81 (1H, m, H-4'), 4.31 (2H, s, H-3'''), 4.03 (2H, t, *J* = 4.9 Hz, H-9'''), 3.84 (2H, q, *J* = 6.6 Hz, H-2'''''), 3.74 (2H, t, *J* = 4.9 Hz, H-8'''), 3.68 (3H, s, OCH₃), 3.66-3.58 (6H, m, H-5', 2 × OCH₂), 2.90 (2H, t, *J* = 6.6 Hz, H-1'''''); ¹³C NMR (75 MHz, DMSO-d₆): δ 179.1 (C=S), 161.3 (C-4), 153.1 (C-4''), 152.1 (C-2'''''), 150.6 (C-1''), 149.5 (C-2), 145.6 (C-6'''''), 144.5 (C-6), 141.0 (C-4'''''), 135.2 (C-3'), 128.4 (C-2''), 127.4 (C-2'), 116.8 (C-3''), 114.3 (C-3'''''), 113.4 (C-6''), 111.6 (C-5''), 111.4 (C-5'''''), 97.5 (C-2''), 89.4 (C-1'), 88.5 (C-1''), 87.5 (C-4'), 78.1 (C-5), 69.5 (OCH₂), 68.9 (OCH₂), 68.5 (OCH₂), 68.2 (OCH₂), 61.7 (C-5'), 58.0 (C-3'''), 55.1 (OCH₃), 44.5 (C-2'''''), 28.9 (C-1'''''); HRMS (ES): *m/z* found 716.1389 (M⁺ + H), C₃₁H₃₅N₅O₈SBr requires (M⁺ + H) 716.1390.

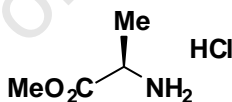
5-{15-[2-(2-(5-Bromo-2-pyridinylamino thiocarbonylamino)ethyl)-4-methoxyphenoxy]pentadeca-4,7,10,13-tetraoxa-1-ynyl}-2',3'-dideoxyuridine (80)



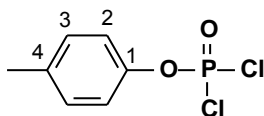
A solution of NaOMe in methanol (0.02 mL, 2M, 0.04 mmol), was added to a solution of the nucleoside **119** (70 mg, 0.08 mmol) in MeOH (1 mL) and THF (1 mL) at 0 °C. The mixture was stirred for 30 min, then acetic acid (0.05 mL) was added and the crude product was subjected to column chromatography employing EtOAc/ MeOH (8 / 2) to give the title product **80** as a white solid (32 mg, 52%): m.p: 63-65 °C; $[\alpha]_D^{25} + 53.2^\circ$ (c 1.0, DMSO); IR (DMSO): ν_{\max} 3442, 3283 (NH, OH), 2246, 2123 (C≡C), 1660 (C=O), 1469 (C=S), 1226 (C-N) cm^{-1} ; $^1\text{H NMR}$ (400 MHz, DMSO- d_6): δ 11.60 (1H, brs, NH), 11.09 (1H, t, $J = 4.8$ Hz, NH), 10.62 (1H, brs, NH), 8.12 (1H, s, H-6), 8.09 (1H, d, $J = 2.4$ Hz, H-6'''), 7.93 (1H, dd, $J = 2.4, 8.8$ Hz, H-4'''), 7.09 (1H, d, $J = 8.8$ Hz, H-3'''), 6.89 (1H, d, $J = 8.8$ Hz, H-6''), 6.81 (1H, d, $J = 3.2$ Hz, H-3''), 6.78 (1H, m, H-1'), 6.75 (1H, dd, $J = 3.2, 8.8$ Hz, H-5''), 6.38 (1H, dt, $J = 1.7, 6.0$ Hz, H-3'), 5.91 (1H, dq, $J = 1.4, 6.0$ Hz, H-2'), 5.02 (1H, t, $J = 5.2$ Hz, OH), 4.79 (1H, m, H-4'), 4.28 (2H, s, H-3''), 4.00 (2H, t, $J = 4.9$ Hz, H-15''), 3.81 (2H, q, $J = 6.6$ Hz, H-2'''), 3.71 (2H, t, $J = 4.9$ Hz, H-14''), 3.66 (3H, s, OCH₃), 3.60-3.47 (14H, m, H-5', 6 × OCH₂), 2.87 (2H, t, $J = 6.6$ Hz, H-1''); $^{13}\text{C NMR}$ (75 MHz, DMSO- d_6): δ 179.1 (C=S), 161.4 (C-4), 153.0 (C-4''), 152.2 (C-2'''), 150.6 (C-1''), 149.6 (C-2), 145.6 (C-6'''), 144.6 (C-6), 141.1 (C-4'''), 135.2 (C-3'), 128.4 (C-2''), 125.5 (C-2'), 116.8 (C-3''), 114.3 (C-3'''), 113.3 (C-6''), 111.6 (C-5''), 111.5 (C-5'''), 97.5 (C-2''), 89.4 (C-1'), 88.5 (C-4'), 87.5 (C-1''), 78.2 (C-5), 69.8 (OCH₂), 69.7 (OCH₂), 69.6 (2 × OCH₂), 69.4 (OCH₂), 68.9 (OCH₂), 68.4 (OCH₂), 68.2 (OCH₂), 61.7 (C-5'), 58.0 (C-3''), 55.1 (OCH₃), 44.5 (C-2'''), 29.0 (C-1''); HRMS (ES): m/z found 804.1932 ($M^+ + H$), C₃₅H₄₃N₅O₁₀SBr requires ($M^+ + H$) 804.1914.

2',3'-Didehydro-2',3'-dideoxy-5-iodouridine (122)¹⁸³

To a solution of 5'-benzoyl-5-iodouridine **47** (0.80 g, 1.82 mmol) in dry MeOH (15 mL), was added a solution of NaOMe in methanol (0.90 mL, 2M, 1.82 mmol) at 0 °C. The mixture was stirred at rt for 2 h. The crude residue was diluted with aq NH₄Cl (25 mL) and then was extracted using CHCl₃: MeOH (4:1) (40 mL), the organic extract dried over MgSO₄ and the solvent removed in *vacuum* to give a crude product, which was purified on silica-gel using EtOAc to give compound **122** as a colourless solid (0.45 g, 74%): m.p.:176-177 °C; ¹H NMR (300 MHz, DMSO-d₆): δ 11.58 (1H, brs, NH), 8.23 (1H, s, H-6), 6.78 (1H, m, H-1'), 6.40 (1H, dt, *J* = 1.7, 6.0 Hz, H-3'), 5.94 (1H, dq, *J* = 1.4, 6.0 Hz, H-2'), 5.01 (1H, t, *J* = 4.9 Hz, OH), 4.83 (1H, m, H-4'), 3.62 (2H, m, H-5'); ¹³C NMR (75 MHz, DMSO-d₆): δ 160.3 (C-4), 150.3 (C-2), 145.7 (C-6), 135.2 (C-3'), 125.7 (C-2'), 89.1 (C-1'), 87.4 (C-4'), 68.6 (C-5), 61.5 (C-5').

L-Alanine methyl ester hydrochloride (141)¹⁷²

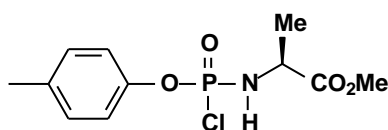
To a solution of L-alanine (1.00 g, 11.22 mmol) in MeOH (20 mL) was added thionyl chloride (0.82 mL, 11.22 mmol) at 0 °C after which the mixture was warmed to rt and stirred for 20 h. The solvent was evaporated and diethyl ether (5 mL) was added to precipitate the product. The resultant product was filtered and washed with diethyl ether (10 mL) to give **141** a colourless solid (1.8 g, 100%): ¹H NMR (400 MHz, DMSO-d₆): δ 8.74 (3H, brs, NH₃Cl), 4.00 (1H, q, *J* = 7.0 Hz, CH), 3.70 (3H, s, CO₂CH₃), 1.42 (3H, d, *J* = 7.0 Hz, CH₃).

***p*-Methylphenyl phosphorodichloridate (120)**¹⁷²

A solution of *p*-methylphenol (10.0 g, 92.50 mmol) and triethylamine (12.90 mL, 92.50 mmol) in anhydrous diethyl ether (200 mL) was added dropwise to a vigorously stirred solution of

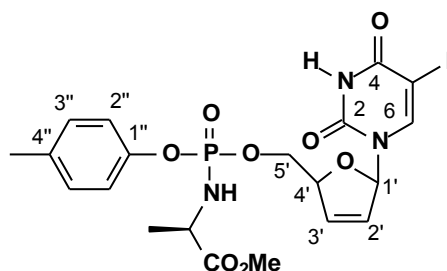
phosphoryl chloride (10.30 mL, 111.0 mmol) in diethyl ether (100 mL) at 0 °C over 2 h. The mixture was allowed to warm to rt with stirring for 15 h, and then refluxed for 2 h. The mixture was filtered, and the precipitate was washed with diethyl ether. The combined filtrate and washings were evaporated under reduced pressure to give a coloured oil. This was subjected to a vacuum distillation to give the product **120** as a colourless oil (16.80 g, 81%): (bp 85-90 °C, 0.1 mmHg), (lit. bp 80-85 °C, 0.1 mmHg); ¹H NMR (400 MHz, CDCl₃): δ 7.19 (4H, m, ArH), 2.38 (3H, d, *J*_{HP} = 2.4 Hz, ArCH₃); ³¹P NMR (CDCl₃): δ 3.9.

***p*-Methylphenyl methoxyalaninyl phosphorochloridate (121)¹⁷²**



A solution of triethylamine (2.80 mL, 20.00 mmol) in dry CH₂Cl₂ (60 mL) was added drop wise with vigorous stirring to a solution of L-alanine methyl ester hydrochloride **141** (1.40 g, 10.04 mmol) and *p*-methylphenyl phosphorodichloridate **120** (2.26 g, 10.04 mmol) in CH₂Cl₂ (80 mL) at -78 °C over 2 h. The reaction mixture was slowly warmed to rt with stirring for 12 h, and the solvent was then removed *in vacuo*. The residue was treated with diethyl ether (30 mL), and the solid formed filtered and washed with diethyl ether (20 mL). The solvent was evaporated *in vacuo* to give the product **121** as a colourless oil (2.90, 100%), which was used in the next step without further purification.

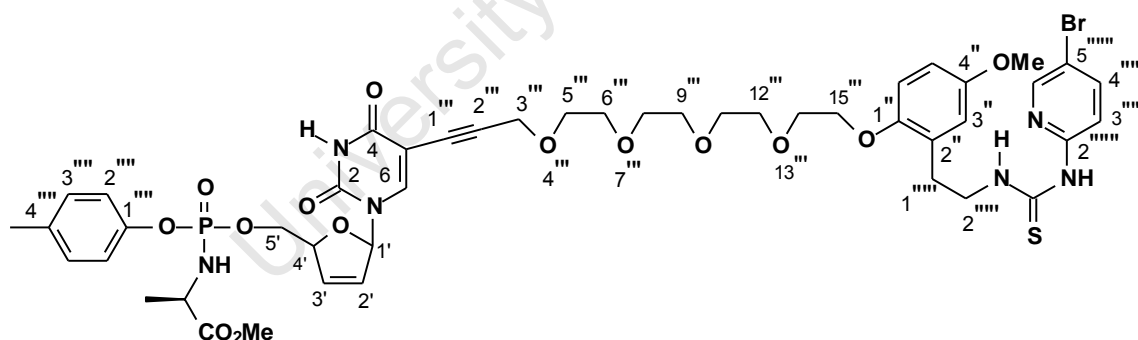
2',3'-Didehydro-2',3'-dideoxy-5-iodouridine-5'-[*p*-methylphenyl methoxyalaninyl phosphate] (123)



p-Methylphenyl methoxyalaninyl phosphorodichloridate **121** (1.77 g, 6.42 mmol) and 5-iodouridine **122** (0.72 g, 2.14 mmol) were dissolved in THF (25 mL) and *N*-methylimidazole (1.02 mL, 12.84 mmol), was added with vigorous stirring. After 24 h at rt the solvent was removed under vacuum. The residue was dissolved in CHCl₃ (50 mL) and washed with hydrochloric acid solution (1M, 2 × 60 mL), aq NaHCO₃ (2 × 40 mL), and then water (3 × 40

mL). The organic layer was dried over MgSO_4 , and evaporated under vacuum, and the residue was purified by chromatography on silica-gel by elution with 3% MeOH in CHCl_3 to give the product **123** as a (1:1) mixture of diastereoisomers and as a colourless solid (0.45 g, 54%): m.p: 40-44 °C; IR (CHCl_3): ν_{max} 3384 (NH), 3007 (C-H), 1743, 1704 (C=O), 1505 (C=C), 1245 (P=O) cm^{-1} ; ^1H NMR (400 MHz, CDCl_3): δ (peaks are split due to diastereoisomers at P) 8.91 (1H, brs, NH), 7.92, 7.90 (1H, s, H-6), 7.11 (4H, m, ArH), 6.94, 6.92 (1H, m, H-1'), 6.38, 6.32 (1H, dt, $J = 1.7, 6.0$ Hz, H-3'), 5.94, 5.86 (1H, dq, $J = 1.3, 6.0$ Hz, H-2'), 5.05 (1H, m, H-4'), 4.46-3.82 (4H, m, H-5', Ala-CH, Ala-NH), 3.72, 3.71 (3H, s, OCH_3), 2.31 (3H, s, ArCH_3), 1.41, 1.36 (3H, d, $J = 7.6$ Hz, Ala- CH_3); ^{13}C NMR (75 MHz, CDCl_3): δ (starred peaks are split due to diastereoisomers: δ values given as an average) 173.9* (CO_2Me), 159.9* (C-4), 150.3 (C-2), 148.2* (C-1''), 144.6* (C-6), 134.6 (C-4''), 133.7* (C-3'), 133.0* (C-3'', C-5''), 126.9* (C-2'), 120.0* (C-2'', C-6''), 90.2* (C-1'), 85.3* (C-4'), 69.0* (C-5), 66.6* (C-5'), 52.4* (Ala- OCH_3), 50.0* (Ala-CH), 21.0* (Ala- CH_3), 20.8* (ArCH_3); ^{31}P NMR (CDCl_3): δ 3.7, 3.5 (1:1); HRMS (ES): m/z found 592.0356 ($\text{M}^+ + \text{H}$), $\text{C}_{20}\text{H}_{24}\text{N}_3\text{O}_8\text{P}$ requires ($\text{M}^+ + \text{H}$) 592.0346.

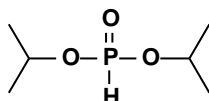
5-{15-[2-(2-(5-Bromo-2-pyridinylaminothiocarbonylamino)ethyl)-4-methoxyphenoxy]pentadeca-4,7,10,13-tetraoxa-1-ynyl}-2',3'-dideoxy-5-iodouridine-5'-5'-(*p*-methylphenyl methoxyalaninyl phosphate)-2',3'-dideoxy-2',3'-dideoxyuridine (81**)**



Trifluoroacetic acid (0.20 mL) was added to a solution of alkyne **70r** (92 mg, 0.19 mmol) in CH_2Cl_2 (2 mL) at 0 °C, and the solution stirred for 2 h. Anhydrous K_2CO_3 (80 mg, 0.57 mmol) was added, the mixture was stirred for a further 15 min and then filtered through Celite, The solvent was then evaporated *in vacuo*, the crude amine dried under vacuum for 1 h and then used in the next step without further purification. The crude amine was dissolved in dry THF (3 mL), DMF (2 mL), and 5-iodouridine-5'-[*p*-methylphenyl methoxyalaninyl phosphate] **123** (0.10 g, 0.17 mmol), triethylamine (0.05 mL, 0.34 mmol) were added, The mixture was thoroughly degassed with nitrogen for 1h. CuI (17 mg, 0.09 mmol) and $\text{Pd}(\text{PPh}_3)_4$ (20 mg, 0.02 mmol) were added to the degassed solution under a nitrogen atmosphere. The mixture

was left stirring at rt for 2h. The crude was dissolved in MeOH: CHCl₃ (1: 4) (20 mL), which was washed with portions (10 mL) of 5% aq disodium EDTA, water (10 mL) and finally dried over MgSO₄. Filtration and solvent evaporation under reduced pressure gave a crude product, which was flashed through a silica-gel column employing EtOAc/ MeOH/ Et₃N (5/ 4/ 1) as eluent. The amine product was dissolved in dry THF (3 mL), thiourea **49** (65 mg, 0.23 mmol) was added and the mixture was stirred at room temperature for 20h. Following evaporation of solvent, the residue was subjected directly to column chromatography using EtOAc/ MeOH (9/ 1) to give a yellow solid **81** (36 mg, 20% over the 3 steps): m.p: 51-54 °C; [α]_D +4.4 ° (c 1.0, CHCl₃); IR (CHCl₃): ν_{max} 3391 (NH), 3007, 2928 (C-H) 1707 (C=O), 1505 (C=C), 1462 (C=S), 1259 (P=O), 1223 (C-N) cm⁻¹; ¹H NMR (300 MHz, CDCl₃): δ (peaks are split due to diastereoisomers) 11.11 (1H, t, *J* = 4.9 Hz, NH), 9.11 (1H, brs, NH), 9.05, 9.00 (1H, s, NH), 8.03 (1H, d, *J* = 2.4 Hz, H-6'''), 7.79, 7.78 (1H, s, H-6), 7.66, 7.63 (1H, dd, *J* = 2.4, 8.8 Hz, H-4'''), 7.08 (4H, s, ArH), 6.96, 6.94 (1H, m, H-1'), 6.80 (1H, d, *J* = 3.0 Hz, H-3''), 6.78 (1H, d, *J* = 8.8 Hz, H-6''), 6.74 (1H, d, *J* = 8.8 Hz, H-3'''), 6.72 (1H, dd, *J* = 3.0, 8.8 Hz, H-5''), 6.37, 6.27 (1H, dt, *J* = 1.7, 6.0 Hz, H-3'), 5.91, 5.81 (1H, dq, *J* = 1.4, 6.0 Hz, H-2'), 5.02 (1H, m, H-4'), 4.41-3.97 (10H, m, Ala-CH, Ala-NH, H-5', H-15'', H-2''', H-3'''), 3.81 (2H, t, *J* = 4.9 Hz, H-14''), 3.75 (3H, s, OCH₃), 3.68, 3.67 (3H, s, CO₂CH₃), 3.70-3.57 (12H, m, 6 × CH₂O), 2.97 (2H, t, *J* = 6.6 Hz, H-1'''), 2.28 (3H, s, ArCH₃), 1.37, 1.33 (3H, d, *J* = 6.3 Hz, Ala-CH₃); ¹³C NMR (75 MHz, CDCl₃): δ (starred peak are split due to diastereoisomers: δ values given as an average) 179.2 (C=S), 173.9* (CO₂Me), 161.2 (C-4), 153.6 (C-4''), 151.9 (C-2'''), 151.3 (C-1''), 149.6 (C-2), 148.3* (C-1'''), 146.5 (C-6'''), 143.1* (C-6), 141.0 (C-4'''), 134.7 (C-4'''), 133.8 (C-3'), 130.1* (C-3''', C-5'''), 128.8 (C-2''), 126.7* (C-2'), 120.0* (C-2''', C-6'''), 117.5 (C-3''), 113.6 (C-3'''), 112.7 (C-6''), 112.4 (C-5'''), 111.5 (C-5''), 99.9 (C-2''), 91.3* (C-1'), 90.2 (C-1''), 85.4* (C-4'), 77.2 (C-5), 70.8 (OCH₂), 70.6 (OCH₂), 70.5 (2 × OCH₂), 70.2* (OCH₂), 69.9 (OCH₂), 69.2* (OCH₂), 68.4 (OCH₂), 66.7 (d, *J*_{cp} = 4.5 Hz, C-5'), 58.9 (C-3'''), 55.6 (OCH₃), 52.5 (CO₂CH₃), 50.3* (Ala-CH), 45.8 (C-2'''), 29.8 (C-1'''), 20.9* (Ala-CH₃), 20.7 (Ph-CH₃); ³¹P NMR (CDCl₃): δ 3.63, 3.56 (1:1); HRMS (ES): *m/z* found 1059.2548 (M⁺ + H), C₄₆H₅₇N₆O₁₄SBrP requires (M⁺ + H) 1059.2574.

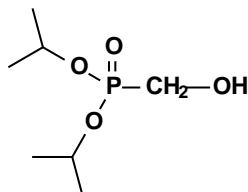
Diisopropyl hydrogen phosphonate (**124**)¹⁷⁷



Isopropanol (5.24 g, 68.82 mmol) was added dropwise to a suspension of NaH (60% in mineral oil, 1.84 g, 45.88 mmol) in THF (60 mL) and the mixture was stirred for 15 min at 0 °C. Phosphorus trichloride (2.00 mL, 22.94 mmol) was added dropwise and then the mixture

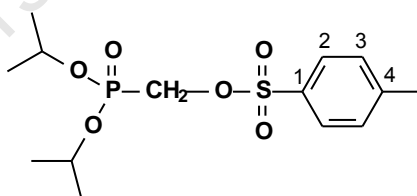
was warmed to rt with stirring for 1h. The reaction was quenched using aqueous NH_4Cl (10 mL). The mixture was diluted with EtOAc (80 mL), washed with aq NH_4Cl (50 mL), water (2×40 mL), dried over MgSO_4 and the solvent was evaporated under reduced pressure to give the product **124** without purification as a colourless oil (11.20 g, 98%): ^1H NMR (300 MHz, CDCl_3): δ 6.77 (1H, d, $J_{\text{HP}} = 687.0$ Hz, H-P=O), 4.67 (2H, m, $\text{CH}(\text{CH}_3)_2$), 1.30 and 1.28 ($2 \times 6\text{H}$, $2 \times$ d, $\text{CH}(\text{CH}_3)_2$); ^{31}P NMR (CDCl_3): δ 4.6.

Diisopropyl hydroxymethylphosphonate (**125**)¹⁷⁷



To a solution of diisopropyl hydrogen phosphonate **124** (5.00 g, 30.10 mmol), paraformaldehyde (1.05 g, 36.12 mmol) in isopropanol (20 mL) was added anhydrous potassium carbonate (0.21 g, 1.51 mmol). The mixture was stirred vigorously for 1h at 60 °C, filtered through Celite and the solvent was evaporated in *vacuum* to give the product **125** as a colourless oil (5.81 g, 98%) pure enough for the next step: ^1H NMR (300 MHz, CDCl_3): δ 4.73 (2H, m, $\text{CH}(\text{CH}_3)_2$), 3.82 (2H, d, $J_{\text{HP}} = 6.6$ Hz, CH_2P), 2.15 (1H, brs, OH), 1.32 (12H, d, $J = 6.3$ Hz, $\text{CH}(\text{CH}_3)_2$); ^{31}P NMR (CDCl_3): δ 22.9.

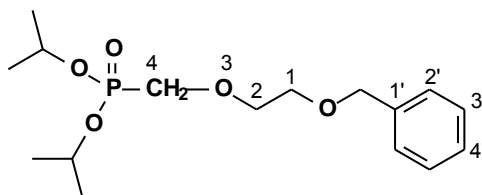
Diisopropyl *p*-toluenesulphonyloxymethylphosphonate (**126**)



To a solution of diisopropyl hydroxymethyl phosphonate **125** (5.00 g, 25.49 mmol) in dry CH_2Cl_2 (30 mL), were added triethylamine (4.26 mL, 30.59 mmol) and *p*-toluenesulfonyl chloride (5.81 g, 30.59 mmol) followed by DMAP (0.02 g). The reaction mixture was stirred at rt for 16h. The mixture was diluted with CH_2Cl_2 (120 mL), washed with aq. NH_4Cl (60 mL), water (70 mL), dried over MgSO_4 and solvent was removed under reduced pressure. Purification by column chromatography using EtOAc / pet ether (6 / 4) gave a colourless oil **126** (8.20 g, 92%): IR (CHCl_3): ν_{max} 2986 (C-H), 1252 (P=O), 1176 (O-SO₂-), 1003 (P-O) cm^{-1} ; ^1H NMR (400 MHz, CDCl_3): δ 7.80 (2H, d, $J = 8.0$ Hz, H-2, H-6), 7.36 (2H, d, $J = 8.0$ Hz, H-3, H-5), 4.73 (2H, m, $\text{CH}(\text{CH}_3)_2$), 4.12 (2H, d, $J_{\text{HP}} = 10.0$ Hz, CH_2P), 2.46 (3H, s, ArCH_3), 1.33 and 1.29 ($2 \times 6\text{H}$, $2 \times$ d, $J = 6.2$ Hz, $\text{CH}(\text{CH}_3)_2$); ^{13}C NMR (100 MHz, CDCl_3): δ 145.3 (C-1),

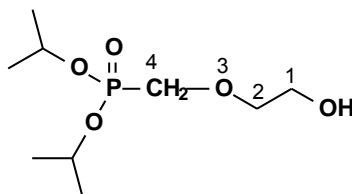
131.8 (C-4), 129.9 (C-3, C-5), 128.1 (C-2, C-6), 72.3 (d, $J_{CP} = 6.1$ Hz, $CH(CH_3)_2$), 61.9 (d, $J_{CP} = 169.1$ Hz, CH_2P), 23.9 (d, $J_{CP} = 3.8$ Hz, $CH(CH_3)_2$) 23.7 (d, $J_{CP} = 4.6$ Hz, $CH(CH_3)_2$), 21.5 (Ph- CH_3); ^{31}P NMR ($CDCl_3$): δ 13.3; HRMS (ES): m/z found 351.1044 ($M^+ + H$), $C_{14}H_{24}O_6SP$ requires ($M^+ + H$) 351.1031.

Diisopropyl (2-benzyloxyethoxy)methylphosphonate (127)



2-Benzyloxyethanol **72** (2.09 g, 13.70 mmol) was added dropwise to a suspension of NaH (60% mineral oil, 0.69 g, 17.13 mmol) in THF (60 mL) at 0 °C. The mixture was stirred for 30 min and the tosylate **126** (4.00 g, 11.42 mmol) was added. The mixture was heated at reflux for 3 h. The crude mixture was added to EtOAc (80 mL), which was washed with aqueous NH_4Cl (50 mL), water (2 × 40 mL), dried over $MgSO_4$ and the solvent evaporated under reduced pressure. The crude product was purified by column chromatography employing EtOAc / pet ether (7 / 3) to give compound **127** as a colourless oil (2.70 g, 72%): IR ($CHCl_3$): ν_{max} 2986, 2935 (C-H), 1241 (P=O), 999 (P-O) cm^{-1} ; 1H NMR (400 MHz, $CDCl_3$): δ 7.31 (4H, m, ArH), 7.29 (1H, m, H-4'), 4.76 (2H, m, $CH(CH_3)_2$), 4.54 (2H, s, $ArCH_2O$), 3.82 (2H, d, $J_{HP} = 8.4$ Hz, CH_2P), 3.79 (2H, t, $J = 4.7$ Hz, H-2), 3.66 (2H, t, $J = 4.7$ Hz, H-1), 1.33 and 1.31 (2 × 6H, 2 × d, $J = 6.3$ Hz, $CH(CH_3)_2$); ^{13}C NMR (100 MHz, $CDCl_3$): δ 138.2 (C-1'), 128.3 (C-2', C-6'), 127.6 (C-3', C-5'), 127.5 (C-4'), 73.2 ($ArCH_2O$), 72.5 (d, $J_{CP} = 10.5$ Hz, C-2), 71.0 (d, $J_{CP} = 6.6$ Hz, $CH(CH_3)_2$), 69.4 (C-1), 66.1 (d, $J_{CP} = 165.9$ Hz, CH_2P), 24.0 (m, $CH(CH_3)_2$); ^{31}P NMR ($CDCl_3$): δ 19.7; HRMS (ES): m/z found 331.1668 ($M^+ + H$), $C_{16}H_{28}O_5P$ requires ($M^+ + H$) 331.1674.

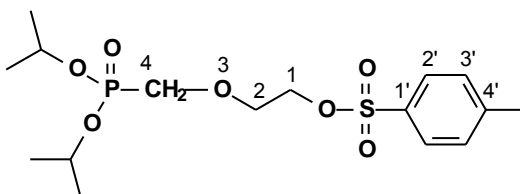
Diisopropyl (2-hydroxyethoxy)methylphosphonate (128)



Hydrogen gas was introduced at atmospheric pressure to compound **127** (2.00 g, 6.05 mmol) and a suspension of 10% palladium-on-carbon (0.65 g, 0.61 mmol) in MeOH: THF (1: 1) (15 mL). The mixture was stirred at room temperature for 6 h. The catalyst was filtered through a pad of Celite, washed with MeOH (2 × 15 mL) and the filtrate evaporated in *vacuo* to give the

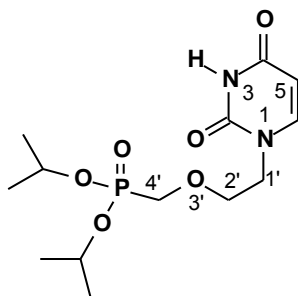
product **128** as a colourless oil pure enough for the next step (1.12 g, 77%): IR (CHCl₃): ν_{\max} 3200(OH), 2986 (C-H), 1234 (P=O), 996 (P-O) cm⁻¹; ¹H NMR (300 MHz, CDCl₃): δ 4.75 (2H, m, CH(CH₃)₂), 3.79 (2H, d, J_{HP} = 7.8 Hz, CH₂P), 3.72 (4H, m, H-1, H-2), 2.52 (1H, brs, OH), 1.33 (12H, d, J = 6.2 Hz, CH(CH₃)₂); ¹³C NMR (75 MHz, CDCl₃): δ 75.0 (d, J_{CP} = 9.5 Hz, C-2), 71.2 (d, J_{CP} = 6.6 Hz, CH(CH₃)₂), 66.0 (d, J_{HP} = 167.3 Hz, CH₂P), 61.5 (C-1), 23.9 (m, CH(CH₃)₂); ³¹P NMR (CDCl₃): δ 20.2.

Diisopropyl (2-*p*-toluenesulfonyloxyethoxy)methylphosphonate (**129**)



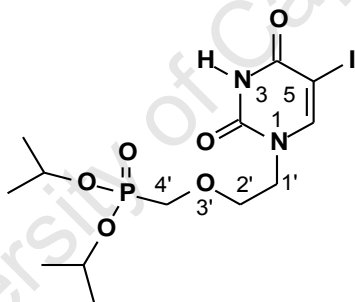
p-Toluenesulfonyl chloride (1.05 g, 5.50 mmol) was added to a stirring solution of the alcohol **128** (1.10 g, 4.58 mmol) containing triethylamine (0.77 mL, 5.50 mmol), and a catalytic amount of DMAP in dry CH₂Cl₂ (20 mL) at 0 °C. The reaction mixture was stirred at rt for 16 h. The mixture was diluted with CH₂Cl₂ (80 mL), washed with aq NH₄Cl (25 mL), water (30 mL), dried over MgSO₄ and the solvent removed under reduced pressure. Purification by column chromatography using EtOAc / pet ether (9 / 1) gave a colourless oil **129** (1.63 g, 90%): IR (CHCl₃): ν_{\max} 2986 (C-H), 1234 (P=O), 1176 (O-SO₂), 999 (P-O) cm⁻¹; ¹H NMR (300 MHz, CDCl₃): δ 7.78 (2H, d, J = 8.3 Hz, H-2', H-6'), 7.33 (2H, d, J = 8.3 Hz, H-3', H-5'), 4.71 (2H, m, CH(CH₃)₂), 4.14 (2H, t, J = 4.8 Hz, H-1), 3.77 (2H, t, J = 4.8 Hz, H-2), 3.69 (2H, J_{HP} = 8.4 Hz, CH₂P), 1.31 and 1.28 (2 × 6H, 2 × d, J = 6.0 Hz, CH(CH₃)₂); 2.43 (3H, s, ArH); ¹³C NMR (75 MHz, CDCl₃): δ 144.8 (C-1'), 132.9 (C-4'), 129.8 (C-3', C-5'), 127.9 (C-2', C-6'), 71.2 (d, J_{CP} = 6.6 Hz, CH(CH₃)₂), 70.4 (d, J_{CP} = 11.0 Hz, C-2), 68.7 (C-1), 66.1 (d, J_{CP} = 166.5 Hz, CH₂P), 24.0 (m, CH(CH₃)₂), 21.5 (d, J_{CP} = 3.7 Hz, ArCH₃); ³¹P NMR (CDCl₃): δ 18.6; HRMS (ES): m/z found 395.1297 (M⁺ + H), C₁₆H₂₈O₇PS requires (M⁺ + H) 395.1293.

1-{2-[(diisopoxyphosphoryl)methoxy]ethyl}uracil (**131**)¹⁷⁶



A mixture of uracil (0.61 g, 5.47 mmol) and caesium carbonate (1.64 g, 5.02 mmol) in DMF (10 mL) was heated at 100 °C for 1 h. A solution of the tosylate **129** (1.80 g, 4.56 mmol) in DMF (2 mL) was added to the mixture and stirred for 20 h at 100 °C. The reaction mixture was diluted with CHCl₃ / MeOH (4 / 1) (40 mL) and washed with aqueous NH₄Cl (25 mL), water (3 × 30 mL), dried over MgSO₄ and the solvent was removed under reduced pressure. The crude product was purified on silica-gel using EtOAc / MeOH (8 / 2) to give compound **131** as a colourless oil (0.35 g, 35%): IR (CHCl₃): ν_{\max} 3413 (NH), 2986 (C-H), 1707, 1660 (C=O), 1241 (P=O), 999 (P-O) cm⁻¹; ¹H NMR (300 MHz, CDCl₃): δ 8.90 (1H, brs, NH), 7.36 (1H, d, J = 7.8 Hz, H-6), 5.64 (1H, d, J = 7.8 Hz, H-5), 4.72 (2H, m, CH(CH₃)₂), 3.94 (2H, t, J = 4.5 Hz, H-1'), 3.80 (2H, t, J = 4.5 Hz, H-2'), 3.72 (d, J_{HP} = 8.1 Hz, CH₂P), 1.34 and 1.32 (2 × 6H, 2 × d, J = 6.2 Hz, CH(CH₃)₂); ¹³C NMR (100 MHz, CDCl₃): δ 163.5 (C-4), 150.8 (C-2), 145.8 (C-6), 101.5 (C-5), 71.2 (d, J_{CP} = 6.8 Hz, CH(CH₃)₂), 71.0 (d, J_{CP} = 10.6 Hz, C-2'), 66.2 (d, J_{CP} = 166.9 Hz, CH₂P), 48.3 (C-1'), 24.0 (m, CH(CH₃)₄); ³¹P NMR (CDCl₃): δ 18.8; HRMS (ES): m/z found (M⁺ + H), 335.1376, C₁₃H₂₄N₂O₆P requires (M⁺ + H) 335.1376.

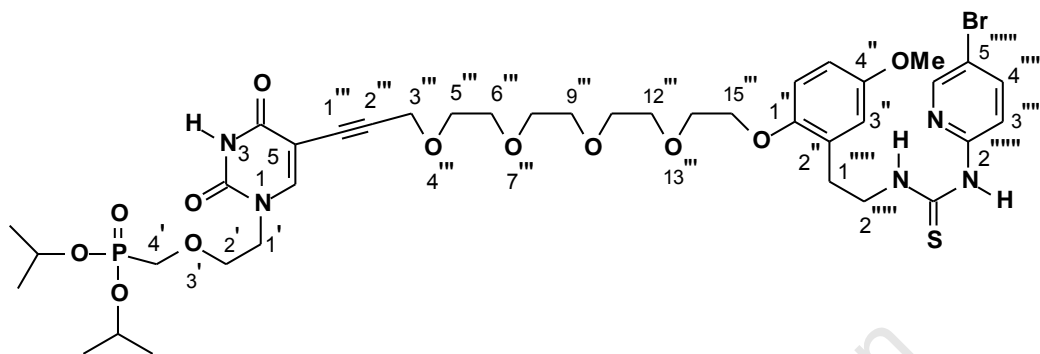
5-Iodo-1-{2-[(diisopropoxyphosphoryl)methoxy]ethyl}uracil (**132**)



Cerium ammonium (IV) nitrate (0.18 g, 0.32 mmol) and iodine (96 mg, 0.38 mmol) were added to the uracil phosphonate **131** (0.21 g, 0.63 mmol) in CH₃CN (8 mL). The mixture was stirred at 40 °C for 4 h. The solvent was then reduced under vacuum after which the crude residue was diluted with a solution of sodium thiocyanate (20 mL) and extracted with EtOAc / MeOH (4 / 1) (2 × 30 mL). The organic fractions were dried over MgSO₄ and the solvent reduced under vacuum. Purification by chromatography using a silica-gel column with EtOAc gave compound **132** as a yellow solid (0.18 g, 62%): m.p: 89-91 °C; IR (CHCl₃): ν_{\max} 3377 (NH), 2986 (C-H), 1711, 1689 (C=O), 1241 (P=O), 999 (P-O) cm⁻¹; ¹H NMR (300 MHz, CDCl₃): δ 9.00 (1H, brs, NH), 7.78 (1H, s, H-6), 4.76 (2H, m, CH(CH₃)₂), 3.94 (2H, t, J = 4.7 Hz, H-1'), 3.79 (2H, t, J = 4.7 Hz, H-2'), 3.73 (2H, J_{HP} = 8.4 Hz, CH₂P), 1.34, 1.30 (2 × 6H, 2 × d, J = 6.0 Hz, CH(CH₃)₂); ¹³C NMR (100 MHz, CDCl₃): δ 160.7 (C-4), 150.6 (C-2), 150.0 (C-6), 71.2 (d, J_{CP} = 6.1 Hz, CH(CH₃)₂), 70.6 (d, J_{CP} = 10.7 Hz, C-2'), 67.2 (C-5), 66.0 (d, J_{CP} =

166.9 Hz, CH₂P), 48.5 (C-1'), 23.9 (d, J_{CP} = 3.1 Hz, CH(CH₃)₂); ³¹P NMR (CDCl₃): δ 18.7; HRMS (ES): *m/z* found (M⁺ + H), 461.0341 C₁₃H₂₃N₅O₆PI requires (M⁺ + H) 461.0339.

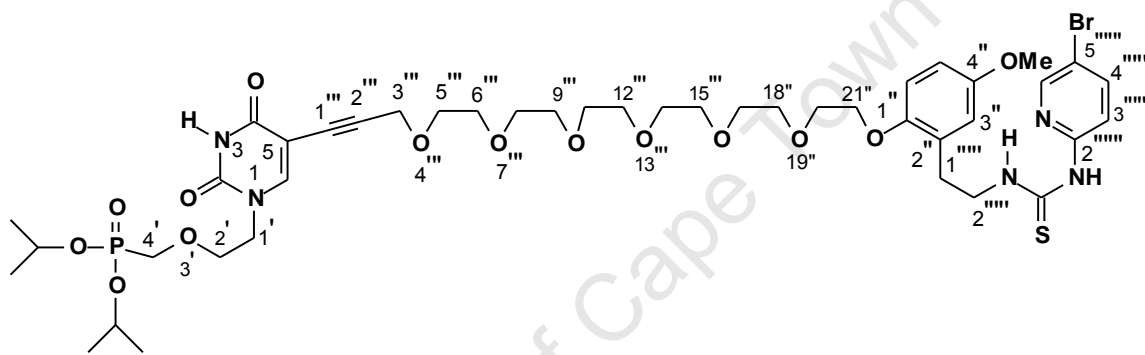
5-{15-[2-(2-(5-Bromo-2-pyridinylaminothiocarbonylamino)ethyl)-4-methoxyphenoxy]pentadeca-4,7,10,13-tetraoxa-1-ynyl}-1-{2-[(diisopropoxyphosphoryl)methoxy]ethyl}uracil (134)



Trifluoroacetic acid (0.20 mL) was added to a solution of the alkyne **70r** (0.12 g, 0.25 mmol) in CH₂Cl₂ (3 mL) at 0 °C, and the solution stirred for 2 h. Anhydrous K₂CO₃ (0.10 g, 0.75 mmol) was added, the mixture was stirred for a further 15 min, then filtered through Celite and the solvent evaporated *in vacuo*. The crude amine was dried under vacuum for 1 h and used in the next step without further purification. The crude amine was dissolved in dry THF (3 mL)/ DMF (2 mL), and iodide **132** (0.10 g, 0.22 mmol) and triethylamine (0.06 mL, 0.44 mmol) were added, The mixture was thoroughly degassed with nitrogen for 1 h. Cul (21 mg, 0.11 mmol) and Pd(PPh₃)₄ (23 mg, 0.02 mmol) were added to the degassed solution under a nitrogen atmosphere. The mixture was left stirring at rt for 2 h. The crude was dissolved in MeOH: CHCl₃ (1: 4) (25mL) which was washed with portions of 5% aq disodium EDTA (15 mL), water (15 mL) and dried over MgSO₄. Filtration and a solvent removal under reduced pressure gave the crude product, which was flushed through a column of silica-gel employing EtOAc / MeOH / Et₃N (5 / 4 / 1) to afford the coupled amine product, which was dissolved in dry THF (4 mL). Thiourea **49** (85 mg, 0.30 mmol) was then added and the mixture was stirred at room temperature for 20 h. Following evaporation of solvent, the residue was subjected directly to column chromatography to give **134** as a colourless oil (40 mg, 20% over the 3 steps): IR (CHCl₃): ν_{max} 3406, 3167 (NH), 3000 (C-H), 2232 (C≡C), 1693 (C=O), 1501 (C=C), 1465 (C=S), 1230 (P=O), 1097 (C-N), 999 (P-OCH) cm⁻¹; ¹H NMR (400 MHz, CDCl₃): δ 11.20 (1H, t, J = 5.0 Hz, NH), 9.12 (1H, brs, NH), 8.04 (1H, d, J = 2.4 Hz, H-6'''), 7.70 (1H, s, NH), 7.68 (1H, dd, J = 2.4, 8.8 Hz, H-4'''), 7.58 (1H, s, H-6), 6.82 (1H, d, J = 8.8 Hz, H-6''), 6.80 (1H, d, J = 2.9 Hz, H-3''), 6.78 (1H, d, J = 8.8 Hz, H-3'''), 6.73 (1H, dd, J = 2.9, 8.8 Hz, H-5''), 4.74 (2H, m, CH(CH₃)₂), 4.33 (2H, s, H-3'''), 4.02 (4H, m, H-15''', H-2'''), 3.95 (2H, t, J = 4.8 Hz, H-1'), 3.82 (4H, m, H-2', H-14'''), 3.75 (3H, s, OCH₃), 3.70-3.64 (14H, m, 6 × CH₂O, H-4'), 2.98 (2H, t, J = 6.4 Hz, H-1'''), 1.32 (12H, m, CH(CH₃)₂); ¹³C NMR (75 MHz, CDCl₃): δ

179.2 (C=S), 162.2 (C-4), 153.5 (C-4''), 151.9 (C-2'''''), 151.1 (C-1''), 149.8 (C-2), 148.7 (C-6), 146.4 (C-6'''''), 140.9 (C-4'''''), 128.8 (C-2''), 117.5 (C-3''), 113.6 (C-3'''''), 112.7 (C-6''), 112.4 (C-5'''''), 111.5 (C-5''), 98.7 (C-2''), 89.7 (C-1''), 77.3 (C-5), 71.3 (d, $J_{CP} = 6.2$ Hz, $CH(CH_3)_2$), 70.7 (CH₂O), 70.6 (CH₂O), 70.5 (2 × CH₂O), 70.3 (CH₂O), 69.8 (CH₂O), 69.1 (CH₂O), 68.3 (CH₂O), 66.1 (d, $J_{CP} = 166.7$ Hz, C-4'), 59.0 (C-3'''), 55.5 (OCH₃), 48.8 (C-1'), 45.6 (C-2'''''), 29.8 (C-1'''''), 23.9 (m, $CH(CH_3)_2$); ³¹P NMR (CDCl₃): δ 18.7; HRMS (ES): *m/z* found ($M^+ + H$), 928.2603, C₃₉H₅₆N₅O₁₂PSBr requires ($M^+ + H$) 928.2567.

5-{21-[2-(2-(5-Bromo-2-pyridinyl)amino thiocarbonylamino)ethyl)-4-methoxyphenoxy]heneicosa-4,7,10,13, 16,19-heptoxa-1-ynyl}-1-{2-[(diisopropoxyphosphoryl)methoxy]ethyl}uracil (135)



Trifluoroacetic acid (0.12 mL) was added to a solution of the alkyne **70s** (80 mg, 0.14 mmol) in CH₂Cl₂ (2 mL) at 0 °C, and the solution stirred for 2 h. Anhydrous K₂CO₃ (58 mg, 0.42 mmol) was added, the mixture was stirred for a further 15 min before being filtered through Celite and the solvent evaporated *in vacuo*. The crude amine was dried under vacuum for 1 h and used in the next step without further purification. It was dissolved in dry THF (3 mL)/DMF (1 mL) and the iodide **132** (60 mg, 0.13 mmol), and triethylamine (0.04 mL, 0.26 mmol) were then added. The mixture was thoroughly degassed with nitrogen for 1h. CuI (13 mg, 0.07 mmol) and Pd(PPh₃)₄ (15 mg, 0.013 mmol) were added to the degassed solution under a nitrogen atmosphere and the mixture was left stirring at rt for 2h. The crude was dissolved in MeOH: CHCl₃ (1: 4) (20 mL), which was washed with portions (10 mL) of 5% aq disodium EDTA, water (10 mL) and dried over MgSO₄. Filtration and solvent removal under reduced pressure gave a crude product, which was flushed through a column of silica-gel employing EtOAc / MeOH / Et₃N (5 / 4 / 1). The amine product was dissolved in dry THF (2 mL), thiourea **49** (48 mg, 0.17 mmol) was then added and the mixture stirred at room temperature for 20h. Following evaporation of solvent, the residue was subjected directly to column chromatography to afford **135** as a colourless oil (20 mg, 15% over the 3 steps): IR (CHCl₃): ν_{max} 3413, 3167 (NH), 3007 (C-H), 2239 (C≡C), 1693 (C=O), 1501 (C=C), 1469 (C=S), 1259,

1230 (P=O), 1097 (C-N), 1006 (P-O) cm^{-1} ; ^1H NMR (400 MHz, CDCl_3): δ 11.17 (1H, t, $J = 4.7$ Hz, NH), 9.00 (1H, brs, NH), 8.06 (1H, d, t, $J = 2.4$ Hz, H-6'''''), 7.74 (1H, brs, NH), 7.69 (1H, dd, $J = 2.4, 8.8$ Hz, H-4'''''), 7.61 (1H, s, H-6), 6.81 (1H, d, $J = 3.2$ Hz, H-3''), 6.79 (1H, d, $J = 8.8$ Hz, H-3'''''), 6.79 (1H, d, $J = 8.8$ Hz, H-6''), 6.74 (1H, dd, $J = 3.2, 8.8$ Hz, H-5''), 4.75 (2H, m, $\text{CH}(\text{CH}_3)_2$), 4.37 (2H, s, H-3'''), 4.02 (4H, m, H-21'', H-2'''''), 3.96 (2H, t, $J = 4.7$ Hz, H-1'), 3.83 (4H, m, H-2', H-20''), 3.76 (3H, s, OCH_3), 3.75-3.63 (22H, m, $10 \times \text{CH}_2\text{O}$, H-4'), 2.99 (2H, t, $J = 6.6$ Hz, H-1'''''), 1.33 (12H, m, $\text{CH}(\text{CH}_3)_2$); ^{13}C NMR (75 MHz, CDCl_3): δ 179.3 (C=S), 161.8 (C-4), 153.6 (C-4''), 151.8 (C-2'''''), 151.2 (C-1''), 149.6 (C-2), 148.7 (C-6), 146.5 (C-6'''''), 141.0 (C-4'''''), 128.8 (C-2''), 117.5 (C-3''), 113.6 (C-3'''''), 112.8 (C-6''), 112.4 (C-5'''''), 111.5 (C-5''), 98.8 (C-2'''), 89.9 (C-1'''), 77.1 (C-5), 71.3 (d, $J_{\text{CP}} = 6.2$ Hz, $\text{CH}(\text{CH}_3)_2$), 70.8 (CH_2O), 70.7 ($2 \times \text{CH}_2\text{O}$), 70.5 ($5 \times \text{CH}_2\text{O}$), 70.4 (CH_2O), 69.9 (CH_2O), 69.1 (CH_2O), 68.4 (CH_2O), 66.2 (d, $J_{\text{CP}} = 166.7$ Hz, C-4'), 59.0 (C-3'''), 55.6 (OCH_3), 48.9 (C-1'), 45.7 (C-2'''''), 29.8 (C-1'''''), 24.0 (m, $\text{CH}(\text{CH}_3)_2$); ^{31}P NMR (CDCl_3): δ 18.7; HRMS (ES): m/z found ($\text{M}^+ + \text{H}$), 1016.3100, $\text{C}_{43}\text{H}_{64}\text{N}_5\text{O}_{14}\text{PSBr}$ requires ($\text{M}^+ + \text{H}$) 1016.3091.

APPENDIX

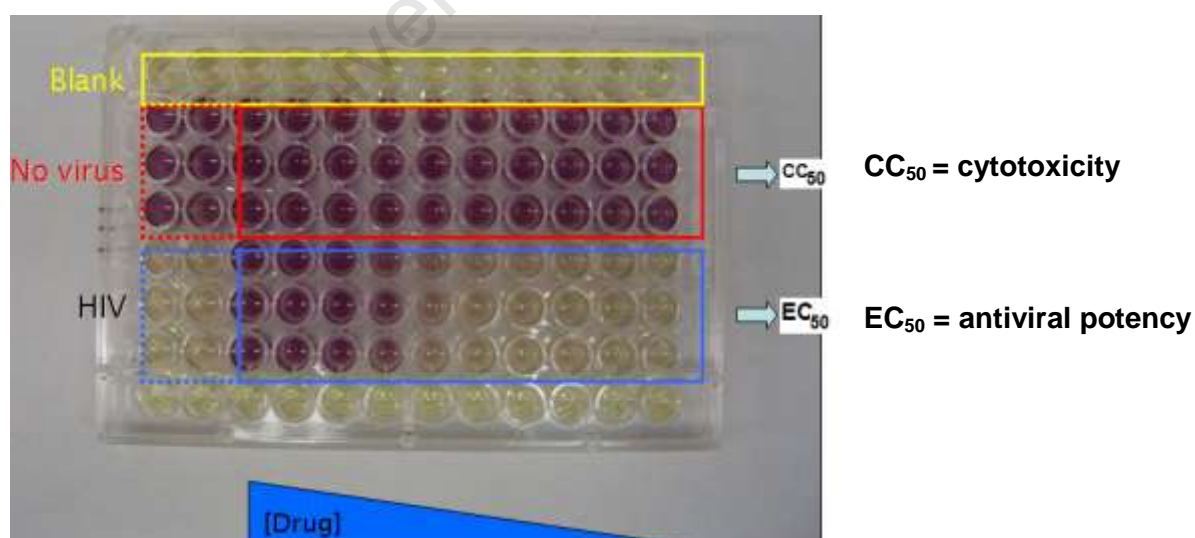
AN MTT-ASSAY

An MTT-assay was carried out at Yale University to determine the target compounds have been synthesized in this project. The tetrazolium-based colorimetric (MTT) assay using MT-4 cells for detection of anti-HIV compounds has been widely used, since 20 years ago. This method, which remains popular, provides more information than more recently developed methods and very efficiently.

An MTT-assay procedure

1×10^5 MT-2 cells per millilitre were infected with HIV-1 IIIB at a 0.1 multiplicity of infection (MOI). 100 μ L of of this solution was mixed with each serial dilution of inhibitor in triplicate on a 96-well plate. Mock infected cells were also mixed with inhibitor in a similar manner. After five days of incubation, a cell-permeable tetrazolium dye (MTT) was added. The MTT reaction was stopped after 5 h adding acidified isopropanol. The plates were gently shaken overnight, quantitated on a plate reader and the absorbance measured at 595 nm. The absorbance values were then plotted versus inhibitor concentration (EC_{50}) and 50% cytotoxic concentration (CC_{50}) of the test compounds were defined as the compound concentrations required to inhibit cell viability (MT-2) by 50% or to reduce by 50% the number of viable cells in mock-infected cell cultures, respectively.

Cell-Culture Assay



REFERENCES

1. Barré-Sinoussi, F.; Chermann, J.C.; Rey, F.; Nugeyre, M. T; Charnart, S.; Gruest, J.; Dauguet, C.; Axler-Blin, C.; Venzinet-Brun, F.; Rouzioux, C.; Rozenbaum, W.; Montagnier, L. *Science* **1983**, 220, 868-871.
2. Weiss, R. A. *Trop. Med. Int. Health* **2000**, 5, A-10-A15.
3. Aiken, C.; Trono, D. *J. Virol* **1995**, 69, 5048-5056.
4. Cooley, L. A.; Lewin, S. R. *J. Clin. Virol.* **2003**, 26, 121-132.
5. (a) Lodish, H.; Baltimore, D.; Berk, A.; Zipursky, S. L.; Matsudaira, P.; Darnell, J. *Molecular Cell Biology*, Third Edition, Scientific American Books, Inc. **1995**, 330-331. (b) AIDS/ HIV information from AVERT.org (available at <http://www.avert.org/virus.htm>).
- 6.(a) UNAIDS/WHO Epidemiological Fact Sheets on HIV/AIDS and Sexually Transmitted Infections, 2007 Epidemic Update: December **2007**. (b) UNAIDS/WHO Epidemiological Fact Sheets on HIV/AIDS and Sexually Transmitted Infections, 2008 Epidemic Update: July **2008**.
7. De Clercq, E. *Nature Rev.* **2007**, 6, 1001-1018.
8. De Clercq, E. *Biochem. Pharmacol.* **1994**, 47, 155-169.
9. Kwong, P. D.; Wyatt, R.; Robinson, J.; Sweet, R.W.; Sodroski, J.; Hendrickson, W. A. *Nature* **1998**, 393, 448.
10. Wyatt, R.; kwong. P. D.; Desjardins, E.; Sweet, R. W.; Robinson. J.; Hendrickson, W. A.; Sodroski, J. G. *Nature* **1998**, 280, 705
11. Rizzuto, C. D.; Wyatt, R.; Hernandez-Ramos, N.; Sun, Y.; Kwong, P. D.; Hendrickson, W. A.; Sodroski, J. *Science* **1998**, 280, 1949.
12. Borkow, G.; Lapidot, A. *J. Infect. Dis.* **2005**, 5, 3-15.
13. De Clercq, E. *Int. J. Biochem. Cell Biol.* **2004**, 36, 1800-1822.
14. (a) Ren, J.; Esnouf, R. M.; Hopkins, A. L.; Warren, J.; Balzarini, J.; Stuart, D. I.; Stammers, D. K. *Biochemistry*, **1998**, 37, 14394-14403. (b) Auwerx, J.; Stevens, M.; Van Rompay, A. R.; Bird, L. E.; Ren, J.; De Clercq, E.; Oeberg, B.; Stammers, D. K.; Karlsson, A.; Balzarini, J. *J. Virol.* **2004**, 78, 7427-7437.
15. Monini, P.; Sgadari, C.; Toschi, E.; Barillari, G.; Ensoli, B. *Nature Rev.* **2004**, 4, 861-875.
16. (a)Gottlieb, M. S.; Schroff, R.; Schanker, H. M. *New Engl. J. Med.* **1981**, 305, 1425-1431.(b) Scott, K.; Blankson, J. N. *Hopkins HIV report*, **2007**, 19, 2, 10-12.
17. Budner, M.; Falzone, C.; Lantz, C.; Uy, J. HIV and AIDS: The Biochemistry Behind the Disease, 2002 (available at <http://www.denison.edu/chem/DCS/journal/budnerv1n1.html>).
18. Jacobo-Molina, A.; Ding, J.; Nanni, R. G.; Clark Jr, A. D.; Lu, X.; Tantillo, C.; Willians, R. L.; Kamer, G.; Ferris, A. L.; Clark. P. *Proc. Natl. Acad. Sci. USA*, **1993**, 90, 6320-6324.
19. Pata, J. D.; Stirtan, W. G.; Goldstien, S. W.; Steitz, T. A. *Proc. Natl. Acad. Sci. USA*, **2004**, 101, 10548-10553.
20. Kohlstaedt, L. A.; Wang, J.; Friedman, J. M.; Rice, P. A.; Steitz, T. A. *Science*, **1992**, 256, 1783-1790.
21. Zhou, Z.; Lin, X.; Madura, J. D. *J. Infect.Dis.* **2006**, 6, 391-413.
22. Sluis-Cremer, N.; Tachedjian, G. *Virus Res.* **2008**, 134, 147-156.

23. De Clercq, E. *Curr. Med. Chem.* **2001**, 8, 1543-1572.
24. Henry, K.; Erice, A.; Tierney, C.; Balfour, H. H. Jr.; Fischl, M. A.; Kmack, A.; Liou, S-H.; Kenton, A.; Hirsch, M. S.; Phair, J.; Martinez, A.; Kahn, J. O. *J. Acquir. Immun. Defic. Syndr. Hum. Retrovirol.* **1998**, 19, 339-349.
25. Bisset, L. R.; Cone, R. W.; Huber, W.; Battegay, M.; Vernazza, P. L.; Weber, R.; Grob, P. J.; Opravil, M. *AIDS*, **1998**, 12, 2115-2123.
26. Woods II, M. L.; MacGinley, R.; Eisen, D. P.; Allworth, A. M. *AIDS*, **1998**, 12, 1491-1494.
27. Mitsuya, H.; Weinhold, K. J.; Furman, P. A.; St Clair, M. H.; Nusonoff-lehrman, S.; Gallo, R. C.; Bolognesi, D. P.; Barry, D. W.; Broder, S. *Proc. Natl. Acad. Sci. USA.* **1985**, 82, 7096-7100.
28. Coates, J. A. V.; Cammack, N. S.; Jenkinson, H. J.; Jowett, A. J.; Jowett, M. I.; Pearson, B. A.; Pen, C. R.; Rouse, P. L.; Viner, K. C.; Cameron, J. M. *Antimicrob. Agents Chemother.* **1992**, 36, 733-739.
29. Ahluwalia, G.; Cooney, D. A.; Mitsuya, H.; Fridland, A.; Flora, K. P.; Hao, Z.; Dalal, M.; Broder, S.; Johns, D. G. *Biochem. Pharmacol.* **1986**, 35, 3797-3800.
30. Cooney, D. A.; Dalal, M.; Mitsuya, H.; McMahon, J. B.; Nadkarni, M.; Balzarini, J.; Broder, S.; Johns, D. G. *Biochem. Pharmacol.* **1986**, 35, 2065-2068.
31. Balzarini, J.; Kang, G. J.; Dalal, M.; Herdewijn, P.; De Clercq, E.; Broder, S.; Johns, D. G. *Mol. Pharmacol.* **1987**, 32, 162-167.
32. Crimmins, M. T.; King, B. W.; *J. Org. Chem.* **1996**, 61, 4192-4193.
33. (a) Liotta, D. G.; Choi, W. -B. *PCT Int. Appl. WO 91252418*, **1991**. (b) Liotta, D. C.; Schinazi, R. F.; Choi, W. -B. *PCT Int. Appl. WO 9214743*, **1992**.
34. (a) De Clercq, E. *Clin. Microbiol. Rev.* **1995**, 8, 200-239. (b) McComsey, G. A.; Lo Re, V., III.; O'Riordan, M.; Walker, U. A.; Laberecht, D.; Baron, E.; Mounzer, K.; Frank, I. *Clin. Infect. Dis.* **2008**, 46, 1290-1296.
35. Meyer, P. R.; So, A. G.; Scott, W. A. *Proc. Natl. Acad. Sci. USA.* **1998**, 95, 13471-13476.
36. Miller, M. D.; Margot, N. A.; Hertogs, K.; Larder, B.; Miller, V. *Nucleos. Nucleot. Nucleic Acids* **2001**, 20, 1025-1028.
37. De Clercq, E. *Expert Opin. Emerging Drugs* **2005**, 10, 241-274.
38. De Clercq, E. *Nature Rev. Drug Discov.* **2002**, 1, 13-25.
39. (a) Hurwitz, S. J.; Otto, M. J. *Antiviral Chem. Chemother.* **2005**, 16, 117-127. (b) Feng, J. Y.; Junxing, S.; Schinazi, R. F.; Anderson, K. S. *FASEB*, **1999**, 13, 1511-1517.
40. De Clercq, E. *Antiviral Res.* **2007**, 75, 1-13.
41. De Clercq, E. *Biochem. Pharmacol.* **2007**, 73, 911-922.
42. Holy, A. *Antiviral Res.* **2006**, 71, 248-253.
43. Tantillo, C.; Ding, J.; Jacobo-Molina, A.; Nanni, R. G.; Boyer, P. L.; Hughes, S. H.; Arnold, E. *Proc. Natl. Acad. Sci. USA* **1993**, 90, 6320-6324.
44. Marx, A.; Detmer, I.; Gaster, J.; Summerer, D. *Synthesis* **2004**, 1, 1-14.
45. Perigaud, C.; Aubertin, A. -M.; Benzaria, S.; Pelicano, H.; Girardet, J. -L.; Maury, G.; Gosselin, G.; Kirn, A.; Imbach, J. -L. *Biochem. Pharmacol.* **1994**, 48, 11-14.
46. McGuigan, C.; Tsang, H. -W.; Cahard, D.; Turner, K.; Velazquez, S.; Salgado, A.; Bidios,

- L.; Naesens, L.; De Clercq, E.; Balzarini, J. *Antiviral Res.* **1997**, 35, 195-204.
47. Siddiqui, A. Q.; Ballatore, C.; McGuigan, C.; De Clercq, E.; Balzarini, J. *J. Med. Chem.* **1999**, 42, 393-399.
48. Siddiqui, A. Q.; McGuigan, C.; Ballatore, C.; Zuccotto, F.; Gilbert, I. H.; De Clercq, E.; Balzarini, J. *J. Med. Chem.* **1999**, 42, 4122-4128.
49. Balzarini, J.; Karlsson, A.; Aquaro, S.; Perno, C. -F.; Cahard, D.; Naesens, L.; De Clercq, E.; McGuigan, C. *Proc. Natl. Acad. Sci. USA* **1996**, 93, 7295-7299.
50. Aquaro, S.; Wedgwood, O.; Yarnold, C.; Cahard, D.; Pathinara, R.; Velazquez, S.; McGuigan, C.; Calio, R.; De Clercq, E.; Balzarini, J.; Perno, C. F. *Antimicrob. Agents Chemother.* **2000**, 44, 173-177.
51. Meier, C.; Lorey, M.; De Clercq, E.; Balzarini, J. *Bioorg. Med. Chem. Lett.* **1997**, 7, 99-104.
52. Meier, C.; Knispel, T.; De Clercq, E.; Balzarini, J. *J. Bioorg. Med. Chem. Lett.* **1997**, 7, 1577-1582.
53. Meier, C.; Lorey, M.; De Clercq, E.; Balzarini, J. *J. Med. Chem.* **1998**, 41, 1417-1427.
54. Meier, C.; Knispel, T.; De Clercq, E.; Balzarini, J. *J. Med. Chem.* **1999**, 42, 1604-1614.
55. Abert, A. *Selective toxicity*. Chapman and Hall Editors London, **1951**.
56. Anastasi, C.; Quelever, G.; Burlet, S.; Garino, C.; Souard, F.; Kraus, J. -L. *Curr. Med. Chem.* **2003**, 10, 1825-1843.
57. (a) Meier, C. *Eur. J. Org. Chem.* **2006**, 1081-1102. (b) Gisch, N.; Balzarini, J.; Meier, C. *J. Med. Chem.* **2007**, 50, 1658-1667.
58. Wagner, C. R.; Iyer, V. V.; McIntee, E. J. *Med. Res. Rev.* **2000**, 20, 417-451.
59. Meier, C. *Synlett* **1998**, 233-242.
60. Khan, S. R.; Nowak, B.; Plunkett, W.; Farquhar, D. *Biochem. Pharmacol.* **2005**, 69, 1307-1313.
61. Meier, C. *Mini-Rev. Med. Chem.* **2002**, 2, 219-234.
62. Meier, C.; Ruppel, M. F. H.; Vukadinovic, D.; Balzarini, J. *Mini. Rev. Med. Chem.* **2004**, 4, 383-394.
63. De Clercq, E.; Holy, A. *Nat. Rev. Drug Discov.* **2005**, 4, 928-940.
64. De Clercq, E.; Holy, A.; Rosenberg, I.; Sakuma, T.; Balzarini, J.; Maudgal, P. C. *Nature* **1986**, 323, 464-467.
65. De Clercq, E.; Descamps, J.; De Somer, P.; Holy, A. *Science* **1978**, 200, 563-565.
66. Shafer, R. W. *Clin. Microbiol. Rev.* **2002**, 247-277.
67. Meyer, P. R.; Matsuura, S. E.; So, A. G.; Scott, W. A. *Proc. Natl. Acad. Sci USA* **1998**, 13471-13476.
68. De Clercq, E. *Antiviral Res.* **1998**, 38, 153-179.
69. (a) Sluis-Cremer, N.; Temiz, N. P.; Bahar, I. *Curr. HIV Res.* **2004**, 2, 323-332. (b) Haubrich, R. ; Gubernick, S. ; Yasothan, U. ; Kirkpatrick, P. *Nature*, **2008**, 7, 287. (c) Martins, S.; Ramos, M.J.; Fernandes, P.A. *Curr. Med. Chem.* **2008**, 15, 1083-1095.
70. Pauwels, R.; Andries, K.; Desmyter, J.; Schols, D.; Kukla, M. J.; Breslin, H. J.; Raeymaeckers, A.; Van Gelder, J.; Woestenborghs, R.; Heykants, J.; Schellekens, K.; Janssen, M. A. C.; De Clercq, E.; Janssen, P. A. J. *Nature* **1990**, 343, 470-474.
71. Janssen, P. A. J.; Lewi, P. J.; Arnold, E.; Daeyaerts, F.; de Jonge, M.; Heeres, J.; Koymans, L.; Vinkers, M.; Guillemont, J.; Pasquier, E.; Kukla, M.; Ludovici, D.; Andries,

- K.; de Bethune, M. -P.; Pauwels, R.; Das, K.; Clark, A. D.; Frenkel, Y. V.; Hughes, S. H.; Medaer, B.; De Knaep, F.; Bohets, H.; De Clercq, F.; Lampo, A.; Williams, P.; Stoffels, P. *J. Med. Chem.* **2005**, 48, 1901-1909.
72. Pauwels, R.; Andries, K.; Debyser, Z.; Van Daele, P. V.; Schols, D.; Stoffels, P.; De Vreese, K. D.; Woestenborghs, R.; Vandamme, A.; Janssen, C. G. M.; Anne, J.; Cauwenbergh, G.; Desmyter, J.; Heykants, J.; Janssen, M. A. C.; De Clercq, E.; Janssen, P. A. J. *Proc. Natl. Acad. Sci. USA* **1993**, 90, 1711-1715.
73. Ludovici, D. W.; Kukla, M. J.; Grous, P. G.; Krishnan, S.; Andries, K.; de Bethune, M. -P.; Azijn, H.; Pauwels, R.; De Clercq, E.; Arnold, E.; Janssen, P. A. J. *Bioorg. Med. Chem. Lett.* **2001**, 11, 2225-2228.
74. Ludovici, D. W.; Kavash, R. W.; Kukla, M. J.; Ho, C. Y.; Ye, H.; De Corte, B. L.; Andries, K.; de Bethune, M. -P.; Azijn, H.; Pauwels, R.; Moereels, H. E.; Heeres, J.; Koymans, L. M.; de Jonge, M. R.; Van Aken, K. J.; Daeyaert, F. F.; Lewi, P. J.; Das, K.; Arnold, E.; Janssen, P. A. J. *Bioorg. Med. Chem. Lett.* **2001**, 11, 2229-2234.
75. Sankatsing, S.; Weverling, G.; van 't Klooster, G.; Prins, J.; Lange, J. 9th Conference on Retroviruses and Opportunistic Infections, Seattle, WA, February 24-28, 2002. Abstract 5.
76. Das, K.; Bauman, J. D.; Clark, A. D.; Frenkel, Y. D.; Lewi, P. J.; Shatlin, A. J.; Hughes, S. H.; Arnold, E. *Proc. Natl. Acad. Sci. USA* **2008**, 105, 1466-1471.
77. Hsiou, Y.; Ding, J.; Das, K.; Clark, A. D.; Hughes, S. H.; Arnold, E. *Structure* **1996**, 4, 853-860.
78. Rodgers, D. W.; Gamblin, S. J.; Harris, B. A.; Ray, S.; Culp, J. S.; Hellmig, B.; Woolf, D. J.; Debouck, C.; Harrison, S. C. *Proc. Natl. Acad. Sci. USA* **1995**, 92, 1222-1226.
79. Smith, M. B. K.; Lamb, M. L.; Tirado-Rives, J.; Jorgensen, W. L.; Michejda, C. J.; Ruby, S. K.; Smith, Jr. R. H. *Protein Eng.* **2000**, 13, 413-421.
80. Madrid, M.; Jacobo-Molina, A.; Ding, J.; Arnold, E. *Proteins* **1999**, 35, 332-337.
81. Rodgers, D. W.; Gamblin, S. J.; Harris, B. A.; Ray, S.; Culp, J. S.; Hellmig, B.; Woolf, D. J.; Debouck, C.; Harrison, S. C. *Proc. Natl. Acad. Sci. U.S.A.* **1995**, 92, 1222-1226.
82. Esnouf, R.; Ren, J.; Ross, C.; Jones, Y.; Stammers, D.; Stuart, D. *Nat. Struct. Biol.* **1995**, 2, 203-308.
83. Esnouf, R. M.; Ren, J.; Garman, E. F.; Somers, D. O. N.; Ross, C. K.; Jones, E. Y.; Stammers, D. K.; Stuart, D. I. *Acta Crystallogr.* **1998**, D 54, 938-954.
84. Ren, J.; Esnouf, R.; Garman, E.; Somers, D.; Ross, C.; Kirby, I.; Keeling, J.; Darby, G.; Jones, Y.; Stuart, D.; Stammers, D. *Nat. Struct. Biol.* **1995**, 2, 293-302.
85. Spence, R. A.; Kati, W. M.; Anderson, K. S.; Johnson, K. A. *Science* **1995**, 267, 988-993.
86. Das, K.; Sarafianos, S. G.; Clark Jr, A. D.; Boyer, P. L.; Hughes, S. H.; Arnold, E. *J. Mol. Biol.* **2007**, 365, 77-89.
87. Huang, H.; Chopra, R.; Verdine, G. L.; Harrison, S. C. *Science* **1998**, 282, 1669-1675.
88. Xia, Q.; Radzio, J.; Anderson, K. S.; Sluis-Cremer, N. *Protein. Sci.* **2007**, 16, 1728-1737.
89. Hsiou, Y.; Ding, J.; Das, K.; Clark Jr, A. D.; Hughes, S. H.; Arnold, E. *Structure* **1996**, 4, 853-860.
90. Hopkins, A. L.; Ren, J.; Esnouf, R. M.; Willcox, B. E.; Jones, E. Y.; Ross, C.; Miyasaka, T.;

- Walker, R. T.; Tanaka, H.; Stammers, D. K.; Stuart, D. I. *J. Med. Chem.* **1996**, 39, 1589-1600.
91. Campiani, G.; Ramunno, A.; Maga, G.; Nacci, V.; Fattorusso, C.; Catalanotti, B.; Morelli, E.; Novellino, E. *Curr. Pharmaceut. Des.* **2002**, 8, 615-657.
92. Parniak, M. A.; Sluis-Cremer, N. *Adv. Pharmacol.* **2000**, 49, 67-109.
93. Tronchet, J. M.; Seman, M. *Curr. Topics Med. Chem.* **2003**, 3, 1496-1511.
94. Ding, J.; Das, K.; Moereels, H.; Koymans, L.; Andries, K.; Janssen, P. A.; Hughes, S. H.; Arnold, E. *Nature Struct. Biol.* **1995**, 2, 407-415.
95. Das, K.; Lewi, P. J.; Hughes, S. H.; Arnold, E. *Progr. Biophys. Mol. Biol.* **2005**, 88, 209-231.
96. De Corte, B. L. *J. Med. Chem.* **2005**, 48, 1689-1696.
97. Das, K.; Clark, A. D.; Lewi, P. J.; Heeres, J.; de Jonge, M. R.; Koymans, L. M. H.; Vinkers, H. M.; Daeyaert, F.; Ludovici, D. W.; Kukla, M. J.; De Corte, B.; Kavash, R. W.; Ho, C. Y.; Ye, H.; Lichtenstein, M. A.; Andries, K.; Pauwels, R.; de Bethune, M. -P.; Boyer, P. L.; Clark, P.; Hughes, S. H.; Janssen, P. A. J.; Arnold, E. *J. Med. Chem.* **2004**, 47, 2550-2560.
98. Rodriguez-Barrios, F.; Balzarini, J.; Gago, F. *J. Am. Chem. Soc.* **2005**, 127, 7570.
99. Cantrell, A.S.; Engelhardt, P.; Högberg, M.; Jaskunas, S.R.; Johansson, N.G.; Jordan, C.L.; Kangasmesä, J.; Kinnick, M.D.; Lind, P.; Morin, J.M.; Muesting, M.A.; Noréen, R.; Öberg, B.; Pranc, P.; Sahlberg, C.; Ternansky, R.J.; Vasileff, R.T.; Vrang, L.; West, S.J.; Zhang, H. *J. Med. Chem.* **1996**, 39, 4261-4274.
100. Ahgren, C.; Backro, K.; Bell, F. W.; Cantrell, A. S.; Clemens, M.; Colacino, J. M.; Deeter, J. B.; Engelhardt, J. A.; Hogberg, M.; Jaskunas, S. R.; Johansson, N. G.; Jordan, C. L.; Kasher, J.S.; Kinnick, M. D.; Lind, P.; Lopez, C.; Morin, J. M. Jr.; Muesing, M. A.; Noréen, R.; Oberg, B.; Paget, C. J.; Palkowitz, J. A.; Parrish, C. A.; Pranc, P.; Rippey, M. K.; Rydergard, C.; Sahlberg, C.; Swanson, S.; Ternansky, R. J.; Unge, T.; Vasileff, R. T.; Vrang, L.; West, S. J. Zhang, H.; Zhou, X-X. *Antimicrob. Agents Chemother.* **1995**, 39, 1329-1335.
101. Bell, F. W.; Cantrell, A. S.; Högberg, M.; Jaskunas, S. R.; Johansson, N. G.; Jordan, C. L.; Kinnick, M. D.; Lind, P.; Morin, J. M. Jr.; Noréen, R.; Oberg, B.; Palkowitz, J. A.; Parrish, C. A.; Pranc, P.; Sahlberg, C.; Ternansky, R. J.; Vasileff, R. T.; Vrang, L.; West, S. J.; Zhang, H.; Zhou, X-X. *J. Med. Chem.* **1995**, 38, 4929-4936.
102. Vig, R.; Mao, C.; Venkatachalam, T.K.; Tuel-Ahlgren, L.; Sudbeck, E.A.; Uckun, F.M. *Bioorg. Med. Chem. Lett.* **1998**, 8, 1461-1466.
103. D'Cruz, O.J.; Uckun, F. M. *Enzym. Inhib. Med. Chem.* **2006**, 21, 329-350.
104. Venkatachalam, T. K.; Sudbeck, E. A.; Mao, C.; Uckun, F. M. *Bioorg. Med. Chem. Lett.* **2001**, 11, 523-528.
105. Ren, J.; Diprose, J.; Warren, J.; Ensouf, R. M.; Bird, L. E.; Ikemizu, S.; Slater, M.; Milton, J.; Balzarini, J.; Stuart, D. I.; Stammers, D. K. *J. Biol. Chem.* **2000**, 275, 5633-5639.
106. D'Cruz, O. J.; Uckun, F. M. *Curr. HIV Res.* **2006**, 4, 329, 345.
107. Mao, C.; Sudbeck, E. A.; Venkatachalam, T. K.; Uckun, F. M. *Biochem. Pharmacol.* **2000**, 60, 1251-1265.
108. Balzarini, J.; Karlsson, A.; Perez-Perez, M. J.; Camarasa, M. J.; Tarpley, W. G.; De Clercq, E. *J. Virol.* **1993**, 67, 5353-5359.
109. Bacheler, L.; Jeffrey, S.; Hanna, G.; D'Aquila, R.; Wallace, L.; Logue, K.; Cordova, B.; Hertogs,

- K.; Larder, B.; Buckery, R.; Baker, D.; Gallagher, K.; Scarnati, H.; Tritch, R.; Rizzo, C. *J. Virol.* **2001**, *75*, 4999-5008.
110. Ren, J.; Milton, J.; Weaver, K. L.; Short, S. A.; Stuart, D. I.; Stammers, D. K. *Struct. Folds Des.* **2000**, *8*, 1089-1094.
111. Hsiou, Y.; Das, K.; Ding, J.; Clark, A. D.; Kleim, J. P.; Rosner, M.; Winkler, I.; Riess, G.; Hughes, S. H.; Arnold, E. *J. Mol. Biol.* **1998**, *284*, 313-323.
112. Ren, J.; Stammers, D. *Vir. Res.* **2008**, *134*, 157-170.
113. Udier-Blagovic, M.; Watkins, E. K.; Tirado-Rives, J.; Jorgensen, W. L. *Bioorg. Med. Chem. Lett.* **2003**, *13*, 3337-3340.
114. Das, K.; Ding, J.; Hsiou, Y.; Clark, A. D.; Moereels, H.; Koymans, L.; Andries, K.; Pauwels, R.; Janssen, P. A.; Boyer, P. L.; Clark, P.; Smith, R. H. Jr.; Kroeger Smith, M. B.; Michejda, C. J.; Hughes, S. H.; Arnold, E. *J. Mol. Biol.* **1996**, *264*, 1085-1100.
115. Ren, J.; Nichols, C.; Bird, L.; Chamberlain, P.; Weaver, K.; Short, S.; Stuart, D. I.; Stammers, D. K. *J. Mol. Biol.* **2001**, *312*, 795-805.
116. Nanni, R. G.; Ding, J.; Jacobo-Molina, A.; Hughes, S. H.; Aronld, E. *Perspect. Drug Dis. Dis.* **1993**, *1*, 129.
117. (a) périgaud, C.; Gosselin, G.; Lefebvre, I.; Girardet, J-L, Benzaria, S.; Barker, I.; Imbach, J-L. *Bioorganic. Med. Chem. Lett.* **1993**, *3*, 2521. (b) Xia, Z.; Wiebe, L. I.; Miller, G. G.; Kanaus, E. E. *Arch. Der Pharmazie* **1999**, *332*, 286-294.
118. Nudelman, A.; Rephaedli, A. *J. Med. Chem.* **2000**, *43*, 2962-2966.
119. Romeo, S.; Dell'Agli, M.; Parapini, S.; Rizzi, L.; Galli, G.; Mondani, M.; Sparatore, A.; Taramelli, D.; Bosisio, E. *Bioorg. Med. Chem. Lett.* **2004**, *14*, 2931-2934.
120. Biot, C.; Dessolin, J.; Grellier, P.; Davioud-Charvet, E. *Redox Rep.* **2003**, *8*, 280-283.
121. Davioud-Charvet, E.; Delarue, S.; Biot, C.; Schwobel, Boehme, C. C.; Mussigbrodt, A.; Maes, L.; Sergheraert, C.; Grellier, P.; Schirmer, R. H.; Becker, K. *J. Med. Chem* **2001**, *44*, 4268-4276.
122. Muhanji, C. I.; Hunter, R. *Curr. Med. Chem* **2007**, *14*, 127.
123. Wang, Z.; Bennett, E. M.; Wilson, D. J.; Salomon, C.; Vince, R. *J. Med. Chem.* **2007**, *50*, 3416-3419.
124. (a) Matsumoto, H.; Hamawaki, T.; Ota, H.; Kimura, T.; Goto, T.; Sano, K.; Hayashi, Y.; Kiso, Y. *Bioorg. Med. Chem. Lett.* **2000**, *10*, 1227-1231. (b) Kimura, T.; Matsumoto, H.; Matsuda, T.; Hamawaki, T.; Akaji, K.; Kiso, Y. *Bioorg. Med. Chem. Lett.* **1999**, *9*, 803-806.
125. Tamamura, H.; Omagri, A.; Hiramatsu, K.; Kanamoto, T.; Gotoh, K.; Kanbara, K.; Yamamoto, N.; Nakahima, H.; Otaka, A.; Fujii, N. *Bioorg. Med. Chem.* **2001**, *9*, 2179-2187.
126. Daoudi, J. M.; Greiner, J.; Aubertin, A. M.; Vierling, P. *Bioorg. Med. Chem. Lett.* **2004**, *14*, 495-498.
127. Vliegheer, P.; Clerc, T.; Pannecouque, C.; Witvrouw, M.; De Clercq, E.; Salles, J-P.; Kraus, J-L. *J. Med. Chem.* **2002**, *45*, 1275-1283.
128. Gavriiliu, D.; Fossey, C.; Ciurea, A.; Delbederi, Z.; Sugeac, E.; Ladurée, D.; Schmidt, S.; Laumond, G.; Aubertin, A. M. *Nucleos. Nucleot. Nucleic Acids* **2002**, *21*, 505-533.

129. Ladurée, D.; Sugeac, E.; Fossey, C.; Schmidt, S.; Laumond, G.; Aubertin, A. M. *Nucleos. Nucleot. Nucleic Acids* **2003**, *22*, 873-875.
130. Sugeac, E.; Fossey, C.; Ladurée, D.; Schmidt, S.; Laumond, G.; Aubertin, A. M. *J. Enzym. Inhib. Med. Chem.* **2003**, *18*, 175-186.
131. Ijichi, K.; Fujiwara, M.; Mori, K.; Morozumi, M.; Machida, H.; Shigeta, S.; Konno, K.; Yokota, T.; Baba, M. *Antiviral Res.* **1996**, *31*, 115-120.
132. (a) Mohamed, L. A.; Taourirte, M.; Rochdi, A.; Lazrek, H. B.; Vasseur, J. -J.; Engels, J. W.; Pannecouque, C.; De Clercq, E. *Nucleot. Nucleos. Nucleic Acids* **2003**, *22*, 829-831; (b) Taourirte, M.; Mohamed, L. A.; Rochdi, A.; Vasseur, J. -J.; Fernández, S.; Ferrero, M.; Gotor, V.; Pannecouque, C.; De Clercq, E.; Lazrek, H. B. *Nucleos. Nucleot. Nucleic Acids* **2004**, *23*, 701714.
133. Peterson, L.; Jørgensen, P. T.; Nielsen, C.; Hasen, T. H.; Nielsen, J.; Pederson, E. B. *J. Med. Chem.* **2005**, *48*, 1211-1220.
134. Basavapathruni, A.; Bailey, C. M.; Anderson, K. S. *J. Biol. Chem.* **2004**, *279*, 6221-6224.
135. (a) Velázquez, S.; Alvarez, R.; San-Félix, A.; Jimeno, M. L.; De Clercq, E.; Balzarini, J.; Camarasa, M.-J. *J. Med. Chem.* **1995**, *38*, 1641-1649; (b) Velázquez, S.; Tuñón, V.; Jimeno, M. L.; Chamorro, C.; De Clercq, E.; Balzarini, J.; Camarasa, J.-M. *J. Med. Chem.* **1999**, *42*, 5188-5196.
136. McGuigan, C.; Devine, K. G.; O'Connor, T. J.; Galpin, S. A.; Jeffries, D. J.; Kinchington, D. *Antiviral Chem. Chemother.* **1990**, *1*, 107-113.
137. Velázquez, S.; Lobatón, E.; De Clercq, E.; Koontz, D. L.; Mellors, J. W.; Balzarini, J.; Camarasa, M.-J. *J. Med. Chem.* **2004**, *47*, 3418-3426.
138. (a) Oberg, B. *Pharmacol. Ther.* **1989**, *40*, 213-285; (b) Wagstaff, A. J.; Bryson, H. M. *Drugs* **1994**, *48*, 199-226; (c) Chrisp, P.; Clissold, S. F. *Drugs* **1991**, *41*, 104-129.
139. Feltcher, C. V.; Collier, A. C.; Rhame, F. S.; Bennet, D.; Para, M. F.; Beatty, C. C.; Jones, C. E.; Balfour, H. H. Jr. *Antimicrob. Agents Chemother.* **1994**, *38*, 604-607.
140. Renoud-Grappin, M.; Fossey, C.; Fontaine, G.; Ladurée, D.; Aubertin, A. M.; Kirn, A. *Antiviral Chem. Chemother.* **1998**, *9*, 205-223.
141. Pontikis, R.; Dollé, V.; Guillaumel, J.; Dechaux, E.; Note, R.; Nguyen, C. H.; Legraverend, M.; Bisagni, E.; Aubertin, A.-M.; Grierson, D. S.; Monneret, C. *J. Med. Chem.* **2000**, *43*, 1927-1939.
142. Hunter, R.; Muhanji, C.I.; Hale, I.; Bailey, C. M.; Basavapathruni, A.; Anderson, K. S. *Bioorg. Med. Chem.* **2007**, *17*, 2614.
143. (a) Ruth, J. L.; Cheng, Y. C. *Mol. Pharmacol.* **1981**, *20*, 415-422. (b) Ruth, J. L.; Cheng, Y. C. *J. Biol. Chem.* **1982**, 10261-10266.
144. Mao, C.; Sudbeck, E. A.; Venkatachalam, T. K.; Uckun, F. M. *Bioorg. Med. Chem. Lett.* **1999**, *9*, 1593-1598.
145. Hö gberg, M.; Engelhardt, P.; Vrang, L.; Zhang, H. *Bioorg. Med. Chem. Lett.* **2000**, *10*, 265-268.
146. (a) Glennon, R. A.; Liebowitz, S. M.; Leming-Doot, D.; Rosecrans, J. A. *J. Med. Chem.* **2005**, *23*, 990. (b) Lin, C. H.; Yang, J. S.; Chang, C. Y.; Kuo, S. C.; Lee, M. R.; Haung, L. *J. Bioorg. Med. Chem.* **2005**, *13*, 1537-1544.
147. Brossi, A.; Teitel, S. *Helv. Chim. Acta.* **1970**, *53*, 1779-1787.

148. Hunter, R.; Younis, Y.; Muhanji, C-I.; Curtin, T-L.; Naidoo, K. J.; Petersen, M.; Baily, C. M.; Basavapathruni, A.; Anderson, K. S. *Bioorg. Med. Chem.* **2008**, 16, 10270-10280.
149. Marshall, J. A.; Trometer, J. D.; Blough, B. E.; Crute, T. D. *J. Org. Chem.* **1988**, 53, 4274-4282.
150. Pannecouque, C.; Daelemans, D.; De Clercq, E. *Nat. Protoc.* **2008**, 3, 427-434.
151. Morris, G. M.; Goodsell, D. S.; Halliday, R. S.; Huey, R.; Hart, W. E.; Belew, R. K.; Olson, A. J. *J. Comput. Chem.* **1998**, 19, 1639.
152. (a) Venkatachalam, T. K.; Sudbeck, E.; Uckun, F. M. *J. Mol. Struct.* **2005**, 751, 41; (b) Sudbeck, E. A.; Jennissen, J. D.; Venkatachalam, T. K.; Uckun, F. M. *Acta Crystallogr. Sect. C: Cryst. Struct. Commun.* **1999**, C55, 2122.
153. Barreiro, G.; Kim, J. T.; Guimaraes, C. R. W.; Bailey, C. M.; Domaoal, R. A.; Wang, L.; Anderson, K. S.; Jorgenson, W. L. *J. Med. Chem.* **2007**, 50, 5324.
154. Chen, C-L.; Venkatachalam, T. K.; Waurzyniak, B.; Chestrom, L.; Uckun, F. M. *Arzneimittel-Forschung* **2001**, 51, 574.
155. Sonogashira, K.; Todha, Y.; Hagihara, N. *Tetrahedron Lett.* **1975**, 16, 4467-4470.
156. Ciurea, A.; Fossey, C.; Benzaria, S.; Gavriuiu, D.; Delbederi, Z.; Lelong, B.; Ladurée, D.; Aubertin, A. M.; Kirn, A. *Nucleos. Nucleot. Nucleic Acids* **2001**, 20, 1655-1670.
157. De Clercq, E. *J. Clin. Virol.* **2004**, 30, 115-133.
158. (a) Horwitz, J. P.; Chua, J.; Da Rooga, M. A.; Noel, M. *Tetrahedron Lett.* **1964**, 2725-2727. (b) Horwitz, J. P.; Chua, J.; Klundt, I. L.; Da Rooge, M. A.; Noel, M. *J. Am. Chem. Soc.* **1964**, 86, 1896. (c) Horwitz, J. P.; Chua, J.; Da Rooge, M. A.; Noel, M.; Klundt, I. L. *J. Org. Chem.* **1966**, 31, 205-211.
159. Chen, B-C.; Quinlan, S. L.; Ried, J. G.; Spector, R. H. *Tetrahedron Lett.* **1998**, 39, 729732.
160. Chen, B-C.; Quinlan, S. L.; Stark, D. R.; Ried, G.; Audia, V. H.; George, J. G.; Eisenreich, E.; Brundidge, S. P.; Racha, S.; Spector, R. H. *Tetrahedron Lett.* **1995**, 36, 7957.
161. Agrofoglio, L. A.; Gillaizeau, I.; Saito, Y. *Chem. Rev.* **2003**, 103, 1875-1916.
162. Crisp, G.; Flynn, B. L. *J. Org. Chem.* **1993**, 58, 6614-6619.
163. Robins, M. J.; Barr, P. J. *J. Org. Chem.* **1983**, 48, 1854-1862.
164. Hobbs, F. W. Jr. *J. Org. Chem.* **1989**, 54, 3420-3422.
165. Robins, M. J.; Vinayak, R. S.; Wood, S. G. *Tetrahedron Lett.* **1990**, 31, 3731-3734.
166. Garg, N. K.; Woodroffe, C. C.; Lacenere, C. J.; Quake, S. R.; Stoltz, B. M. *Chem. Commun.* **2005**, 4551-4553.
167. Asakura, J.; Robins, M. J. *J. Org. Chem.* **1990**, 55, 4928-4933.
168. Olivi, N.; Spruyt, P.; Peyrat, J-F.; Alami, M.; Brion, J-D. *Tetrahedron Lett.* **2004**, 45, 2607-2610.
169. (a) McGuigan, C.; Nicholls, S. R.; O'Connor, T. J.; Kinchington, D. *Antiviral Chem. Chemother.* **1990**, 1, 25-33. (b) McGuigan, C.; O'Connor, T. J.; Nicholls, S. R.; Nickson, C.; Kinchington, D. *Antiviral Chem. Chemother.* **1990**, 1, 355-360.
170. McGuigan, C.; Cahard, D.; Sheeka, H. M.; De Clercq, E.; Balzarini, J. *J. Med. Chem.* **1996**, 39, 1748-1753.
171. McGuigan, C.; Cahard, D.; Sheeka, H. M.; De Clercq, E.; Balzarini, J. *Bioorg. Med. Chem. Lett.* **1996**, 6, 1183-1186.
172. McGuigan, C.; Pathirana, R.; Balzarini, J.; De Clercq, E. *J. Med. Chem.* **1993**, 36, 1048-1052.

173. McGuigan, C.; Tsang, H-W.; Cahard, D.; Turner, K.; Velazquez, S.; Salgado, A.; Bidois, L.; Naesens, L.; De Clercq, Balzarini, J. *Antiviral Res.* **1997**, 35, 195-204.
174. Murakami, E.; Feng, J.Y.; Lee, H.; Hanes, J.; Johnson, K.A.; Anderson, K.S. *J. Biol. Chem.* **2003**, 278, 36403-36409.
175. Kerr, S.G.; Anderson, K.S. *Biochemistry* **1997**, 36, 14064-14070.
176. Pomeisl, K.; Votruba, I.; Holy, A.; Pohl, R. *Collect. Czech. Chem. Commun.* **2006**, 71, 595-624.
177. Fakharian, H.; Mirzaei, A. *Organic Process Research and Development* **2004**, 8, 401-404.
- 178.(a) Pudovik, A. N.; Zimin, M. G.; Kurguzova, A. M. *J. Gen. Chem. SSSR*, **1971**, 41, 1981.
(b) Jeanmaire, T.; Hervaud, Y.; Boutevin, B. *Phosphorous, Sulfur and Silicon*, **2002**, 177, 1137- 1145.
179. I. G. Farbenindustrie AG. *FR Patent No.* 655871, **1928**.
180. Hammerschmidt, F.; Kahlig, H. *J. Org. Chem.* **1991**, 56, 2364-2370.
181. Otter, B. A.; Falco, E. A.; Fox, J. J. *J. Org. Chem.* **1969**, 34, 1390-1395.
182. Codington, J. F.; Fecher, R.; Fox, J. J. *J. Am. Chem. Soc.* **1960**, 82, 2794-2803.
183. Johar, M.; Manning, T.; Kunimoto, D. Y.; Kumar, R. *Bioorg. Chem.* **2005**, 13, 6663-6671.